The University of Sydney

Copyright in relation to this thesis*

Under the Copyright Act 1968 (several provisions of which are referred to below), this thesis must be used only under the normal conditions of scholarly fair dealing for the purposes of research, criticism or review. In particular no results or conclusions should be extracted from it, nor should it be copied or closely paraphrased in whole or in part without the written consent of the author. Proper written acknowledgement should be made for any assistance obtained from this thesis.

Under Section 35(2) of the Copyright Act 1968 'the author of a literary, dramatic, musical or artistic work is the owner of any copyright subsisting in the work'. By virtue of Section 32(1) copyright 'subsists in an original literary, dramatic, musical or artistic work that is unpublished' and of which the author was an Australian citizen, an Australian protected person or a person resident in Australia.

The Act, by Section 36(1) provides: 'Subject to this Act, the copyright in a literary, dramatic, musical or artistic work is infringed by a person who, not being the owner of the copyright and without the licence of the owner of the copyright, does in Australia, or authorises the doing in Australia of, any act comprised in the copyright'.

Section 31(1)(a)(i) provides that copyright includes the exclusive right to 'reproduce the work in a material form'. Thus, copyright is infringed by a person who, not being the owner of the copyright and without the licence of the owner of the copyright, reproduces or authorises the reproduction of a work, or of more than a reasonable part of the work, in a material form, unless the reproduction is a 'fair dealing' with the work 'for the purpose of research or study' as further defined in Sections 40 and 41 of the Act.

Section 51(2) provides that 'Where a manuscript, or a copy, of a thesis or other similar literary work that has not been published is kept in a library of a university or other similar institution or in an archives, the copyright in the thesis or other work is not infringed by the making of a copy of the thesis or other work by or on behalf of the officer in charge of the library or archives if the copy is supplied to a person who satisfies an authorized officer of the library or archives that he requires the copy for the purpose of research or study'.

Keith Jennings
Registrar and Deputy Principal

*'Thesis' includes 'treatise', 'dissertation' and other similar productions.

R. B. LIB

CHARACTERISATION AND PULMONARY DEPOSITION OF THERAPEUTIC AND DIAGNOSTIC AQUEOUS AEROSOLS

Submission in fulfilment of the requirements for the degree

of Doctor of Philosophy

by

Paul R. Phipps, B. Pharm.

Department of Pharmacy University of Sydney

October, 1990

PREFACE

The work presented for examination in this thesis was carried out under the supervision of Dr Igor Gonda. No portion of this work has been submitted by the candidate for the award of any other degree.

ACKNOWLEDGMENTS

The work covered by this thesis has been made possible only with the help of the staff of a number of Departments at Royal Prince Alfred Hospital and Sydney University.

It has been my very good fortune to have had Dr Igor Gonda as my supervisor. With his mix of enthusiasm, friendship and ability to always choose the right moment to give advice, direction and ideas, he has provided momentum to this work as well as making it enjoyable.

I would like to sincerely thank all the physicists, medical staff and technologists of the Department of Nuclear Medicine at Royal Prince Alfred Hospital for their friendly help and encouragement, especially Peter Borham, Steve Meikle and Roger Fulton. Special thanks are due to Dale Bailey whose expertise and fervour has provided an important contribution to this work.

The Respiratory Lab staff at Royal Prince Alfred Hospital have always been eager to help and inform and I would like to thank them, including Dr Christine Smith, Lily Daviskas, Robyn Schoeffel and Leanne Rodwell. I would like to particularly thank Dr Sandra Anderson who has been a special source of inspiration for me, I owe much of my postgraduate training to her experience and understanding.

Thanks also go to the subjects who volunteered for the aerosol deposition studies, Dr Wayne Castle who provided some of the software for the aerosol inhalation apparatus and Kathie Smith who prepared many of the graphs and diagrams.

I have been the recipient of a Commonwealth postgraduate award and I would like to acknowledge those authorities as well as the help of the Asthma Foundation of New South Wales in providing a generous equipment grant in support of this work.

I am grateful to my parents, brother and sister for their willing support and assistance.

My deepest gratitude is for my wife, Debbie and daughter Jessica whose constant encouragement and companionship has meant so much to me.

PUBLICATIONS AND COMMUNICATIONS

Some of the work presented in this thesis has been described in the following publications and communications.

PHIPPS, P.R., GONDA, I., BAILEY, D.L., BORHAM, P. & BAUTOVICH, G. December 1985. Characterisation of aqueous aerosols. Asthma workshop, Melbourne, Australia.

PHIPPS, P.R., BAILEY, D.L., BORHAM, P.W. & GONDA, I. (1986). Rapid droplet size analysis of diagnostic aerosols. Aust. J. Hosp. Pharm., 16, 60.

BORHAM, P.W., PHIPPS, P.R., BAILEY, D.L., GONDA, I., BAUTOVICH, G.J., MURRAY, C. & MEIKLE, S. (1987). In Vitro assessment of radioaerosol delivery systems. Aust. N.Z. J. Med., 17 [suppl. 2], 468.

PHIPPS, P.R., GONDA, I., BAILEY, D.L., BORHAM, P.W., ANDERSON, S.D. & BAUTOVICH, G.J. November 1986. Deposition of diagnostic aerosols. Asthma workshop, Sydney, Australia.

PHIPPS, P.R., GONDA, I., BAILEY, D.L., BORHAM, P.W., ANDERSON, S.D. & BAUTOVICH, G.J. (1987). Quantitative SPECT aerosol penetration index. Aust. N.Z. J. Med., 17 [suppl. 2], 483.

PHIPPS, P.R., GONDA, I., BAILEY, D.L., BORHAM, P.W., ANDERSON, S.D. & BAUTOVICH, G.J. August 1987. Penetration index of inhalation aerosols obtained by 2-dimensional and tomographic methods. IUPHAR Xth meeting, World Congress, Sydney, Australia. Published in proceedings, 1988.

PHIPPS, P.R., GONDA, I., BAILEY, D.L., BORHAM, P.W., ANDERSON, S.D. & BAUTOVICH, G.J. September 1987. Assessment of regional deposition of saline aerosols by tomographic methods. Airways '87 IUPHAR satellite meeting, Ayers Rock. Australia.

PHIPPS, P.R. & GONDA, I. (1987). Concentration of solution in aqueous aerosol droplets. J. Pharm. Pharmacol., 39 (suppl.), 74p.

PHIPPS, P.R., GONDA, I., BAILEY, D.L., BORHAM, P.W., BAUTOVICH, G.J. & ANDERSON, S.D. (1987). Comparison of methods for the measurement of regional aerosol deposition. J. Pharm. Pharmacol., 39 (suppl.), 72p.

PHIPPS, P.R., GONDA, I., BAILEY, D.L., BORHAM, P.W., BAUTOVICH, G.J. & ANDERSON, S.D. November 1988. The regional deposition of non-isotonic aerosols in normal and asthmatic subjects. Asthma workshop, Melbourne, Australia.

PHIPPS, P.R., BORHAM, P., GONDA, I., BAILEY, D.L., BAUTOVICH, G. & ANDERSON, S.D. (1987). A rapid method for the evaluation of diagnostic radioaerosol delivery systems. Eur. J. Nucl. Med., 134, 183-6.

PHIPPS, P.R., GONDA, I., BAILEY, D.L., BORHAM, P., ANDERSON, S.D. AND BAUTOVICH, G. (1988). Studies of regional deposition of aqueous aerosols in the human respiratory tract. 7th Int. Congr. Aerosols in Medicine, Rochester, USA. J. Aerosols in Med., 1, 208-209.

PHIPPS, P.R., GONDA, I., BAILEY, D.L., BORHAM, P., BAUTOVICH, G. & ANDERSON, S.D. (1989). Comparisons of planar and tomographic gamma scintigraphy to measure the penetration index of inhaled aerosols. Am. Rev. Respir. Dis., 139, 1516-23.

PHIPPS, P.R., GONDA, I., BAILEY, D.L., BORHAM, P., BAUTOVICH, G. & ANDERSON, S.D. Deposition of unstable aqueous droplets in the human respiratory tract. Australian Pharmaceutical Sciences Association meeting, July

1989, Melbourne, Australia.

PHIPPS, P.R. & GONDA, I. (1990). Droplets produced by medical nebulisers: some factors affecting their size and solute concentration. Chest, 97, 1327-1332.

PHIPPS, P.R. AND GONDA, I. (1990). Some consequences of instability of aqueous aerosols produced by jet and ultrasonic nebulisers. Proc 3rd Internat. Aerosol Conf., September 1990, Kyoto, Japan. Published in: Aerosols: science, industry, health and environment. Eds. Masuda, S and Takahashi, K. Pergamon Press, Oxford, vol. 1. p 227-230.

SYNOPSIS

The main body of this thesis consists of nine chapters in the following order:

The general introductory material is presented in chapter 1 where the overall aims are explained. Chapters 2 - 8 have been written in the format of research papers; there are therefore only few cross references and, instead, the reader may directly consult the publications attached to this thesis.

Chapters 2 - 7 are concerned with the development of the methodology used in the *in vivo* experiments described in chapter 8. This latter chapter presents the work to date on the experimental regional deposition of hygroscopic aerosols in normal and asthmatic volunteers. The last chapter summarises the findings and lists suggestions for future work.

CONTENTS

ABSTRACT

Our ultimate aim was to measure the deposition pattern of non-isotonic aerosols in the lungs of normal and asthmatic subjects. These aerosols cause airway narrowing in hypersensitive subjects and are used as an aid to the diagnosis of asthma.

A rapid method for assessing the droplet size generated by aerosol delivery systems to be used in these experiments was designed and evaluated. These methods were then applied to assess, i) diagnostic radioaerosol delivery systems and ii) therapeutic aerosol systems used in the treatment and prevention of *Pneumocystis carinii* infections.

The humidity of the air inhaled along with the aerosol stream and the fall in temperature of the nebuliser solution during generation were found to be important in controlling the size and concentration of solutes within the droplets. To gain a full understanding of the mechanisms involved, droplet concentrations and sizes were predicted by considering mass balance of water and solutes.

Non-isotonic aerosols have the capacity to grow (if hypertonic) or shrink (if hypotonic) during their passage through the respiratory tract. The regional deposition of a hyper- and hypo- tonic aerosol of the same initial droplet size could therefore be different if growth or shrinkage takes place before deposition

has occurred. The deposition patterns of two isotonic aerosols of sizes similar to the range possible after equilibration of the hypertonic (4.5% saline) and hypotonic (0.3% saline) aerosols in the respiratory tract were assessed. The breathing pattern during aerosol inhalation was monitored and reproduced on both occasions with the aid of a microcomputer.

Three-dimensional gamma scintigraphic techniques were found to provide the most sensitive method of detecting differences in regional deposition.

Differences in the deposition patterns of hypertonic and hypotonic aerosols of the same initial size were found in normal subjects, but they were not as great as expected if rapid complete equilibration of the droplets before deposition is assumed. In particular, tracheal deposition was greater with the hypertonic aerosol. Hyper- and iso- tonic aerosols of the same initial size also deposited with different patterns in asthmatic subjects. The effects were due to a combination of hygroscopic growth, bronchoconstriction during aerosol inhalation and the baseline lung function of the subjects.

Chapter 1

Introduction

1. Background

Deposition mechanisms and factors effecting deposition

The factors that effect the regional and total deposition of aerosols in the lungs can be divided into three areas: physical, physiological and anatomical.

A] Physical factors

The physical factors that govern the behaviour of airborne particles were first described by physicists (Findeisen 1935; Landahl 1950; Fuchs 1964). The forces that act on an airborne particle depend on its size. Small particles of a size in the order of magnitude or less than the mean free path (0.1 μm) of the gas molecules in which they are suspended, receive energy from collision with individual molecules. The forces acting on the particle are therefore of a diffusive nature. The motion is random because the particles are too small to be significantly affected by gravitational forces. Deposition of these particles is dependent on time and the distance they must travel to meet a surface, so diffusional deposition occurs most readily in the smaller airways where residence

time is high (Landahl 1950) and diffusion distance is small.

Larger particles, greater than 0.5μm in diameter, are acted upon by two opposing forces, gravity and the resistance of the air to relative motion, as described by Stokes' Law, such that they reach a steady velocity when these two forces balance:

So, a spherical particle will have a constant terminal settling velocity V,

$$V \propto D^2 \rho/\nu$$

ν = viscosity of the air

ρ = density of the particle

D = particle diameter

V is reached typically in 10^{-2} seconds (Fuchs 1964).

Therefore in air, with a constant ν value, deposition occurs in relation to $D^2\rho$. The aerodynamic diameter (D_a) of a spherical particle is described by $\sqrt{(D^2\rho)}$ (Fuchs 1964), so for a sphere of unit density, the geometric diameter is equal to the aerodynamic diameter. The definition of D_a is "the diameter of a unit density sphere which would have the same terminal sedimentation velocity as the particle in question". This makes the aerodynamic diameter a useful descriptor, since it can be measured directly without knowing the density, geometric size or shape of

the particles being sized.

Sedimentational deposition is therefore increased with terminal settling velocity which in turn depends on the diameter and density of the particle. The distance travelled increases with time, so prolonged residence time increases the probability of sedimentational deposition.

As the aerosol stream is deflected during passage through the respiratory tract, the inertia of an aerosol particle must be overcome before it can follow the direction of flow. The inertia of a particle is the product of its mass and velocity, so larger particles will tend to resist the change in direction of the aerosol stream and deposit by impaction. The probability of impaction is related to the Stokes' (Stk) number (Brain & Valberg 1979):

$Stk = D^2\rho v/18\nu R$

v = average velocity

R = radius of tube

Impaction therefore occurs in regions where the aerosol stream changes direction, such as bifurcations. It is also more likely for large particles with high velocity and in small airways. Clearly, impaction (through Stk) is also dependent upon the product $D^2\rho = (D_a)^2$ for a sphere. However, impaction also increases with

increasing particle velocity.

Other mechanisms of deposition include electrostatic deposition. Particles or droplets that carry a charge are able to induce a charge of the opposite sign on the surface of the airway due to its conducting covering. The force of attraction will therefore enhance deposition of the particle when it comes close to the airway wall. These effects are difficult to measure (Brain & Valberg 1979) and they have only been shown with highly charged particles (Brain & Valberg 1979; Melandri et al, 1977).

Particles will always deposit as they come close enough to the surface of an airway, this mechanism is termed interception, but the number will be small as deposition will only occur within a particle diameters' width of the airway wall. For fibres, however, interception becomes important as the fibre's long axis and airway attains similar dimensions (Harris 1976).

In considering aqueous aerosol droplets, with a spherical shape and density often close to unity, the major determinants of deposition are aerodynamic diameter and velocity. The most important mechanisms of deposition may be classified as time and velocity dependent. Time dependent mechanisms include diffusion and sedimentation, where the average time taken to travel to the airway wall is finite. Inertial impaction, however, is a velocity dependent mechanism, where for a given

particle in air, its probability of impaction at a particular bifurcation is directly related to its velocity.

B] Physiological factors.

The physical behaviour of aerosol particles may be used to conceptually and mathematically (Lippmann et al, 1980) predict the effect of breathing pattern on total and regional deposition. Deposition by diffusion predominates in the small airways and alveoli and is enhanced by long residence times, so a long inspiratory pause or breath-holding time will maximise deposition of particles small enough to be affected by this mechanism (< 0.5μm, Byron 1986). Larger particles are effected by gravity, and settling time will be fast if the particles have a short distance to travel. Inspiratory pause and breath-holding time will, therefore, also increase sedimentational deposition in the small airways. Deposition in larger airways is limited to sedimentation of larger droplets and inertial impaction. The inspired airstream has a high velocity on entry into the trachea, but as the flow is divided at airway bifurcations, the velocity falls. Inhalation velocity, or flow rate will therefore be the most critical factor in deposition by inertial impaction (Newman 1984). Particles escaping impaction in the more proximal airways will then sediment as the velocity declines.

For a particular inspiratory flow rate tidal volume will control the time of respiration. Deep, slow breathing will therefore increase residence time and

peripheral deposition will be enhanced.

C] Anatomical factors

Deposition depends on lung morphometry (Yu et al, 1979) and changes brought about to the dimensions of the airways whether structural (eg. airway damage) or non structural (secretions), permanent (such as fibrosis) or temporary (bronchoconstriction).

The anatomical factors influencing deposition include the airway branching angles, radii of specific airway generations, and length and volume dimensions of regions and airways (Yu et al, 1979). Landahl (1963) has developed expressions for the probability of deposition by diffusion, sedimentation and impaction which depend on these anatomical factors. Mathematical predictions of regional deposition probabilities will therefore require a model of the lungs, the one most often used is that quoted by Weibel (1963).

Alterations to the dimensions of the respiratory tract are present in many disease states, and since therapeutic and diagnostic aerosols are delivered under these circumstances, much work has been undertaken to evaluate the effects of disease on regional and total deposition (Goldberg and Lourenco 1973; Dolovich et al, 1976) and on the therapeutic effects of the aerosols.

The diameter of an airway is an important determinant of deposition probability, as it affects impaction, sedimentation and diffusion. Many diseases of the lungs reduce airway diameter by a number of mechanisms such as bronchoconstriction, oedema and excess mucus. Such dimensional changes within the lung will have important influences on aerosol deposition. A number of studies have shown that deposition in more proximal airways is enhanced by bronchoconstriction as determined by FEV_1 (Laube et al, 1986; Agnew et al, 1981; Pavia et al, 1977). There is some evidence that local obstructions cause enhanced inertial deposition downstream of the blockage by increasing turbulence and linear airflow velocities (Itoh et al, 1976). This may account for patchy hot spots seen in chronic bronchitis patients (Hayes 1980; Greening et al, 1980) and may be a consequence of local mucus plugs (Agnew 1984) or uneven airway narrowing. Radioaerosol techniques have been shown to be sensitive to changes in airway dimensions in smokers that lung function techniques such as spirometry are unable to detect (Dolovich et al, 1976), other studies have used different indices of deposition pattern such as skew and kurtosis from analysis of aerosol deposition images (Garrard et al, 1981) or a distribution index (Agnew et al, 1982a), both of which found good correlation between deposition pattern and non-radioaerosol indices of small airways function.

Small alterations in airway dimensions can therefore dramatically effect the deposition probabilities of aerosol particles by deposition mechanisms already

described. Mathematical modelling of deposition in obstructed airways predicts similar effects (Agnew 1982).

1.2. Hygroscopic Growth

A hygroscopic substance is one that tends to absorb moisture from an unsaturated environment. A particle of such a substance, suspended in an atmosphere of high humidity, will therefore attract water vapour and grow in size. A sudden phase transition from dry particle to a solution droplet may occur when the relative humidity exceeds that of the saturated solution of the solute (deliquescence point). A droplet containing solutes is also hygroscopic because the vapour pressure of the droplet is reduced by the presence of solutes according to Raoults' Law for ideal solutions:

$$P = a_w P_o$$

a_w = water activity as mole fraction

P_o = saturation vapour pressure

The droplet will therefore continue to grow and the vapour pressure of the droplet will increase as the concentration of solutes fall. The droplet no longer grows in size when there is an equilibrium between the vapour pressure of the droplet and its immediate surroundings. For a droplet suspended in air, this

point will be when the water vapour pressures of the droplet and air are equal. Small droplets (<0.1 μm) suspended in air exhibit an enhanced vapour pressure due to their high curvature. This effect was described by Kelvin (Kelvin 1870) and expressed as the Kelvin equation (Findeisen 1935). Therefore, small droplets of dilute solutions can have a vapour pressure exceeding that of larger droplets and will preferentially evaporate. This effect can usually be neglected for most clinically used aerosol with droplets greater than 2μm (Gonda et al, 1982).

The majority of aerosol particles used clinically, and many environmental pollutant aerosols, whether solids, liquids or solutions, are hygroscopic in nature. This fact has lead to the consideration of the effects of hygroscopic growth on deposition patterns in the lungs (Morrow 1986).

The majority of work undertaken has been in the theoretical prediction of hygroscopic growth in the lungs with the aid of *in vitro* data on droplet growth and mathematical models of heat and water transport to and from particles travelling in the respiratory tract (Ferron 1977). This data has then been applied to models of deposition probability in the lungs during inspiration to arrive at a theoretical assessment of the effect of growth or shrinkage on regional mass deposition. Evidence that hygroscopic growth of particles is an important determinant of regional deposition comes from interrelated areas of study:

Physical	Physiological
1. The effect of ambient relative humidity (RH) and temperature (T) on the equilibrium size of the particles.	The RH and T profile within the respiratory tract.
2. The rate of particle growth or shrinkage.	The residence time in each longitudinal segment of the airways.
3. The aerodynamic size of particle at any one time in relation to its position in the respiratory tract.	The deposition probability in each longitudinal segment of the particles as a function of size.

Growth and shrinkage of particles as a function of relative humidity and temperature.

Evaporation and condensation growth theory originates from Fick, whose laws can be applied to vapour diffusion from a droplet, and Maxwell (1890) who gave expressions for heat transfer. The growth of NaCl particles with increasing RH was shown by Covert and Frank (1980). NaCl shows a hysteresis effect, where no growth occurs until an RH of 75% is reached. The equilibrium diameter then starts to rise sharply as the RH approaches 100% (Figure 1).

Figure 1. The ratio of the equilibrium droplet size (D) to the initial droplet size (D_o) as a function of environmental humidity. (Adapted from Covert and Frank 1980).

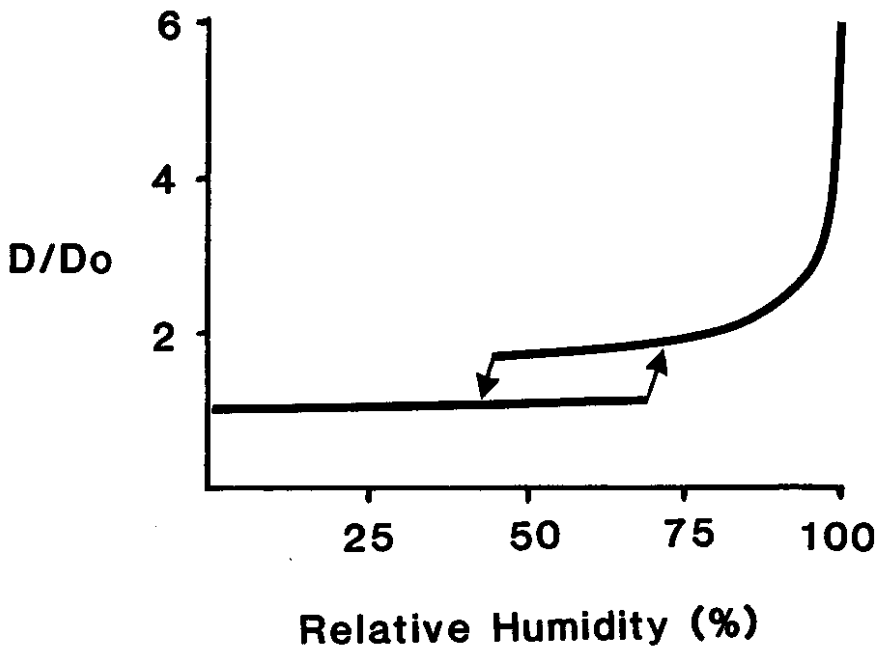

The effects of hygroscopic growth can therefore be seen to be highly dependent on RH when close to saturation. Small miscalculations of RH in the large airways will thus lead to poor predictions of deposition in these airways. The temperature is an important component in calculations of hygroscopic growth because of the relationship between particle (droplet) temperature on inhalation and that of the respiratory tract. Since the transfer of water to or from a surface involves heat, temperature and humidity need to be considered together.

RH and temperature profile of the respiratory tract

The warm, humid environment of the respiratory tract provides an ideal environment for hygroscopic growth to take place. The meaningful prediction of dynamic droplet growth or shrinkage, is reliant on a working knowledge of the temperature and humidity profile of the respiratory tract. Studies of the regional temperature and relative humidity of the airways have been limited by techniques. Early studies indicated that the expired air was completely saturated with water, from which it was concluded that the alveolar air was similarly saturated (Osborne 1913), this was however contended, since the water covering the respiratory surfaces is 'impure' (Burch 1945).

The RH of alveolar air can be calculated from the deep lung temperature (Edwards et al, 1963) and the saturated vapour pressure of the airway fluid, assumed to be isoosmotic with blood plasma (Ferron 1977; Ferron and Hornick

1984). The RH of more proximal airways during inspiration and expiration has proven difficult to measure. Ferron et al (1984) calculated RH profiles in the lungs for nose breathing by solving equations for water vapour and heat transfer simultaneously. They found that the RH reaches a maximum of 99.8% during inhalation which occurs near the tracheal bifurcation, and then falls to 99.5% over the next 10 generations. The fact that the diffusivity of water molecules is approximately 10% greater than that of heat (Ferron et al, 1981) means that air of high initial RH is likely to be supersaturated near the carina. This may be important for the consideration of hygroscopic growth, because if the RH in the trachea is high, growth will be rapid before reaching the carina. Another factor that was found to be important in Ferron's study was the effect of the non-laminar airflow pattern that exists in the first few generations. He found that by taking this into account, the thermal and vapour transport was increased by a factor of 5 (Ferron et al, 1981) and a closer approximation to experimental data was found.

A commonly used profile assumes an RH of 90% at the mouth with a 1% increase per generation to 99%, then 99.5% throughout the rest of the respiratory tract (Martonen et al, 1985; Martonen and Clarke 1983). Growth is then calculated in a stepwise manner in each airway generation (in some studies it is assumed that they reach equilibrium before moving on to the next generation).

The rate of particle growth or shrinkage.

For growth or evaporation to alter regional deposition, it must at least partially occur on a time scale similar to that of the respiratory cycle. The growth or shrinkage rate in an atmosphere of constant temperature and humidity depends on the particle size, concentration and solute composition. Growth rate curves under these circumstances can be derived from laws governing the physicochemical behaviour of the salt solution and heat and mass balance (Mercer 1973; Crider et al, 1956; Pruppacher and Klett 1978; Wagner 1982).

Ferron gives condensation growth curves for various salts, assuming ideal solution behaviour, as a function of the residence time in the lungs (Ferron 1977) with an assumed constant temperature and RH of 37°C and 99.5% respectively. The growth of sodium chloride particles starts abruptly and increase rapidly, slowing towards equilibrium. With particles of other salts there is an initial delay, then a rapid growth until there is again a slowing towards equilibrium, producing a sigmoid shape (Figure 2).

Ferron showed that the time for shrinkage to equilibrium of droplets of low sodium chloride solutions can be estimated by the stabilisation times of pure water droplets. For a 4μm droplet, for example, this will be approximately 4 seconds at an RH of 99.5%.

Figure 2. The ratio of the equilibrium droplet size (D) to the initial droplet size (D_0) as a function of time. (Adapted from Ferron 1988b).

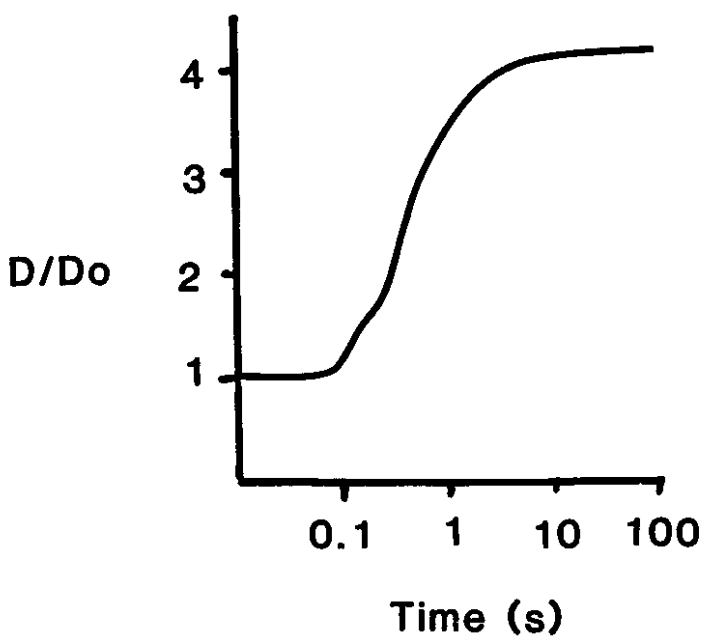

Ferron also considered initially dry NaCl particles growing in an atmosphere of 99.5% RH and found that a 1μm particle of sodium chloride reached 4.1μm in 2 seconds and after one second it has reached 80% of its equilibrium diameter (Ferron et al, 1988b).

The RH and temperature, however, rises throughout the respiratory tract as already discussed and since growth rate is exquisitely sensitive to RH, attempts have been made to introduce this into theoretical growth curves. Martonen and Clarke (1983) use an expression for the aerodynamic diameter of a particle at each airway generation, calculated from the combination of growth and position in the respiratory tract with time. However, they assume equilibrium is reached in each generation. A changing humidity in the respiratory tract means that at each segment (however defined - usually by generation number) the droplet undergoes a different growth curve, related to the size and concentration on entry and the particular RH and temperature of that segment. Martonen's assumption that the droplets reach equilibrium at each generation before moving to the next may be incorrect, and therefore probably overestimate the effects of growth.

The effects of hygroscopic growth and shrinkage on regional deposition.

Once derived, mathematical models of hygroscopic growth and aerosol deposition may be applied to various aerosol inhalation conditions to predict the effects of inhaling hygroscopic aerosols on total and regional deposition. The initial size

and composition of the inhaled particles are the most important factors that determine the site of deposition. Ferron (1977) applied the effect of growth on the Task Group on Lung Dynamics regional deposition model for non-hygroscopic aerosols and found that the total and regional particle deposition fraction was increased for all sizes above 0.5μm, reflecting the greater deposition probabilities as the droplet size increased during growth.

The altered deposition of hygroscopic aerosols is important in both environmental aerosol toxicology and therapeutics because it relates to the changes in the local burden of therapeutic, diagnostic or pollutant substances and responses of the lungs.

More recently, Ferron (1984) has calculated the deposition as % of the inhaled particle concentration of dry NaCl particles assuming a) no growth, b) hygroscopic growth according to the RH profile described in a previous section and c) assuming an RH of 99.5% upon inhalation. The greatest differences in deposition were found for 1μm particles having a 3 fold increase in both TB and P deposition, while 5μm particles had an increased TB deposition by a factor of just more than 2 and decreased P by a factor just less than 2.

Breathing pattern also affects the magnitude of hygroscopic growth. (Ferron et al, 1984) showed that reducing tidal volume reduces the effect of growth on

deposition, especially in the pulmonary regions, because of shorter residence times. Anselm et al (1986) measured the droplet size on expiration of initially dry 0.5μm NaCl particles. The aerosol bolus was inhaled to different lung depths to assess the effect of residence time on growth. The droplets exhaled were up to 2.6μm (5.5 times the initial particle size), indicating that growth had occurred. The deeper the aerosol was inhaled (longer residence time) the greater the growth factor.

Implications of droplet growth

The first studies on hygroscopic aerosols were concerned with atmospheric particles (Milburn et al, 1957; Fuchs 1959; Landahl 1963; Findeisen 1935) and later with atmospheric pollutants such as phosphoric (Martonen and Clarke 1983) and sulphuric acid droplets (Amdur et al, 1952; Martonen et al, 1985). As aerosol therapy became more popular, the models of hygroscopic growth were applied to therapeutic aerosols (Byron et al, 1977; Persons et al, 1987).

The majority of studies of hygroscopic growth have been concerned with the inhalation of dry solute particles. Medicinal aerosols are, however, often derived from nebulisers and are delivered as droplets. On attainment of equilibrium size deep within the lungs, droplets will approach a solute concentration giving the same vapour pressure as the fluid lining the lungs, assumed to be isotonic with plasma (RH = 99.5%). The inhalation of hypertonic solutions means that the

growth factor may be no more than 2 or 3.

There is mathematical evidence that small hygroscopic particles of the atmospheric type are capable of hygroscopic growth within the respiratory tract of a sufficient degree to affect the total and regional deposition (Nair and Vohra 1975). The application to therapeutic nebulised aerosols has, however, not been studied to a great extent.

The only comprehensive theoretical study of hygroscopic growth of nebulised aqueous aerosols was made by Persons et al (1987a) who developed a model for mouth inhalation of aqueous sodium chloride aerosols. The model was compared with data derived from other theoretical predictions and experimental deposition data. The model uses growth theory similar to Ferron (1977) and the results compare favourably with his. Figure 3 is reproduced from Persons et al (1987b) and shows the effect of hygroscopic growth and evaporation after inhaling saline droplets with initial concentrations of 3.5% (hypertonic) and 0.45% (hypotonic) saline. Medical aerosols are usually in the range of 2-5 μm so for an initial droplet size in this range the fractional deposition can be significantly altered between tonicities of 3.5 and 0.45% saline (Figure 3).

Figure 3. The fractional deposition of hypertonic (3.5 % NaCl, unbroken lines) and hypotonic (0.35 % NaCl, broken lines) aerosols as a function of mass median diameter (MMD). T = Total, T-B = Tracheobronchial and A = Alveolar deposition. (Adapted from Persons et al, 1987b).

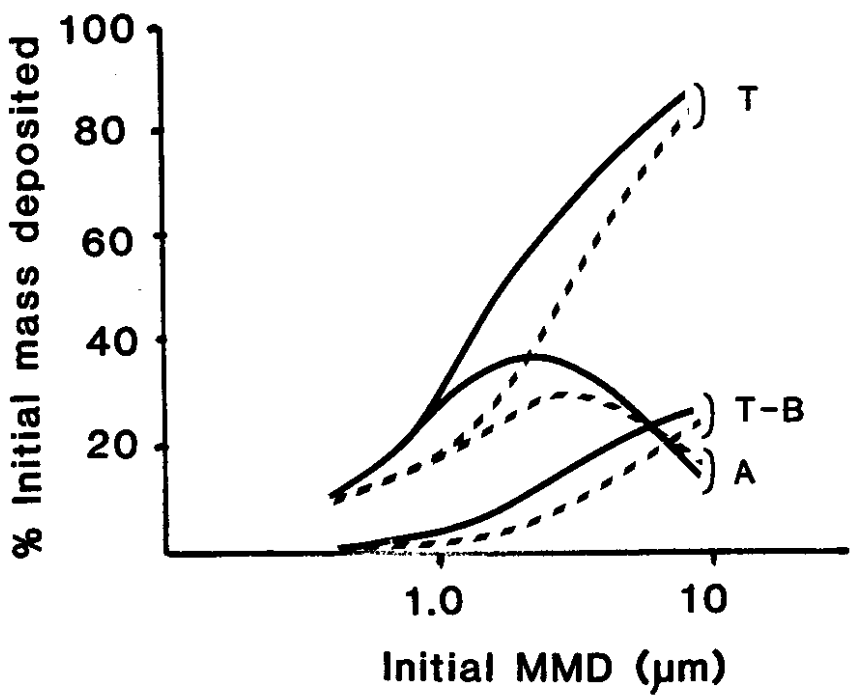

The majority of evidence of the occurrence and effects of hygroscopic growth is theoretical and often, only single droplets within the respiratory tract are considered. In fact, little experimental data exists, particularly on the effects of droplet solute concentration on regional deposition of aqueous aerosols in vivo.

1.3. Nebulised aerosols in asthma diagnosis and therapy

The fact that nebulised non-isotonic aerosols are able to cause airway narrowing in subjects with lung disease was first demonstrated by Abernathy (1968) which was later followed up by Allegra et al (1974, 1975). In 1981, it was shown that asthmatics but not normals were hypersensitive to non-isotonic aerosols, the degree of airway narrowing being increased by greater departures of the nebuliser solution from isotonicity (Schoeffel et al, 1981).

Of the challenge agents now used to aid the diagnosis of asthma, non-isotonic aerosols have the advantage that they cause mediator release, they therefore simulate natural challenge agents such as allergens and exercise more closely than pharmacological agents (Smith and Anderson 1986). They are becoming more popular as a result. The hygroscopic nature of these aerosols, together with evidence of the importance of the large airways as their site of action (Anderson et al, 1989) makes an understanding of the effects of tonicity on regional deposition a necessity.

1.4. Overall aims

The aims of this thesis are i) to determine the factors that govern the physical characteristics of aqueous aerosol droplets generated by nebulisers for use in therapy and diagnosis and ii) to study the effects of hygroscopic growth or shrinkage of non-isotonic aerosols, and the airway narrowing they provoke in asthmatic subjects, on regional deposition.

The work described in the first five chapters is concerned with the detailed characterisation of jet and ultrasonically nebulised aerosols to gain a better understanding of the specific factors involved in controlling the physical dimensions and composition of aqueous aerosol droplets.

The use of nebulisers in therapy and diagnosis is widespread due to the ease with which physiologically active agents may be administered to the lungs. In Chapters 2, 3 and 4 the beneficial and unwanted characteristics of aerosol droplets are identified. Thus, by assessing the operation of nebuliser systems currently in use, the medical community will be able to prescribe and administer therapeutic and diagnostic agents to the lungs more effectively. The assessment of aerosol delivery systems and the detailed consideration of the water and solute dynamics occurring during aerosol nebulisation and inhalation are also performed in Chapters 3 and 5.

The comparison of medications or diagnostic tests that involve aerosol delivery to the lungs requires a knowledge of the total and often regional deposition of the aerosols in question. A number of techniques have therefore been developed to measure delivery to the lungs. The most highly developed has been gamma scintigraphic techniques that enable quantitation of the aerosol deposition by non-invasive methods involving the use of radio-isotopes. The three dimensional nature of the lungs limits the specificity of the two dimensional data obtained by these methods. The aim in Chapter 7 was therefore to develop more sensitive methods of determining regional deposition with the three dimensional imaging now available. However, before aerosol inhalation imaging studies can be performed, a suitable system for monitoring and controlling the breathing pattern during aerosol inhalation must be found so that aerosols can be inhaled on more than one occasion with the same breathing pattern (Chapter 6).

Ultrasonically nebulised non-isotonic aerosols have become popular as an aid in the diagnosis of asthma (Smith and Anderson 1989), but the droplets generated have the potential to change in size while passing through the respiratory tract and alter the deposition pattern depending on their initial tonicity. The bronchoconstriction they provoke may also alter the total delivery to certain regions of the respiratory tract. These effects were, therefore, also studied with the help of normal and asthmatic volunteers in Chapter 8.

Chapter 2

A rapid method for the evaluation of diagnostic radioaerosol delivery systems.

2.1. Introduction

Radioaerosol ventilation agents such as those containing ^{99m}Tc-DTPA are used for the assessment of regional ventilation and alveolar clearance. They are produced and delivered to patients via radioaerosol delivery systems (ADS) consisting of jet nebulisers and associated tubing. To be effective, these systems must produce a uniform peripheral aerosol deposition while minimising a) the radiation dose to the patient, b) the radiation exposure to personnel administering the dose and c) the cost of the procedure. It is therefore important to reduce as much as possible both the duration of administration and the unusable portion of the radioactive aerosol, the latter including that depositing in the delivery tubing, mouth, oropharynx and central airways and that exhaled by the patient. Regional deposition of aerosols is determined by their physical characteristics, such as size distribution and droplet composition together with patient parameters, such as inhalation flow rate and severity of lung disease; the variability of all these has complicated previous clinical assessments of ADS (Hayes et al, 1979; Foulds and Smithuis 1983; Trajan et al, 1984; Alderson et al, 1984; Matthys and Kohler 1985; Wollmer et al, 1985).

Nuclear medicine departments are responsible for the choice of ADS and the quality control of radioaerosols. We therefore wished to define meaningful parameters for the assessment of the quality of radioaerosols used for ventilation studies, and to develop rapid experimental methods to measure those parameters, using, as far as possible, equipment already available in a typical nuclear medicine department (Borham et al, 1986).

The droplet size distribution of ADS is known to depend on operating parameters (Mercer et al, 1965; Ferron et al, 1976; Ryan et al, 1981; Clay et al, 1983; Sterk et al, 1984) and also on environmental conditions (Porstendorfer et al, 1977). In many ADS, ambient dilution air is inhaled along with the aerosol. A potential therefore exists for the humidity of the dilution air to affect the aerosol droplet size and this was also investigated.

2.2. Materials and Methods

Droplet size determination. Particle size distribution, expressed as the mass median aerodynamiç diameter (MMAD) and the geometric standard deviation (σg) was measured using a seven stage cascade impactor (DC16, Delron, Columbus, Ohio, USA). ^{99m}-pertechnetate in normal saline was added to the nebuliser solution to an approximate concentration of 100 MBq/ml. The aerosol was generated from the nebuliser using compressed oxygen. The dilution air required to make up a fixed flow of 12.5 l/min through the impactor was humidified or dried by bubbling through water or a saturated solution of lithium chloride, respectively.

After generation of the aerosol for approximately 60 s, the impactor slides, precoated with silicone fluid (Dow Corning 200/60 000 cs, Midland, Michigan, USA) were removed and simultaneously counted on a large field of view gamma camera (GE 400AT, Milwaukee, Wisconsin, USA) fitted with a low energy, all purpose, collimator. A 5 min image was recorded by an on line computer (DEC PDP11, Maynard, MA, USA). Regions of interest were drawn around the image of each slide and total counts within each were recorded. These values, corrected for background and expressed as a percentage of the total count, together with the previous impactor calibration results for particles and droplets (Gonda et al, 1982) were analysed by a least squares program to determine the MMAD and σg of the aerosol sample. Dead time correction was not necessary at the count rate observed.

The method was validated by placing small volumes of 100 MBq/ml ^{99m}Tc-pertechnetate onto seven coated impactor slides from a pipette (Phipps et al, 1986). The activity in the pipette was measured by a dose calibrator (Capintec Inc. New Jersey, USA) before and after application. The slides were counted for 5 mins on the gamma camera 5 times over a period of 48 h and the results pooled to test for linearity. The activity values ranged from 14.91 to 0.00524 MBq per slide. The correlation equation produced was then used to convert impactor slide counts into activity values. In the experimental runs, the highest activity on any one slide was approximately 6 MBq and 0.1% of the lowest total activity was still greater than the lowest point on the calibration.

* Pictures of these nebulisers are shown in the addendum at the back of this thesis.

Aerosol delivery system characterisation. Droplet size distribution measurements as described above were carried out in triplicate on four commercially available ADS; Ultravent (Mallinckrodt Inc., St Louis, USA), Venticis (Cis UK Ltd., North Finchley, London), Mistyneb (Airlife Inc., Montclair, California USA) and Cadema (Cadema Medical Products Inc., Middletown, N.Y., USA). Each system was set as for patient use with the mouthpiece of the delivery tubing connected to the impactor. The aerosol was generated by compressed oxygen at the manufacturer's recommended flow rate (10 l/min in each case) and supplemented with humid dilution air.

The results from the droplet size analysis were used to calculate both the mass fraction of droplets in the respirable size range and the total activity caught in the impactor per min. The respirable size range was taken to be the cumulative activity below stage three of the cascade impactor [50% cutoff diameter = 3.3μm (Gonda et al, 1982)]. All results were corrected for decay and to an original nebuliser concentration of 100 MBq/ml.

The effective delivery (ED) of each ADS was calculated as the amount of activity leaving the mouth piece in MBq/min contained in droplets in the respirable size range. The wasted delivery (WD) was defined as the amount of activity leaving the mouthpiece outside the respirable range, i.e., the amount of activity in droplets depositing on or above stage three of the impactor. The results were expressed as the mean ± standard deviation of three determinations.

Effect of dilution air humidity on the droplet size distribution of the Cadema ADS. The droplet size distribution was measured on the Cadema ADS as described above, with dilution air comprising 4.5 l/min and aerosol 8.0 l/min of the 12.5 l/min total flow through the impactor. Several determinations were carried out on three nebulisers using humid and dry dilution air. The MMAD and σg values for dry and humid dilution air were then compared with the use of a Mann-Whitney *U* test and the standard deviations with an *F*-test.

2.3. Results

The pooled data from the gamma camera calibration was used to plot counts (*Y* in units of cpm) against activity (*X* in MBq). The equation of the regression line produced was

$$Y = 9492(\pm 1.8\%)\, X + 91.4(\pm 747\%) \qquad (1)$$

where standard deviation in % is given in parentheses, n=35 (pooled results of 7 slides at 5 times) and $r^2 = 0.9997$.

The regression equation (1) shows that a 25 % error is found at a count rate of 4×10^3 cpm. From experience, it was noted that up to 10% of the total cpm could vary by as much as 25% without changing the calculated values of MMAD and σg to one decimal place. Therefore a total cpm of over 4×10^4 is required for suitable precision of the method.

Values of activity were calculated from impactor slide counts (A in units of cpm) using Eq. (1), to give the ED and WD values shown in Table 1 from:

$$ED = (A/T_g) \times F \qquad (2)$$

and

$$WD = (A/T_g) \times (1-F) \qquad (3)$$

where

T_g = generation time (min).

F = Fraction depositing below stage three.

The effect of dilution air humidity on the MMAD of droplets produced by the three Cadema ADS is shown in Table 2. The mean MMAD of the pooled results for humid dilution air is 2.55 ± 0.1 μm (SD) where n = 22, indicating a low inter- and intra-nebuliser variability. Dry dilution air reduces the pooled mean MMAD by 22% ($p<0.01$) and increases the variability [mean = 1.99 ± 0.32 μm (SD), n = 17]. The standard deviations of the dry dilution air MMAD and σg results were both significantly greater ($P<0.01$) than those of humid dilution air.

2.4. Discussion

The effect of droplet size on the regional deposition of aerosols in the human respiratory tract has now been well documented by both *in vivo* determination and mathematical models (see reviews, eg., Ferron et al, 1985; Stahlhofen 1984).

Table 1. ED, WD and aerosol characteristics of four ADS.

	MMAD (μm)	σg	(F × 100) % below Stage 3	Mean ED[a] MBq/min	Mean WD[a] MBq/min
Ultravent	1.1 (0.1)	1.7 (0.1)	99.2 (0.3)	6.44 (0.46)	0.05 (0.02)
Venticis[b,c]	1.0 (0.1)	1.8 (0.1)	99.8 (0.1)	8.06 (0.86)	0.02 (0.01)
Mistyneb	3.7 (0.1)	1.5 (0.1)	42.3 (0.8)	11.3 (0.2)	15.4 (0.5)
Cadema	2.3 (0.1)	1.4 (0.1)	92.0 (3.1)	14.0 (0.8)	1.24 (0.61)

Values expressed as mean of three results (standard deviation)

[a]Corrected for decay and activity concentration in the nebuliser to 100 MBq/ml

[b]The venticis aerosol delivery system includes a settling bag which fills during patient use but not during particle size determination due to the continuous negative pressure supplied to the system

[c]The first run on the venticis used some of the output to soak the ball bearing filled filter system

MMAD = Mass median aerodynamic diameter

σg = Geometric standard deviation

RH = Relative humidity

Particles of mass median aerodynamic diameter between 3 and 1 μm, at resting inhalation flow rates, are of the optimum size for pulmonary deposition. Larger particles tend to deposit in the central airways or mouth, while particles in the region of 0.5 μm are exhaled. A better estimation of the effective aerosol delivery may therefore be obtained by excluding those droplets likely to be exhaled. We chose to disregard the exhaled portion of the aerosol in defining our respirable range but droplets of around 0.5μm may be easily excluded from the results. As the droplet size decreases below 0.5μm, the alveolar deposition increases, starting from a minimum around 10% (Ferron et al, 1985). However, the fraction of radioactivity carried by such small droplets is low in ADS used clinically at present, as shown by our results.

Marked differences in the performance of different ADS are shown in Table 1. The Venticis and Ultravent produce droplets all within the respirable size range but their output is low, requiring either a high nebuliser activity concentration or a long inhalation time. The Venticis incorporates a settling bag as part of the delivery tubing which failed to fill during the droplet size analysis, due to the constant negative pressure applied. If some of the larger droplets settle in this bag the MMAD will decrease (possibly increasing the proportion exhaled). The output will also decrease as a result, but this may be offset by the storage capacity of the bag during exhalation. The Mistyneb nebuliser has a high output of droplets in the respirable range but it produces an even larger portion that will deposit outside the pulmonary region. The

Cadema nebuliser, however, has optimum operating characteristics with a high delivery rate and little waste of aerosol.

The aerosol samples for the droplet size measurements were taken at the mouthpiece of the delivery system which did not take into account the amount of aerosol depositing in any unshielded tubing, an important hazard consideration. The amount of aerosol caught in the tubing would depend on droplet size, flow rate and tubing geometry so ADS with high WD values and tortuous tubing are more likely to deposit aerosol before the mouthpiece.

The droplet size distribution and output from a nebuliser may change markedly with generation flow rate (Mercer 1973; Ryan et al, 1981; Clay et al, 1983) and this will in turn lead to different D and WD values. It may thus be possible to modify the effectiveness of an ADS by changing its operating flow rate.

Table 2 shows the results of changing the dilution air humidity passing through the Cadema ADS. Dilution air mixes with the aerosol at the exit from the nebuliser in all of the systems tested. Dry dilution air caused the droplets to evaporate and probably concentrate, and in so doing the droplet size was reduced by 22% and became more variable. During inhalation of diagnostic radioaerosols, patients require dilution air to supplement the 8 or 10 l/min flowing through the nebuliser with a flow rate often far in excess of the aerosol flow.

Table 2. Effect of ambient dilution air humidity on MMAD and σg of droplets produced by the Cadema ADS.

Nebuliser No.	Humid dilution air 88 - 100 % RH			Dry dilution air 12 - 17 % RH		
	No of repeats	MMAD (μm)	σg	No of repeats	MMAD (μm)	σg
1	5	2.64 (0.04)	1.40 (0.04)	5	2.41 (0.08)	1.37 (0.03)
2	8	2.51 (0.07)	1.36 (0.04)	8	1.77 (0.15)	1.62 (0.11)
3	9	2.53 (0.13)	1.34 (0.02)	4	1.90 (0.25)	1.55 (0.12)

Values expressed as mean (standard deviation)

MMAD = Mass median aerodynamic diameter

σg = Geometric standard deviation

ED = Effective delivery

WD = Wasted delivery

F = Fraction depositing below stage 3 (cut-off diameter 3.3µm)

The humidity of this dilution air, and the proportion of it, will effect the droplet size and the variability of the aerosol leaving the mouthpiece to a greater extent than in the reported experiments, and this may have some effect on the droplet deposition. A theoretical explanation and the practical implications of the greater sensitivity of the droplet size and σg to fluctuations of water content at a low relative humidity, is the subject of another paper. However, it is possible that the variability of the results of penetration of aerosols in the diagnosis of chronic obstructive pulmonary disease (Ruffin et al, 1981) could have been due, not to clinical variability, but to variable aerosol delivery. The pooled σg values and their variability are also increased with dry dilution air ($P<0.01$) and this too, may have an effect on the deposition of the aerosols (Gonda 1981).

The breathing pattern is also important in relation to the general deposition of the droplets. A high inspiratory flow rate will cause greater deposition of the larger droplets outside the pulmonary region by impaction, while a low flow rate will increase the pulmonary deposition of those same droplets (Agnew et al, 1985). Therefore, the respirable size ranges and hence the values of ED and WD will change with inhalation flow rate, which could be readily accommodated in new definitions of ED and WD.

Lung disease may effect the ED values by a number of mechanisms. Increased inhalation flow rate, bronchoconstriction and excessive mucus secretions may all lead to reduced pulmonary deposition of aerosol (Taplin et

al, 1977) making fine droplets preferable for imaging the alveoli.

The continuous output of the nebulisers makes it possible to estimate the total dose inhaled by the patient as half the sum of ED and WD values if expiration and inhalation times are assumed to be equal and exhaled dose ignored (with the exception of the Venticis which stores aerosol in a settling bag during expiration).

Conclusions

These results show that it is possible to characterise and compare ADS by a simple, quick *in vitro* method using readily available equipment as an aid to the evaluation of aerosol delivery systems.

The droplet sizing technique was found to be suitable precise provided the total impactor slide counts were greater than 4×10^4 cpm. The system was linear over the range 10^2 - 10^4 cpm per slide.

Environmental conditions such as ambient air humidity may have an effect on the droplet size distribution produced by some ADS.

Chapter 3

Droplets produced by medical nebulisers: some factors affecting their size and solute concentration.

3.1. Introduction

Although there is increasing evidence that metered dose inhalers alone, or with spacers, are at least as effective as nebulisers in the prophylaxis and acute treatment of asthma (Newhouse and Dolovich 1987; Jenkins et al, 1987; Turner at al, 1987), the latter continue to be used in both hospital and home treatment. The administration of antibiotics as aerosols generated by nebulisers is also becoming increasingly popular in patients with cystic fibrosis (Hodson et al, 1981; Newman et al, 1987). With the advent of AIDS, there has been much recent effort in testing nebulised pentamidine for the treatment of *Pneumocystis carinii* (Montgomery et al, 1987; Montgomery 1988). Other medications administered as nebulised aerosols include local anaesthetics (Kirkpatrick et al, 1987), adrenalin for the treatment of croup (Remington and Meakin 1986), vaccines (Sabine et al, 1984) and mucolytics (Wanner and Rao 1980).

Nebulised aerosols are also used extensively in diagnosis. The diagnosis of asthma and assessment of its severity is aided by challenge testing with inhaled

aqueous aerosols containing pharmacological agents such as histamine and methacholine (Hargreave et al, 1981), or non-isotonic aerosols (Anderson et al, 1983). This mode of administration has also proven useful in ventilation imaging as an aid in the diagnosis of pulmonary embolism (Alderson et al, 1984). In fact, it is the ease with which solutions or suspensions of therapeutic and diagnostic agents can be nebulised which makes the use of this type of aerosol so widespread.

The importance of the characterisation of nebuliser systems for clinical applications has been recognised by a number of authors (Newman et al, 1986; Newman et al, 1987; Phipps et al, 1987 [Chapter 2]; Matthys and Kohler 1985). The clinical efficacy of nebulised aerosol treatment depends primarily on the amount of active substance depositing at various sites in the respiratory tract, which in turn is dependent on the droplet size (Stahlhofen et al, 1983; Ferron et al, 1981) and output from the nebuliser as well as patient parameters such as inspiratory flow rate, respiratory tract morphology and disease state of the lungs (Ilowite et al, 1987). The wide variation in performance of nebuliser delivery systems (Newman et al, 1988; Newman et al, 1985; Sterk et al, 1984; Dahlback et al, 1986), and the lack of information provided by the manufacturers makes it likely that a failure in therapy may often be explained by poor aerosol delivery rather than a poor response to the drug therapy. An important determinant of droplet size distribution is the pressure-flow relationship of the nebuliser and the capacity of the supply of compressed air to drive the aerosol generator adequately (Newman et al,

1988; Davis 1978; Mercer et al, 1968).

It is well known that the nebuliser solution cools and concentrates during nebulisation (Davis 1978; Mercer et al, 1968), and it has been reported that the humidity of the air inhaled along with the aerosol effects droplet characteristics (Phipps et al, 1987 [Chapter 2]; Porstendorfer et al, 1977). We wished to look directly at the effects of nebuliser cooling and dilution air humidity on a) the size and b) the concentration of solutes, in the aerosol droplets generated by a number of different medical nebuliser systems.

3.2. Methods.

Nebuliser systems tested

The following products were assessed:

a) Cadema nebuliser (Cadema Medical Products Inc., Middletown, NY, USA) with compressed oxygen at 8 l/min.

b) Up-Draft nebuliser (Hudson Up-Draft Oxygen Therapy Sales Co., Temecula, CA., USA) with compressed oxygen at 8 l/min.

c) Up-Draft nebuliser with Flatus Mk.V air compressor (Maymed, Anaesthetic Supplies Pty. Ltd., Sydney, Australia. This system is equivalent to: Tote-A-Neb, Hospitak Inc., Lindenhurst, NY., USA [private communication, Mefar SRL, Italy]).

d) Up-Draft nebuliser with Aerosol-One air compressor (Medical Industries America, Desmoines, Iowa, USA).

e) Mist-O_2-Gen ultrasonic nebuliser (Model EN143A, Timeter, Penn., USA).

Flow/Pressure curves

The flow/pressure characteristics of the Aerosol-One and the Flatus air compressors were measured by directing the air flow through a rotameter (Platon Ltd., Basingstoke, Hants, UK) via a mercury manometer. The resistance to flow was produced by a needle valve on the flow meter and the resulting pressure recorded in mm of mercury. The flow rate through an Up-Draft nebuliser was also measured.

Temperature/time curves

The change in temperature of each system was measured with an oesophageal thermistor probe (YSI series 400, temperature recorder Model 46TUC, Yellow Springs Instruments Co. Inc., Yellow Springs, Ohio USA) placed in the nebuliser solution, and the temperature recorded at set times during aerosol generation until the temperature had reached a steady value (T_s). The initial volume of solution in the nebuliser was 5ml (jet nebulisers) or 200ml (ultrasonic nebuliser). The ambient temperatures varied between 23 and 24°C.

Concentration measurement

Jet nebulisers: The concentration of sodium chloride in the aerosol droplets was measured for different, constant, nebuliser solution temperatures. The lowest temperature used for each nebuliser was the value reached after running the nebuliser without heating to a steady temperature T_s, determined as described above. The nebuliser bowl, containing 5 ml normal saline, was

cooled to a nominated temperature by immersion in a cold water bath. The aerosol was then generated and the nebuliser solution temperature kept at the nominated value by immersion in a warm water bath. The temperature of the nebuliser solution was monitored with the miniature oesophageal thermistor probe. The temperature was controlled to ± 0.3 degrees during a generation time of 10 to 25 minutes and generated volume of 1 to 3 ml. The aerosol was passed via a short length of tubing (30 cm) through the last two stages of a cascade impactor (DCI6, Delron, Columbus, Ohio, USA) and collected in a small container of similar dimensions to a cascade impactor slide. The flow through the impactor stages was 12.5 l/min and the dilution air necessary to supplement the flow through the nebuliser was supplied either at ambient temperature (23 - 24 °C) and humidity (65 - 75%) or fully humidified at ambient temperature via a Douglas bag.

After collection of the aerosol droplets, the containers were re-weighed and droplets diluted with normal saline if their volume was insufficient for the determination of their solute concentration. The concentration of sodium chloride was then measured by vapour pressure osmometry (Model 1100, Knauer, Bad Homberg, W. Germany).

Ultrasonic nebuliser: The solute concentration of the aerosol droplets generated by the Mist-O_2-Gen nebuliser was measured by the above methods, except that aerosol droplets were collected in 30 second samples at set times during continuous nebulisation.

Determination of Output

The output of nebuliser solution from the jet nebuliser systems was measured by weighing after generation for different periods off time.

The output of solution from the ultrasonic nebuliser was measured by weighing the nebuliser continuously during generation. The output from the mouthpiece with a two-way valve (model 2700, Hans Rudolf Inc., Kansas, Mis., USA) in line, was also tested at various flow rates.

Droplet sizing

The droplet size of the jet nebulisers at various operating solution temperatures was measured in separate experiments. The nebuliser was cooled to a set temperature and aerosol generated as in the concentration measurements for 2 minutes. The nebuliser solution contained approximately 100 MBq/ml of $^{99m}TcO_4^-$ in normal saline. The aerosol was passed through the 7-stage cascade impactor and the coated glass impactor slides containing the deposited radioaerosol were counted on a previously calibrated gamma camera (Phipps et al, 1987 [Chapter 2]) and the droplet size distribution calculated by a least squares fit to the data (Gonda et al, 1982).

The size of the droplets produced by the ultrasonic nebuliser was measured with and without the two-way valve in line, using the same methods as above.

To test the effect of nebuliser temperature on the size of the primary droplets

produced by the Cadema and Hudson nebulisers, droplet sizing was carried out in a cold room at 7.5 °C with humid dilution air equilibrated at the same temperature.

3.3. Results

Flow / pressure curves

The flow pressure curves for the Flatus and the Aerosol-One compressors can be seen in Figure 1. The Aerosol-One was a weaker pump and the flow rate produced was lower than that of the Flatus at the same pressure. The Flatus produced a flow rate of 6.3 and the Aerosol-One 5.0 l/min through the Up-Draft nebuliser.

Temperature/time curves

The fall in temperature with time of nebulisation for each of the nebuliser/generator systems is shown in Figure 2. For the jet nebulisers, the temperature falls to a steady value T_s which is 5-6 °C below the ambient temperature at the lower flow rates of the air compressors, and 11-15 °C at 8 l/min flow rate from a gas cylinder. Most of this temperature change occurs in the first four minutes of aerosol generation.

By contrast, the ultrasonic nebuliser increases in temperature by approximately 18°C during the first 20 minutes of generation (Figure 3). The temperature change occurs over a longer time scale than in the jet nebulisers, the majority occurring within 15 mins.

Figure 1. Graph of flow vs pressure for the Aerosol-One (*squares*) and Flatus (*diamonds*) air compressors.

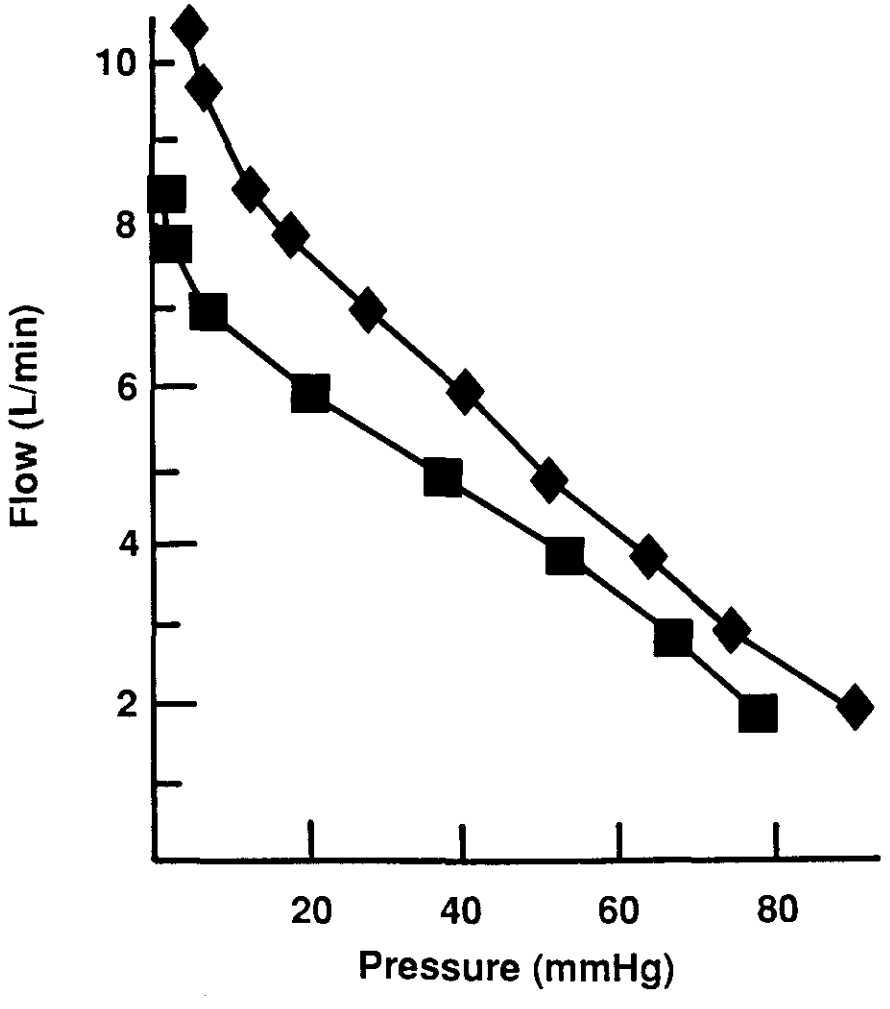

Figure 2. Graph of nebuliser solution temperature below ambient (23-24 °C) vs time of generation for the four jet nebuliser systems: Up-Draft/Aerosol-One (*squares*), Up-Draft/Flatus (*diamonds*), Cadema/compressed oxygen (*circles*) and Up-Draft/compressed oxygen (*triangles*).

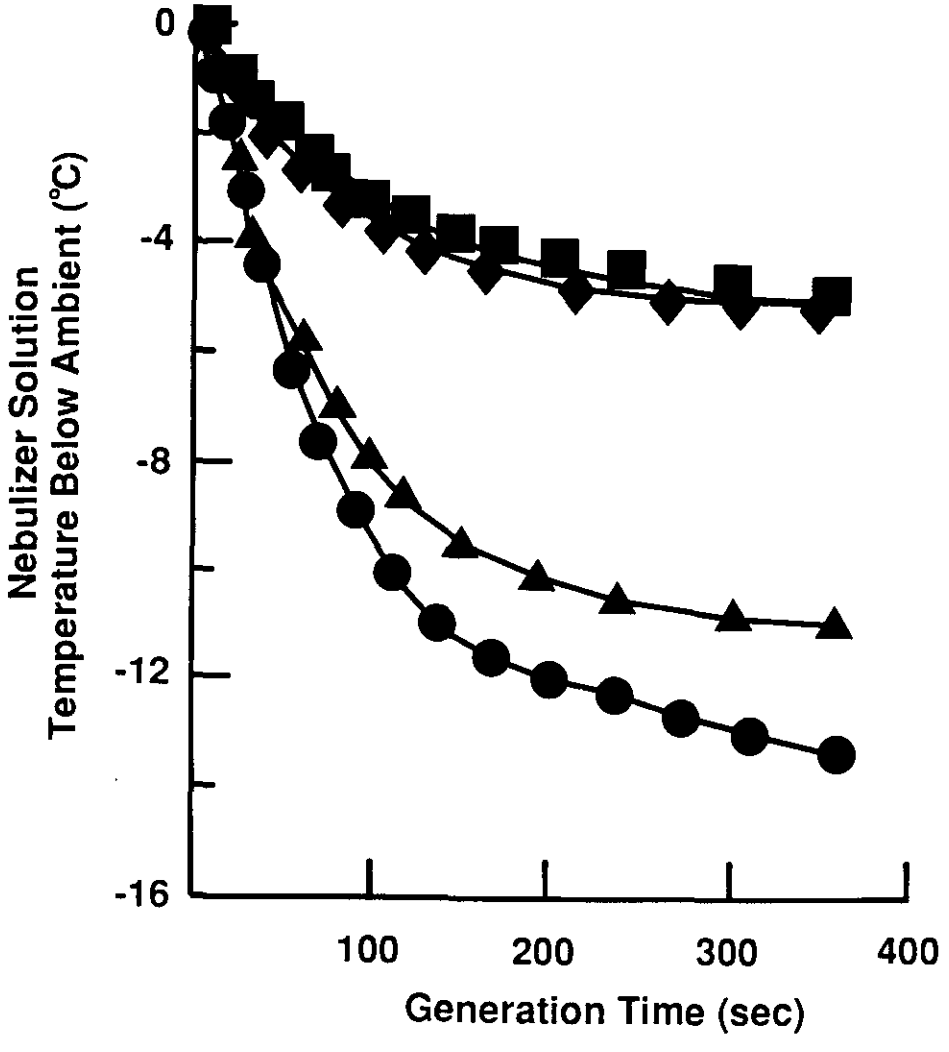

Figure 3. Graph of nebuliser solution temperature vs generation time for the Mist-O_2-Gen ultrasonic nebuliser.

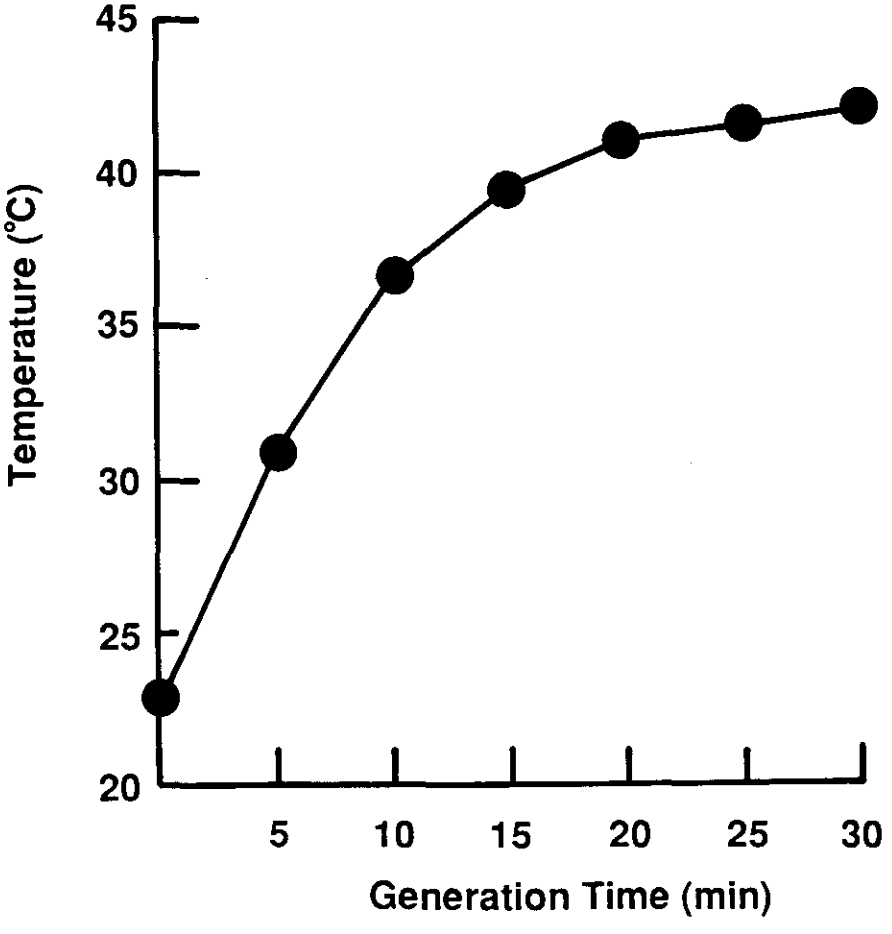

Output

The total output of the jet nebuliser systems are plotted against generation time in Figure 4. The total output fell during nebulisation for all of the jet nebuliser systems tested. The magnitude of the fall was similar for both the Cadema and Up-Draft with reductions in total output of approximately 45-65 mg/min for temperature falls of 11-15 °C (over 6 minutes of generation).

The reduction in output with generation time for the two air compressor driven systems was lower; approximately 15 and 27 mg/min for the Aerosol-One and the Flatus respectively, after a temperature fall of 5-7 °C during 6 minutes of generation.

The ultrasonic nebuliser solution output is very much larger than that of the jet nebulisers. The output vs time graph is shown in Figure 5. The output without tubing or valve was found to be approximately constant at 4.8 ml/min over the time period tested. The output through the two-way valve was found to be much reduced and was dependent on the flow rate of the aerosol through it (Figures 5 and 6). The output was found to be greatest at a flow rate of 20 l/min above and below this value, the mass output fell (Figure 6).

Concentration of solution in the droplets

The change in concentration of solution in the nebulised aerosol droplets can be seen for each nebuliser system in Figure 7.

Figure 4. Graph of nebuliser output vs generation time for the four jet-nebuliser systems: Up-Draft/Aerosol-One (*squares*), Up-Draft/Flatus (*diamonds*), Cadema/compressed oxygen (*circles*) and Up-Draft/compressed oxygen (*triangles*).

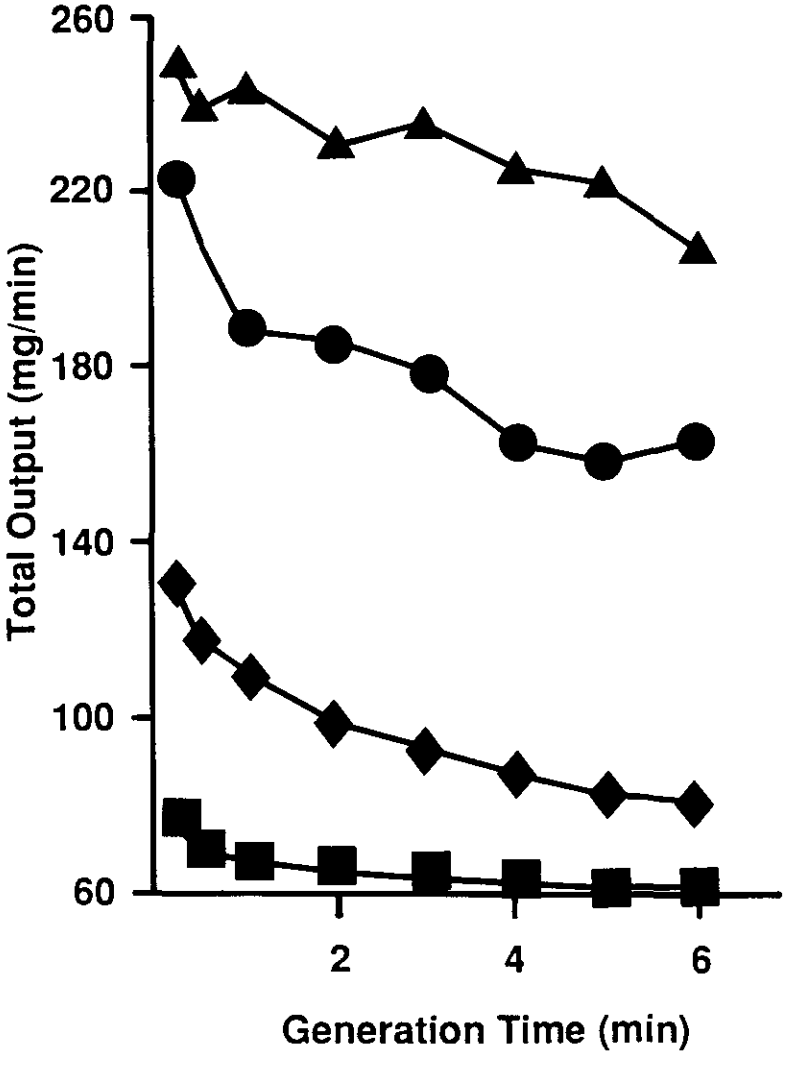

Figure 5. Graph of output vs generation time for the Mist-O_2-Gen ultrasonic nebuliser: no tubing or valve (*circles*), Bennett tubing and valve (model 2700, Hans Rudolf Inc., Kansas, Mis., USA) attached; 10 l/min flow rate (*triangles*), 20 l/min (*squares*), 30 l/min (*diamonds*) and 50 l/min (*crosses*).

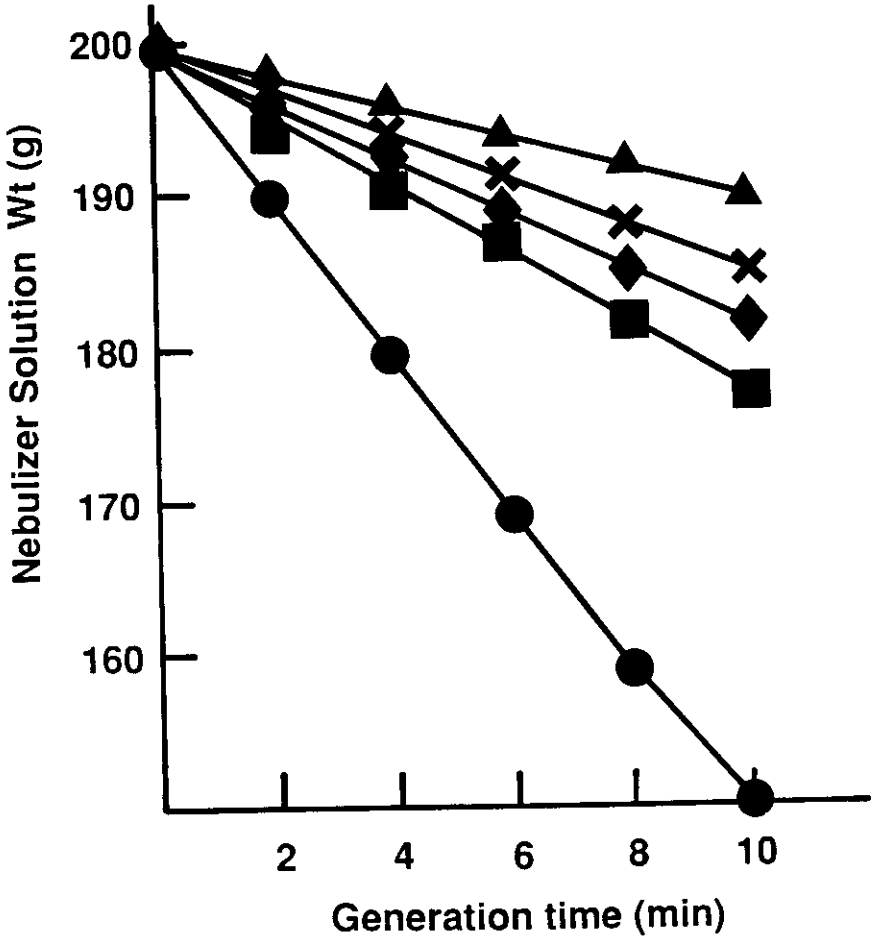

Figure 6. Graph of output vs flow rate for the Mist-O_2-Gen ultrasonic nebuliser, Bennett tubing and valve in place.

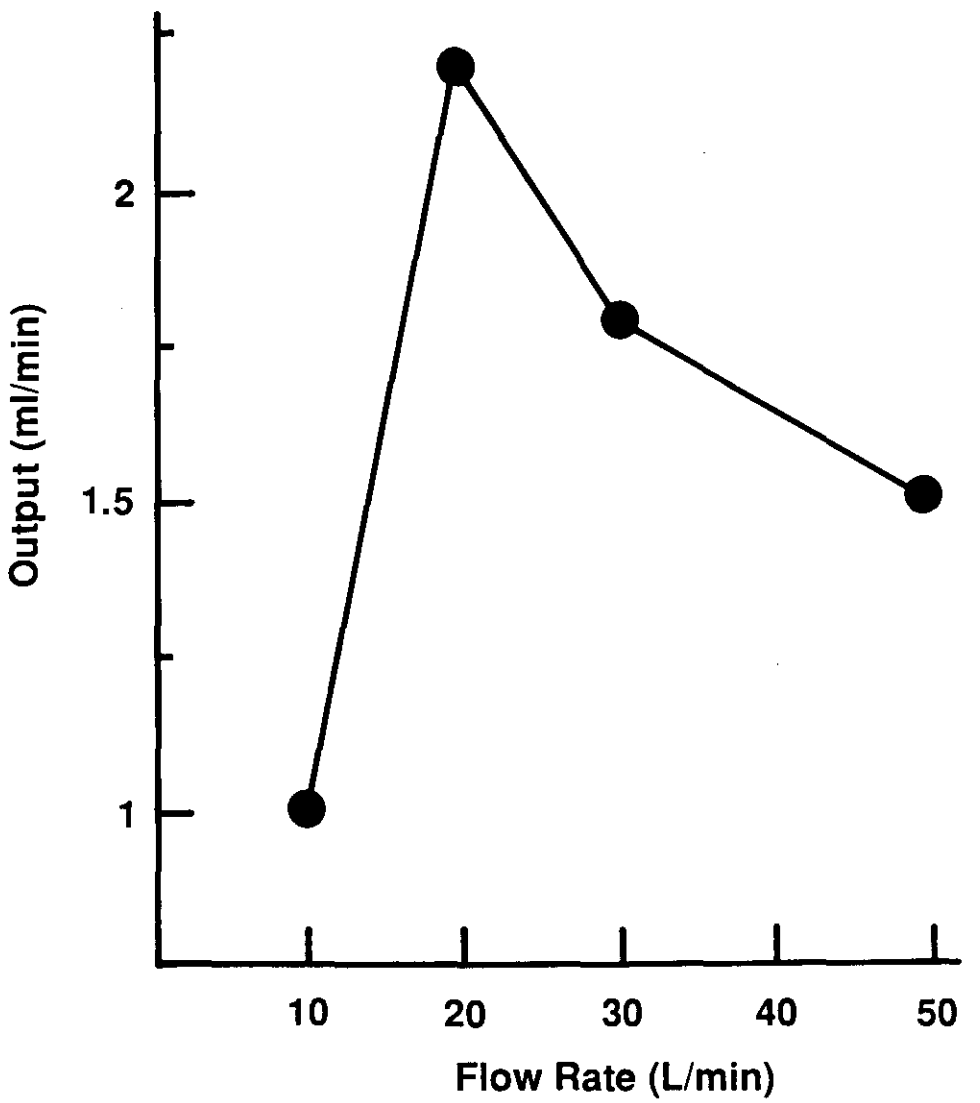

Figure 7. Graph of droplet solute concentration (% w/v) vs nebuliser solution temperature for the four jet-nebuliser systems: Up-Draft/Aerosol-One (*squares*), Up-Draft/Flatus (*diamonds*), Cadema/compressed oxygen (*circles*) and Up-Draft/compressed oxygen (*triangles*). Note that the ambient temperature is the highest value on each graph.

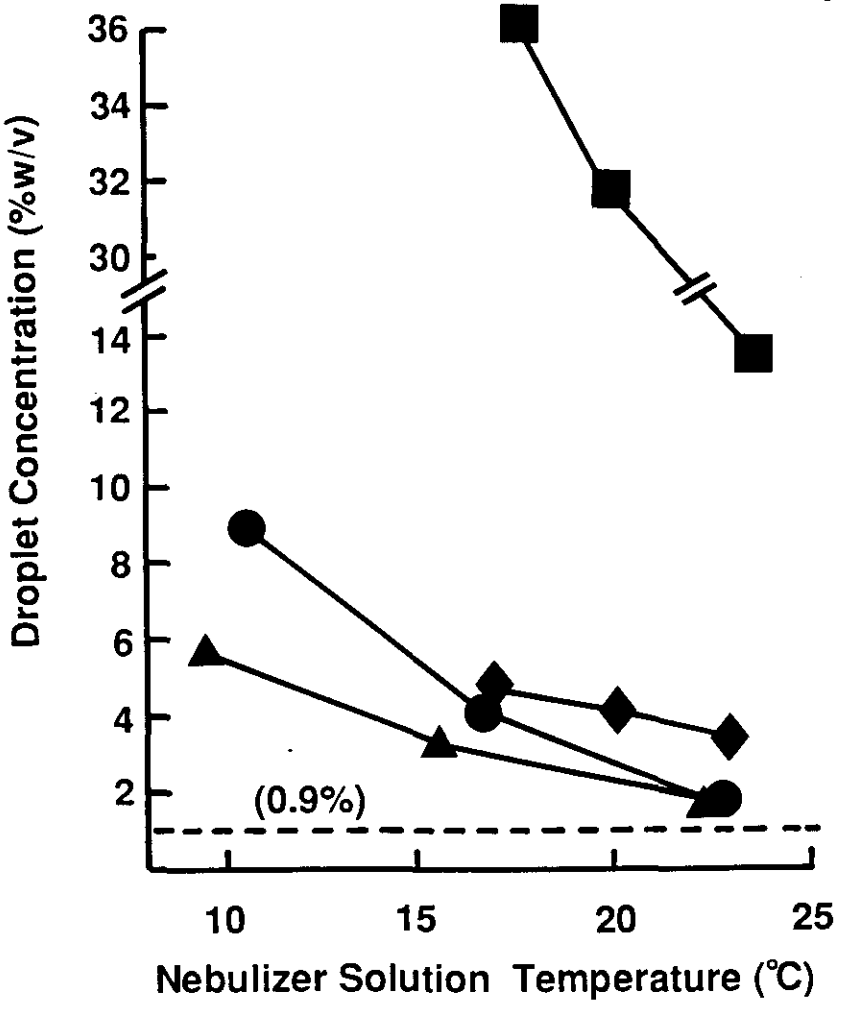

The solute concentration contained in the aerosol produced by the jet nebulisers increases significantly with fall in nebuliser temperature and with reduction in the dilution air humidity. At the steady temperature T_s the droplet solution reaches 5.8 and 9.2 % NaCl for the Cadema and Up-Draft nebulisers respectively, using 8 l/min of compressed oxygen as the generation gas. The Flatus/Up-Draft system reaches a little less than 5% and the Aerosol-One/Up-Draft reaches approximately 36% saline after the same generation time.

The effect of dilution air humidity alone on the droplet solute concentration with the nebuliser at room temperature for each jet nebuliser system can be seen in Table 1. The droplet solute concentration reaches 1.1 - 1.5% with saturated dilution air at ambient temperature. Ambient dilution air with relative humidity of 65-75% at ambient temperature increased the droplet solute concentration to 1.86 and 2.46% for the Up-Draft and Cadema respectively, generated with compressed oxygen. The effect with the air compressors was greater with the Up-Draft, the Flatus compressor producing a concentration of 3.45% and the Aerosol-One 13.5%.

The droplet solution concentration generated from the ultrasonic nebuliser changes very little with time. The maximum effect is seen at the start of generation (0.93 % saline from 0.9 % initial value) and as nebulisation progresses, the concentration returns toward isotonic, reaching it after approximately 13 minutes.

Table 1. Effect of dilution air humidity on droplet solute concentration at ambient temperature.

Nebuliser/Generator System	droplet solute concentration (% w/v Saline)	
	100% RH	65-75% RH
Up-Draft/Aerosol-One	1.5 ± 0.3	13.5 ± 1.8
Up-Draft/Flatus	1.1 ± 0.1	3.5 ± 0.6
Up-Draft/Compressed O_2	1.3 ± 0.2	1.9 ± 0.3
Cadema/Compressed O_2	1.5 ± 0.2	2.5 ± 0.2

#Results expressed as mean ± range (number of determinations = 2 or 3).

Droplet sizing

The droplet size distributions of the jet-nebuliser systems fall with reduced dilution air humidity and with falling in temperature in the nebuliser, in parallel with the increase in solute concentration in the aerosol droplets. Figure 8 shows the effect of nebuliser temperature on aerosol droplet size. The effect of temperature change is greater when compressed oxygen is used at 8 l/min, the droplet size falling by 33 and 36% of the size at ambient temperature for the Cadema and Up-Draft respectively. With Flatus and Aerosol-One generation, the size change is smaller (19 and 11% fall from ambient temperature value respectively). Conversely, the effect of dilution air humidity at ambient temperature is greater with the air compressor generation than with the compressed oxygen (Table 2). The changes that would be seen in practice with unheated nebulisers are shown in Table 3.

The droplet size measured in a cold environment was found to be the same as that measured at room temperature (MMAD = 4.0 and σ_g = 1.4 on both occasions).

The ultrasonic nebuliser droplet size changes when a two-way valve is included in-line but is not affected by changes in relative humidity of the dilution air (Table 4).

Figure 8. Graph of droplet size (μm, mass median aerodynamic diameter) vs nebuliser solution temperature for the four jet nebuliser systems: Up-Draft/Aerosol-One (*squares*), Up-Draft/Flatus (*diamonds*), Cadema/compressed oxygen (*circles*) and Up-Draft/compressed oxygen (*triangles*). Note that ambient temperature is the highest value on each graph.

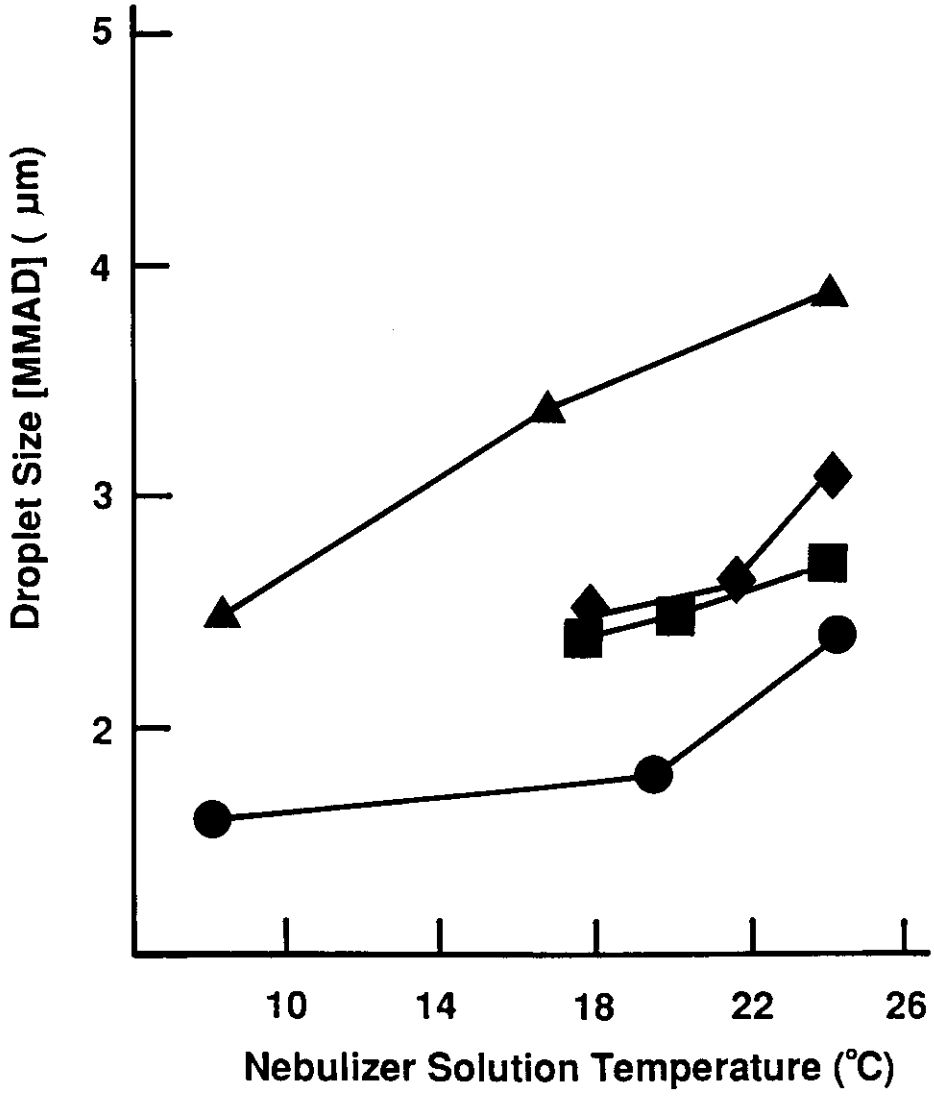

Table 2. Effect of dilution air humidity on droplet size at ambient temperature.

nebuliser/generator system	mass median aerodynamic diameter in μm# (geometric standard deviation*)	
	100% RH	65-75% RH
Up-Draft/Aerosol-One	4.2 ± 0.3 (1.5)	2.7 ± 0.3 (1.5)
Up-Draft/Flatus	4.1 ± 0.2 (1.6)	3.1 ± 0.3 (1.6)
Up-Draft/Compressed O_2	4.2 ± 0.1 (1.4)	3.9 ± 0.2 (1.5)
Cadema/Compressed O_2	2.7 ± 0.1 (1.4)	2.4 ± 0.2 (1.4)

#Results expressed as mean ± range (number of determinations = 2 or 3).

*Geometric standard deviation values all ± 0.1.

Table 3. Change of concentration and droplet size between ambient and steady state temperature, T_s (65 - 75% relative humidity dilution air).

nebuliser/generator system	droplet size % fall	droplet Conc % rise
Up-Draft/Aerosol-One	11.1	170
Up-Draft/Flatus	5.2	39.1
Up-Draft/Compressed O_2	35.9	392
Cadema/Compressed O_2	2.4	244

Calculated as:

$$\frac{|X(T_a) - X(T_s)|}{X(T_a)} \times 100$$

where:

X = droplet size or droplet solution concentration at ambient temperature T_a or

steady state temperature T_s (lowest steady temperature reached by each system).

Table 4. Size of droplets generated by the Mist-O_2-Gen ultrasonic nebuliser.

Amb Temp °C	Dilution air relative humidity %	Mouthpiece and valve Yes or No	mass median aerodynamic diameter (μm)	geometric standard deviation
19.5 ± 0.3	99.0 ± 1	Y	3.6 ± 0.1	1.1 ± 0.1
19.0 ± 0.3	53.1 ± 1	Y	3.5 ± 0.2	1.1 ± 0.1
19.0 ± 0.3	53.5 ± 1	N	5.7 ± 0.1	1.4 ± 0.1

Results expressed as mean ± range (number of determinations = 2 or 3)

3.4. Discussion

The nebuliser systems chosen are representatives of those used in diagnosis and therapy. The Cadema is used for ventilation imaging in the diagnosis of pulmonary embolism and the Mist-O_2-Gen in non-isotonic challenge testing in asthma diagnosis (Anderson et al, 1983). The Up-Draft nebuliser is used for drug delivery in a number of lung diseases using compressed gas, or domiciliary nebulisation with portable air compressors such as the Flatus and Aerosol-One.

The performance of air compressors can be assessed and compared with the aid of Flow/Pressure curves (Newman et al, 1988; Newman et al, 1986). In general, it is known that the greater the flow rate, the smaller the droplet size (Clay et al, 1983), so the compressor that is able to generate higher flow at high back pressures (Flatus compressor compared to the Aerosol-One) will produce an aerosol with a greater proportion capable of reaching the lungs.

The fact that the nebuliser solution temperature of jet nebulisers falls during generation is well documented (Mercer 1981). The heat loss is due to the evaporation of the nebuliser solution to saturate the gas used to generate the aerosol and some cooling due to adiabatic expansion of the generating gas (Davis 1978; Mercer 1981). This evaporation also leads to an increase in solute concentration of the nebuliser solution (Mercer 1981). The gas from a compressed gas cylinder contains no water vapour, while an air compressor supplies air of ambient humidity. Less vapour is therefore required from the

nebuliser solution to saturate the air from an air compressor and heat loss is therefore reduced. Of the energy imparted to the solution of an ultrasonic nebuliser, however, part is used to overcome the surface tension to disperse solution droplets and part to heat the solution itself. The nebuliser solution therefore warms during generation (Figure 3).

The initial output from the nebuliser depends on the type, the flow rate, and the saturation of the generating gas. The change in jet nebuliser output measured during generation depends almost solely on the temperature of the nebuliser solution. The nebuliser solution provides both the solution output and the output of vapour necessary to saturate the generation gas with water vapour at the nebuliser temperature. Therefore, the amount of vapour carried by the generation gas decreases as the temperature falls and the total output is reduced as a result. The fall in output reflects the fall in temperature within the nebuliser and thus levels off after 4-6 minutes.

As the temperature of the ultrasonic nebuliser solution increases, the extra water needed to saturate the air is likely to come from the dense aerosol cloud within the nebuliser chamber. The output is therefore not likely to change as the nebuliser temperature rises as suggested by the results (Figure 5). The two-way valve situated before the mouthpiece of the ultrasonic nebuliser filters a high proportion of the larger droplets from the aerosol stream. The effect is therefore to reduce the output and MMAD of the droplets. This effect depends on the flow rate of the aerosol stream and

hence the velocity of the droplets. There is an optimum flow rate, however, due to opposing effects: at the lower flow rate, the droplets tend to settle into the nebuliser solution or within the tubing and the output is reduced. At the higher flow rates, the droplets are more likely to impact within the tubing and on the valve. The optimum flow rate for this system was found to be approximately 20 l/min (Figure 6).

Although it is known that the concentration of the solution in the jet nebuliser bowl increases with generation due to the release of vapour in addition to the liquid droplets (Davis 1978; Mercer et al, 1968), the changes in solution concentration in the droplets measured in the experiments reported here, are generally much greater. This is because the cold aerosol droplets generated from the jet nebuliser solution will evaporate a substantial amount of water as they rapidly warm up to room temperature. Therefore, the concentration of solutes in the droplets increases to a value determined by the difference between the ambient temperature and the temperature of the nebuliser solution and to a lesser extent due to the gradual increase of the concentration in the nebuliser.

The nebuliser solution equilibrates to a lower steady temperature T_s when the dry gas from a compressed gas cylinder is used to generate the aerosol, compared to the air compressors. The droplet solute concentration thus increases to a greater extent (relative to the value at ambient temperature) as a result (Table 3).

The ambient air inhaled along with the aerosol that makes up the inspiratory flow is likely to have a lower relative humidity than that corresponding to the nebuliser solution, therefore it has the effect of drying the aerosol droplets as it mixes before inhalation (Phipps et al, 1987 [Chpater 2]). This concentrating effect is quite marked, especially when the generation flow and the output of solution from the nebuliser is low. The consequence of the low output is that there is only a small volume of water present in the droplets to re-saturate the aerosol stream (see results for Up-Draft/Flatus and especially the Up-Draft/Aerosol-One systems, Figure 7 and Table 1). The ambient relative humidity was comparatively high during these experiments (65-75%), a lower ambient RH such as that found in air-conditioned rooms would be expected to greatly enhance these effects.

The ultrasonic nebuliser has a higher output and larger droplet size, so more water is available for saturation of the dilution air and the concentration change of the droplet solution is hence much smaller than that of the jet nebulisers. The droplet concentration therefore starts off greater than isotonic but as the tubing becomes saturated, this is able to supply the vapour necessary to saturate the dilution air. Although the nebuliser solution temperature is increasing, the droplets do not become hypotonic due to water vapour condensing on them as the aerosol stream cools, rather the excess vapour will condense on the walls of the conducting tubing (Mercer et al, 1968).

Schoeffel et al (1981) found that small amounts of hypertonic (3.6% NaCl) aerosol caused bronchoconstriction in asthmatic subjects. Lewis and Tattersfield (1980 and 1982) found that a number of asthmatics bronchoconstricted after inhaling a jet nebulised aerosol of isotonic saline, but not to an aerosol generated by a nebuliser heated to 37°C. This was explained in terms of a reduction in airway cooling by the warm aerosol, but it may have been due to a reduction in the concentrating effects that the nebuliser temperature fall imparted on the droplets. The possibility that initially isotonic, or even hypotonic, solutions may produce hypertonic aerosol droplets should therefore be accounted for when delivering therapeutic aerosols to patients with hyperreactive airways.

Bronchial challenge tests are most often performed using jet nebulisers, and the possibility that the solutions being administered are hypertonic, even though isotonic solutions are initially placed in the nebuliser bowl, may affect the results and should be considered. The necessity for nebulisation to be reproducible for bronchial challenge testing, has led to some careful characterisation of nebulisers (Tsanakas et al, 1987; Sterk et al, 1983; Ryan et al, 1981); nebuliser temperature change may, however, add to the variability in dose and site of delivery of challenge agents.

The size of the aerosol droplets falls with generation time in conjunction with the increase in concentration. The magnitude of this is variable but it is likely to affect the deposition pattern of aerosol within the lungs (Stahlhofen et al,

1983). This change in droplet size is not due to a direct effect of cooling of the nebuliser, since there was no change in droplet size when the nebuliser system and environment were kept at a low temperature of 7.5 °C. Large differences in regional deposition as measured by 'Penetration Index' on tomographic slices have been found in normal subjects inhaling mildly polydisperse aerosols with mass median aerodynamic diameters of 2.6 and 5.5 μm (Phipps et al, 1989 [Chapter 7]). The smaller droplet size showed a much higher relative deposition in the small airways and lung parenchyma. This may or may not be clinically desirable, but the change in droplet size depending on the time since the start of generation and the humidity of dilution air (for example, from an initial droplet size of 4.2μm with 100% RH dilution air to 2.4 μm after the equivalent of 4 minutes generation for the Up-Draft/Aerosol-One system) may be important in therapeutic, diagnostic or experimental applications when reproducibility of aerosol deposition or clinical response is important (Clay and Clarke 1987; Mitchell et al, 1987). It is of course, very likely that some subsequent adjustment of droplet size will take place in the respiratory tract (Morrow 1986).

The Flatus compressor produces a droplet size similar to the Aerosol-One, with the Up-Draft nebuliser, but with the higher flow rate of the Flatus, a smaller droplet size may be expected. The discrepancy may be due to the fact that the Aerosol-One droplets are evaporating to a greater extent than with the Flatus at ambient temperature and saturated dilution air (1.5 and 1.14% respectively, see Table 1). The lower output of the Aerosol-One/Up-Draft

system is likely to be responsible for this.

The effect of the increase in temperature of the ultrasonic nebuliser solution on the droplet solute concentration is small. Also, the effect of dilution air humidity on the droplet size (and presumably the droplet solute concentration) is small due to the much higher output from the Mist-O_2-Gen nebuliser. The larger droplet size generated by the ultrasonic nebuliser means that they are more easily deposited on the tubing and valves within the system.

Conclusions

The unsaturated dilution air and fall in temperature of jet-nebulisers with time cause the initial aerosol droplets to reduce in size and increase their solute concentration. These effects can be much greater than that caused by the well-known increase in concentration of the solution in the nebuliser bowl (Davis 1978; Mercer 1968). These phenomena may be critical in some therapeutic, diagnostic and experimental applications of jet nebulised aqueous aerosols and the effects are especially marked when the aerosol output is low.

The droplet solute concentrating effects are caused more by dilution air humidity with the lower flow rate and output of the air compressors. The fall in nebuliser solution temperature has a greater effect on the size of the droplets and the concentration of solution within them when dry gas such as that supplied from compressed oxygen cylinders.

To reduce these effects, the generating gas and dilution air should be saturated with water vapour at ambient temperature and the nebuliser solution should be maintained at ambient temperature.

The higher output and droplet size occurring with the Mist-O_2-gen ultrasonic nebuliser makes the droplet size and solute concentration less susceptible to large changes during nebulisation. However, the presence of tortuous tubing, valves and high inhalation flow rate will cause a large reduction in the output available to the patient because the large droplets will deposit in the apparatus.

Chapter 4

The assessment of aerosol delivery systems used in the pentamidine treatment of *Pneumocystis carinii.*

4.1. Introduction

Although nebulisers have been used to deliver bronchodilator and other drugs in the treatment of asthma and bronchitis for some considerable length of time, it is only relatively recently that anti-infective drugs have proven to be effective by inhalation (Heley 1987; Newman et al, 1985; Montgomery et al, 1987; Clarke and Newman 1984). Drug delivery by aerosol inhalation has obvious advantages in that it enables a high local concentration and low systemic levels to be achieved, thus overcoming many of the problems associated with systemic administration.

The main problem with inhaled anti-infective drugs lies in achieving a consistent delivery to the areas of infection in high enough doses to be effective. Due to the wide choice of aerosol delivery systems and compressors it is necessary to understand the factors which determine the effective delivery of inhaled drugs to be able to compare and choose the best system. There is no doubt that some nebuliser systems are ineffective (Foulds and Smithuis 1983; Simonds et al, 1989).

Inadequate or inappropriate characterisation of the system is likely to lead to a failure of therapy that may be interpreted as a failure in the drug treatment rather than the system of delivery.

The delivery of pentamidine by inhalation in the treatment and prophylaxis of *Pneumocystis carinii* has recently been reviewed (Corkery et al, 1988) and its use is likely to increase as a means of reducing the systemic side effects of this drug (Wharton et al, 1986). However, despite the continued popularity of drug delivery to the respiratory tract via nebulisation, there has not been enough detailed, specific and quantitative assessment of the physicochemical factors affecting the dose and site of deposition.

The effect of deposition site is likely to be of particular importance for pentamidine for two reasons: the infection is localised in the alveolar regions (Hughes 1987) and deposition in the large airways is likely to cause local and possibly systemic side effects (O'Doherty et al, 1988). Therefore, it is sensible to develop an *in vitro* test in order to predict the amount of drug which is likely to deposit at desired and unwanted sites in a defined period of inhalation.

The aim of this report is to identify, *in vitro*, some of the important factors which determine the delivery of pentamidine by inhalation in the therapy of *P carinii* and to assess the characteristics of three systems used in inhalation therapy with

two modes of generation; compressed oxygen and air compressor for home use.

4.2. Methods.

The nebuliser systems tested were:

RespirGard II (Marquest Medical Products Inc., Englewood, Co, USA), Aerotech II (Cadema Medical Products Inc., Middletown, New York, USA) and Provent II (Protech Services, Sydney, Australia). The former and latter systems incorporate an in-line filter to remove large droplets.

The air compressor used in this study was the Vitalair (Allersearch, Sydney, Australia). The pentamidine isethionate (May and Baker Ltd., Dagenham, England and Lyphomed Inc. Rosemont, Illinois, USA) was made up as a 100 mg/ml solution in distilled water. The osmolarity of the pentamidine solution was measured by vapour pressure osmometry (Model 1100, Knauer, Bad Homberg, W. Germany).

The Vitalair compressor flow rate was assessed by passing the pump flow through a rotameter (Platon Ltd., Basingstoke, Hants, England). The flow rate produced by the pump through the Provent II nebuliser containing either 5 ml of normal saline or 5 ml of the pentamidine solution was also measured.

The droplet size and total output of the RespirGard II and Provent II nebulisers using the Vitalair pump were measured as described below.

The total output and the output of pentamidine alone from the mouthpiece of each aerosol delivery system was measured by operating each nebuliser unit for 5, 10 or 15 minutes at both 6 and 10 l/min and measuring the weight before and after aerosol generation. The solution left in the nebuliser and tubing was then thoroughly rinsed and the washings collected and accurately weighed (Model A 200 S, Sartorius, Goettingen, W. Germany). The washings were then further diluted and the solution immediately assayed by ultra violet spectrophotometry (DMS 70, Varian Associates Inc., Palo Alto, California, USA) at a wavelength of 262 nm (Clarke 1986). The concentration of pentamidine was then calculated with reference to a previously determined standard curve of absorbance vs concentration (Figure 1).

The efficiency of collecting pentamidine from the nebuliser system was assessed by placing a known amount (approximately 6 ml) of an accurately prepared 100 mg/ml pentamidine solution in each of the three nebulisers. The solution was recovered in the same way as before, by repeated washings. The washings were diluted and the concentration measured by ultra violet spectrophotometry. The recovery of pentamidine was found to be 99.2 ± 0.7%.

The output of sodium chloride was measured by including 2 MBq/ml of $^{99m}TcO_4^-$ in 5 ml of isotonic saline, generating for 5, 10 or 15 minutes at 6 or 10 l/min, weighing the nebuliser and collecting the remaining activity by repeated washings.

Figure 1. Standard curve of absorbance at 262 nm vs pentamidine concentration.

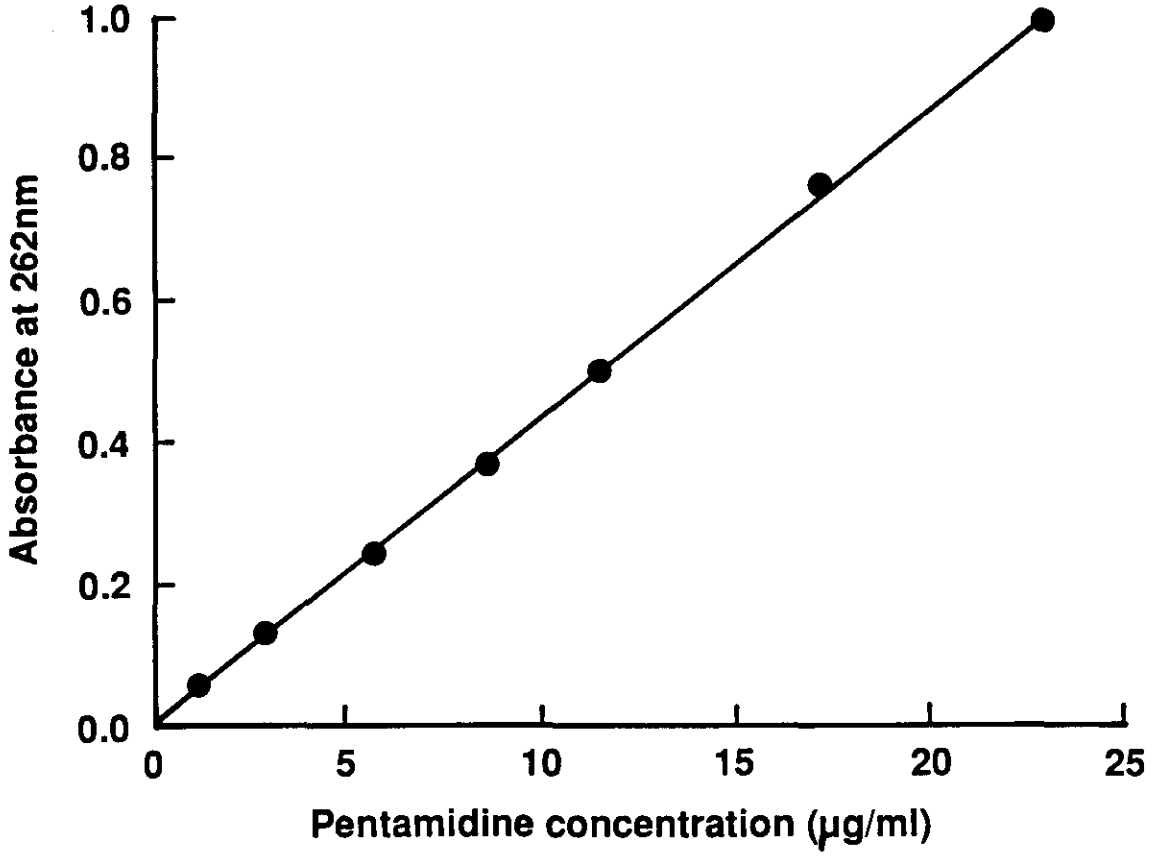

The concentration of $^{99m}TcO_4^-$ was measured by placing 2ml of the washings into a scintillation detector (Model 802, Canberra Industries Inc., Connecticut, USA) and obtaining counts per ml. This was compared with 2ml of the initial nebuliser solution, having been diluted in the same manner. The linearity of the well counter was assessed by counting 2 ml solutions containing known amounts of $^{99m}TcO_4^-$ (Figure 2; $r^2 = 0.998$).

The effectiveness of $^{99m}TcO_4^-$ solution collection from the nebuliser units was assessed by including 20 MBq of ^{99m}Technetium pertechnetate ($^{99m}TcO_4^-$) in 5 ml of normal saline in each nebuliser unit, generating the aerosol for 10 minutes and washing the nebuliser unit as before and collecting the washings. The washings and the nebuliser unit were then placed on a collimated gamma camera (Diagnost Tomo Phillips, Hamburg, FDR) and counts collected for 5 minutes (PDP-11, Digital Equipment Corp., Maynard, USA). The counts remaining in the nebulisers after the washings were always less than 0.5% of the total.

Outputs of pentamidine were measured for each of the three nebuliser brands for generation times of 5, 10 and 15 minutes. This was carried out at a compressed oxygen flow rate of 10 l/min for all three nebuliser brands and at 6 l/min for the RespirGard II and Provent II nebulisers. The saline output measurements were carried out in triplicate to asses variability, and the pentamidine measurements in duplicate.

Figure 2. Standard curve of counts per second vs. radioactivity for the well counter described in the text.

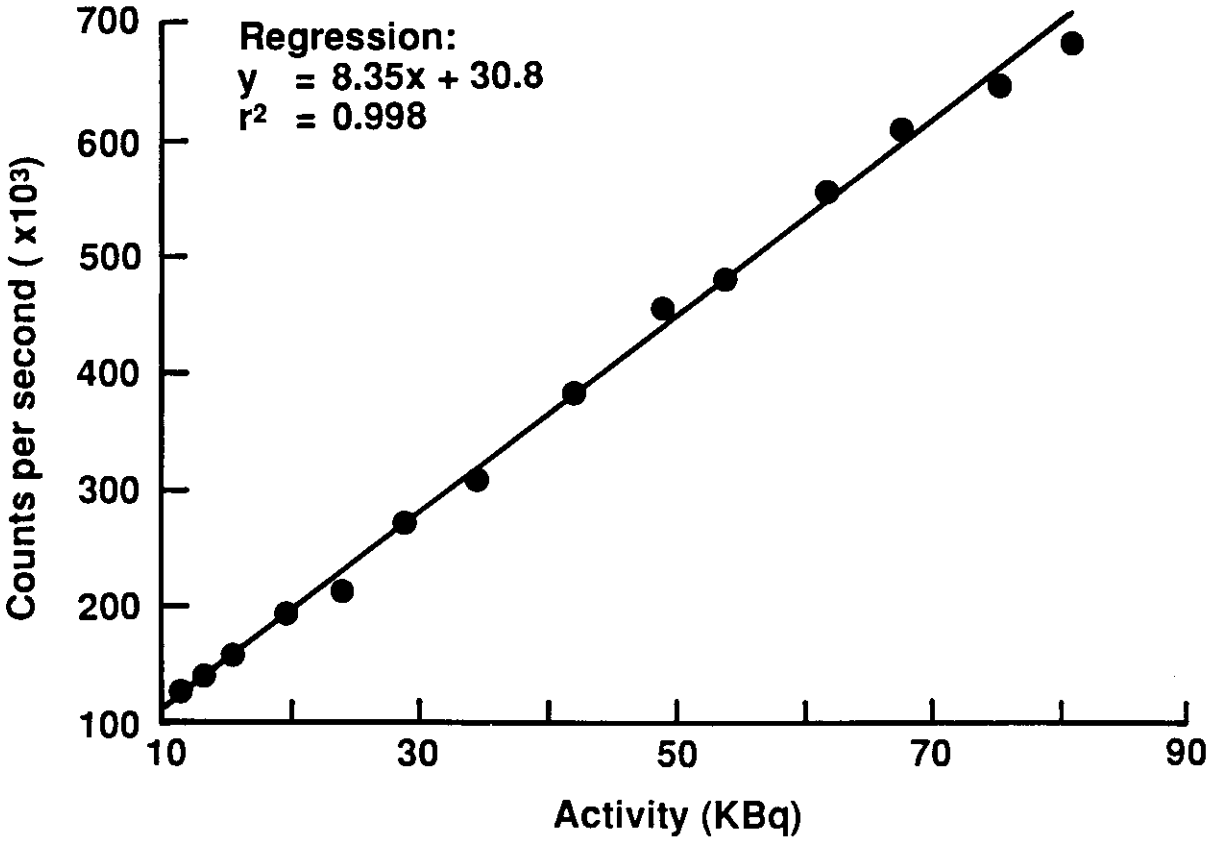

A calibrated 7-stage cascade impactor (DCI6, Delron, Columbus, Ohio, USA) was used to measure droplet size produced by the aerosol delivery systems (Phipps et al, 1987 [Chapter 2]). The nebuliser solution was made up containing 100 MBq/ml of $^{99m}TcO_4^-$. The aerosol was generated by either a Vitalair compressor or oxygen from a compressed gas cylinder. The dilution air was at ambient temperature (20 - 23 °C) and relative humidity (RH, 40-50%), or at ambient temperature and 100% RH.

The cascade impactor slides were placed on a previously calibrated gamma camera (Phipps et al, 1987 [Chapter 2]), and the distribution of aerosol droplets calculated from a least squares fit to the data (Gonda et al, 1982). The effect of pentamidine, humidity, multiple usage and method of generation on the droplet size was also determined. Droplet sizing was performed in triplicate.

The mass fraction of the output below a droplet size of 2 μm (the 50 % cut off diameter of stage 4 of the impactor [Gonda et al, 1982]) was also calculated.

4.3. Results.

The flow\pressure curve for the Vitalair compressor is seen in Figure 3. The flow rate from the compressor without nebuliser or tubing was found to be 12 l/min.

Figure 3. Graph of maximum flow rate generated by the Vitalair compressor vs. back pressure.

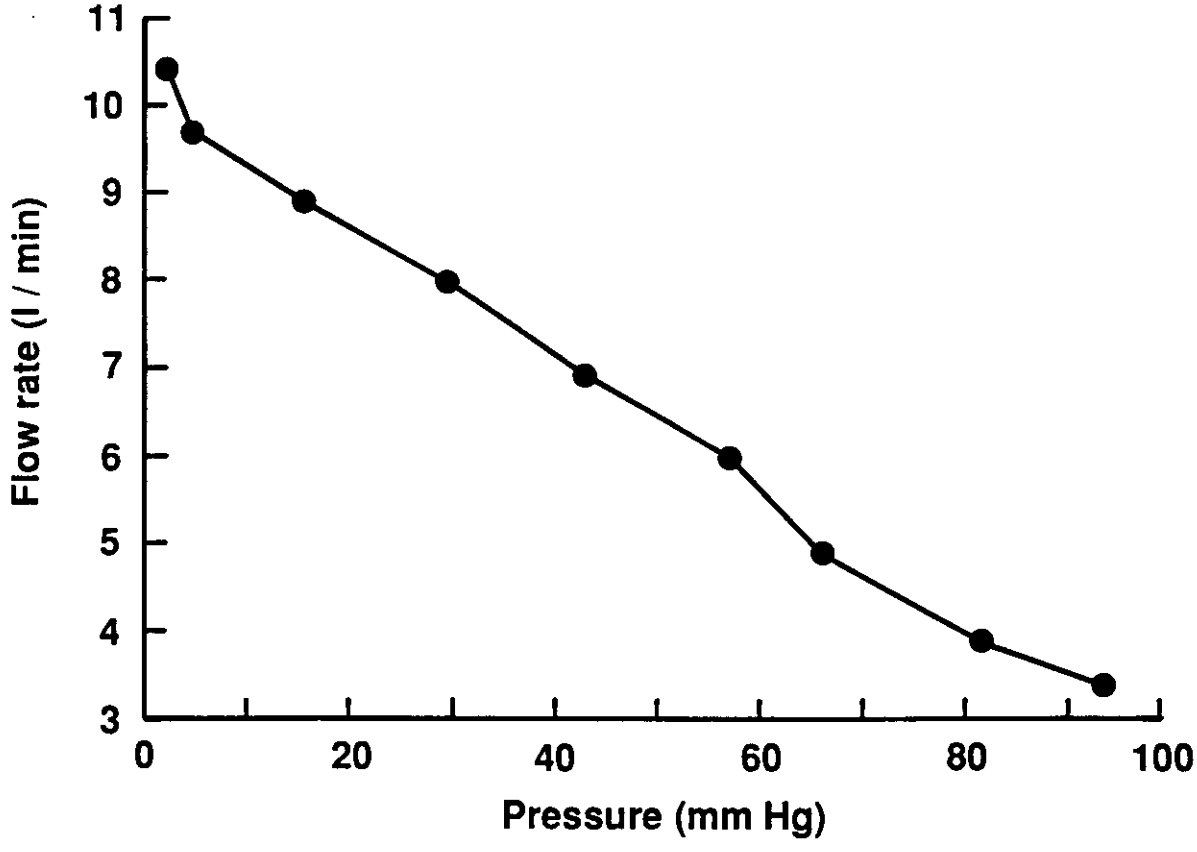

If the Provent II or RespirGard II nebulisers were included with 5 ml of normal saline, the flow rate fell to 5.5 l/min, corresponding to an increase of differential pressure (due to the resistance of the nebuliser) to approximately 60 mmHg. The same is expected with the pentamidine solutions.

A precipitate of pentamidine was observed in the nebuliser bowl and on the baffles of the nebuliser systems during nebulisation shortly after the commencement of nebulisation.

The size of the droplets and total outputs generated from the RespirGard II and Provent II by the Vitalair compressor were similar to that at 6 l/min of compressed oxygen for both pentamidine and saline aerosols (Table 1).

The total output falls with time of generation for all nebuliser solutions and systems tested (Table 2). While the solute output remains relatively constant for sodium chloride, it falls with generation time for pentamidine (Table 2). At 10 l/min, the cumulative pentamidine output after 5 minutes of generation is 29.5 and 30.5 mg for the Provent II and RespirGard II respectively, however, the cumulative output after 15 minutes is not proportionally higher at 51.0 and 60.0 mg respectively. The total pentamidine output after 15 minutes at 6 l/min is less than half the value at 10 l/min. The Aerotech II has a pentamidine output approximately 1.6 to 1.9 times that of the other two systems.

Table 1. Droplet size and total output using the Vitalair compressor or compressed oxygen at a flow rate of 6 l/min. Results are expressed as mean (standard deviation)

		Vitalair compressor (5.5 l/min)			Compressed oxygen (6 l/min)		
	Saline (S) or Pentamidine (P)	MMAD* μm	σ_g#	Output mg / min	MMAD μm	σ_g	Output mg / min
Provent II	S	1.2 (0.2)	1.8 (0.2)	89.3 (6.2)	0.9 (0.1)	2.0 (0.1)	81.3 (4.4)
	P	1.7 (0.2)	1.6 (0.1)	78.2 (5.0)	1.7 (0.1)	1.8 (0.1)	91.7 (7.1)
RespirGard II	S	1.1 (0.2)	1.8 (0.1)	94.5 (8.6)	1.1 (0.1)	1.8 (0.1)	99.3 (3.0)
	P	1.7 (0.1)	1.7 (0.1)	75.8 (3.1)	1.9 (0.1)	1.7 (0.1)	89.5 (5.2)

Notes:

* Mass median aerodynamic diameter.

Geometric standard deviation.

Table 2a. Total mass output and output of sodium chloride (Table 2a) or pentamidine (Table 2b) for each system. Results are expressed as mean (standard deviation).

	Flow rate (l/min)	Time (min)	Total output (mg/min)	sodium chloride solute output (mg/min)
RespirGard II	10	5	170.1 (5.5)	0.472 (0.009)
		10	156.4 (3.2)	0.485 (0.01)
		15	-	-
	6	5	99.3 (3.0)	0.179 (0.011)
		10	77.3 (6.5)	0.187 (0.013)
		30	68.1 (3.2)	-
Provent II	10	5	157.1 (8.8)	0.442 (0.012)
		10	150.4 (2.1)	0.425 (0.012)
		13	149.7 (3.5)	0.482 (0.015)
	6	5	81.3 (4.0)	0.176 (0.015)
		10	71.3 (5.2)	0.173 (0.016)
		15	70.0 (2.2)	0.169 (0.010)
Aerotech II	10	5	243.2 (11.0)	1.02 (0.008)
		12	217.4 (5.6)	0.98 (0.01)

Table 2b.

	Flow rate (l/min)	Time (min)	Total output (mg/min)	sodium chloride solute output (mg/min)
RespirGard II	10	5	167.3 (12.1)	6.1 (0.9)
		10	152.1 (13.2)	4.6 (0.3)
		15	147.6 (8.3)	4.0 (0.3)
	6	5	93.7 (4.8)	3.8 (0.4)
		10	81.2 (4.2)	2.4 (0.3)
		15	73.9 (6.2)	1.8 (0.3)
Provent II	10	5	171.9 (15.2)	5.9 (1.0)
		10	144.2 (12.1)	4.3 (0.2)
		15	131.8 (7.0)	3.4 (0.3)
	6	5	95.2 (7.1)	3.5 (1.0)
		10	86.0 (9.2)	2.1 (0.7)
		15	75.4 (8.9)	1.6 (0.9)
Aerotech II	10	5	229.4 (9.6)	9.6 (1.2)
		13.5	205.9 (10.1)	7.3 (0.3)

The droplet size of the pentamidine solution was greater than that of saline for the RespirGard II and Provent II but not for the Aerotech II (Table 3). The variability in droplet size within and between brands at 10 l/min flow rate was low (MMAD of less than ± 0.2 μm and σ_g of less than ± 0.1).

The dilution air humidity had no effect on droplet size for the Provent II and RespirGard II, but the droplet size produced by the Aerotech II was slightly higher when dilution air of 100% RH was used (2.5μm [SD = 0.2] for 40% RH and 2.7μm [SD = 0.2] for 100% RH). The droplet size of the Provent II also remained relatively constant with repeated usage (a total of 5 hours continual use) at 6 l/min, (initial MMAD = 1.75μm, σ_g = 1.6 and final MMAD = 1.8μm, σ_g = 2.0).

The 'effective delivery' of the pentamidine aerosols can be calculated as the drug output multiplied by the fraction of 'respirable' droplets (Phipps et al, 1987 [Chapter 2]). In the case of pentamidine aerosols, the respirable droplets are those that will have a high probability of alveolar deposition. We have arbitrarily decided to include those droplets depositing below stage 4 of the cascade impactor (less than 2μm [Gonda et al, 1982]). The 'wasted delivery' is defined as the output of pentamidine contained in droplets outside this respirable range (Phipps et al, 1987 [Chapter 2]).

Table 3. Droplet size of the three aerosol delivery system brands at 6 and 10 l/min for pentamidine (P) and normal saline (S) solutions. Results are expressed as mean (standard deviation)

		10 l/min		6 l/min	
		MMAD* (μm)	σ_g#	MMAD (μm)	σ_g
Provent II	S	0.9 (0.1)	2.0 (0.2)	0.9 (0.1)	2.0 (0.1)
	P	1.5 (0.2)	1.7 (0.1)	1.7 (0.1)	1.8 (0.1)
RespirGard II	S	1.0 (0.1)	1.9 (0.0)	1.1 (0.1)	1.8 (0.1)
	P	1.6 (0.1)	1.6 (0.1)	1.9 (0.1)	1.7 (0.1)
Aerotech II	S	2.5 (0.2)	1.3 (0.1)		
	P	2.4 (0.2)	1.4 (0.1)		

Notes:

* Mass median aerodynamic diameter.

Geometric standard deviation.

The effective delivery (ED) is more than double for the RespirGard II and Provent II when a flow rate of 10 l/min is used in comparison to 6 l/min, while the wasted delivery (WD) is a lower proportion of the total at the higher flow rate. The Aerotech II system has a comparable ED at 10 l/min to the other two systems, but the WD is much greater (Table 4).

The osmolarity of the 100 mg/ml pentamidine solution in water was found to be equivalent to 0.945 % NaCl solution.

4.4. Discussion

The study clearly demonstrates some important factors involved in the aerosol delivery of pentamidine. a) The output of a 10% pentamidine solution falls with generation time due to precipitation. b) While the effective delivery is similar for all three systems tested and is greater at higher flow rates, the Aerotech II has a higher wasted delivery than the other systems. c) The air compressor generates a flow rate of 5.5 l/min and an aerosol with similar characteristics to 6 l/min of compressed oxygen. d) There is little effect of humidity of dilution air or repeated usage on the droplet characteristics.

Chronic and prophylactic therapy of *P carinii* with pentamidine is likely to require home therapy and thus use of a portable air compressor.

Table 4. Effective delivery ED, (the output of pentamidine contained in droplets less than 2 μm) and wasted delivery, WD (the pentamidine output contained in droplets greater than 2μm) after 15 minutes generation.

	Flow rate l/min	% below stage 4	ED mg/min	% on stage 4 or above	WD mg/min
Provent II	10	71.0 (1.6)	2.4	29.0 (1.6)	1.0
	6	60.2 (0.9)	1.0	39.8 (0.9)	0.6
RespirGard II	10	66.5 (0.6)	2.7	33.5 (0.6)	1.3
	6	58.5 (0.9)	1.4	41.5 (0.9)	1.1
Aerotech II	10	34.9 (1.2)	2.5	65.1 (1.2)	4.7

These results show that the output may be poor if the flow rates are low, especially if appreciable precipitation of the drug occurs. If powerful compressors are unavailable, the use of compressed oxygen cylinders should be recommended for home use.

A flow rate of 12 l/min is quoted by the manufacturers of the Vitalair. This value is the maximum flow rate able to be produced by the compressor, but it is considerably reduced by the resistance of the attached nebulisers. The low flow rate of the Vitalair can limit the output and suitable droplet size generated by the nebulisers used in pentamidine therapy. The flow rate generated by a compressor through any given nebuliser should therefore be independently assessed for each system with the aid of a rotameter. The effective delivery of pentamidine should also be measured on each nebuliser / compressor combination, to provide domiciliary treatment comparable to that received in hospital.

The loss in weight of the nebuliser systems represents the total output from the mouthpiece. This value falls with increasing generation time from 5 to 15 minutes. This effect is likely to be due to the cooling of the nebuliser with time of generation (Phipps and Gonda 1990 [Chapter 3]; Mercer 1981) which reduces the amount of vapour accompanying the aerosol. The output can be segregated into solution and vapour output since the generating gas contains either no water vapour in the case of compressed oxygen or the room air humidity if the air compressor is used. Upon generation, the aerosol stream

will be virtually equilibrated to the humidity corresponding to the solution and temperature in the nebuliser. Thus, a portion of the output is in the form of water vapour rather than aerosol droplets (Phipps and Gonda 1990 [Chapter 3]). The cooling of the nebuliser solution will result in a reduction in the amount of water vapour (the solution vapour pressure is reduced at the lower temperature) and the output will fall as a result (Phipps and Gonda 1990 [Chapter 3]) (Table 2).

The solubility of pentamidine is low in saline and is near its solubility limit in water at 100 mg/ml (Martindale 1982). As the nebuliser solution cools and concentrates, the pentamidine precipitates. Less pentamidine will therefore be available for nebulisation if the precipitate is too coarse for effective nebulisation as a suspension. This may explain the fall in pentamidine output with generation time that is not observed when normal saline is used (Table 2). This effect is likely to be reduced with the use of lower concentrations of pentamidine (Simonds et al, 1989).

It is important to take into account the output of water in the form of vapour when calculating the dose of a solute drug delivered during nebulisation (O'Callaghan et al, 1989). If the drug concentration in the aerosol droplets is assumed to be the same as that of the nebuliser solution, then the output of solution alone should be used to calculate the solute output rather than the total output of solution plus vapour. For example, at a room temperature of 22 °C, using compressed oxygen or compressed air to generate the aerosol at

10 l/min, the saturated water vapour content of the aerosol stream will be approximately 19 mg/litre, so 190 mg/min of the total output will be water vapour. This vapour output will of course fall as the nebuliser solution cools, and is complicated by the fact that the solute concentration in the nebuliser, and that of the droplets, rises with time (Phipps and Gonda 1990 [Chapter 3]). The water output as vapour when an air compressor is used will be lower due to the supply of some water vapour from the room air.

The cough and bronchoconstriction reported as side effects in aerosolized pentamidine therapy (O'Doherty et al, 1988; Simonds et al, 1989) is unlikely to be due to non-isotonicity of the aerosol, since a 10% solution has an osmolarity close to that of normal saline. However, the absence of a permeant anion has been shown to cause cough in normal and asthmatic subjects (Eschenbacher et al, 1984). The bronchoconstriction may therefore be due to a direct irritant effect of the drug in the large airways. The reduced concentrations of pentamidine often used in prophylaxis (O'Doherty et al, 1988) will be hypotonic and therefore, likely to be more potent at causing cough and bronchoconstriction (Schoeffel et al, 1981).

Although the droplet size produced by all three systems was reproducible, the droplet size of the pentamidine aerosols was found to be greater than those of normal saline for the RespirGard II and Provent II. The reason for this is obscure, but is possibly a result of differences in surface tension and viscosity of the two solutions or the deposition of pentamidine precipitate on the

baffling devices, since there was no differences observed for the Aerotech II. The greater droplet size of the pentamidine aerosols to that of saline has been reported previously (Smaldone et al, 1988). These authors, however, obtained lower droplet sizes for the Aerotech II and RespirGard II than those reported here, this may be due to the fact that the aerosol stream for droplet size analysis was sampled via a T-piece, resulting in preferential selection of the smaller droplets.

It has been noted by Smaldone et al (1988) that the droplet size and output of the pentamidine aerosols are dependent on inhalation flow rate. The impaction filter device incorporated into some aerosol delivery systems will remove droplets according to their velocity. We have used a flow rate of 12.5 l/min in these experiments, similar to very slow deep inhalation, which patients should try to achieve for maximum alveolar deposition (Pavia et al, 1977). It should therefore be noted that both the droplet size and output will fall with increasing flow rate with the RespirGard II and the Provent II, but little change is expected with the Aerotech II. Smaldone et al, used a particular breathing pattern in determining output, but another breathing pattern will give different results. The dose received by the patient therefore, will be a function of the inhalation flow rate and the time of inhalation (often taken to be a third of the breathing cycle, but usually longer in slow deep inspiratory manoeuvres). The dose to the patient can therefore be estimated for

comparison between systems as:

$$M_d \times T_i/T_{rc}$$

where:

M_d = Total drug output (output per minute × time of administration).

T_i/T_{rc} = inspiration time (T_i) as a fraction of the total breathing cycle (T_{rc})

The irritant and toxic properties of pentamidine has made it necessary to reduce its delivery to areas other than the alveoli, the site of *P carinii* infection, as much as possible. Droplets of approximately 2μm have been calculated to have a maximal fractional deposition in the non-ciliated regions of the lung (Yu et al, 1977) and a much larger proportion of 2.6 μm droplets have been shown to deposit in peripheral lung regions than 5.5 μm droplets in normal subjects (Phipps et al, 1989 [Chapter 7]) but this value will vary if the lungs are diseased and smaller droplets may conceivably be necessary to penetrate to the alveolated regions of the lung. The effective droplet size range is therefore likely to be less than 1 - 2μm, depending on the morphology and disease state of the lungs and breathing pattern (Brain and Valberg 1979). The effective delivery (ED) has been defined as the dose of drug contained in droplets of 'respirable size range' delivered to the mouthpiece (Phipps et al, 1987 [Chapter 2]). The ED values are useful for nebuliser comparisons and to estimate the rate of delivery of useful drug to the patient. The 'wasted delivery' is also relevant in this case, since pentamidine delivered to the large airways is not of any therapeutic use, and can cause toxic effects. The ideal pentamidine delivery device will therefore have a large ED and low WD. Of

the devices tested, the most effective are the two systems with in-line filters at a generation flow rate of 10 l/min (the Aerotech II has a similar ED but greater WD).

The effective delivery (ED) and wasted delivery (WD) of the pentamidine aerosols can be used to compare the amounts of clinically useful and potentially toxic fractions of pentamidine being delivered to the mouthpiece of each system. Of the devices tested, the most effective are the two systems with in-line filters at a generation flow rate of 10 l/min. Although the manufacturer's recommended generation flow rate for the RespirGard II is 5 - 7 l/min, the smaller droplet size and greater output of pentamidine at the higher flow rate of 10 l/min is more desirable. All of the systems can be considered to have a low efficiency, the systems with in-line filters lose much of the aerosol before reaching the mouthpiece, while the Aerotech may waste some of its delivered dose by deposition in large airways.

Although the humidity of dilution air being inhaled along with the aerosol stream has been shown to effect the droplet size in other aerosol delivery systems (Phipps et al, 1987 [Chapter 2]; Phipps and Gonda 1990 [Chapter 3]), there is no effect found with Provent II or RespirGard II, due to the abundance of deposited water at the filter being able to provide the excess vapour necessary. A Cadema nebuliser (Cadema Medical Products Inc., Middletown, New York, USA) has been tested previously and the droplet size found to decrease with dilution air of low RH (Phipps et al, 1987 [Chapter 2]),

this effect is likely to be similar for the Aerotech II, a modification of the original Cadema nebuliser.

Repeated usage of the Provent II seems to render the size distribution a little wider and more variable. This is probably clinically insignificant. The nebuliser systems characterised are designed to be disposable, mainly for the reason of contamination and although the characteristics of the systems do not change upon re-use, the contamination of the nebulisers and tubing with potentially pathogenic organisms is a limiting factor, especially in immunocompromised patients (Higgs et al, 1987; Barnes et al, 1987; Popa et al, 1988).

In summary, a number of recommendations can be made as a result of this study. a) A powerful compressor or compressed gas should be used to provide a flow rate of at least 10 l/min, to give a greater ED, lower WD and shorter delivery time. b) Pentamidine solution concentrations lower that 10% should be used to minimise precipitation of the drug. c) The characteristics of each nebuliser - generator system should be carried out with the drug solution to be used, prior to patient use. d) The 'effective dose' of drug can be calculated with some degree of accuracy and may be more useful than the amount added to the nebuliser (which is unrelated to dose received by the patient) for comparisons of drug delivery. The fact that the weight output of the nebuliser is not directly related to the output of drug should also be noted.

An improved nebuliser system would incorporate a baffling device that returns the larger droplets to the nebuliser solution to prevent wastage of the drug. The cooling and concentrating effects that cause the precipitation may be overcome by using generating gas and dilution air saturated with water vapour.

In conclusion, careful attention to the factors which determine the output of the drug from the nebuliser and its subsequent deposition in the alveoli may be expected to improve the effectiveness of pentamidine treatment and to decrease the side effects which may result.

Chapter 5

Jet-nebulised aqueous aerosols: mass balance prediction of solute concentration.

5.1. Introduction

The median droplet size of aqueous nebulised aerosols used in therapy and diagnosis, together with the width of the size distribution (usually characterised by the geometric standard deviation) are important determinants of the total and regional deposition in the respiratory tract (Stahlhofen et al, 1983; Ferron et al, 1981; Gonda 1981). The accurate prediction of the sites of delivery of therapeutic agents within the lung for any given aerosol, therefore, requires the characteristics of the droplets on inspiration to be known.

The droplet solute concentration is also important, since initially non-isotonic droplets can effect deposition by hygroscopic growth or shrinkage as they attain a new equilibrium within the respiratory tract (Ferron 1977; Persons et al, 1987; Morrow 1986). Non-isotonic droplets may also effect the deposition pattern by causing a change in airway resistance via bronchoconstriction in hypersensitive subjects (Schoeffel et al, 1981), a fact that has lead to the greater control of nebuliser solution tonicity (Mann et al, 1984; Fois et al, 1986).

Jet-nebulisation of aqueous aerosols is a dynamic process that involves breaking a stream of fluid into primary droplets by a high velocity air-jet. Heat is thus lost from the nebuliser solution as a result of the adiabatic expansion and evaporation of the solution to supply the generating gas with water vapour (Mercer et al, 1968). Since more than 99% of the primary droplets return to the nebuliser solution (Mercer et al, 1968), the end result is that the nebuliser solution and the droplets produced by it, cool and concentrate (Mercer 1981; Phipps and Gonda 1990 [Chapter 3]).

The instability of aqueous aerosol droplets is manifested by changes in their dimensions and composition while attaining an equilibrium with their immediate environment. The time delay between generation of the droplets and inhalation depends on the nebuliser system being used, the inhalation flow rate, and the geometry of the connection between nebuliser and mouthpiece or mask. This delay is likely to be sufficient for significant changes in droplet size and solute concentration to occur prior to inhalation (Phipps and Gonda 1990 [Chapter 3]). Dilution air (i.e. room air) inhaled along with the aerosol during the time when the inspiratory flow rate is greater than that of the aerosol generating gas, has also been shown to effect droplet characteristics (Phipps and Gonda 1990 [Chapter 3]; Phipps et al, 1987 [Chapter 2]).

We have previously reported the effect of temperature fall and dilution air

humidity on the concentration of solutes in aerosol droplets delivered by various jet nebuliser / generator systems (Phipps and Gonda 1990 [Chapter 3]). It was found that the fall in nebuliser solution temperature during nebulisation, together with unsaturated dilution air, caused the aerosol droplets to evaporate during rapid rewarming towards ambient temperature. In so doing, the droplets concentrated their solutes and decreased in volume.

The aim of this chapter is to apply mass balance considerations to the nebuliser systems to explain and predict in theoretical terms the physical changes occurring within the nebuliser bowl and the dynamics of the aerosol droplets being produced. We will then compare theoretical and experimental results.

5.2. Methods

Theoretical mass-balance considerations

To obtain information about the changes occurring within the aerosol droplets, it is necessary to consider the movement and conservation of water and solute during aerosol generation. Most medical aqueous nebuliser solutions contain solutes and sodium chloride in proportions that render them isotonic. For this reason, we shall consider the effects of nebulising solutions of isotonic saline (these are likely to behave in a manner similar to isotonic aerosols containing dissolved drug as long as surface tension and to some extent viscosity are similar to that of normal saline).

The mathematical treatment in the first instance makes some assumptions about the system:

1. The aerosol stream is constantly saturated with water vapour (i.e. equilibrium between the droplets and surrounding air is rapid).

2. There is no loss of aerosol by deposition in the connecting tubing.

The equations are presented in Appendices I and II.

Experimental

Nebuliser systems studied:

a) Cadema nebuliser (Cadema Medical Products Inc., Middletown, NY, USA) with compressed oxygen.

b) Up-Draft nebuliser (Hudson Up-Draft Oxygen Therapy Sales Co., Temecula, CA., USA) with compressed oxygen.

c) Up-Draft nebuliser with Flatus Mk.V air compressor (Maymed, Anaesthetic Supplies Pty. Ltd., Sydney, Australia. This system is equivalent to: Tote-A-Neb, Hospitak Inc., Lindenhurst, NY., USA [private communication, Mefar SRL, Italy]).

d) Up-Draft nebuliser with Aerosol-One air compressor (Medical Industries America, Desmoines, Iowa, USA).

Temperature / time curves

The temperature of the nebuliser solution during aerosol generation was previously measured for each of the nebuliser systems tested (Phipps and Gonda 1990 [Chapter 3]). The temperature was recorded at set times until it reached a steady value (T_s). The initial volume of solution in the nebuliser was 5 ml and the ambient temperatures varied between 23.5 and 25.2 °C.

Output

As described previously (Phipps and Gonda 1990 [Chapter 3]), the mass output from the nebuliser systems was measured for different, constant, nebuliser solution temperatures by weighing the nebuliser. The temperature was controlled to ± 0.3 degrees with the aid of a warm water bath during a generation time of 3 or 4 minutes.

At the end of each run, the concentration of sodium chloride left in the nebuliser was measured by vapour pressure osmometry (Model 1100, Knauer, Bad Homberg, W. Germany). The output of solution and vapour was then calculated from the total mass output and the rise in nebuliser solution concentration during the time of aerosol production (Mercer et al, 1968):

$$W = [(V_o - V_t) / F \times t] \times Ln\ (C_t/C_o) / Ln\ (V_o/V_t) \quad ....(i)$$

$$A = [(V_o - V_t) / F \times t] - W \quad ....(ii)$$

where:

C_o = Concentration at zero time

C_t = Concentration at time t

V_o = Volume at zero time

V_t = Volume at time t

W = Vapour output (vol/vol)

A = Solution output (vol/vol)

F = Flow rate through nebuliser (vol/time)

t = Generation time

The predicted vapour concentration was calculated assuming that the vapour was supplied by the nebuliser solution alone ie,

$$M_{vI} = P_o\, a_w\, (M_w / (R\, T_I)) \qquad \text{....(iii)}$$

where:

P_o = Saturated vapour pressure at T_I.

a_w = water activity (see Appendix I) at the nebuliser concentration which was taken to be the average $(C_o\text{-}C_t) / 2$

M_w = Mol wt water

R = gas constant

T_I = nebuliser solution temperature (K)

Solute concentration in the droplets

The concentration of sodium chloride in the aerosol droplets was measured for different, constant, nebuliser solution temperatures as previously described (Phipps and Gonda 1990 [Chapter 3]). The aerosol was passed via either a short length of tubing (30 cm long and 2 cm diameter, volume = 94 ml, residency time = 0.45 s) or a long length of tubing (61 cm long and 5 cm diameter, volume = 1198 ml, residency time = 5.75 s) through the last stage of a cascade impactor (DCI6, Delron, Columbus, Ohio, USA) and collected in a small container of similar dimensions to a cascade impactor slide. The flow through the impactor stage was 12.5 l/min and the dilution air necessary to supplement the flow through the nebuliser was supplied either at ambient temperature (21 - 27 °C) and humidity (31 - 45%) or at ambient temperature and fully saturated with water vapour via a Douglas bag. After collection of the aerosol droplets, the concentration of sodium chloride was measured by vapour pressure osmometry.

Prediction of droplet solute concentration as a function of nebuliser solution temperature and dilution air humidity.

The mathematical treatment to predict the final droplet solute concentration at the mouthpiece is given in Appendix I. The parameters measured during each run (Table 1) were substituted into equations 13 (assuming ideal behaviour of the solution) and 15 (assuming non-ideal behaviour) to give the expected droplet solute concentration at the mouthpiece.

Table 1. Parameters measured

Generation time (t)

Initial mass of nebuliser solution (M_{ni})

Final mass of nebuliser solution (M_{nf})

Temperature of nebuliser solution (T_I)

Flow rate of generating gas (Q_I)

Relative humidity of dilution air (RH_d)

Relative humidity of generating gas (RH_g)

Initial concentration of nebuliser solution (C_{ni})

Final concentration of nebuliser solution (C_{nf})

Ambient temperature (T_{II})

The predicted values calculated by the two equations were compared with each other and with the measured droplet solute concentration values using the short and long connecting tubing.

Droplet sizing

The droplet size of the aerosols produced by the nebuliser systems at various operating solution temperatures was measured in separate experiments (Phipps and Gonda 1990 [Chapter 3]). The aerosol containing ^{99m}Tc pertechnetate was passed through the 7-stage cascade impactor via either the short or long connection tubing. The impactor slides containing the deposited radioaerosol were counted on a previously calibrated gamma camera (Phipps et al, 1987 [Chapter 2]) and the droplet size distribution calculated by a least squares fit to the data (Gonda et al, 1982).

In a separate experiment, the droplet size was measured with the nebuliser solution at ambient temperature with dilution air saturated with water vapour. This value was assumed to be the initial droplet size of the aerosol generated by the nebuliser.

The parameters given in Table 1 were measured during each run, and the predicted droplet size calculated from equation 20 (ideal solutions) and equation 21 (non-ideal solutions) in Appendix I. The predicted and measured droplet sizes

were then compared.

It was impossible to repeat each data point exactly, so the variability of the measurements was assessed using the Cadema nebuliser at 8 l/min (42 - 52% RH) and 10 l/min (43 - 56% RH and 100% RH). The droplet concentration was measured numerous times at various nebuliser solution temperatures. The parameters in Table 1 were again measured for each experimental point, and the theoretical droplet solute concentration (using the non-ideal equations of Cinkotai only) also calculated.

5.3. Results

Temperature vs time graphs

The fall in nebuliser solution temperature with time of generation has already been assessed for these systems (Phipps and Gonda 1990 [Chapter 3]). The temperature fell to reach a steady value of 11-15 °C after 4-5 minutes for the Up-draft and Cadema nebulisers with compressed oxygen, while with the Flatus and Aeromist compressors with the Up-Draft nebuliser, the temperature fell by 5-6 °C after the same generation time.

Output

The effect of nebuliser solution temperature on the total, solution and vapour outputs is shown in Figures 1-5.

Figure 1. Mass output at 8 l/min (*open squares*) and 10 l/min (*closed squares*) flow rate vs nebuliser solution temperature for the Cadema nebuliser (short tubing).

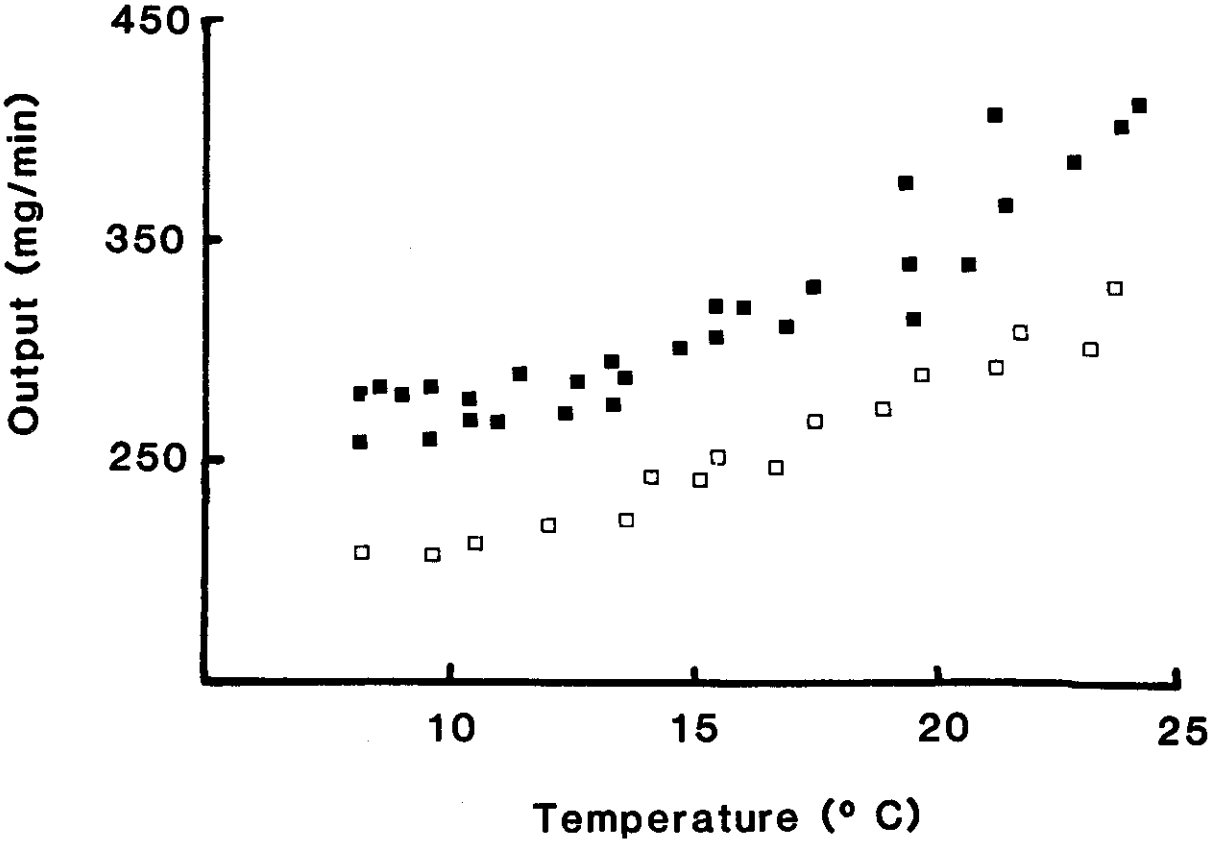

Figure 2 and 3. Output of the Cadema (Figure 2) and Up-Draft (Figure 3) nebulisers at 8 l/min flow rate vs. nebuliser solution temperature. Total mass output (*circles*), solution (droplets) output (*triangles*), vapour output (*diamonds*) and calculated water content at each nebuliser temperature (*squares*).

Figure 2.

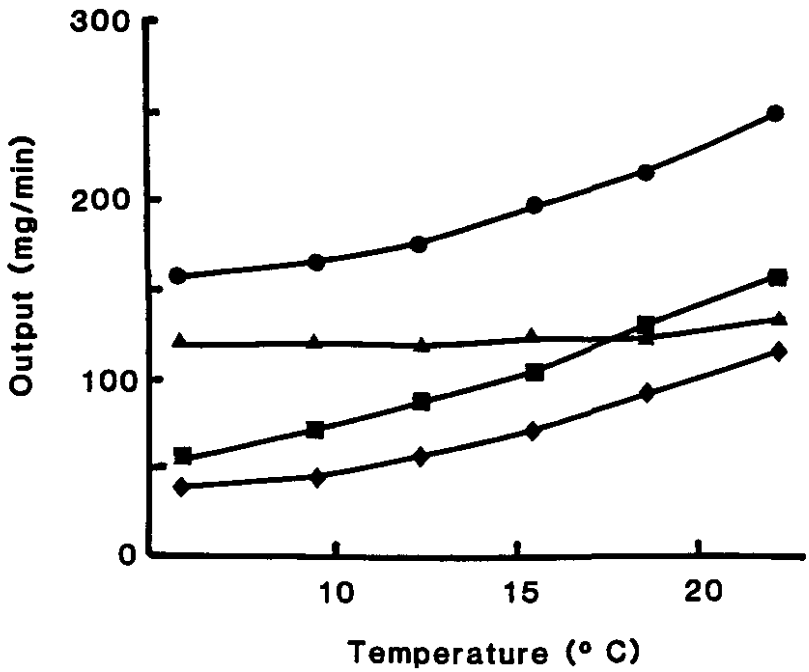

Figure 3.

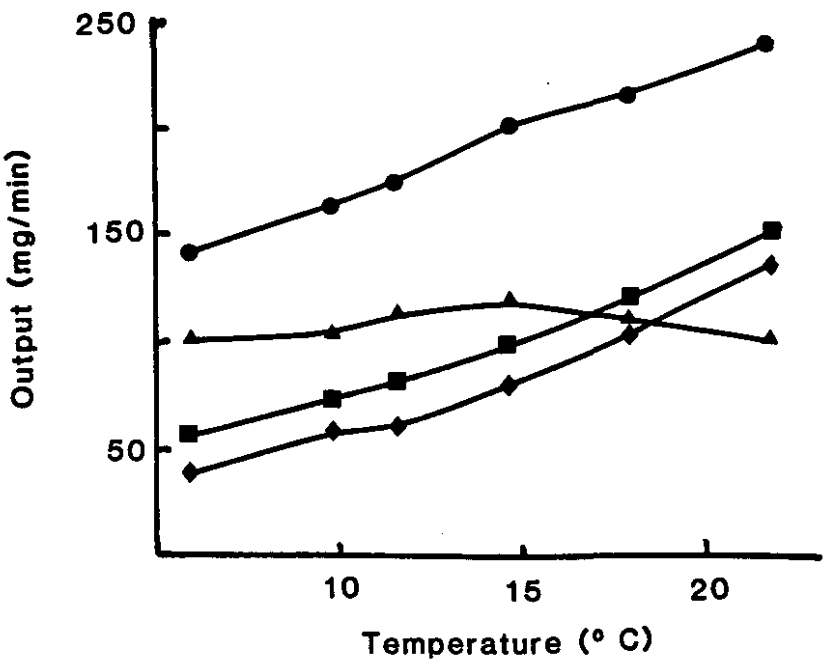

Figure 4 and 5. Output of the Up-Draft nebuliser driven by the Aerosol-1 (Figure 4) and Flatus (Figure 5) air compressors. Total mass output (*closed circles*), solution output (droplets) (*triangles*), vapour output (*diamonds*), calculated water content at each nebuliser temperature (*squares*) and water vapour contribution by the generating gas (*open circles*).

Figure 4.

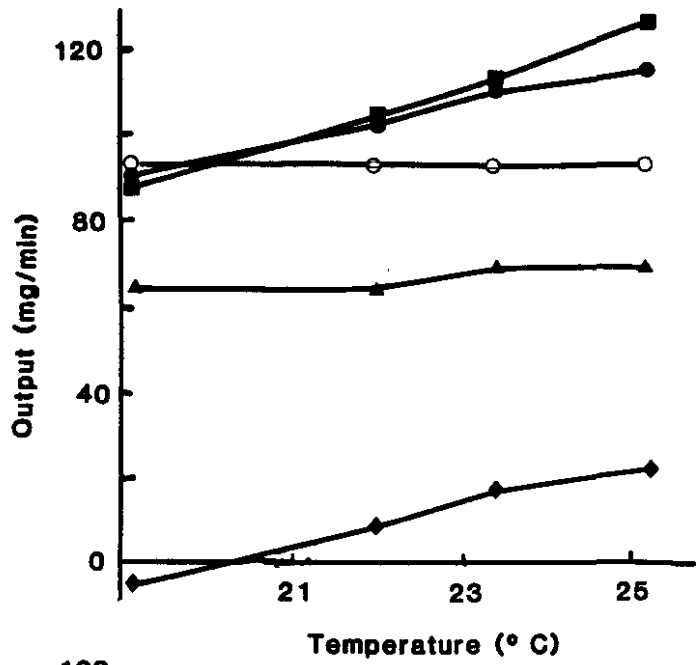

Figure 5.

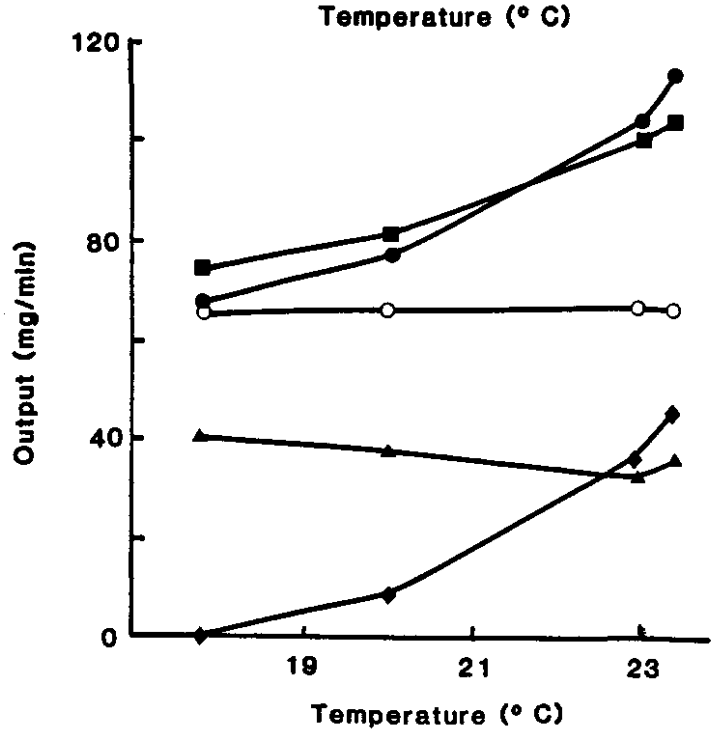

In general, the total output is lower as the nebuliser solution temperature drops, the variability being greater at temperatures close to ambient. This is demonstrated in Figure 1, for the Cadema nebuliser. By segregating the output, it can be seen that the solution output remains constant, so the fall in output is due to a fall in the vapour output alone. The vapour output required to saturated the aerosol stream at each nebuliser temperature was calculated from equation (iii) above and plotted in Figures 2-5. These calculated values were found to be greater than the measured nebuliser solution vapour output, suggesting that some of the vapour required to saturate the aerosol stream was supplied by the droplets.

In the case of the systems driven by air compressors, water is added from two sources, the generating gas (room air) which is partially saturated with water vapour and the dilution air. The contribution of vapour from the generating gas is also plotted in Figures 4 and 5. The water vapour required to saturate the aerosol stream [again calculated from equation (iii)], is similar to the total output from the nebuliser (solution plus vapour), highlighting the large amount of water contained in the gas phase in comparison to the droplets. The air compressors show the same pattern of output, with the contributions from the generating gas, dilution air and droplets all remaining constant, while the vapour supplied by the nebuliser solution varies with nebuliser temperature.

Concentration of solute in the droplets

Figure 6 shows the nebuliser solution concentration with generation time for the Cadema nebuliser. The concentration increase for each time increment becomes greater as generation progresses. A similar effect was found with all of the nebuliser systems tested, although the concentration increase was lower when air compressors were used.

The measured and theoretical droplet concentrations (using ideal and non-ideal equations) for each nebuliser temperature are shown in Figures 7-10.

The concentration of the collected droplets increases as the nebuliser cools. The droplet concentration at the mouthpiece for each nebuliser temperature was greater when the long tubing was used (Figures 7 and 8). The lowest temperature used in these experiments was approximately 6 °C, lower than the steady temperature (T_s) reached by the Cadema and Up-Draft with compressed oxygen (approximately 9°C). The greatest concentration at the T_s was 20.3 and 32.2% for the Up-Draft and Cadema respectively (long tubing) and 9.2 and 7.8% for the Up-Draft and Cadema respectively (short tubing). The theoretical concentration results for each experimental point are plotted alongside the measured results.

Figure 6. Nebuliser solution concentration vs. time of nebulisation for the Cadema nebuliser at 8 l/min flow rate.

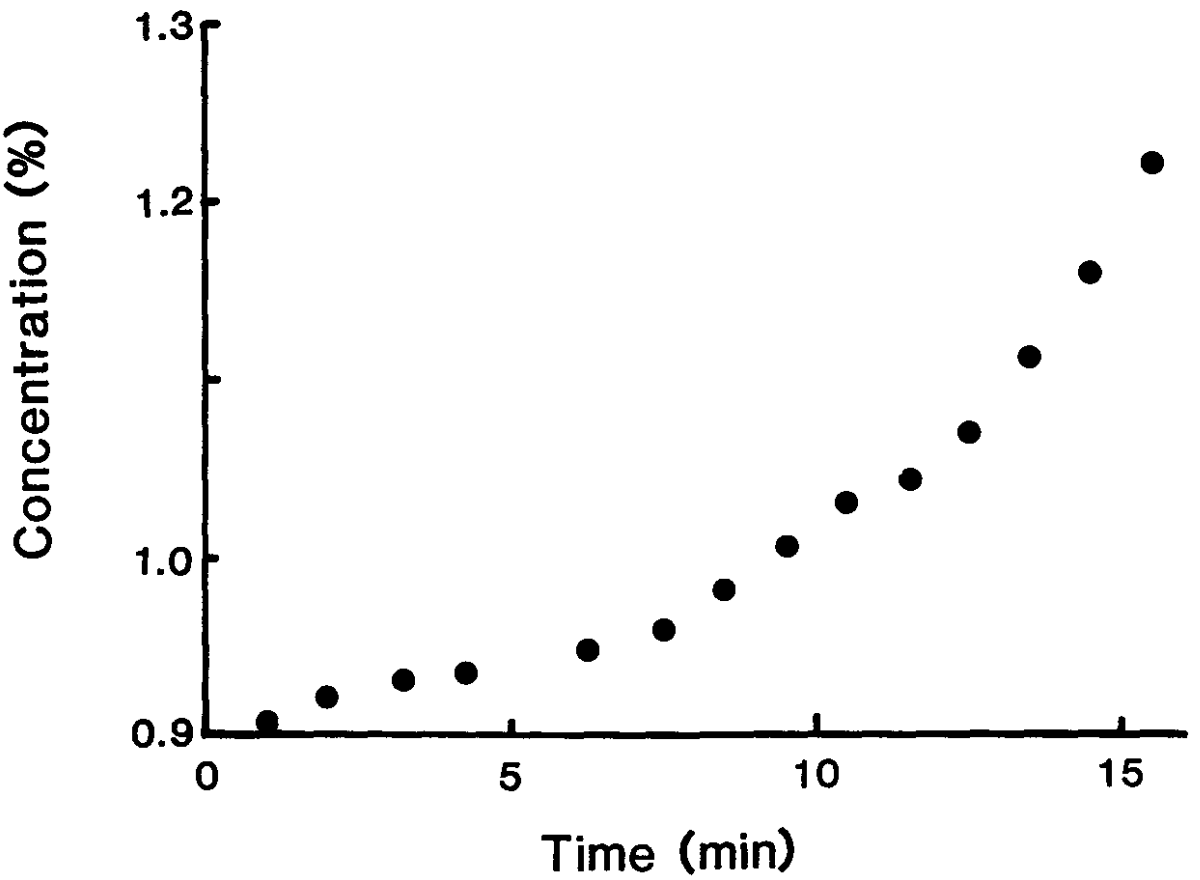

Figure 7. Measured (*circles*) and predicted (*squares*) droplet concentration values at the mouthpiece for the Up-Draft nebuliser at 8 l/min flow rate using long (*open symbols*) or short (*closed symbols*) tubing vs. nebuliser solution temperature. Figure 7a - assuming non-ideal solution behaviour and Figure 7b - assuming ideal solution behaviour.

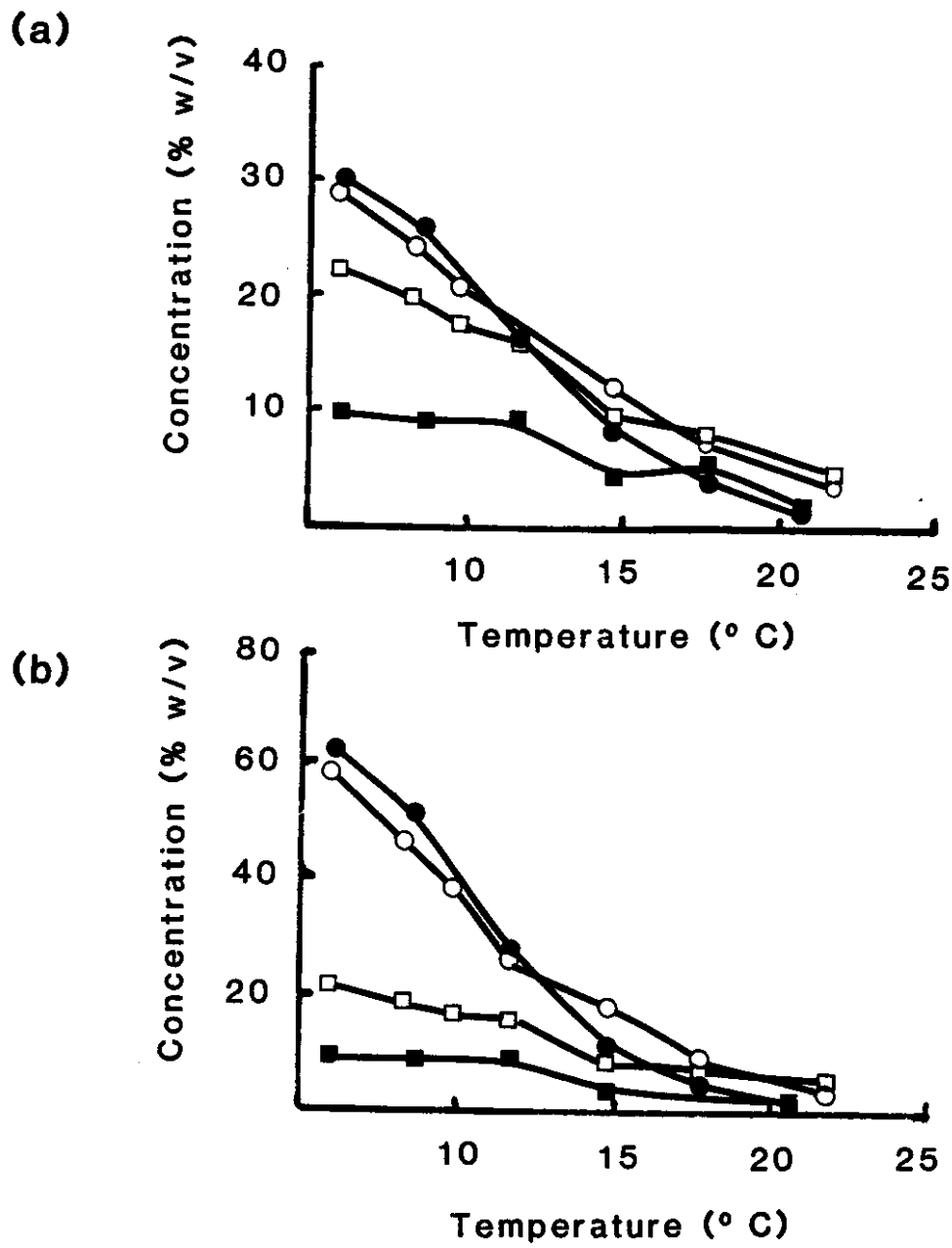

Figure 8. Measured (*circles*) and predicted (*squares*) droplet concentration values at the mouthpiece for the Cadema nebuliser at 8 l/min flow rate using long (*open symbols*) or short (*closed symbols*) tubing vs. nebuliser solution temperature. Figure 8a - assuming non-ideal solution behaviour and Figure 8b - assuming ideal solution behaviour.

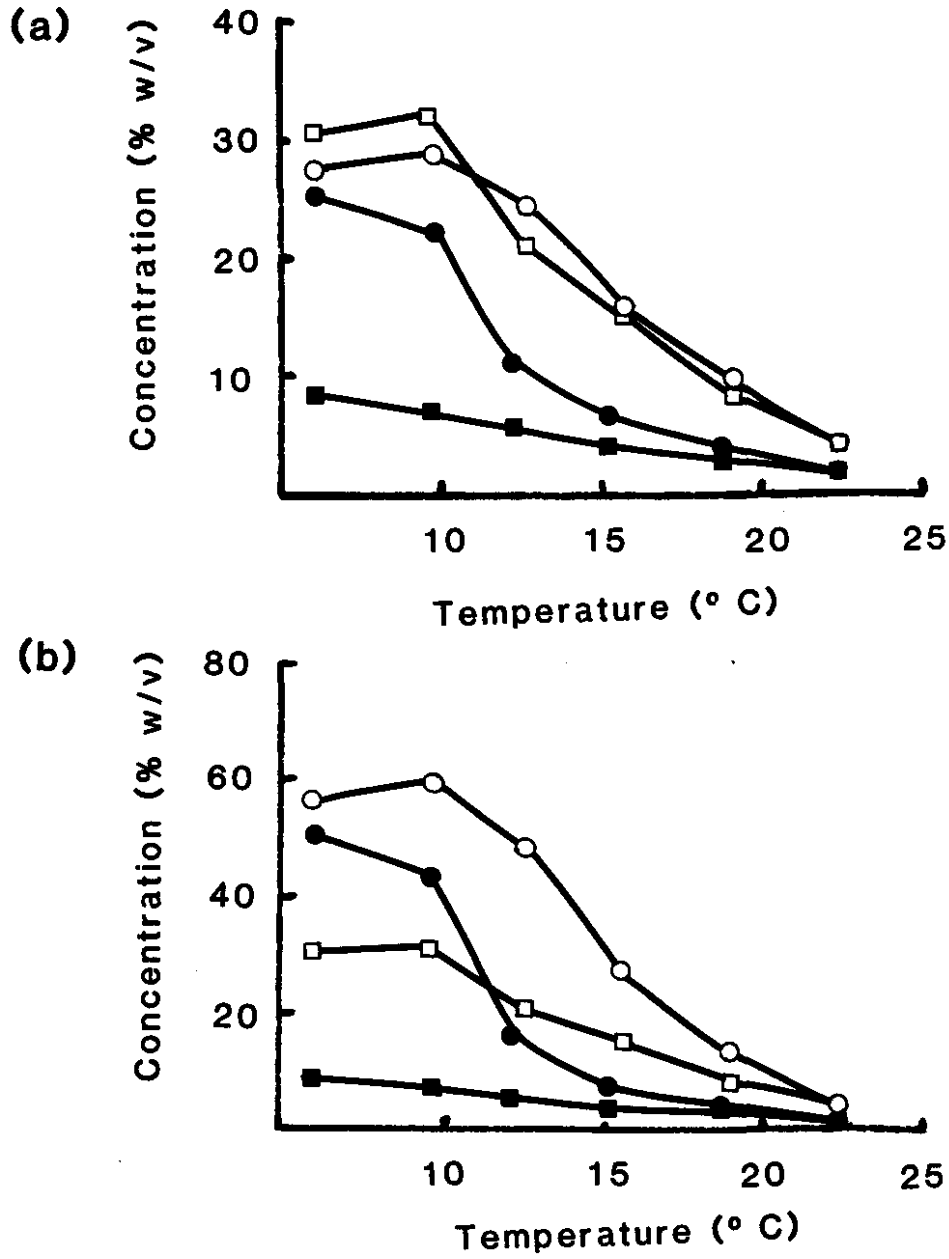

Figure 9. Droplet concentration at the mouthpiece of the Up-draft nebuliser driven by the Aerosol-1 compressor vs. nebuliser solution temperature. Measured concentration (*circles*), results predicted by assuming non-ideal solution behaviour (*open squares*) and assuming ideal solution behaviour (*closed squares*). The isolated data points represent values measured or predicted at ambient temperature with dilution air humidity of 100 %.

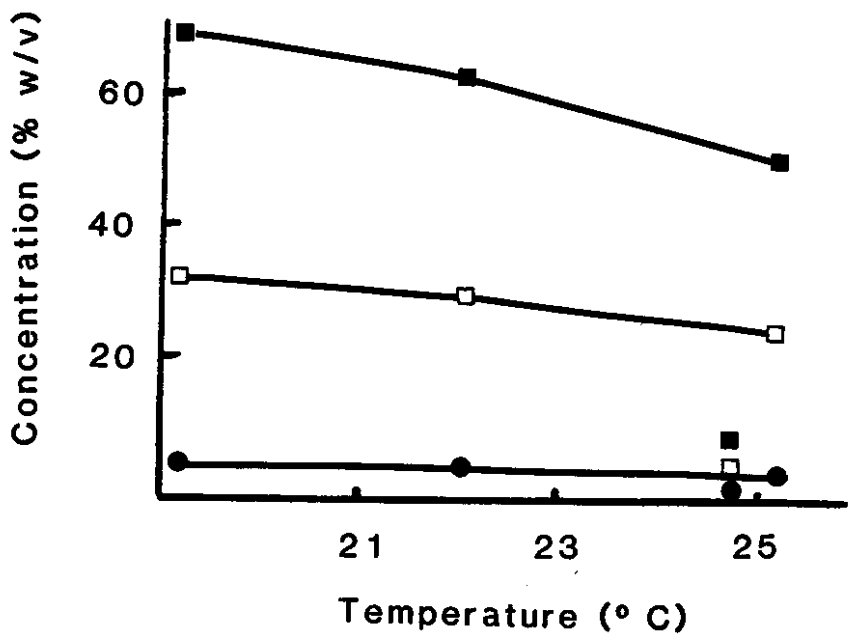

Figure 10. Droplet concentration at the mouthpiece of the Up-draft nebuliser driven by the Flatus compressor vs. Nebuliser solution temperature. Measured concentration (*circles*), results predicted by assuming non-ideal solution behaviour (*open squares*) and assuming ideal solution behaviour (*closed squares*). The isolated data points represent values measured or predicted at ambient temperature with dilution air humidity of 100 %.

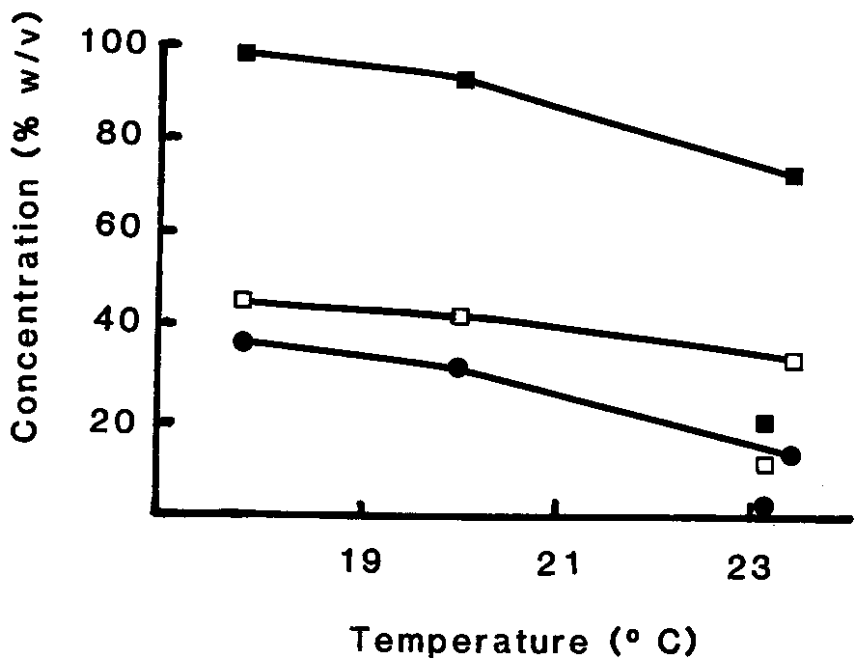

The variability of the data was assessed by repeated experiments, but since the experimental conditions could not be exactly reproduced, all data points have been plotted in Figures 12-14. It can be seen that the greater the likelihood of evaporation (at low temperatures), the bigger the variability in droplet concentration because of the sensitivity to external conditions (Phipps et al, 1987 [Chapter 2]). The variability is also likely to be due to small changes in output that will have disproportionately large effects on the mass of water in solution available for evaporation.

The ideal solution equations of Ferron et al (1976) do not fit the experimental results as closely as those describing non-ideal solution behaviour. The closest agreement between predicted and experimental droplet solute concentrations is therefore found when the long tubing is used and non-ideal solution behaviour assumed. Figure 11 shows the measured vs predicted solute concentration values for the long tubing, assuming ideal solution behaviour (for complete agreement, the data points should lie along the line of identity). Table 2 gives the intercept, slope and correlation coefficients of the measured vs predicted droplet solute concentration results for the Up-Draft and Cadema (non-ideal solution behaviour) with long and short tubing. The long tubing data has a slope much closer to unity, indicating closer correlation of measured with experimental than the short tubing.

The combined effects of changing the RH of dilution air and the proportion of aerosol to dilution air are shown in Figures 12-14. The greater the proportion of dilution air the greater the evaporative effects on the droplets (Figures 12 and 13). When using saturated dilution air, these effects are smaller yet significant (Figure 14).

Figure 11. Graph of measured vs predicted droplet solute concentration for the Cadema (*closed squares and dotted line of best fit*) and Up-Draft (*open squares and dashed line of best fit*) nebulisers, with long tubing (assuming non-ideal solution behaviour). The solid line denotes the line of identity.

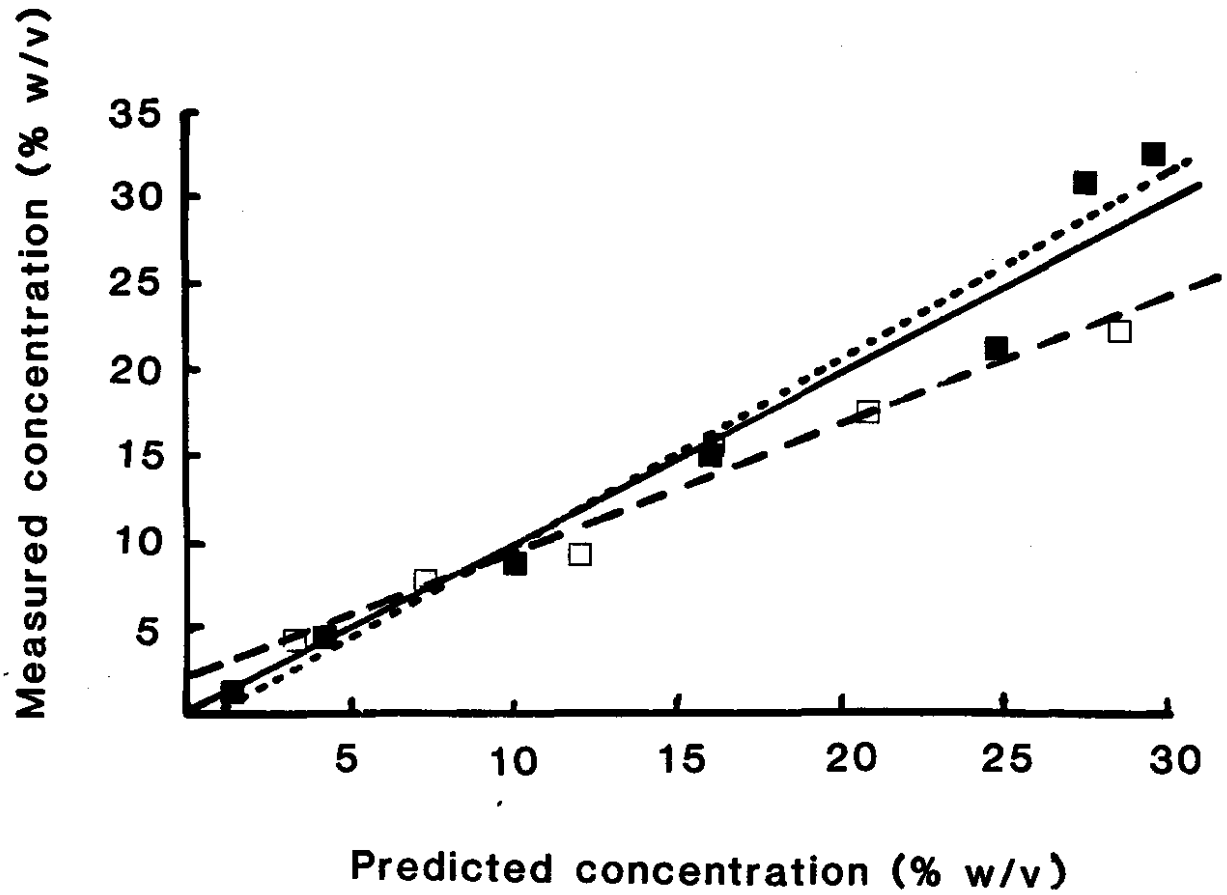

Table 2. Linear regression equations and correlation coefficients of plots of measured vs predicted droplet solute concentrations for the Cadema and Up-Draft nebulisers, long and short tubing (assuming non-ideal solution behaviour). A slope of 1 and intercept of 0 denotes identical measured and predicted values.

	Intercept (% w/v)	Slope	Correlation coefficient
SHORT TUBING			
Cadema	2.7	0.24	0.986
Hudson	2.6	0.27	0.883
LONG TUBING			
Cadema	-0.8	1.06	0.984
Hudson	2.3	0.72	0.984

Figure 12. Measured (*circles*) and predicted (*triangles*) droplet concentration values at the mouthpiece for the Cadema nebuliser at 8 l/min flow rate and dilution air of 50% relative humidity vs. nebuliser solution temperature.

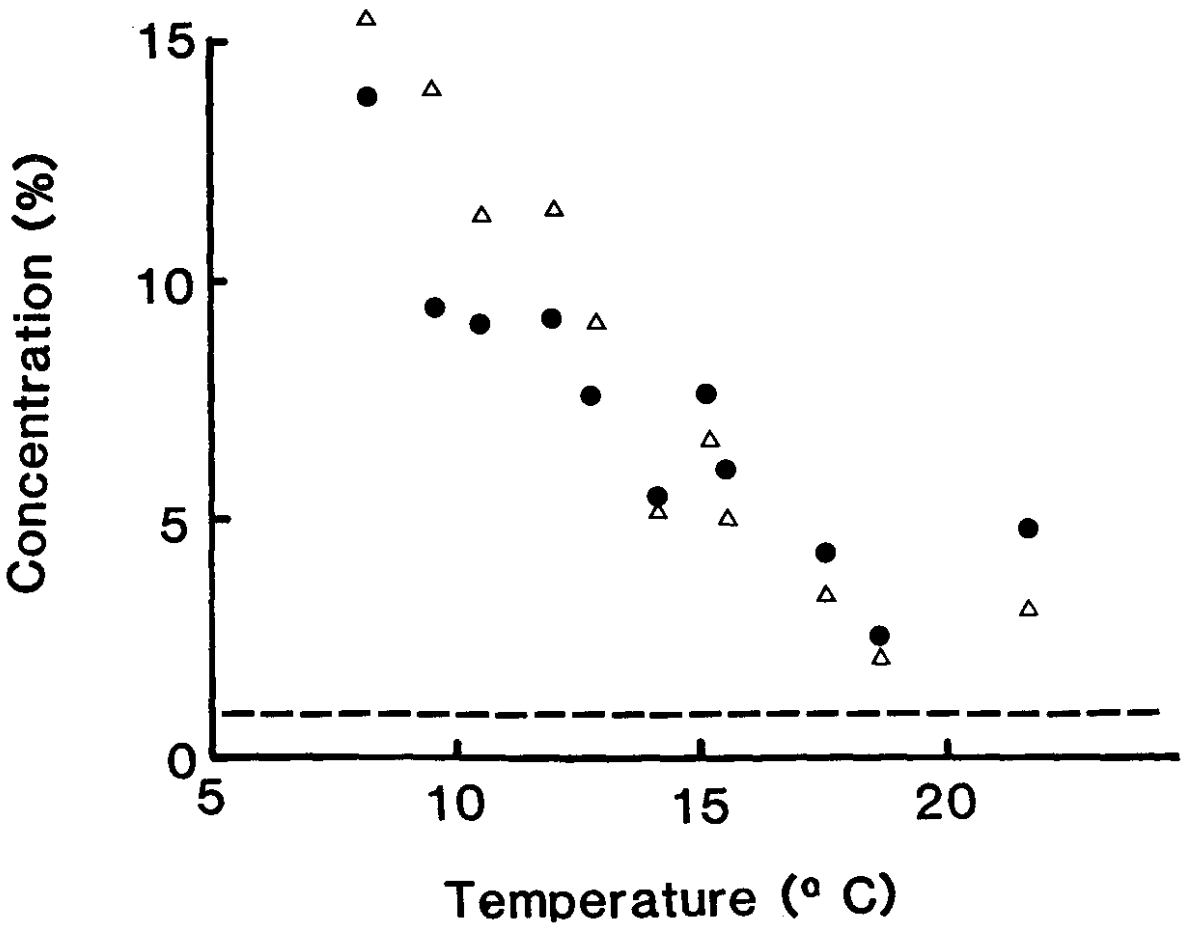

Figure 13. Measured (*circles*) and predicted (*triangles*) droplet concentration values at the mouthpiece for the Cadema nebuliser at 10 l/min flow rate and dilution air of 50% relative humidity vs. nebuliser solution temperature.

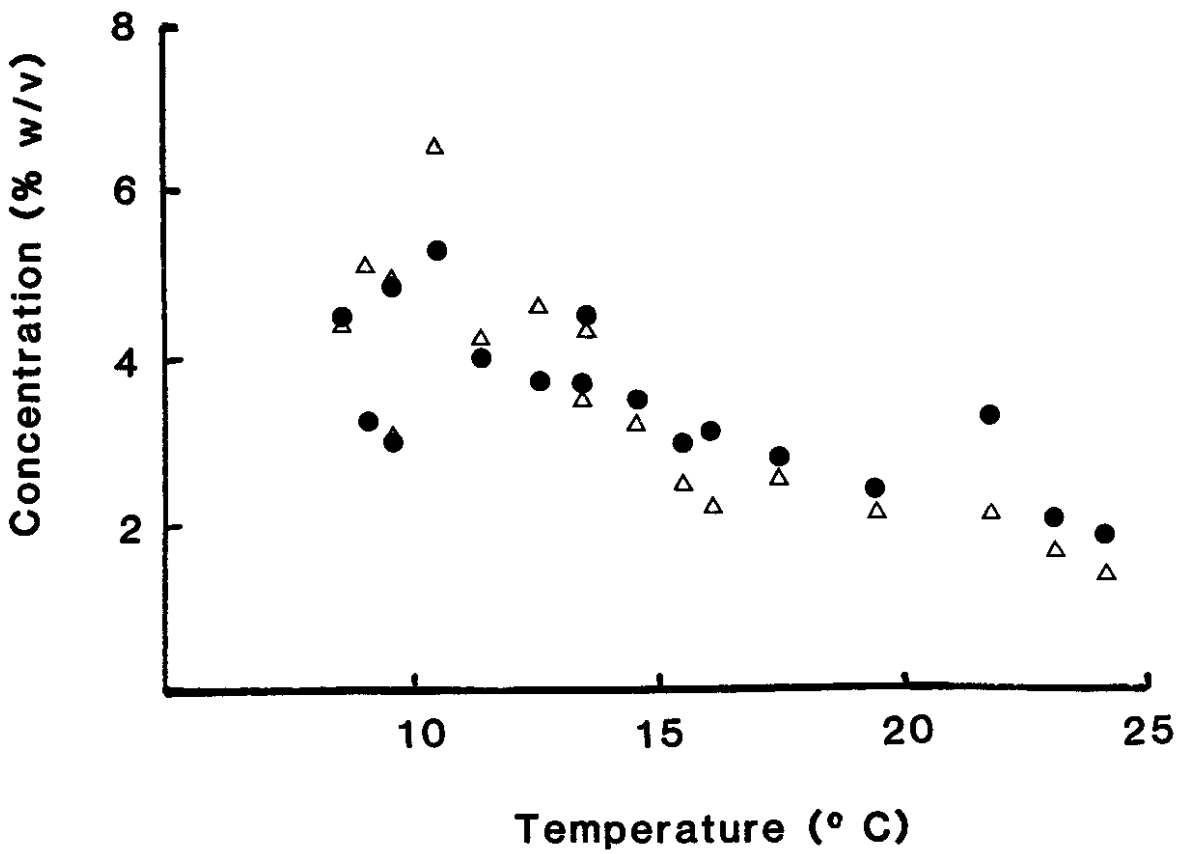

Figure 14. Measured (*circles*) and predicted (*triangles*) droplet concentration values at the mouthpiece for the Cadema nebuliser at 10 l/min flow rate and dilution air of 100% relative humidity vs. nebuliser solution temperature.

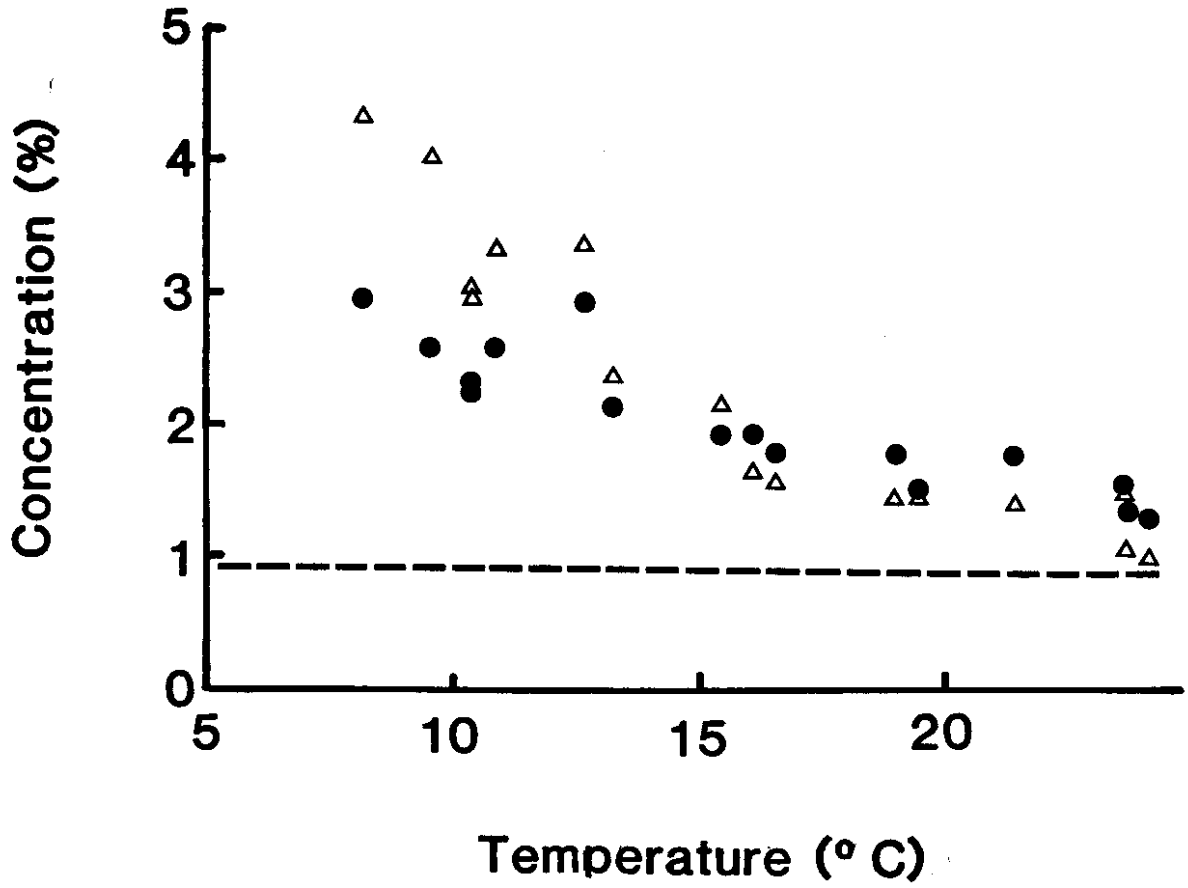

Figure 15. Measured (*circles*) and predicted (*squares*) droplet size for the Cadema nebuliser at 8 l/min flow rate vs. nebuliser solution temperature. Figure 15a - using short tubing (residence time of 0.45 s) and Figure 15b - using long tubing (residence time of 5.75 s).

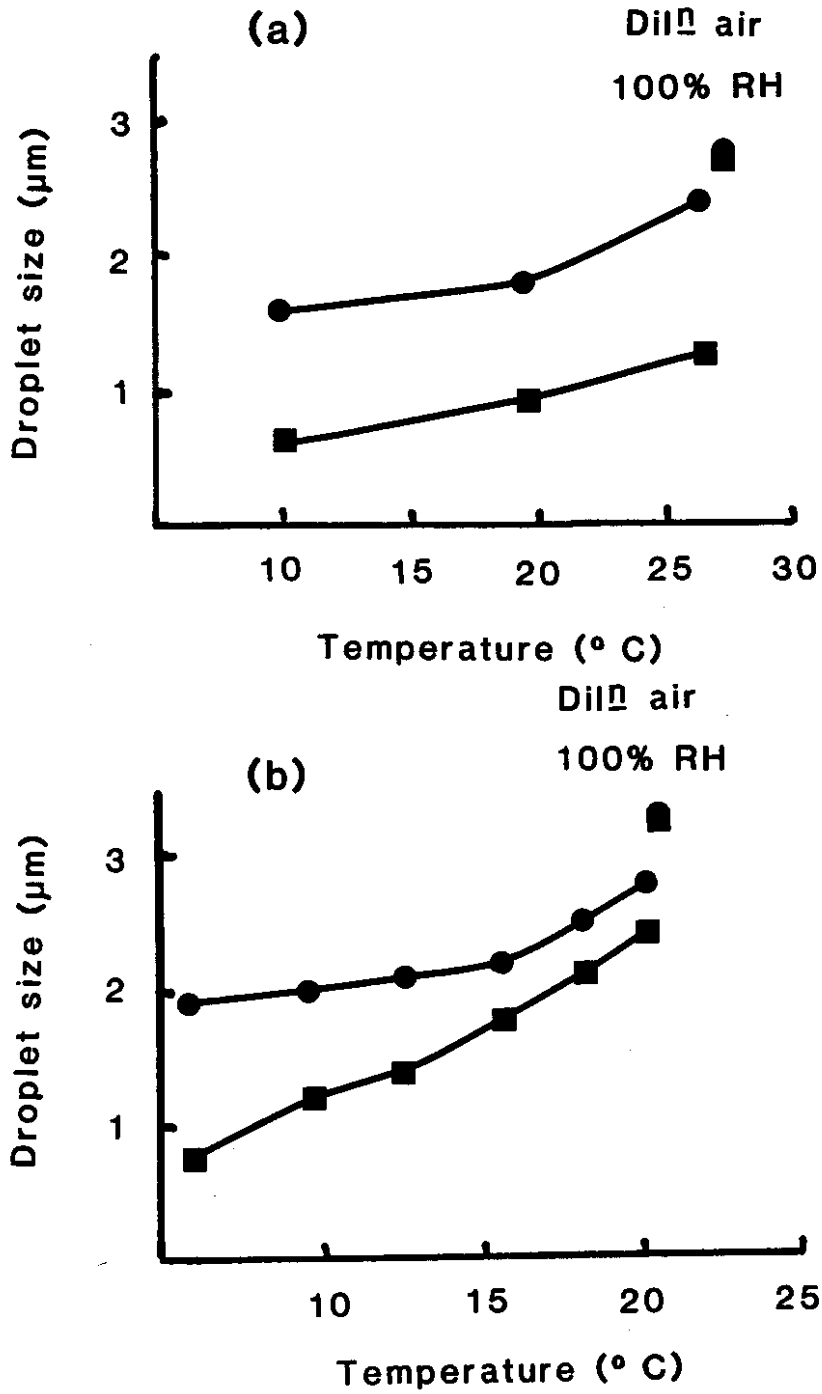

Figure 16. Measured (*circles*) and predicted (*squares*) droplet size for the Up-Draft nebuliser at 8 l/min flow rate vs. nebuliser solution temperature. Figure 16a - using short tubing (residence time of 0.45) and Figure 16b - using long tubing (residence time of 5.75 s).

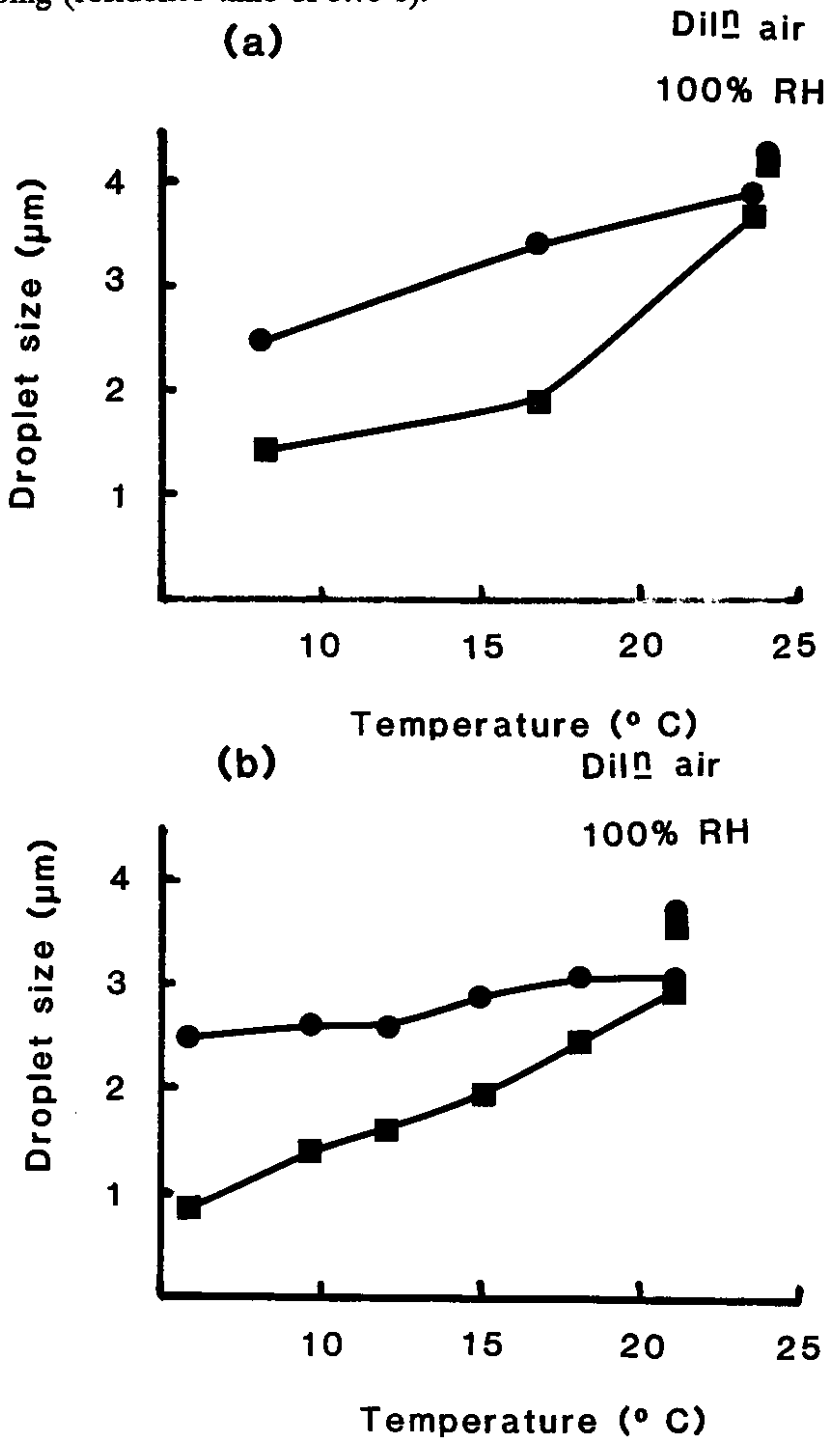

Droplet size

The change in droplet size (MMAD) with nebuliser temperature (Cadema and Up-Draft) is shown in Figures 15 and 16. As expected, the droplet size falls as the nebuliser temperature is reduced. The theoretical MMAD is calculated from equation 21 (for non-ideal solutions, Appendix I) and plotted on the same axes. The difference between theoretical and measured droplet sizes is large for both the long and the short tubing. The expected droplet sizes are approximately 1μm lower at 10°C than those measured, for both the long and short tubing. The disparity is also generally greater at the lower temperatures.

5.4. Discussion

The mass balance equations presented here are an attempt to explain and predict the changes occurring in aerosol droplets before inhalation. The factors effecting the characteristics of droplets generated by jet nebulisers have been studied previously (Ferron et al, 1976; Newman et al, 1986; Sterk et al, 1984; Porstendorfer et al, 1977), but until recently, the specific effects of nebuliser solution temperature on solute concentration as measured directly, have not been studied (Phipps and Gonda 1990 [Chapter 3]). The data presented here shows that droplets move towards an equilibrium that can be predicted, and that the attainment of that equilibrium depends on environmental factors and the time between generation and inhalation.

The output of the aerosol governs the dose of solute delivered to the mouthpiece. The total output decreases as the nebuliser solution temperature falls towards T_S, but this is due to the reduction in vapour output rather than that of the solution, because less water vapour is required to saturate the aerosol stream at lower temperatures (Figures 2-5). The solute output is likely to rise slowly as the solute concentration in the nebuliser solution rises, although this effect is small over the first 10 minutes of generation (Figure 6) and depends on the initial nebuliser loading and rate of evaporation.

The calculated vapour required to saturate the aerosol stream at any nebuliser temperature was greater than the measured vapour output from the nebuliser solution (Figures 2-5). The extra vapour required may therefore come from the droplets that leave the nebuliser, adding to the droplet solute concentration increase. Similar calculations with the compressor driven nebulisers are complicated by the water content of the generating gas, but the generating gas vapour, plus the measured vapour output from the nebuliser was greater than the calculated vapour required.

The concentration of solute in the droplets is expected to increase as the nebuliser solution temperature falls. This effect is primarily due to evaporative water loss as the aerosol stream warms towards room temperature and is compounded by the addition of unsaturated dilution air. The predictions assume

equilibration of the droplets at room temperature by the time they reach the mouthpiece. Using the short tubing, the droplet solute concentration is below that predicted by the ideal and non-ideal solution equations, suggesting that the droplets in the aerosol stream are not reaching room temperature and equilibrium concentration. By increasing the time for droplet equilibration by using connecting tubing with a large volume, and therefore a longer residence time, the solute concentration at the mouthpiece is closer to that predicted by the mass balance equations. It is notable that the droplets produced at the lower nebuliser temperatures are furthest from equilibrium at the mouthpiece because they have more water to lose. The evaporation of the droplets involves loss of heat of vaporisation, keeping the droplets cool. The transfer of heat from the room to the aerosol stream, across the tubing walls, is likely to be the limiting factor.

By measuring the temperature of the aerosol stream at the mouthpiece and substituting this value in place of the ambient temperature in the mass balance equations (T_{II}), a more reliable estimate of droplet concentration using the short connecting tubing may be found.

The comparisons between the predicted droplet solute concentrations using the ideal and non-ideal solution equations with the experimental data shows that by assuming ideal behaviour of the solute, the effects of droplet evaporation

between the nebuliser and mouthpiece are overestimated.

The variability in the droplet solute concentration may be accounted for by experimental error together with variations in the output and temperature of the nebuliser, all of which will effect the droplet solute concentration. In particular, small changes in the output of the nebulisers may have a large effect on the droplet solute concentration because at any nebuliser temperature, the vapour output will be constant and the solution output, being a relatively small fraction of the total, will be affected to a large extent. For example, at 21 °C the Aerosol-1 has a total output of 98 mg/min. The total amount of vapour leaving the nebuliser is expected to be 100 mg/min of which 93 is from the generating gas and 4 from the nebuliser solution, leaving 3 mg/min to come from the 64 mg/min solution output. The output leaving the nebuliser therefore consists of 61 mg/min of solution, and 100 mg/min of vapour. Water vapour required to saturate the aerosol stream as it increases in temperature must come from the solution output. If the droplets have concentrated to 10 %, the solution component will be approximately 5.8 mg/min and vapour 155 mg/min. Any small variations in the final temperature of the aerosol stream (where one degree can alter the vapour component by up to 10 mg/min) could easily alter the droplet solute concentration by a factor of two or more.

The theoretical and measured droplet sizes do not coincide when either the long

or short tubing is used. Although their size has fallen and solute concentration increased, the droplets are clearly not reaching equilibrium in the short tubing and are therefore larger than predicted on reaching the mouthpiece. This is not the case in the long tubing, where the droplet concentration is close to that predicted. The longer residence time and lower velocity of the droplets passing through the long tubing will allow the preferential sedimentation of the larger droplets in the aerosol stream. The assumed initial size of the droplets, measured at ambient temperature and with fully saturated dilution air (no droplet evaporation) will therefore be lower than the actual size leaving the nebuliser. At lower temperatures however, the proportion of larger droplets and hence sedimentation will be reduced as the droplets evaporate. The magnitude of sedimentation may be estimated from a knowledge of the sedimentation velocity of unit density spheres (Hinds 1982). For example, the 10 μm droplets fraction has a settling velocity of 0.305 cm/sec, in the 5.75 seconds residence time of the large tubing, any of these droplets within 1.8 cm vertical distance of the wall will deposit. Assuming even distribution of the droplets in the aerosol stream, the proportion depositing will be approximately equal to 50 % of the difference in cross sectional area between the tubing radius (2.5 cm) and the area of a circle of 1.8 cm smaller radius (2.5 - 1.8 = 0.7 cm) ie. approximately 46 %. Corrections may therefore be attempted, however, other factors such as turbulence will also increase the likelihood of the larger droplets depositing in the tubing.

These results show that although nebulised aerosol droplets are unlikely to reach equilibrium at the mouthpiece of most medical nebulisers, the effects of evaporation due to warming and low dilution air humidity are large, especially if the nebuliser systems have a low output. It may also be concluded that these droplet size and concentration changes may be minimised by using saturated generating gas and dilution air. The actual concentration attained at the mouthpiece will be a function of the residence time, temperature difference between the aerosol stream on production and the room, the volume, RH and temperature of dilution air and the rate of heat transfer across the tubing. The actual reduction in concentration is likely to be higher in reality because the proportion of dilution air to aerosol is usually greater during inspiration than in these experiments. The droplet size at equilibrium is harder to predict, since it depends on size selective losses within the tubing.

The prediction of droplet characteristics at equilibrium is, however, useful in comparing nebuliser systems and assessing the effects of aerosol generation and environmental conditions on droplet size and solute concentration at the mouthpiece. This in turn will allow the prediction of regional deposition and effects within the lung such as the possibility of bronchoconstriction by non-isotonic aerosols (Schoeffel et al, 1981).

Chapter 6

Apparatus for the control of breathing patterns during aerosol inhalation.

6.1. Introduction

The regional and total deposition of therapeutic and diagnostic aerosols has been shown experimentally and mathematically to depend on particle characteristics, dimensions of the lungs and mode of inhalation (Brain and Valberg 1979).

Important particle parameters include mass median aerodynamic diameter (Stahlhofen et al, 1983; Stahlhofen 1984) and the shape of the droplet size distribution (Gonda 1981). Patient parameters effecting deposition pattern include lung morphometry (Yu et al, 1979) and effects of airway obstruction from oedema, bronchoconstriction and excess mucus (Dolovich et al, 1976; Goldberg and Lourenco 1973).

Of particular importance is mode of inhalation, which affects both time and velocity dependent mechanisms of particle deposition within the upper and lower airways (Lippmann et al, 1980). Inhalation parameters known to affect patterns of deposition include; tidal volume, inhalation flow rate, inspiratory pause or

breath holding time and lung volume at the start of inhalation (ie functional residual capacity)(Newman 1984).

Many diagnostic and research study regimes require the subject to inhale an aerosol on more than one occasion; bronchial challenge tests, mucociliary clearance estimation and any studies comparing efficacy of inhaled medications are good examples. The fact that regional and total deposition of aerosols can vary with breathing pattern (Lippmann et al, 1980) means that breathing parameters must be controlled or taken into account during such studies, for example, the necessity for good control of aerosol inhalation during mucociliary clearance studies, has been recognised (Agnew et al, 1981; Dolovich et al, 1987; Pavia 1984).

A number of techniques have been used to monitor and control inhalation: maximal inhalations from residual volume (RV) (Ruffin et al, 1978; Svartengren et al, 1987) or functional residual capacity (Pavia et al, 1980; Oldenburg et al, 1979), single breaths following a kymograph trace (Laube et al, 1986), tidal breathing, following an audible timing device such as a metronome alone (Matthys and Kohler 1985) or with a visual volume target such as an oscilloscope (Phipps et al, 1987 [Chapter 2]; Clay and Clarke, 1987; Ilowite et al, 1987) or a chart recorder trace (Mitchell et al, 1987). In some investigations, breathing pattern was not controlled at all (Isawa et al, 1987; Foulds and Smithuis 1983;

Asmundsson et al, 1973). Many of these methods do not account for changes in all of the breathing parameters thought to be important for aerosol deposition, both during any single aerosol inhalation occasion, and between two occasions. If targets for tidal volume and frequency are used alone, inhalation flow rates are not controlled, because the ratio of time of inspiration and expiration may vary from breath to breath with variation in inspiratory and expiratory pauses (Heyder et al, 1973).

Aerosol inhalation studies may also require the subject to follow a pre-set breathing pattern with well defined parameters of tidal volume, inspiratory flow rate and breath holding, for example in the assessment of the effect of inhalation pattern on regional and/or total deposition (Stahlhofen 1983; Foster et al, 1988; Agnew et al, 1985) or on the clinical response to inhaled therapeutic or diagnostic challenge agents (Ruffin et al, 1981; Ruffin et al, 1978). In this case, variability of inhalation also needs to be controlled with a pre-set target pattern. For single inhalation studies, control should be undertaken to ensure a consistent breathing pattern while the aerosol is being inhaled. For repeat inhalation studies, these variables should also be controlled for each inhalation occasion.

Our aim, therefore, was to produce a breath-by-breath aerosol inhalation monitoring and controlling system with the aid of a microcomputer, that would enable us to record and control the subjects' own tidal breathing pattern during

repeated inhalation of nebulised aerosols.

6.2. Breathing circuit

An aerosol inhalation breathing circuit was set up (Figure 1). It was a one-way, partially closed system. Aerosol was generated with compressed oxygen, or compressed air, via a jet nebuliser. Dilution air to make up the inspiratory flow was supplied via a humidifier (MR 310U, Fisher Paykel Ltd. Auckland, New Zealand). The aerosol was inhaled through a mouthpiece and exhaled through a filter and CO_2 absorber (Durasorb, Medical and Industrial Equipment Ltd. Exeter, England). The inspiratory and expiratory lines passed into a meteorological balloon (Kaysam Corporation, Patterson, New Jersey, USA) in a perspex box, the volume respired being displaced from the box by the balloon. A bell spirometer (Gould Godart BV., Bilthoven, The Netherlands) was connected to the box via a respiratory flow transducer (Hewlet Packard 47304A) and a pneumotachograph (21073B Hewlet Packard, Waltham, MA., USA). The bell spirometer had a servo-potentiometer attached to the bell pulley supplied with 5V DC. A vacuum was applied to the circuit via a needle valve to evacuate from the system an appropriate amount of air to keep the system isovolumetric. The tubing used was clear polypropylene of 2 cm internal diameter.

Figure 1. Diagram of the breathing circuit set-up. Adapted with permission from the publishers (Phipps et al, 1989 [Chapter 7]).

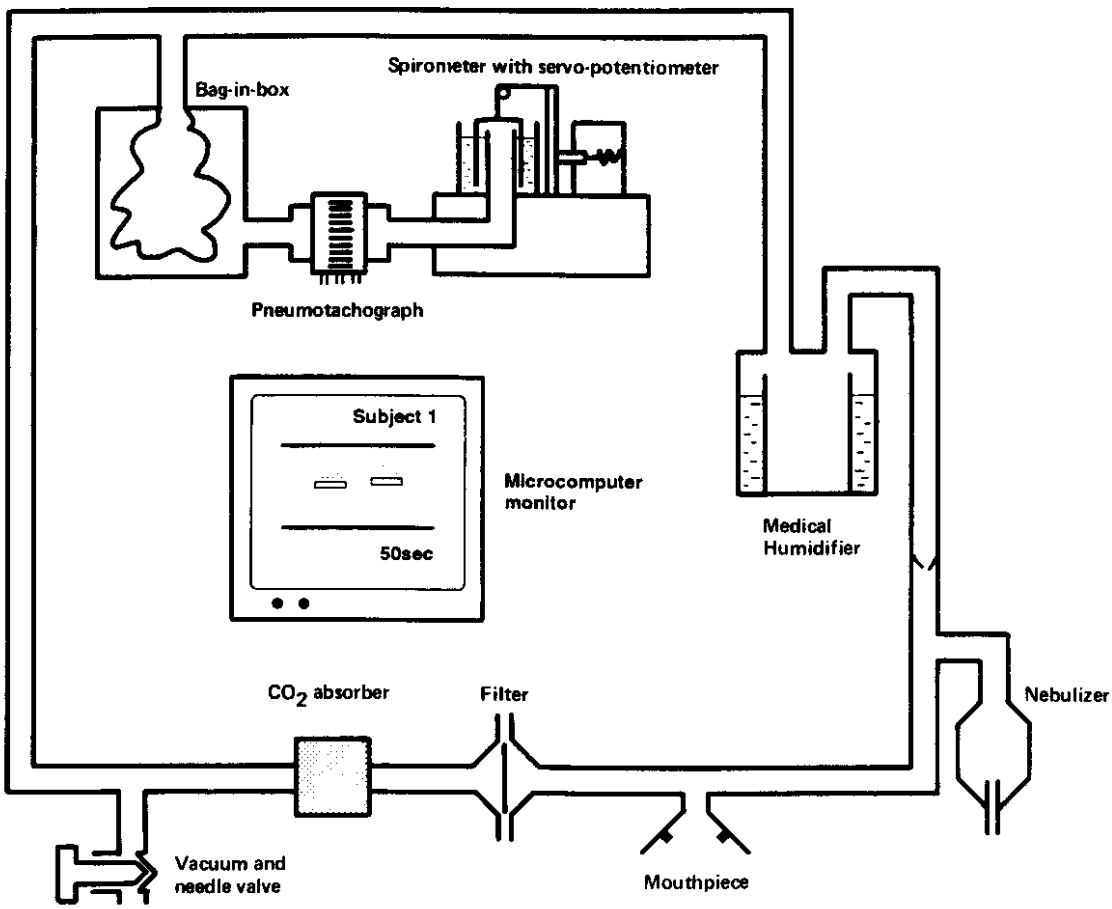

The volume signal from the bell servo and the flow signal from the respiratory flow transducer were passed to an analogue to digital converter (ADC), linked to an IBM PC XT (IBM Corp, Boca Raton, Florida USA), for analysis. The volume was also recorded on the spirometer kymograph trace, and the flow on a chart recorder (Sekonic Instrument Co., Tokyo, Japan).

The flow and volume signals were accessed and manipulated with software written on the IBM PC with the aid of a Turbo Pascal compiler (Borland International Inc., California, USA).

The linearity of the volume and flow signals as sampled from the ADC were obtained by plotting ADC units vs actual volume and flow as measured from the volume kymograph trace and rotameter (Platon Ltd., Basingstoke, England) respectively. The ADC flow and volume values were then related to volume and flow by an equation that was used to convert ADC count into volume and flow.

6.3. Breath monitoring and control system

The program developed is menu driven and includes a number of peripheral functions, these are:

a) Patient data: sex, age, height, weight and other information if necessary, are stored in an output file.

b) Environmental data: The date and ambient conditions of temperature, pressure and humidity are recorded.

c) Calibration: Volume and flow can be calibrated against ADC values.

d) Save and rename files: All data files are renamed to avoid overwriting and saved.

e) Help: Each function is explained.

6.4. Overview

This program is designed to aid in monitoring and controlling a pre-set or a subject's breathing pattern on any number of occasions for aerosol inhalation or any other purpose. The subject breathes on the circuit and the flow and volume signals are passed to a microcomputer. These signals are used to display the tidal breathing pattern on the computer screen. The program then samples a breathing period, defined by the operator. Mean breathing parameters of frequency, inspiratory and expiratory times, expiratory pause and tidal volume are calculated and this pattern is displayed as a target on the computer screen. The subject is then able to follow this pattern with a yellow line which corresponds to the tidal volume produced by the subject in real-time, thus enabling a reproducible breathing pattern to be maintained at all times and on any number of occasions.

After the set test period (ie, time of aerosol inhalation), the program calculates

the breath-by-breath parameters for that period, saves the results in files and displays the results on the screen in the form of a graph with mean and standard deviation values.

6.5. Detailed description.

[1]. Sample breathing:

The subjects' breathing pattern is sampled and the data stored in data files. The values of volume and flow are sampled from the ADC at a rate of approximately 10 Hz. The subject can be instructed to perform normal relaxed tidal breathing or any other pattern. The maximum volume is determined by the spirometer bell (6 l), the maximum flow rate by the limits of the pneumotachograph (linear to 100 l/min). Minimum tidal volume and flow rate is determined by the resolution of the system (approximately 5 ml and 2 l/min respectively).

A period of sampling is initiated by a keystroke and volume, flow rate and time (determined from the sampling frequency; ie time = number of samples / sampling frequency), are saved in arrays in memory.

Sampling is then ended by another keystroke after a suitable length of time as determined by the investigator, the data is then stored in data files.

[2]. Calculation of sample results:

Breath-by-breath mean and standard deviation values of the following parameters are calculated:

Tidal volume, time of expiration, time of inspiration, expiratory pause, inspiratory flow and expiratory flow (the latter two are recorded but not used for target parameters).

The end of a breath is taken to be at the end of expiration. This point in time is found when both of the following conditions are met:

i) Flow is < -2 l/min (i.e., more negative) and

ii) Flow is < the last value of flow (ie more negative) for two consecutive points.

This is not exactly at the point of inspiration but this is accounted for in the calculations by taking the last-but-one value of time increment as the time of end expiration. The delay is to account for small fluctuations in flow during the expiratory pause, where false breaths would otherwise be recorded.

The end of inspiration is found in a similar manner:

i) Flow > 2 l/min, and

ii) Flow > last value of flow for two consecutive points.

Expiratory pause is defined as the time while the following conditions are met (note that inspiratory flow is negative):

a) Expiration = true, and

b) Flow is between +2 and -2 l/min. (2 and -2 l/min was chosen as arbitrary limits to account for small baseline fluctuations).

At the end of a breath, the parameters of that breath are calculated and stored. At the end of the sample calculation procedure, the mean and standard deviation values are calculated and stored in a sample data file.

[3]. Run Test

Target values of tidal volume, time of expiration, time of inspiration and expiratory pause from the sample file produced from [2] are used in a sine wave equation to produce the target volume pattern to be displayed on the screen:

For Inspiration; Target volume = $a \sin (2\pi/f_i)$

For Expiration; Target volume = $a \sin (2\pi/f_e)$

Where:

a = amplitude (tidal volume/2)

$f_i = 2 \times$ time of inspiration (T_i)

$f_e = 2 \times$ time of expiration (T_e)

The reciprocal of inspiratory time is used as the frequency of the sine wave during inspiration, and the expiratory time is used in the same way for expiration. Expiratory pause is built into the pattern separately by halting the target pattern at the end of expiration for the time of expiratory pause (Figure 2).

The screen display is shown in Figure 3. The subject's tidal volume is displayed as a yellow line which is a function of the volume signal entering the ADC. Using the calibration, the ADC value is converted to ml. This value is then converted to screen units (integers between 1 and 200). The screen units are smoothed with a 4-point moving filter before display on the screen. The filter averages the last three and the current value, ie:

(Last-but-two + Last-but-one + Last + Current)/4 = Current

The target is displayed as two horizontal red lines denoting tidal volume limits, between which the subject is instructed to keep his own tidal volume (a yellow line, oscillating in the y-direction). A green line then oscillates next to the yellow (also in the y-direction), between the target volume lines using two sine functions, one for inspiration and one for expiration. The target stays at the expiratory volume line for the duration of the target expiratory pause.

Figure 2. Diagram of the breathing pattern analysis. T_v = tidal volume, P_e = expiratory pause, T_i = inspiratory time and T_e = expiratory time.

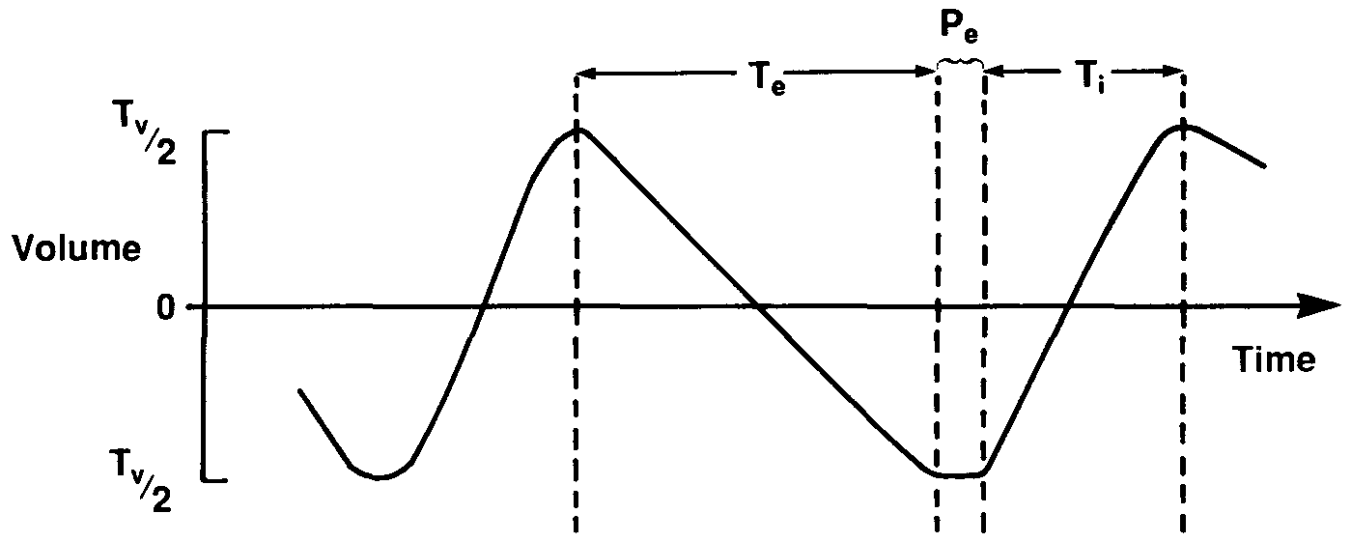

$$T_v = T_{v/2} \sin(2\pi / 2T_e) \text{ : EXPIRATION}$$

$$T_v = T_{v/2} \sin(2\pi / 2T_i) \text{ : INSPIRATION}$$

Figure 3. Diagram of the computer screen display during breathing control.

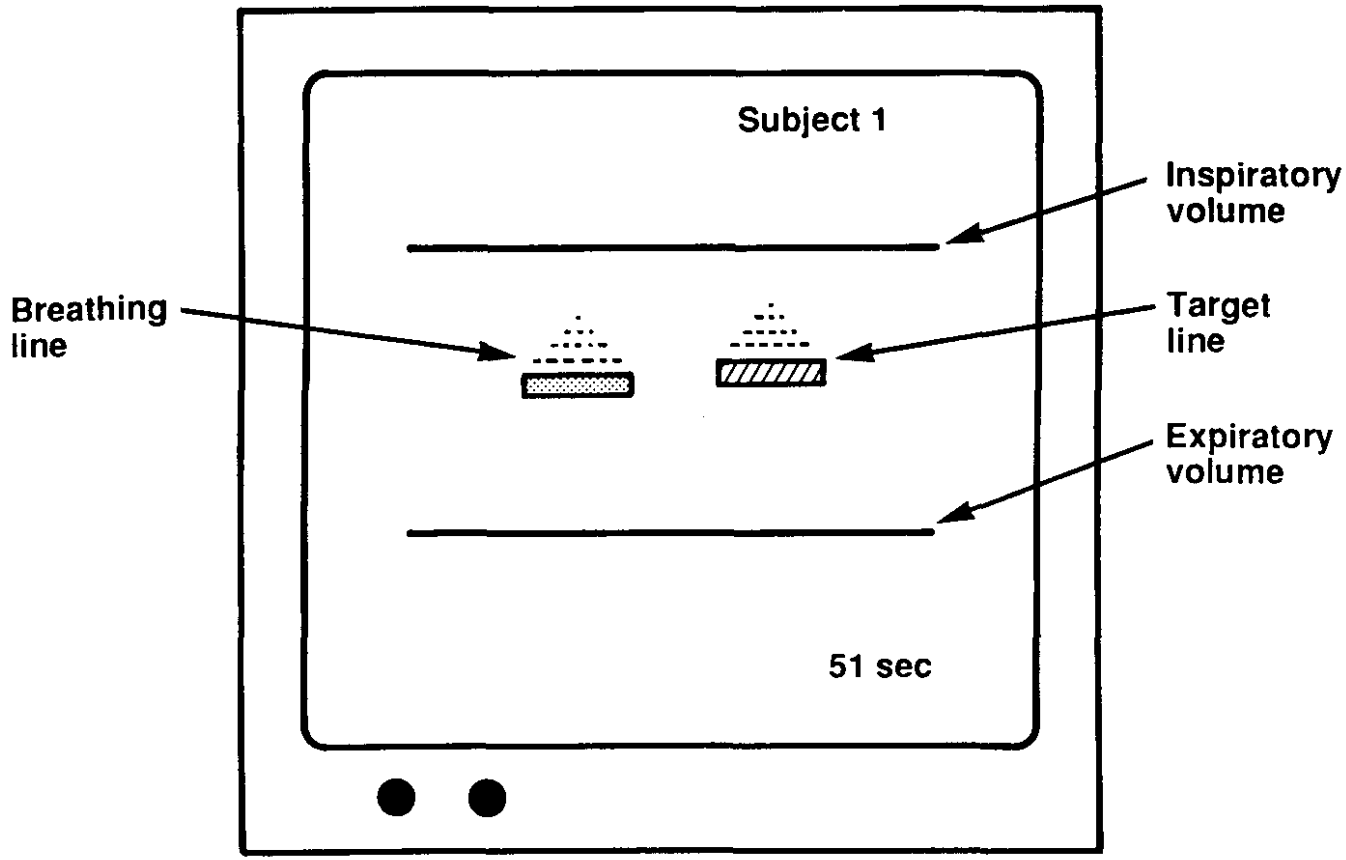

Once the subject has settled and is following the target adequately, the data sampling is started simultaneously with the aerosol inhalation. The sampling is similar to that in [1], the values of volume and flow being saved in arrays at a frequency of approximately 10 Hz. The sampling will continue until any key is pressed. The time is displayed at the bottom right of the screen for convenience. After sampling, volume, flow and time data are stored from buffers to data files and the program returns to the main menu.

[4] Calculate and plot results

This option is used to calculate the mean and standard deviation of the breathing parameters produced by the breathing pattern from [3]. The calculations follow those of [2], using data from the appropriate sampling files. In addition to the parameters already mentioned, the inspiratory pause is also calculated, being defined in a similar way to expiratory pause:

a) Expiration = false, and

b) Flow is between $\pm$2 and -2 l/min.

The parameters for each breath and the mean and standard deviation values for the sampling period are calculated as in [2], stored in data files and plotted on the screen.

6.6. Testing the system

6.6.1. Methods

The linearity of the servo-potentiometer was tested by varying the volume of the bell spirometer and noting the value of ADC counts. ADC counts were then plotted against spirometer volume and linear regression performed (Figure 4a).

The equation thus produced was used to convert counts sampled from the ADC into ml. The linearity of the flow transducer was measured in a similar way, a variable suction was applied via a rotameter to the inspiratory side of the transducer and ADC counts and trace height in mm measured. This was repeated for the expiratory side. The linear regression equation was used to convert ADC counts or trace height into l min^{-1}.

The system was then tested in two ways:

a) Volume, flow and time results as measured by the system and by the chart recorder trace were compared. The aerosol inhalation circuit was set up as described above, with no aerosol solution present, but with compressed oxygen from a cylinder at a flow rate through the nebuliser of 8 l/min. A piston driven animal respirator (C.P. Palmer Ltd. London, England) was used to provide regular simulated breathing with a tidal volume of approximately 500 ml and variable frequency, this was attached to the mouthpiece.

The respirator was turned on, baseline levelled with the aid of the needle

valve and two minutes sampling started. The breath-by-breath values of the following parameters were then calculated by the computer program and measured on the volume and flow chart recorders for comparison:

Tidal volume (V_t), inspiratory flow (F_i), expiratory flow (F_e), expiratory pause (P_e), inspiratory pause (P_i), time of inspiration (T_i) and time of expiration (T_e). The means and standard deviations were then compared.

b) Nine healthy volunteers were chosen to inhale a simulated jet nebulised aerosol on six occasions. The breathing control system was compared with no control and with a target volume and frequency only.

On the first visit, each volunteer was seated in an upright position in front of the computer screen, breathing through the mouthpiece of the aerosol inhalation system. The jet nebuliser contained no solution and the compressed oxygen was passed through at 6 l/min. The baseline, as measured on the computer screen, was steadied by controlling the vacuum outlet flow reduction valve (Figure 1). The breathing was then sampled for two minutes with the monitor turned away from the volunteer. The volume and flow traces were also marked for the beginning and end of sampling.

After sampling, the breathing pattern parameters were computed and stored as the target breathing pattern for future use.

Inhalation [A]. The target breathing pattern, following previously defined parameters, was displayed on the monitor as a vertically oscillating green line and the subject's breathing pattern moving along-side as a yellow line (Figure 3). The subject was asked to keep the two lines in tandem. After 5 - 15 minutes of practice, the mock aerosol delivery commenced. The start of breathing data collection by the computer was simultaneous with the start of the mock aerosol generation and the volume and flow traces were marked. After two minutes of inhalation, the aerosol and data sampling were terminated and mean breathing parameters calculated. The inhalation was repeated on a separate day and the results compared.

Inhalation [B]. On another occasion, the subject was requested to repeat the inhalation in the absence of the oscillating green target line. The tidal volume target was included as two horizontal red lines on the screen and the breathing frequency target consisted of a metronome set to a frequency of half of the subject's time of respiratory cycle (T_{rc}). The subject was instructed to keep the tidal volume oscillating between the target volume lines in time to the metronome signal and sampling was begun after 5 to 15 minutes practice.

Inhalation [C]. On a third occasion the subject repeated the inhalation without a target (blank screen).

The inhalations [A], [B] and [C] were done in random order and repeated, each on a separate day.

6.6.2. Results

The calibration lines for the servo potentiometer and the pneumotachograph are shown in Figure 4. The regression equations and the r^2 values are included in the figures. Figure 5 shows the plot of recorder trace height against inspiratory and expiratory flow rate. The regression equations shown were used to convert mm into expiratory or inspiratory flow rate. Table 1 shows the close agreement between breathing parameters obtained from the computer and measured from the chart recorder when breathing was simulated with an animal respirator. The standard deviations are somewhat greater for the chart recorder in most cases. The means of the breathing parameters for each subject on the six inhalation occasions (two for each of the three methods), were calculated.

To aid comparisons, the difference between day 1 and day 2 were expressed as a percent of the mean of the two days (d value). The d value means for all nine subjects are given in Table 2 together with the range of values in parentheses.

The variation in inspiratory flow rate, tidal volume, time of respiratory cycle (T_{rc}) and inspiratory pause between breathing occasions are all smaller for the full control than either one or other of the other two methods.

Figure 4. (A) Graph of analogue to digital converter (ADC) value vs. spirometer volume as measured by the spirometer potentiometer. (B) Graph of ADC value vs. inspiratory or expiratory flow rate as measured by the pneumotachograph.

A

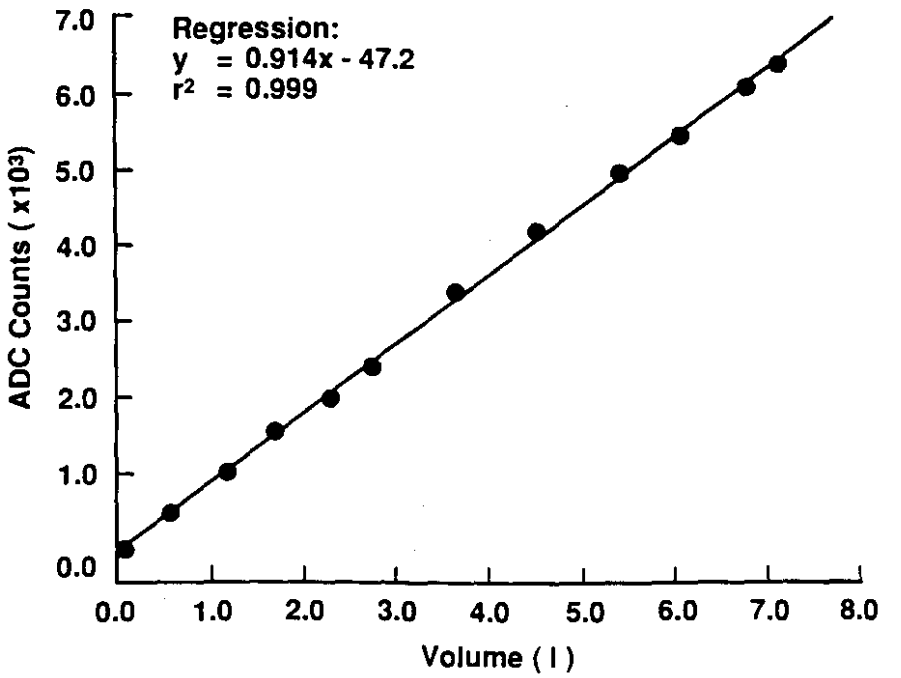

B

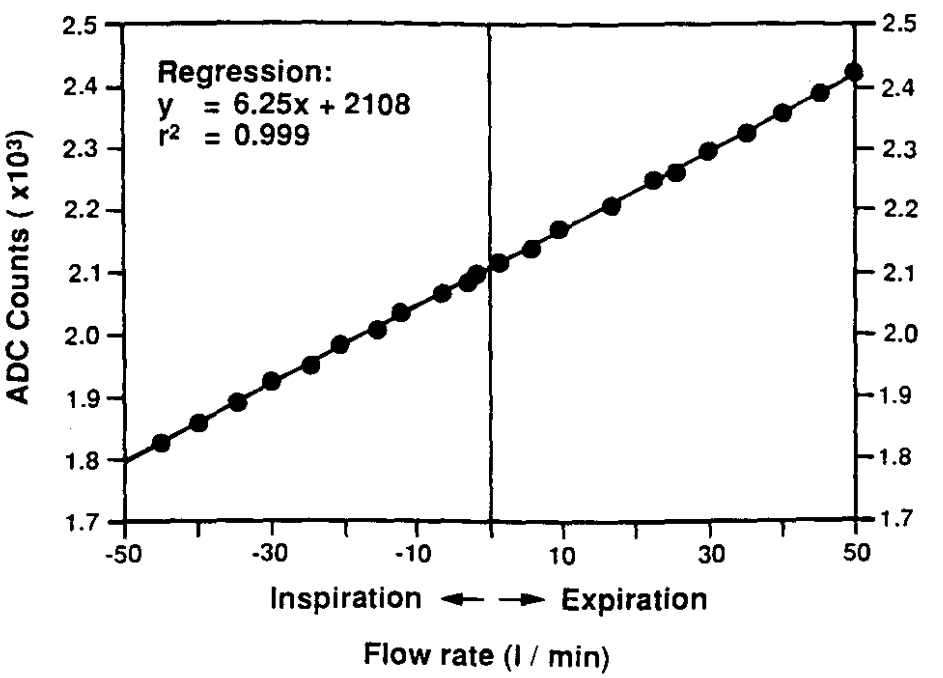

Figure 5. (A) Graph of chart recorder trace height vs. inspiratory flow rate. (B) Graph of chart recorder trace height vs. expiratory flow rate.

A

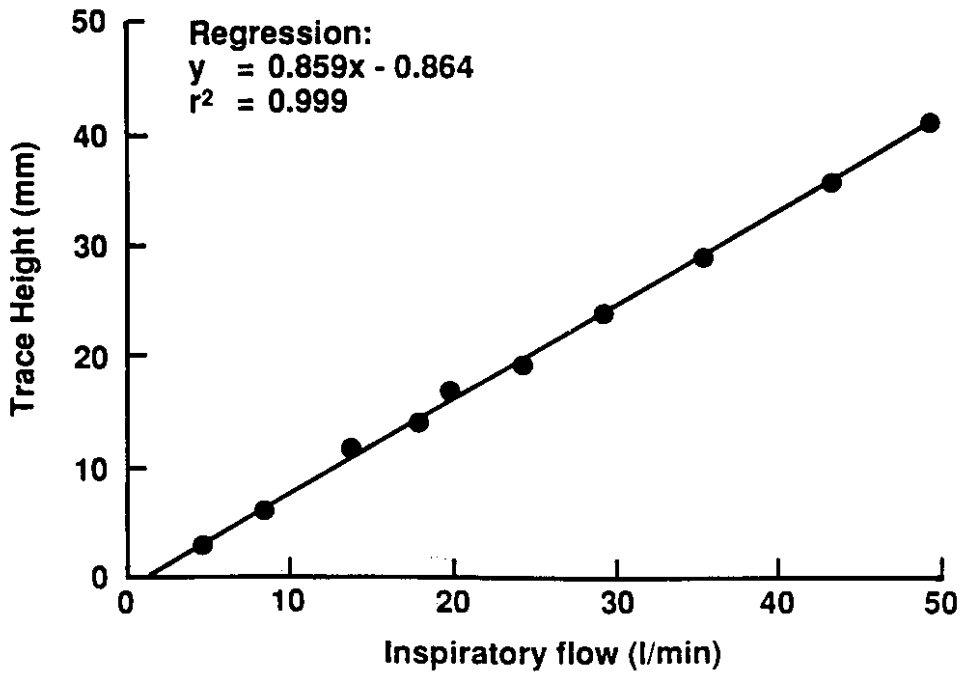

B

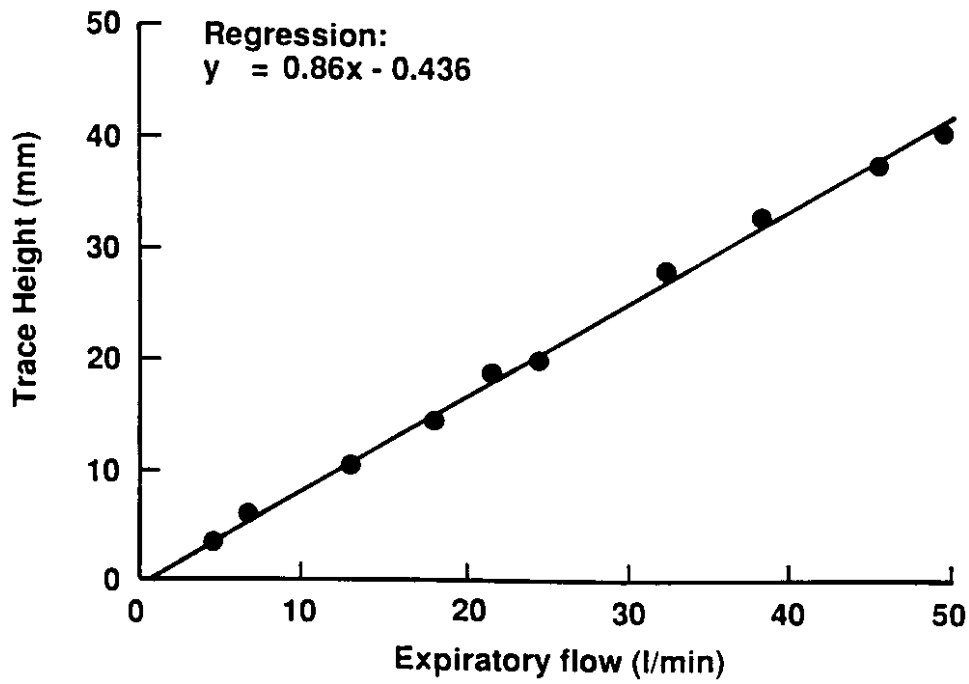

Table 1. Comparison of breathing parameters obtained using the computerised method with the chart recorder trace, mean (SD). Breathing was simulated with an animal respirator.

Parameter		Chart	Computer
Tidal volume (V_t)	ml	413.6 (9.3)	416.3 (8.7)
Inspiratory flow (F_i)	l/min	32.9 (0.5)	33.5 (0.8)
Expiratory flow (F_e)	l/min	22.2 (0.9)	21.7 (0.2)
Expiratory pause (P_e)	sec	*	0.09 (0.03)
Inspiratory pause (P_i)	sec	*	0.10 (0.04)
Time of inspiration (T_i)	sec	1.2 (0.05)	1.2 (0.03)
Time of Expiration (T_e)	sec	2.9 (0.05)	2.9 (0.04)

* Unable to measure respiratory pauses on chart.

Table 2. [1]'d' value means for the nine subjects with range in parentheses:

Method	$^{2}F_{e}$	$^{3}F_{i}$	$^{4}V_{t}$	$^{5}T_{rc}$	$^{6}P_{i}$
No Control	23.8 (0.9 - 45.7)	16.6 (1.7 - 37.6)	19.2 (0.2 - 38)	16.5 (5.7 - 30.8)	51.3 (0.0 - 89)
Metronome + $^{4}V_{t}$	11.4 (4.1 - 25.8)	13.5 (0.0 - 30.0)	3.5 (0.1 - 6.3)	1.5 (0.0 - 9.3)	72 (22 - 160)
Full Control	12.0 (0.4 - 20.2)	6.4 (0.4 - 13.3)	2.5 (0.1 - 4.8)	0.3 (0.0 - 2.9)	26.0 (8.0 - 80.0)

Notes:

1 'd' results are expressed as :

$$d = \frac{\text{day 1 mean parameter - day 2 mean parameter}}{\text{mean of day 1 and day 2}}$$

2 Peak expiratory flow rate; 3 Peak inspiratory flow rate

4 Tidal volume

5 Time of respiratory cycle

6 Inspiratory pause

The difference is statistically significant for inspiratory flow, ($p<0.05$, student's t-test; paired data). The inspiratory pause d values were greater for the metronome control day compared with the full control ($p<0.05$).

In individual cases the inspiratory flow rate varied by as much as 30.0 % from one occasion to another with the metronome and tidal volume target, whereas the greatest difference for the full control was 13.3 %. Similarly for the inspiratory pause, the greatest difference was 114 % and 80 % for the metronome and full control respectively. T_{rc}, F_e and V_t variation was low for both of these methods of control. If no target pattern is used, the day to day variation is greater than either of the other two methods with the exception of inspiratory pause ($p<0.05$). The greatest variation in inspiratory flow rate was found to be 37.6 % for the 'no target' method. Similarly, the greatest variation in tidal volume for this method was 38%, with 24% for T_{rc} and 89% for inspiratory pause. The breath-by-breath variability during each inhalation was found to be similar for all three methods (Table 3).

Table 3. Mean (range) of the breath-by-breath coefficient of variation values (%) for each parameter and method.

Method	$^{1}F_{e}$	$^{2}F_{i}$	$^{3}V_{t}$	$^{4}T_{rc}$	$^{5}P_{i}$
No Control	10.4	9.8	11.2	8.3	64
	(5.1 - 15.6)	(6.7 - 12.7)	(4.7 - 14.2)	(4.2 - 19.6)	(30 - 125)
Metronome	9.5	10.4	7.1	5.1	85
+ $^{3}V_{t}$	(6.3 - 15.9)	(5.6 - 21.4)	(3.1 - 11.1)	(2.1 - 8.8)	(35 - 300)
Full	8.6	9.0	8.1	5.0	67
Control	(4.6 - 12.3)	(4.2 - 13.8)	(4.2 - 13.6)	(2.2 - 9.4)	(36 - 100)

Notes:

1 Peak expiratory flow rate

2 Peak inspiratory flow rate

3 Tidal volume

4 Time of respiratory cycle

5 Inspiratory pause

6.7. Discussion

The inhalation pattern monitoring system described is versatile for a number of reasons: a) any regular target pattern involving multiple breaths can be easily set or each subject's pattern, having been recorded on a previous occasion can be used as the target, b) the target includes expiratory pause and different inspiratory and expiratory times, making it more physiological and easier to follow, with only a visual signal to concentrate on, rather than both audible and visible, c) the breathing parameters are calculated automatically and stored for later use, d) the breath-by-breath and inter-occasion breathing pattern is more reproducible than having either 'no target' or metronome and tidal volume target.

The values calculated are in close agreement with those measured by hand (Table 1). The higher standard deviation values obtained from the chart recorder trace most likely reflect the poorer sensitivity of measurement, since the accuracy of the trace height measurement is $\pm$ 1 mm.

The lung volume at the start of inhalation was not controlled in these experiments. The initial volume was assumed to be at FRC, since the subjects were requested to breath tidally. The initial volume can be checked by requesting an inspiratory capacity manoeuvre of the subject before inhalation. This can be compared with the subject's known value or with the previous day's value prior to inhalation.

The inspiratory pause is usually small in normal tidal breathing, so it was not used in the target pattern. If a target pattern with a long inspiratory pause were required, it could be easily built in to the target by the same mechanism as expiratory pause. If subjects are attempting to control their breathing pattern, however, inspiratory pause may vary. Although breath holding time has been shown to affect deposition in more peripheral airways by sedimentation (Pavia et al, 1980), the differences in inspiratory pause will probably not have a significant effect on deposition unless the values are high. The largest value of inspiratory pause measured was 0.62 seconds (subject 1, metronome target, day 2), the pause on the other metronome day was 0.21, a 0.4 s difference that may be significant for very small droplet sizes. The variations in inspiratory pause were generally greater when a metronome and volume target were used, because the subjects had to 'wait' at end-inspiration for the signal to exhale, on some occasions.

Respiratory flow rates are not necessarily related to time of inspiration and expiration unless respiratory pauses are taken into account. Variations in inspiratory pause with constant time of respiratory cycle, can effect total and regional deposition by both time and velocity dependent mechanisms, as the residence time and the inspiratory flow rate will be affected.

Although high expiratory flow rates have been shown to affect deposition (Foster et al, 1988), variations in normal tidal expiratory flow rates are unlikely to have a large effect.

For the particle sizes used in most clinical applications, inspiratory flow rate is usually the most important breathing parameter with respect to regional deposition (Newman 1984). Bronchial and extrathoracic deposition increase and alveolar deposition decreases with increasing respiratory flow rate (Stahlhofen 1984). The results presented here show that there can be a large difference in inspiratory flow rate (up to 30%), even if the tidal volume and breathing frequency are well controlled. This suggests that if a metronome and frequency target are used alone, flow rates should at least be monitored and taken into account when assessing the data.

A difficulty arises in estimating the effect of small variations in the parameters mentioned on total and regional deposition of the aerosols. In most studies on the effects of breathing pattern on deposition, the differences used have been large to maximise differences in deposition. A clear relationship was however shown between inhalation flow rate and alveolar deposition. In non-smokers below 30 years of age the alveolar deposition value varied from over 60 % at a flow rate of 20 l/min to less than 50 % at 40 l/min (Agnew et al, 1985). These differences may then be further increased by variations in inspiratory pause that may occur if flow rate and volume are not controlled simultaneously. The precise effects of variation in inspiratory flow rate, tidal volume and inspiratory pause will depend on the morphology of the lungs, droplet size and regional ventilation (Trajan et al, 1979).

Chapter 7

Comparisons of Planar and Tomographic Gamma Scintigraphy to Measure the Penetration Index of Inhaled Aerosols.

7.1. Introduction

The ability to differentiate quantitatively between the deposition of inhaled aerosols in large conducting airways and in lung parenchyma is useful in several areas of respiratory and nuclear medicine: for example, the assessment of the initial deposition pattern is necessary in the measurement of mucociliary clearance (Agnew et al, 1981a; Agnew et al, 1986; Gerrard et al, 1986; Dolovich et al, 1987), the 'in vivo' evaluation of devices for production of aerosols and the parameters affecting their performance (Newman et al, 1981; Laube et al, 1984; Newman et al, 1984; Vidgren et al, 1987). The comparison of aerosols with radioactive gases (Royston et al, 1984; Wollmer et al, 1985; Taplin et al, 1977; Susskind et al, 1986), aerosol tests for small airways function (Agnew et al, 1981b; Emmett et al, 1984) and standardisation of inhalation provocation tests (Ryan et al, 1981a; Ryan et al, 1981b; Yan et al, 1983) all require a measure of the distribution of radioactivity between the conducting airways and parenchyma. Perhaps the greatest need for quantitative information on the regional distribution of inhaled materials is necessary in the study of the deposition and elimination of substances with

local pharmacological activity (Vidgren et al, 1987; Ruffin et al, 1978a; Ruffin et al, 1978b; Dolovich et al, 1981) and the pathophysiological (Gerrard et al, 1986; Taplin et al, 1977; Emmett et al, 1984; Dolovich et al, 1976) and pharmaceutical factors affecting these processes (Newman et al, 1981; Vidgren et al, 1987b; Farr et al, 1985).

The most common measure to estimate the relative amounts of aerosol deposited in the large airways and the lung parenchyma is the penetration index (PI) (Dolovich et al, 1976; Agnew 1984; Newman and Pavia 1985): This parameter is obtained by defining peripheral and central regions of the respiratory tract and calculating the ratio of radioactive counts in the two regions; a correction based on comparison with ^{81m}Kr scans is sometimes applied (Agnew et al, 1981b; Emmett et al, 1984; Dolovich et al, 1986), particularly when the gas is used to define the lung boundary, or a volume correction is required for intersubject comparisons.

Conventionally, two-dimensional (2D) gamma scintigraphy has been used to visualise the deposition of radioaerosols in the human respiratory tract by taking posterior, or anterioposterior geometric mean views. The central and peripheral regions of interest for the calculation of PI have been selected assuming that the former would contain predominantly large conducting airways while the latter would represent mostly deposition in the small peripheral airways and, primarily, in the alveoli. It is well known that in reality there are small airways and parenchyma as well as large airways

large airways located in the centre of the lung because of its three-dimensional (3D) structure.

Logus et al, (1984) showed the great value of the 3D technique of single photon emission computed tomography (SPECT) for lung imaging: in animals, SPECT detected ventilation defects caused by artificial obstructions which were not detected by other more conventional methods; while in patients with abnormal lung function, SPECT provided much better information about the regional aerosol deposition than either the posterior or anterior planar views. These workers also studied the qualitative effect of two different breathing patterns on regional aerosol deposition but they could detect no difference either by the 2D or 3D methods, presumably because the aerosol was fine enough (MMAD = 1.2μm, σ_g = 1.8) to deposit primarily in the alveoli (Yu and Taulbee 1977).

We wished to develop a consistent and sensitive method of PI measurement which would enable us to discriminate between deposition in lung parenchyma and conducting airways. To this end, we employed aerosols of different sizes with expected depositions predominantly in these two distinct regions. In order to avoid the possibility of bias due to the effect of different rate and depth of breathing on the individual subject's aerosol deposition (Stahlhofen 1984), we measured PI in each subject for the two aerosol sizes, inhaled using the same pattern of breathing on both occasions. We employed a gamma camera with tomographic acquisition capability, to measure radioaerosol

deposition on a time scale short enough to avoid significant change of the initial deposition pattern by mucociliary transport and absorption.

7.2 Methods

Subjects

Seven healthy non-smoking subjects were studied, five men and two women of mean age 34 years (range 26-39). Lung volumes were obtained from each subject and dynamic lung function tests were carried out immediately before each inhalation study. The study protocol was approved by the Hospital Ethics Review committee and written informed consent was obtained from each subject prior to the studies, after full explanation of the protocol.

The maximum whole body absorbed dose equivalent for each of these studies was estimated to be 0.025 mSv (Appendix III).

Transmission study

A transmission study (Anger and McRea 1968; Bailey et al, 1987) was carried out on each subject to delineate lung fields. Each subject was placed in a supine position over a gamma camera (GE 400AT, Milwaukee, Wisconsin, USA) fitted with a low energy, all purpose, collimator and linked to an on-line computer (DEC PDP 11, Maynard, MA.,USA). A flood source containing approximately 1.5 GBq of ^{153}Gd in water was fixed to a frame in front of the subject's chest. Two ^{57}Co markers were placed on premarked positions on the subject's chest and anterioposterior images collected. The markers were

* Acorn (Medic-Aid, Peckham, Sussex, UK)

then removed with the subject remaining in the same position before a 64 angle tomographic study of 10 to 12 secs per angle (approximately 15 minutes total duration) was acquired in a 64 x 64w matrix. The attenuation images collected were then reconstructed to provide low definition anatomical data in coronal and transverse planes.

Aerosol Deposition

Two radioaerosols with different particle size distributions were inhaled on two occasions by each subject. The aerosols were generated with oxygen from a medical gas cylinder from either a Cadema nebuliser (Cadema Medical Products Inc., Middletown, N.Y.,USA) at 8.0 l/min or a nebuliser of unknown origin* at 6 l/ min. The humidity of the dilution air supplementing the flow to the mouthpiece and the change in temperature of the nebuliser solution during generation were found to affect the droplet characteristics (Phipps and Gonda 1990 [Chapter 3]; Phipps et al, 1987 [Chapter 2]). As a result of these observations, a miniature resistive heater was positioned inside each nebuliser. Power was then applied through a variac to keep the nebuliser as close as possible to room temperature. Dilution air was humidified with the aid of a medical humidifier placed in-line. Droplet sizing was carried out on the radioaerosols produced by the nebulisers under these conditions with the aid of a calibrated 7 stage cascade impactor (Gonda et al, 1982) (DCI-6, Delron, Columbus, Ohio). The coated glass impactor slides containing the deposited radioaerosol were counted on a previously calibrated gamma camera (Phipps et al, 1987 [Chapter 2]) and the droplet size distribution calculated by a least

squares fit to the data (Chang 1978). The droplet sizes of the two aerosols were 2.6 and 5.5μm mass median aerodynamic diameter (MMAD) and 1.4 and 1.7 geometric standard deviation (σ_g) respectively.

Inhalation Circuit.

A closed aerosol inhalation circuit was used to monitor and record the subject's breathing. A target was thus provided to reproduce the breathing pattern on the subsequent inhalation with the aerosol of different size (see Figure 1).

The circuit consisted of a bag in a box system with the humidifier and nebuliser in the inspiratory line and filter and CO_2 absorber in the expiratory line. The volume respired was displaced from the 'box' by the 'bag' which then entered a bell spirometer (Gould Godart BV., Bilthoven, The Netherlands) via a respiratory flow transducer (Hewlet Packard 47304A) and a pneumotachograph (21073B Hewlet Packard, Waltham, MA., USA). The flow signal from the pneumotachograph was integrated (respiratory integrator 8815A, Hewlet Packard, Waltham, MA.,USA) and displayed on a cathode ray oscilloscope (184A and 1805A amplifier, Hewlet Packard, Waltham, MA., USA). A vacuum was applied to the circuit via a needle valve to evacuate from the system an appropriate amount of air to keep the system isovolumetric.

Figure 1. Diagram of aerosol inhalation breathing circuit.

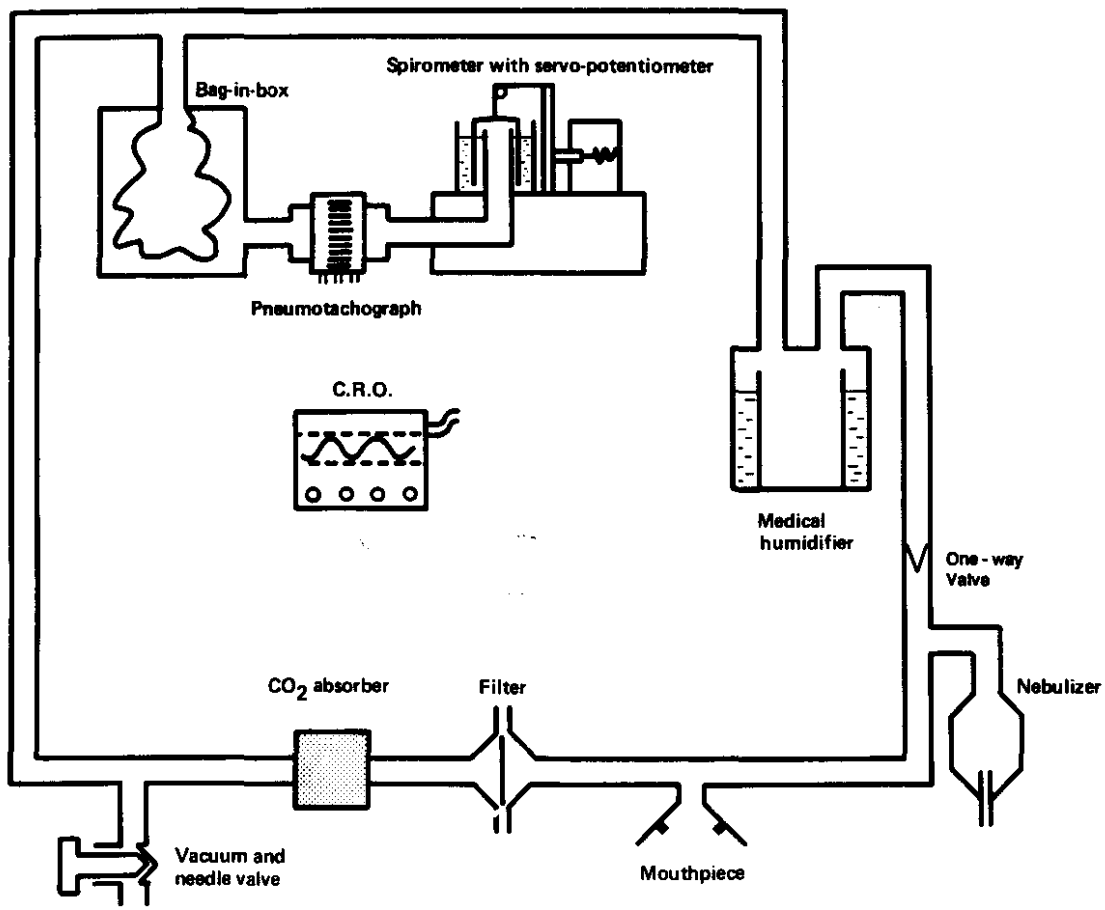

Inhalation

Each subject was seated at the mouthpiece of the aerosol delivery circuit and breathed tidally via the mouth for a few minutes to determine their natural tidal volume, peak flow and frequency of breathing.

The target volume or inspiratory flow was then displayed on the oscilloscope as a base line and target line. The subject followed the tidal volume, or inspiratory flow line, as it moved between the target lines. A facility on the integrator allowed for any small changes in baseline by resetting after the end of every breath. The inspiratory flow was measured from a trace of the original flow signal and tidal volume from the spirometer graph. A metronome was used to provide a target for frequency of breathing. Approximately 5ml of 100 MBq/ml ^{99m}Tc-DTPA in normal saline was then injected into the nebuliser through a rubber septum while the subject remained on the system. The inhalation period was three to four minutes with a further inhalation if lung counts were found to be below 2000 counts per second over the posterior thorax.

Imaging

Immediately after aerosol inhalation, water was gargled and expectorated and the subjects placed in a supine position over the gamma camera. Two-minute anterior and posterior images were then collected before a 10-12 second per angle SPECT study, in a 64 x 64w matrix.

Data Treatment

The images obtained by the gamma camera were displayed on the computer screen in a 64 x 64w matrix (Gamma 11, DEC, Maynard MA, USA). The transmission data were converted to attenuation values and transverse sections reconstructed using conventional convolution back-projection methods (Nuclear Medicine Package, Analogic Corp., Worcester, MA, USA). The emission data were reconstructed by convolution back-projection and a first-order Chang attenuation correction performed employing a constant attenuation coefficient (Chang 1978) derived from the attenuation values described above.

Coronal and transverse sections were formed from the reconstructed images. A number of coronal and transverse central slices were then taken from the mid-portion of the right lung and summed together as shown in Figure 2. The right lung only was assessed to avoid corruption by activity in the stomach adjacent to the left lung. The reconstructed transmission tomographic images were used to define right lung boundaries in transverse, coronal and anterioposterior views for each subject. These were used to derive central and peripheral zones by computer based on pre-defined criteria related to the dimensions of the lung: The central region was drawn along the medial boundary edge of dimensions as shown in Figure 2. The peripheral region was defined by scanning from a point mid-way down the medial side of the lung image, around the lung, drawing a peripheral strip a set distance (1/3 of the lung height) inside the outer boundary (Figure 2).

Figure 2. Diagram of peripheral and central regions and mid-lung slicing.

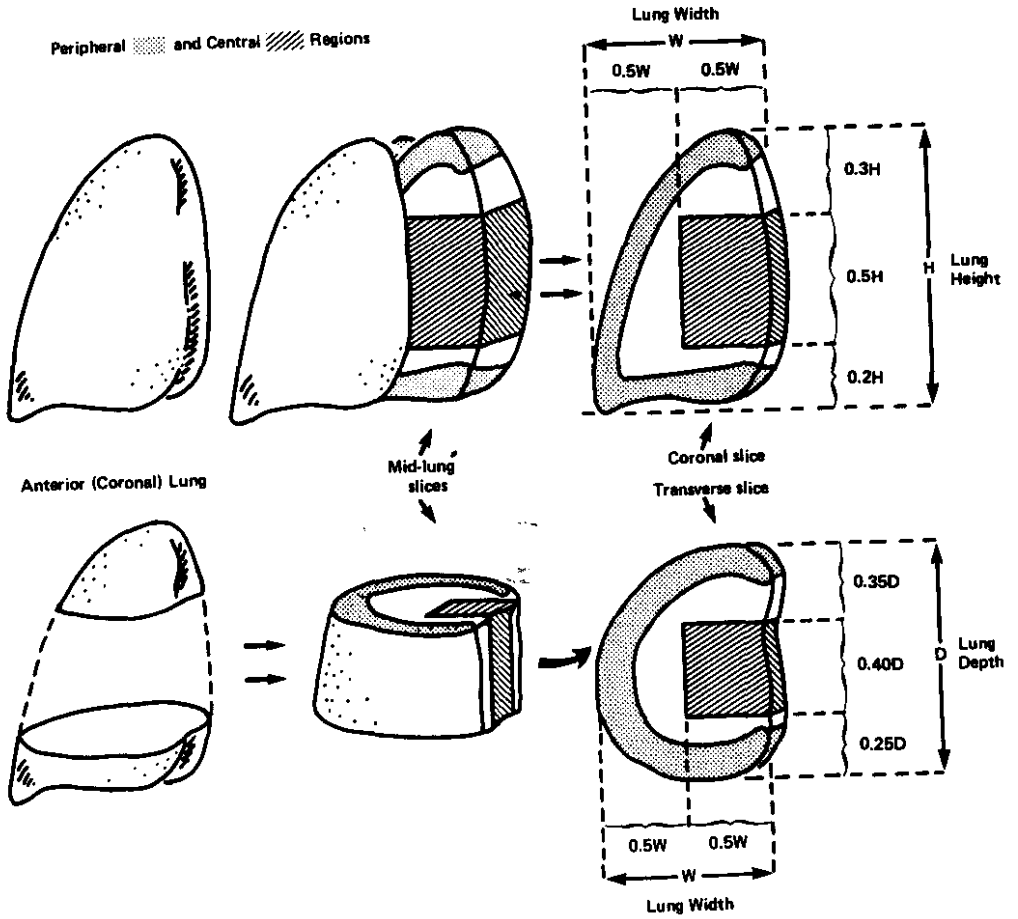

Once a region was defined for a subject, it was stored for all future uses.

The PI was then defined as:

$$PI = \frac{\text{Counts per second (cps)/pixel in peripheral region}}{\text{cps/pixel in central region}}$$

PI measurements were carried out on the following images:

Planar methods:

1. The 2-dimensional posterior image (P), not corrected for attenuation;

2. The anterioposterior geometric mean image (AP), not corrected for attenuation;

Tomographic methods:

3. Transverse central slices (TC) taken through the mid-portion of the lung in transverse view of thickness approximating 50% of the lung height;

4. Coronal central slices (CC), taken through the mid-portion of the lung coronal view of thickness approximating 40% of the lung depth.

The PI of the first and last image of each tomographic study was measured to assess the degree of change in regional deposition during the duration of the SPECT study.

7.3. Results

All subjects' spirometry and lung function results were within the normal range and there was negligible intrasubject variability in performance between 'small' (MMAD = 2.6μm, σ_g = 1.4) and 'large' (MMAD = 5.5μm σ_g = 1.7) aerosol studies (Table 1).This was confirmed by the two tailed paired t-test (Snedecor and Cochran 1967) and the two tailed Wilcoxon rank sum test (Colton 1974) which demonstrated no statistically significant intrasubject differences ($p<0.1$) between the two studies for mean peak inspiratory and expiratory flow, tidal volume and duration of respiratory cycle (Table 2). These are the primary breathing parameters believed to affect the regional deposition of aerosols in the aerodynamic size range used in this work (Stahlhofen 1984).

Figure 3 shows typical AP and CC images for the small and large droplet studies in subject 2. A small qualitative difference in the deposition pattern of the right lung can be observed with the AP images, while a much greater difference in the deposition pattern between large and small droplets with the CC images can be observed.

Figure 4 shows that the PI was smaller for the large droplets in all subjects and in all methods employed.

Table 1. Subject details.

Subject	Sex	Age (Year)	Height (cm)	Weight (Kg)	VC* %	FEV_1 %		FEV_1/VC %		FEF_{50} %	
						S	L	S	L	S	L
1	F	39	154	54	105	97	98	79	84	59	62
2	M	39	182	71	107	105	113	85	83	101	106
3	M	26	191	78	103	103	104	82	84	101	98
4	M	38	154	59	111	116	113	83	88	77	78
5	M	38	165	63	108	111	102	86	89	102	96
6	M	26	171	65	119	130	128	86	87	103	96
7	F	29	166	67	114	104	109	83	86	74	78

* VC - Vital capacity (% predicted),

FEV_1 - Forced expiratory volume in 1 second (% predicted),

FEV_1/VC - FEV_1 as % of VC,

FEF_{50} - Forced expiratory flow at 50% VC (% predicted) (51).

S - 'Small' aerosol droplet study (MMAD = 2.6 μm).

L - 'Large' aerosol droplet study (MMAD = 5.5 μm).

Table 2. Mean breathing parameters (± standard deviation).

SUBJECT	STUDY*	MPIF(l/min) (CV %)	MPEF(l/min) (CV %)	MTV(ml) (CV %)	DRC (sec) (CV %)
	S	25.1 (8.9)	20.6 (7.2)	491.7 (6.9)	4.45 (3.3)
1	L	25.9 (9.4)	19.2 (9.5)	493.9 (8.9)	4.40 (3.8)
	d	3.2	-6.8	0.5	1.10
	S	23.2 (26.7)	16.7 (13.4)	713.8 (9.1)	8.11 (3.8)
2	L	28.4 (23.7)	17.5 (17.8)	730.2 (15.0)	7.96 (4.0)
	d	22.4	4.8	2.3	1.80
	S	41.9 (6.9)	31.1 (6.6)	614.7 (5.3)	5.21 (4.4)
3	L	40.4 (4.7)	27.3 (6.3)	574.8 (5.3)	5.18 (4.1)
	d	-3.6	-9.6	-6.5	0.6
	S	30.4 (15.9)	21.7 (7.5)	682.6 (11.3)	4.91 (3.2)
4	L	8.1 (11.5)	20.5 (7.2)	74.6 (7.7)	4.90 (3.1)
	d	-7.6	-5.5	-1.2	0.2
	S	43.3 (16.1)	34.4 (11.6)	987.6 (3.8)	6.26 (4.4)
5	L	31.1 (8.1)	31.1 (9.6)	1000.1 (3.4)	6.28 (4.8)
	d	-28.2	-9.6	1.3	0.3
	S	31.0 (12.7)	34.3 (8.8)	1254.8 (8.1)	6.43 (3.4)
6	L	34.1 (8.7)	29.6 (12.7)	1244.2 (14.2)	6.44 (4.7)
	d	10.1	-13.7	-0.8	0.2
	S	29.1 (13.7)	19.5 (13.7)	495.0 (12.1)	3.65 (4.2)
7	L	35.3 (10.7)	24.6 (9.3)	633.9 (13.0)	3.60 (4.6)
	d	21.3	26.5	28.1	1.4

*Study
S - 'small' aerosol droplet study (MMAD = 2.6μm),
L - 'large' aerosol droplet study (MMAD = 5.5μm),
d - % difference between large and small study, 100 (L-S)/S
MPIF - mean peak inspiratory flow (l/min),
MPEF - mean peak expiratory flow (l/min),
MTV - mean tidal volume (ml),
DRC - duration of respiratory cycle (sec),
CV - coefficient of variation (%).

Figure 3. Opposite: Deposition images of the small aerosol (3a and 3b) and large aerosol (3c and 3d) in subject 2. Images 3a and 3c are anterioposterior (AP) images, while 3b and 3d are coronal mid-lung slices (CC). The CC images show a larger qualitative difference in deposition pattern between the large and small studies.

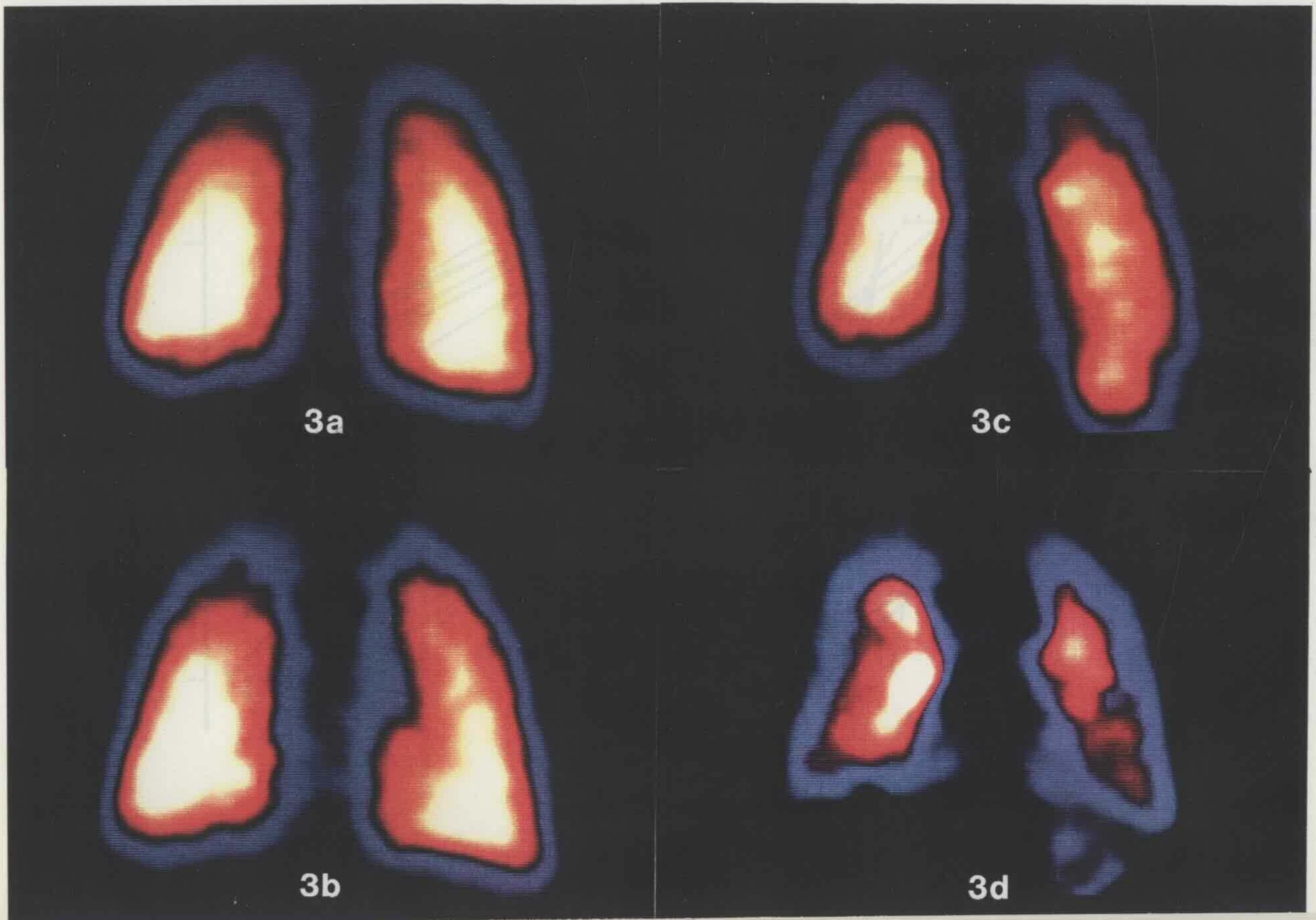
3a
3c
3b
3d

Figure 4. Penetration index (PI) values for small (S) and large (L) droplets. Posterior image (P), anterioposterior image (AP), transverse mid-lung slices (TC) and coronal mid-lung slices (CC). Where a single point for the S aerosol represents two subjects, the first number refers to the subject with a higher PI for the L aerosol.

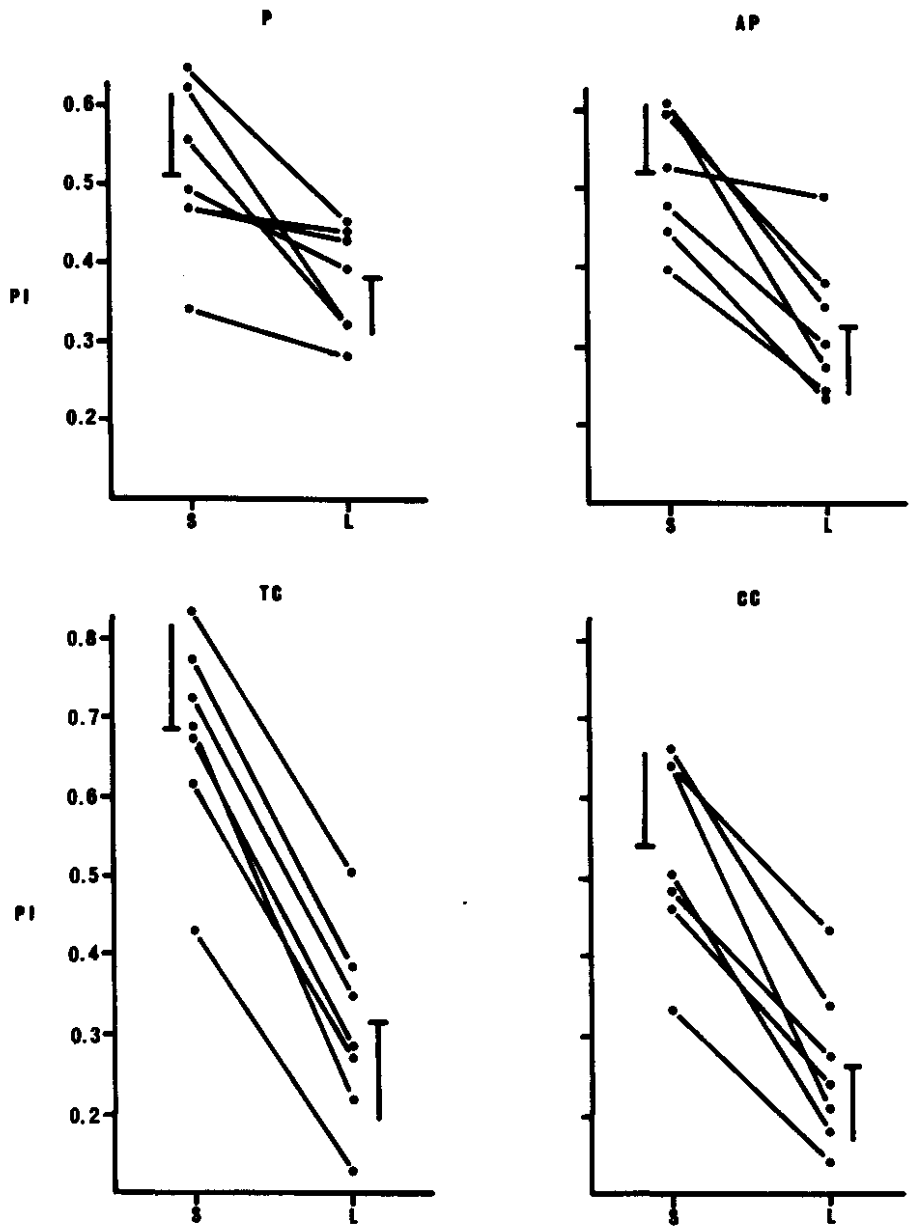

The highest statistical significance was obtained for the transverse ($p<10^{-5}$) and coronal ($p<10^{-3}$) mid-lung slices, while the planar (P) images exhibited the least significant difference ($p = 0.014$). To examine the group response more closely, these differences were further evaluated by calculating the relative increase in PI of the small droplet compared to the large droplet study as a percentage (d):

$$d\ \% = \frac{\text{PI (small droplets) - PI (large droplets)} \times 100}{\text{PI (small droplets)}}$$

The differences in PI between the large and small droplet studies are shown in Figure 5. The d values obtained from the 3D (TC and CC) images are significantly greater than those from the 2D (P and AP) ($P<0.005$), while there was no difference between the two 3D methods nor between the two 2D methods ($p>0.1$). d from the P method was inferior to all other methods tested.

The standard deviation of the mean d values are also shown in Figure 3. PI from TC and CC can be seen to display the most consistent pattern in our subject population and aerosols studied.

There was no trend or significant difference in PI between the first and last frame of the SPECT studies ($p = 0.26$, Table 3).

Figure 5. Chart of d values as the relative difference in penetration index between large and small droplet studies (d values) and standard deviations for posterior (P), anterioposterior (AP), transverse mid-lung slices (TC) and coronal mid-lung slices (CC).

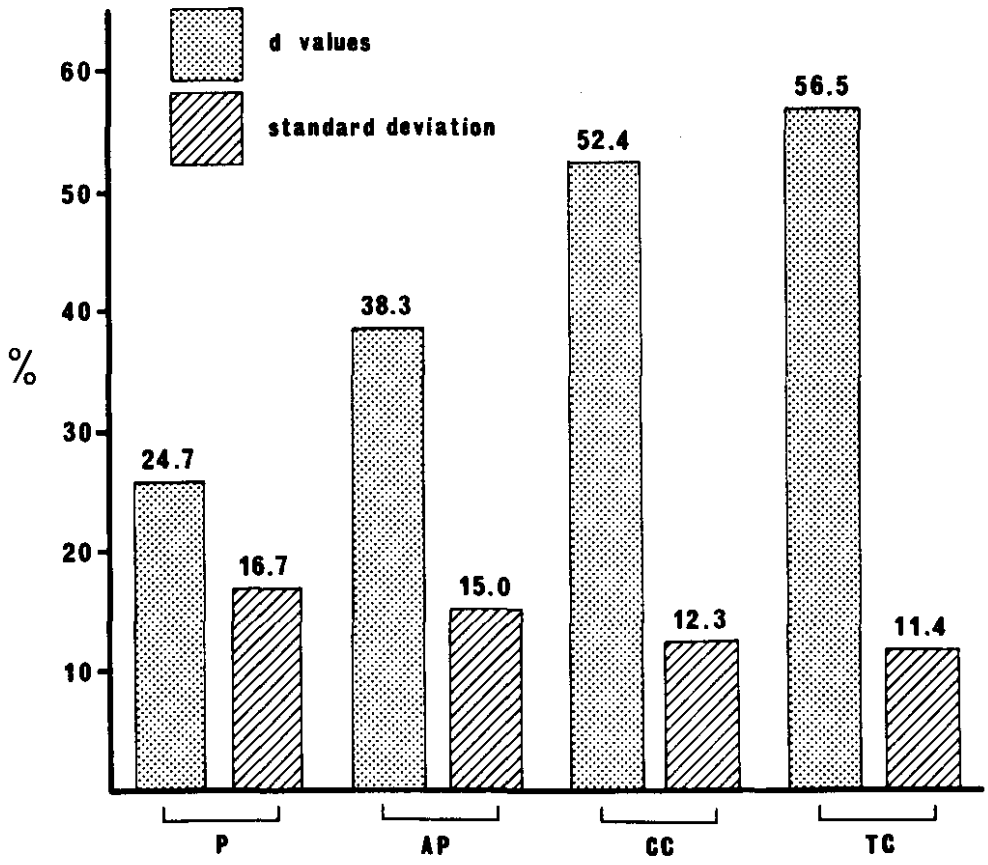

Table 3. Penetration Index (PI) and d values (the difference; frame 64 - frame 1 as a percentage of frame 1) for the first and last frame of each SPECT study.

Subject	Frame	PI	d value (%)
1 small	1	31.1	4
	64	32.4	
1 large	1	60.8	-3
	64	58.9	
2 small	1	40.3	9
	64	44.4	
2 large	1	50.5	14
	64	58.6	
3 small	1	23.3	13
	64	26.3	
3 large	1	44.8	-2
	64	44.1	
4 small	1	40.7	12
	64	45.6	
4 large	1	54.2	-9
	64	49.3	
5 small	1	34.7	-5
	64	33.1	
5 large	1	53.1	5
	64	55.9	
6 small	1	35.1	-11
	64	31.4	
6 large	1	48.9	-15
	64	41.6	
7 small	1	35.7	10
	64	39.2	
7 large	1	56.5	7
	64	60.2	

d value calculated as:

(PI [Frame 1] - PI [Frame 2] / PI [Frame 1]) × 100

7.4. Discussion

Among the various quantitative measures of the distribution of deposited radioaerosols between the airways and the lung parenchyma, the penetration index, PI, is almost certainly the most convenient and readily measurable. However, planar measurements of aerosol deposition suffer from the problem of the inclusion of overlying "peripheral" airways in the central "large" airway region (Logus et al, 1984).

It has been suggested before (Dolovich et al, 1985) that tomography should be better suited to distinguish between deposition in the small and large airways than the conventional 2D images. We therefore attempted to further separate central and peripheral airways by the use of these tomographic techniques. Our results show that in comparison with the conventional techniques based on planar imaging, tomographic methods of measuring regional deposition are superior, with the coronal and transverse mid-lung slices giving a more discriminating measure of PI. This is also likely to be the case with aerosols of different droplet size characteristics to those used, as long as there is a proportion of both peripheral and central deposition.

Mildly polydisperse aerosols with mass median aerodynamic diameters of 5.5μm and 2.6μm were used because the former aerosol would be expected to have a substantially smaller PI than the latter (Gonda et al, 1982; Gonda 1981; Ferron et al, 1985). Impaction in the conducting airways is probably the predominant mechanism of deposition of the 'large' droplets while

sedimentation in the small airways and alveoli becomes important for smaller droplets. The results indicate that the choice of the regions of interest is consistent with the idea that the 'central' region, indeed, contains mainly large conducting airways and the 'peripheral' region consists probably of bronchioli and alveoli; otherwise, we would not expect to obtain such clear differences in PI between the two aerosols in all subjects and methods used. Although there was a difference in the breathing patterns between the large and small aerosol studies in some subjects, there was no significant trend and the changes in PI could not be explained by this. Nevertheless, we would recommend that attempts are made to reproduce as much as possible the breathing pattern in an individual for studies of changes in PI, particularly in subjects with abnormal and variable airway function (Laube et al, 1986).

After the initial deposition, the inhaled aerosol undergoes dynamic changes due to absorption and mucociliary clearance (Lippmann et al, 1980). Although a longer time is required for SPECT image acquisitions (up to 15 mins), these changes are likely to have little effect on the calculated PI values for the following reasons: in normal subjects, the absorption rate half life of Tc-DTPA is 86 ± 26 minutes (Coates and O'Brodovich 1986) and this varies little throughout the respiratory tract over the SPECT acquisition time, especially medio-laterally (O'Doherty et al, 1985; Dusser et al, 1986; Coates and O'Brodovich 1987). Therefore, this route of elimination of the radioactivity will affect approximately equally both the peripheral and the central regions. Similarly, the 'background' radioactivity appearing in the

blood stream will be small and distributed quite uniformly and it will be cleared rapidly with 58% clearing with a biological half-time of 3.8 min, 24% with 15.6 min and 18% greater than 118, min in subjects with normal renal function (McAfee et al, 1979). With regard to the mucociliary clearance, it can be envisaged that at least in normal subjects this process is at steady state, whereby there exists a balance between the rates of supply and removal of material in the more proximal ciliated regions of the respiratory tract. Therefore, we would not expect this process to significantly affect the radioactive counting in the central region over the time period of the SPECT studies. The peripheral region probably contains many non- ciliated surfaces which are therefore not subject to mucociliary clearance. Moreover, all the above processes have half-lives longer than the duration of our SPECT studies (Byron 1986; Becquemin et al, 1987). These assumptions are supported by the insignificant change in PI between the first and last frames of each study.

In conclusion, we have shown that there were significant reductions in the PI values in normal adults when they inhaled two aerosols with MMAD of 2.6 μm (σ_g = 1.4) and 5.5 μm (σ_g = 1.7), respectively, under controlled conditions. These reductions were most pronounced when the PI was calculated from mid-lung coronal or transverse slices obtained by SPECT reconstruction; this former method also gave the most consistent pattern of changes in PI in the subject population studied. The conventional planar images showed the same qualitative behaviour, but their ability to distinguish between deposition of the large and small aerosols was substantially lower,

particularly for the posterior images.

This is the first time that quantitative deposition measurements have been undertaken using SPECT and the advantages of PI obtained in this way are likely to be important in studies requiring a high degree of discrimination between the deposition of aerosols on conducting and respiratory surfaces of the respiratory tract.

Chapter 8

The deposition patterns of non-isotonic challenge aerosols in normal and asthmatic subjects.

8.1. Introduction

The first systematic study of the bronchoconstrictive properties of non-isotonic aerosols was performed by Schoeffel et al, (1981) who found that smaller inhaled doses of aerosols containing 3.6% or 0.3% saline were required to produced a 20% fall in pre-challenge FEV_1 in a group of asthmatics than isotonic aerosols (0.9%). Since that time, non-isotonic ultrasonically nebulised (UN) aerosols have been advocated and used as part of the range of diagnostic tests for asthma (Smith and Anderson 1989) and have increased our understanding of some of the mechanisms involved in this disease.

The droplet size distribution of the inhaled aerosol is a critical factor that determines the site of deposition (Stahlhofen et al, 1983; Ferron et al, 1981). Predictions of regional deposition can be made from a knowledge of the droplet parameters, however, non-isotonic aerosols are unstable in the respiratory tract and are able to undergo hygroscopic growth or shrinkage after inhalation (Ferron

1977). Thus hypertonic aerosols are hygroscopic and will absorb water vapour from a humid environment until the droplet vapour pressure is in equilibrium with that of its surroundings or they deposit. If the airway fluid is isotonic, then the droplets will reach equilibrium when they have absorbed enough water to become isotonic themselves. In so doing, they will increase in size. This will in turn affect the regional and total deposition pattern of the aerosol (Stahlhofen et al, 1983). Hypotonic aerosol droplets however, can evaporate as they come into equilibrium with the lower vapour pressure of the airways and they too will cease to evaporate once they have attained isotonicity or have deposited. Hyper- and hypo- tonic droplets of the same initial size may therefore deposit with very different regional patterns (Byron et al, 1977).

The effects of hygroscopic growth have been predicted by mathematical modelling using growth rate theory and deposition probability functions of particles in the respiratory tract (Ferron 1977; Persons et al, 1987; Martonen et al, 1982). The effects of hygroscopic growth on total deposition has been studied experimentally (Dautrebande and Walkenhorst 1960; Hicks et al, 1986) and growth of sodium chloride aerosols was inferred after larger particles were present on exhalation than on inhalation (Anselm et al, 1986). However, no experimental data exists on the effect of growth or shrinkage on regional deposition of aerosols in the lungs.

It has been proposed that the inhalation of non-isotonic aerosols, exercise and isocapnic hyperventilation (ISH) all lower FEV_1 by provoking bronchoconstriction as a result of increased airway fluid osmolarity (Smith and Anderson 1986). The surface area and airway fluid volume of the proximal airways are small compared to that of the distal airways and alveoli (Anderson et al, 1989). Therefore, the greatest changes in osmolarity due to non-isotonic aerosol deposition or conditioning of the inspired air during ISH or exercise, will occur in the large airways. There is also a direct relationship between the severity of the response and the dose (in terms of water loss from the airways or water required to return the airways to isotonicty) for all three of these stimuli (Smith and Anderson 1989a; Chen and Horton 1977).

The delivery of aerosol to the large airways, rather than the dose to the whole lung may therefore be the most important determinant of the response if the changes in airway fluid concentration (the stimulus) in the small airways and alveoli are minimal in comparison. Factors affecting this large airway dose will then control the response to the aerosol.

Characteristics relating to the subject may also have a profound effect on the regional deposition of the inhaled aerosols. Of particular importance is the geometry of the airways. It has been shown that the reduction in airway calibre occurring during an episode of asthma will increase deposition in the proximal

airways relative to the distal (Laube et al, 1986). This is of importance with challenge agents such as histamine (Ruffin et al, 1978) which may depend for their effect on the site of deposition. The pre-challenge lung function and pattern of bronchoconstriction during the challenge test may therefore alter the deposition pattern and hence the response. The airway narrowing occurring during non-isotonic aerosol challenge is likely to result in a greater proportion of the aerosol depositing on the proximal airways, thereby increasing the dose and altering the response.

If the pattern of deposition is important in diagnosis with non-isotonic aerosols (this includes therapeutic or other challenge agents delivered by nebulisation), then we need to understand and assess the effects of tonicity on regional deposition and the way in which changes in airway calibre affect deposition during the challenge itself.

We have previously demonstrated the use of a three dimensional scintigraphic technique as a sensitive method of distinguishing between the deposition patterns of large (5.5μm) and small (2.6μm) droplets (Phipps et al, 1989 [Chapter 7]). Our aim was therefore to mimic the inhalation of non-isotonic UN aerosols used in asthma diagnosis and compare the regional deposition of 0.3 and 4.5% NaCl aerosols of the same initial droplet diameter in normal subjects. Due to the large volume of radioaerosol and possible uncertainty of dose from the Mist-O_2-Gen

nebuliser, a jet-nebuliser was used with similar droplet characteristics. We also wished to study the effects of bronchoconstriction during inhalation of 4.5 % saline on the deposition pattern in asthmatic subjects.

8.2. Methods

1. Penetration index of hyper- and hypo- tonic aerosols in normal subjects.

An Up-Draft (Hudson Up-Draft Oxygen Therapy Sales Co., Temecula, CA., USA) jet nebuliser was used in this study.

The output of the jet nebuliser was lower than that of the Mist-O_2-Gen ultrasonic nebuliser at 0.23 ml/min (compared to 0.49 ml/min), while the droplet size was similar (mass median aerodynamic diameter (MMAD) = 3.7 - 3.8 μm and geometric standard deviation (σ_g) = 1.4 for the Up-Draft compared to MMAD = 3.6 μm and σ_g = 1.1 for the Mist-O_2-Gen)

The breathing system consisted of an aerosol inhalation circuit as previously described (Phipps et al, 1989 [Chapter 7]). The subject inhaled the aerosol with dilution air supplied via a medical humidifier and exhaled through a filter and carbon dioxide absorber into a bag-in-a-box. A pneumotachograph and potentiometer attached to a bell spirometer provided signals of flow and volume, respectively. A microcomputer was used to display a target volume, frequency and flow rate according to the previously determined respiratory pattern of that

subject. The subject was instructed to follow this target while inhaling the aerosol, thus keeping the breathing pattern similar on both aerosol inhalation occasions (see Chapter 6).

Eleven non-smoking subjects with no history of asthma or any other respiratory disease, and normal lung function tests, inhaled 4.5% and 0.3% NaCl aerosols on separate occasions. The aerosols contained approximately 200 MBq/ml of ^{99m}Technetium-diethyltriaminepenta acetic acid (^{99m}Tc-DTPA). Both aerosols were delivered by the jet nebuliser driven with compressed oxygen at 8 l/min. The droplet size distributions of the aerosols were measured by cascade impaction as previously described (Phipps et al, 1987 [Chapter 2]) and were found to have similar droplet size distributions (MMAD = 3.7 ± 0.1 μm for the hypertonic and 3.8 ± 0.1 μm for the hypotonic and σ_g = 1.4 ± 0.1 for both).

Spirometry was performed prior to, and a single test immediately after, inhalation (subjects were also instructed to gargle and expectorate, then to swallow water to remove mouth and oesophageal activity). Directly after the spirometry, each subject was placed in a supine position over a collimated gamma camera (GE 400AT, Milwaukee, Wisconsin, USA) and a 1 minute anterior and posterior image collected with two small ^{99m}Technetium-pertechnetate markers attached to the subject's chest to assist image alignment, before a 64 angle tomographic study of 12 minutes total duration was performed.

A transmission tomographic scan was performed to delineate the lung fields on a separate occasion. A flood source containing approximately 1.5 GBq of ^{153}Gd in water was fixed to a frame mounted on the camera head. With the subject in a supine position between the flood source and camera, a 64 angle tomographic study of the thorax was acquired in a 64 x 64w matrix. The attenuation images collected were then reconstructed to provide low definition anatomical data in the coronal plane.

2. *Penetration index of hyper- and iso- tonic aerosols in asthmatic subjects.*
Nine otherwise healthy, non-smoking subjects with a documented history of asthma, inhaled isotonic and hypertonic (4.5%) saline aerosols containing approximately 200 MBq/ml of ^{99m}Tc-DTPA on two separate occasions using the Up-Draft nebuliser. The duration of inhalation was decided on a previous occasion as the amount of hypertonic aerosol required to produce a minimum fall in FEV_1 of 20% of the pre challenge value, with 5 minutes the maximum inhalation time. The concentration of ^{99m}Tc-DTPA was adjusted to give a maximum nebuliser output of 100 MBq per study (estimated maximal activity depositing in the respiratory tract for each study = 30 MBq). The maximum whole body absorbed dose equivalent for each of these studies was estimated to be 0.025 mSv (Appendix III)

The subjects were requested to cease all bronchodilator medication for at least 6

hours prior to the aerosol inhalations. Spirometry was performed immediately before and after the aerosol inhalations. Bronchodilator aerosol was administered after the hypertonic aerosol if required (only subjects 1 and 9 required it), otherwise after the imaging was completed.

3. Data treatment for both studies.

The tomographic data were reconstructed and coronal reformatting performed (Phipps et al, 1989 [Chapter 7]). A thick mid-lung coronal slice was used to measure penetration index as described by Phipps et al (1989 [Chapter 7]). The lung regions were drawn with the aid of the transmission scans to delineate the lung boundaries. An example of the use of the transmission scan is shown in Figure 1, which shows a central aerosol deposition pattern and the lung boundary defined by transmission tomography in the subject 12. The penetration index (PI) was defined as the counts in a peripheral region / the counts in a central region. The central region was also modified to include the trachea (Figure 2a).

8.3. Results

The morphometric details of all the subjects are given in Table 1.

There was very little or no difference in any of the breathing parameters between inhalation occasions for all normal or asthmatic subjects (Table 2). The standard deviation of the breathing parameter means was less than 15 %.

Figure 1. Transmission (on the left of the figure) and corresponding emission images of subject 12. Coronal central slices are shown above transverse central slices in this figure. The aerosol has deposited centrally as can be observed by comparison with the lung boundaries shown in the transmission images.

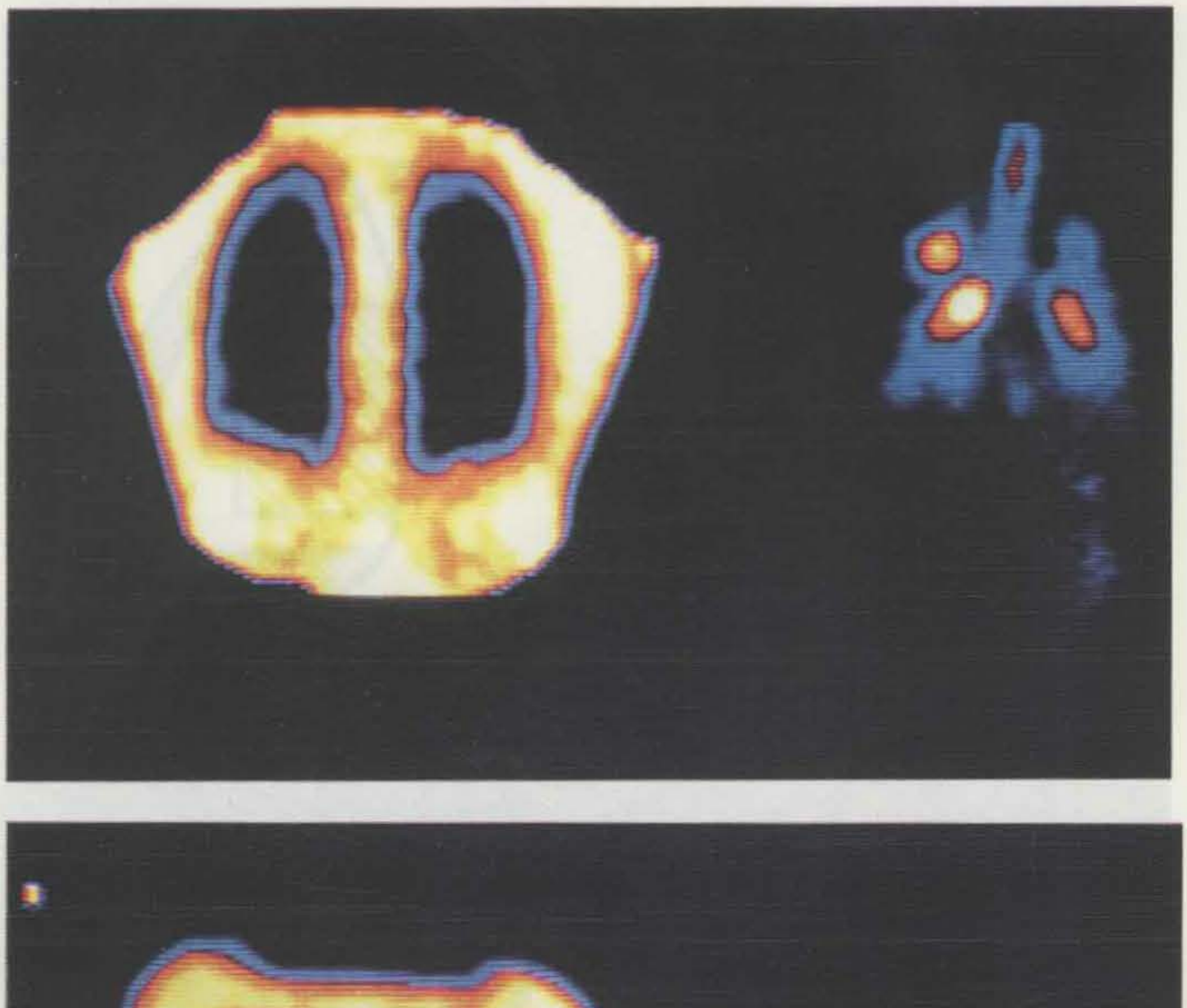

Figure 2. Above; a) Regions of interest as described in Chapter 7 with the central region altered to include the trachea. b) With peripheral region modified to include all but the central region.

Below; Mid-lung coronal slice of hypertonic aerosol study in subject 1, showing the modified central region.

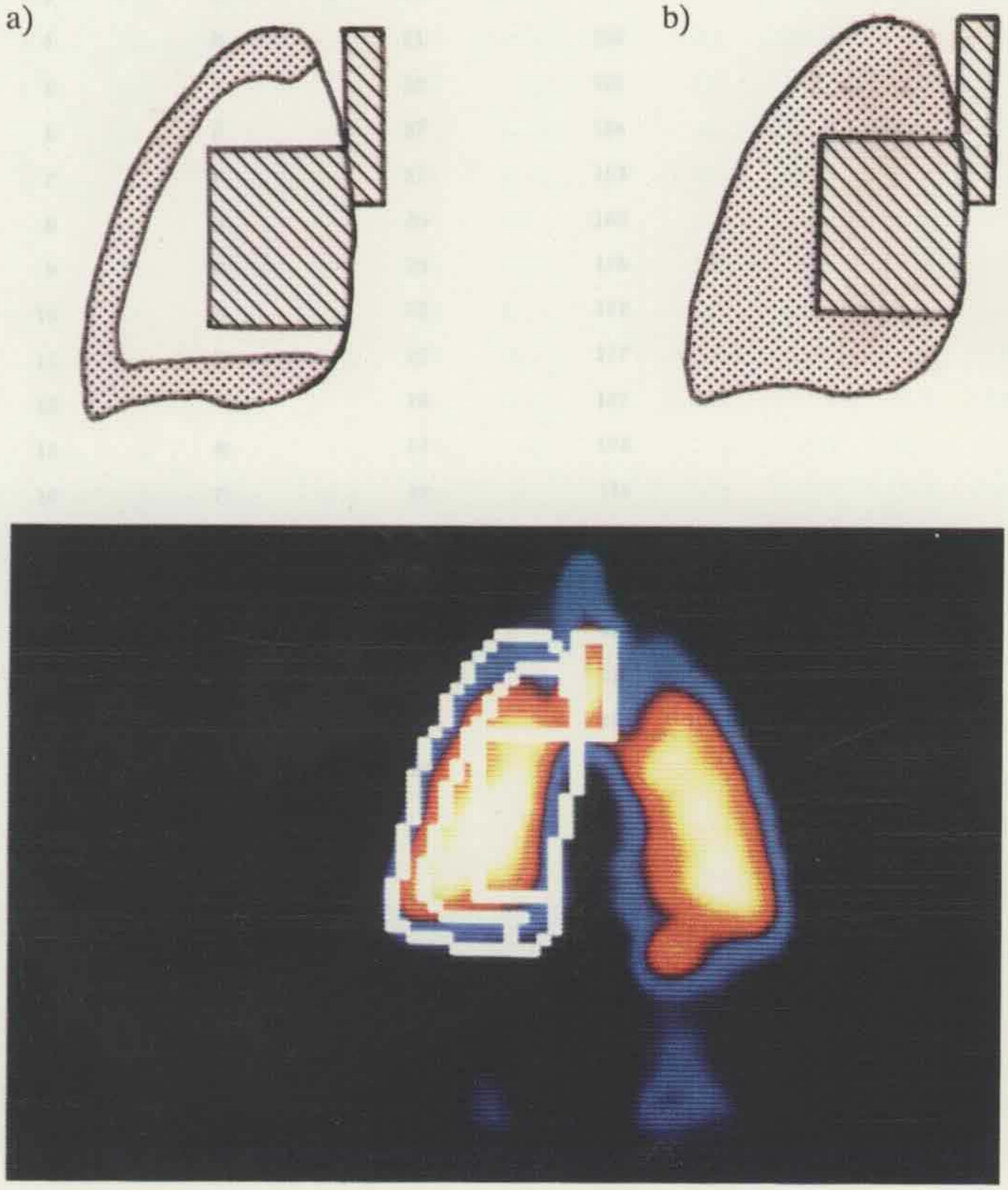

Table 1. Morphometric details of the normal subjects (numbers 1 to 11) and the asthmatic subjects (numbers 12 to 20).

Subject	Sex	Age (Year)	Height (cm)
1	M	23	170
2	M	24	174
3	M	19	170
4	M	21	169
5	M	22	182
6	F	27	164
7	F	27	163
8	M	20	165
9	M	20	176
10	M	23	179
11	M	22	177
12	F	20	167
13	M	27	173
14	M	22	174
15	F	30	156
16	M	25	188
17	M	26	173
18	M	23	179
19	M	22	180
20	M	24	174

Table 2. Mean breathing parameters for each subject (normal and asthmatic).

	Hypotonic or Isotonic aerosol					Hypertonic aerosol				
Subject	V_t	F_i	F_e	T_{tot}	P_i	V_t	F_i	F_e	T_{tot}	P_i
1	423	21.2	12.7	5.1	0.1	412	20.6	12.9	5.2	0.1
2	660	24.4	25.1	3.8	0.22	579	21.6	22.9	3.8	0.21
3	772	17.5	18.1	5.6	0.28	772	17.3	20.1	5.6	0.3
4	550	14.7	21.8	3.6	0.24	478	12.9	20.6	3.7	0.22
5	740	16.2	17.5	5.1	0.45	824	18.6	18.6	5.1	0.36
6	633	16.8	17.0	6.0	0.16	634	17.6	15.0	6.0	0.1
7	401	28.3	20.8	5.9	0.08	391	32.3	18.1	5.8	0.06
8	748	28.4	29.0	4.4	0.22	669	26.0	30.1	4.2	0.19
9	791	25.8	29.6	3.5	0.1	872	28.9	33.4	3.5	0.11
10	449	12.8	12.6	4.7	0.51	416	13.3	12.3	4.7	0.58
11	618	14.4	11.4	6.0	0.27	634	12.4	13.0	6.0	0.28
12	971	22.3	27.9	4.9	0.3	1003	25.4	32.1	4.6	0.22
13	1005	35.9	29.2	5.4	0.19	1101	40.9	29.8	5.5	0.14
14	710	35.8	24	4.4	0.15	752	38.4	26.5	4.4	0.11
15	363	18.6	13.6	5.0	0.3	439	20.0	15.5	5.7	0.5
16	1000	48.7	22.0	4.9	0.4	949	52.9	21.1	5.1	0.43
17	422	11.0	16.8	3.8	0.22	428	9.6	16.2	3.8	0.13
18	566	22.5	15.8	5.4	0.11	595	25.4	14.6	5.9	0.2
19	441	16.4	22.7	3.1	0.08	484	19.9	22.0	3.0	0.06
20	1894	71.5	35.8	6.8	0.06	1773	69.2	36.2	7.0	0.09

Notes:

V_t = Tidal volume [ml]

F_i = Peak inspiratory flow rate [l/min]

F_e = Peak expiratory flow rate [l/min]

T_{tot} = Time of respiratory cycle [s]

P_i = inspiratory pause [s]

The difference in the mean parameter between the two inhalation occasions was also less than 15 %, with the exception of inspiratory pause which was mostly within 0.1 seconds on the two occasions (subject 15 had a difference greater than this of 0.2 secs).

1. Penetration index of hypo and hyper- tonic aerosols in normal subjects.

The pre-test FEV_1 values were greater than 96% of predicted and were similar to the post-test values for all subjects on all study days (intra- and inter- study day differences were < 4.7 %).

There was no significant difference in PI between the hypo- and hyper- tonic aerosols when the tracheal counts were excluded from the central region (Table 3). It was noted however, that there was significantly greater activity in the trachea (as percent of total right lung counts) of the hypertonic compared to the hypotonic studies ($p<0.01$, Table 4 and Figure 3). This trend was also present with the static anterioposterior images taken immediately after inhalation ($p = 0.051$, Table 5). The regions of interest were therefore modified to include the trachea as part of the central region (shown in Figure 2a). The PI values for the small (2.6 μm) and large (5.5 μm) isotonic droplet inhalation studies (Chapter 7) were recalculated using the regions of interest that include the tracheal counts in the central region to assess the effects on PI for the large and small droplet studies.

Table 3. Deposition patterns for eleven normal subjects inhaling hypo- and hyper- tonic aerosols

	PI with tracheal counts excluded from central region.		PI with tracheal counts included in central region.		Central region (including trachea) as % of right lung counts		Modified PI. Non-central counts / central region (incl. trachea)	
Subject	Hypotonic	Hypertonic	Hypotonic	Hypertonic	Hypotonic	Hypertonic	Hypotonic	Hypertonic
1	45.4	51.9	39.9	39.2	62.7	69.8	59.5	43.3
2	47.0	45.2	43.5	34.8	55.4	69.3	80.6	44.3
3	81.7	77.2	73.4	71.1	44.7	44.8	123.6	122.9
4	49.1	50.6	46.3	46.3	52.7	53.0	89.7	88.5
5	71.5	58.6	67.4	52.7	43.4	47.7	130.7	109.6
6	48.6	54.8	42.9	47.0	55.5	54.0	80.1	85.2
7	42.2	45.5	38.1	41.4	55.8	53.0	79.3	88.8
8	42.1	45.9	36.7	35.3	64.0	69.7	56.3	43.4
9	50.1	47.2	48.2	42.5	51.8	55.2	89.6	81.1
10	61.5	63.3	53.0	46.3	53.6	61.7	86.7	62.2
11	54.5	48.6	51.6	42.6	47.6	54.8	110.0	82.4

Table 4. Tracheal counts as % of those in the right lung for all 20 subjects.

Subject	Isotonic or hypotonic aerosol	Hypertonic aerosol
1	7.6	17.1
2	4.1	16.1
3	4.5	3.5
4	3.0	4.5
5	2.5	4.8
6	6.5	7.8
7	5.4	4.8
8	8.3	16.1
9	2.7	5.5
10	7.4	16.6
11	2.5	6.7
12	4.2	22.7
13	1.8	37.8
14	18.5	33.5
15	5.1	14.7
16	1.8	6.7
17	11.3	26.3
18	5.7	7.1
19	7.3	7.6
20	4.1	8.2

Figure 3. Opposite: Mid-lung coronal images from the hypotonic (on the left) and hypertonic (on the right) aerosol studies in subject 1. Note the enhanced tracheal deposition in the hypertonic study.

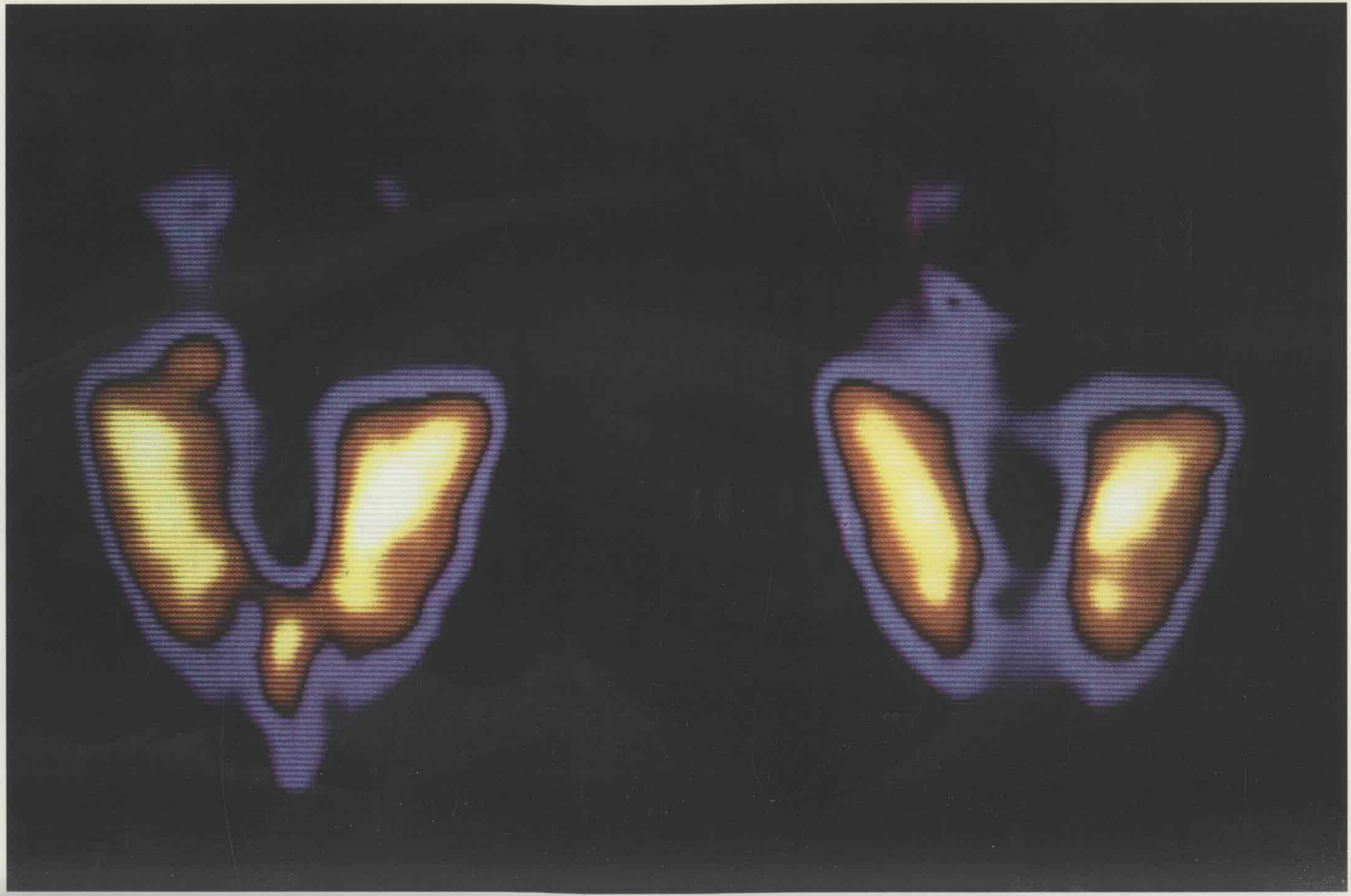

Table 5. Tracheal counts as a % of the right lung counts, obtained from static images taken immediately after inhalation of the hypo- or hyper- tonic aerosols in the normal subjects.

Subject	Hypotonic aerosol	Hypertonic aerosol
1	4.3	5.2
2	5.7	13.8
3	4.5	4.9
4	4.9	4.6
5	5.2	7.9
6	7.2	5.4
7	9.4	7.1
8	9.7	15.5
9	3.8	6.1
10	7.0	14.6
11	3.4	5.9

The difference in PI between large and small droplet studies for the coronal mid-lung slices was found to be significantly greater when the tracheal counts were included in the central region ($p = 0.02$, Table 6). By using the modified regions of interest, the PI from the hypo- and hyper- tonic studies came close to being significantly different ($p = 0.052$, Table 3). By expressing the central region counts (including the trachea) as a percentage of the total counts in the right lung, there was a significant difference between hyper- and hypo- tonic aerosols ($p = 0.02$) (Table 3). If the peripheral region is also modified to include all the counts in the right lung not included in the central region (Figure 2b) the PI values for hypo- and hyper- tonic aerosols are again significantly different ($p = 0.032$, Table 3).

2. Penetration index of hyper- and iso- tonic aerosols in asthmatic subjects.

There was no systematic difference in PI between the hyper- and iso- tonic aerosols for the whole group of asthmatic subjects due to the variations in response. However, a number of observations can be made on small groups of subjects (Table 7).

The difference in PI between the iso- and hyper- tonic aerosol studies may be expressed by the 'd' value, where $d = [PI\ (isotonic) - PI\ (hypertonic)] \times 100 / PI\ (isotonic)$. The provoked fall in pre-challenge FEV_1 and/or hygroscopic growth of the hypertonic aerosol would be expected to result in a smaller PI (positive d).

Table 6. PI values for large (5.5 μm) and small (2.6 μm) isotonic droplet inhalation studies in seven normal subjects. Results include or exclude tracheal counts in the central region. (For details see Chapter 7).

Subject	Tracheal counts excluded from central region			Tracheal counts included in central region		
	Small droplets	Large droplets	d values	Small droplets	Large droplets	d values
1	66.9	27.2	59.3	62.2	24.4	60.8
2	46.3	32.8	29.2	44.0	28.4	35.5
3	42.5	18.8	55.7	36.1	15.1	58.2
4	75.4	46.3	38.6	71.3	35.7	49.9
5	58.6	31.5	46.2	56.8	23.8	58.1
6	78.1	40.3	48.4	71.4	33.1	53.6
7	79.8	22.4	71.9	74.8	20.9	72.1

d value in this case is as defined in Chapter 7 (small - large / small) × 100 - ie percent fall in PI from small to large droplet study.

Table 7. Penetration Index, baseline and post test FEV_1 values for 9 asthmatic subjects for iso- and hyper- tonic aerosol inhalations.

	Coronal Slices				FEV_1 % Predicted			
	ISOTONIC		HYPERTONIC		ISOTONIC		HYPERTONIC	
Subject	Tracheal counts included in central region	Tracheal counts excluded from central region	Tracheal counts included in central region	Tracheal counts excluded from central region	Baseline FEV_1	Post-challenge FEV_1	Baseline FEV_1	Post-challenge FEV_1
12	48.6	60.2	9.7	17.7	82.1	88.2	76.4	16.0
13	37.6	40.7	13.9	30.2	98.3	100.7	100.7	84.4
14	36.9	50.4	31.6	20.4	92.2	92.7	96.5	90.5
15	39.5	48.3	22.5	35.6	118	119	118	117
16	43.3	46.8	36.1	46.5	79.9	77.5	79.6	75.8
17	28.5	39.4	20.8	39.9	70.3	75.6	74.1	80.4
18	27.6	32.8	45.1	58.4	62.3	61.3	85.7	83.8
19	21.8	26	32.9	40.6	73.2	70.6	79.3	73.9
20	18.6	24.6	22.2	39.3	58.1	59.3	70.7	20.2

Table 8. Changes in PI and FEV_1 ('d' values) for the asthmatic subject studies.

Subject	PI with tracheal counts included in central region	PI with tracheal counts excluded from central region	Isotonic % fall in FEV_1 during test	Hypertonic % fall in FEV_1 during test	Baseline FEV_1	Post challenge FEV_1
12	80.0	70.6	-7.4	79.1	6.9	81.9
13	63.0	25.7	-2.4	16.2	-2.4	16.2
14	44.7	3.3	-0.4	6.2	-4.7	2.4
15	43.3	26.3	-0.8	0.8	0.0	1.7
16	16.6	0.64	3.0	4.8	0.4	2.2
17	27.0	-1.3	-7.5	-8.5	-5.4	-6.3
18	-63.4	-78.0	1.6	2.2	-37.6	-36.7
19	-50.9	-56.2	3.6	6.8	-8.3	-4.7
20	-19.4	-59.8	-2.1	71.4	-21.7	65.9

Note:

d values calculated as: $d = [PI\ (isotonic) - PI\ (hypertonic)] \times 100 / PI\ (isotonic)$.

This was the case in subjects 12 to 17 (Tables 7 and 8) who had differences in baseline FEV_1 of less than 7%. Figure 4 shows the effect of bronchoconstriction provoked by the hypertonic aerosol on regional deposition in subject 12. The perihilar deposition pattern is evident when airway narrowing reduces the aerosol penetration.

Conversely, subjects 18 to 20 had a greater PI value for the hypertonic than the isotonic aerosol. All of these subjects had a better baseline (pre-challenge) FEV_1 on the hypertonic day which may account for this finding.

All 9 asthmatic subjects are included in the plot of d value of PI between iso- and hyper- tonic aerosols versus the difference in baseline FEV_1 and the difference in post-challenge FEV_1 between the iso- and hyper- tonic aerosols (Figure 5).

Again, of particular note was the fact that the counts in the trachea were greater on the hypertonic day for every subject ($p<0.01$, Table 4).

Figure 4. Mid-lung coronal slices of the hypertonic aerosol (on the left) and isotonic aerosol for subject 12. Note the effect of bronchoconstriction provoked by the hypertonic aerosol on the deposition pattern.

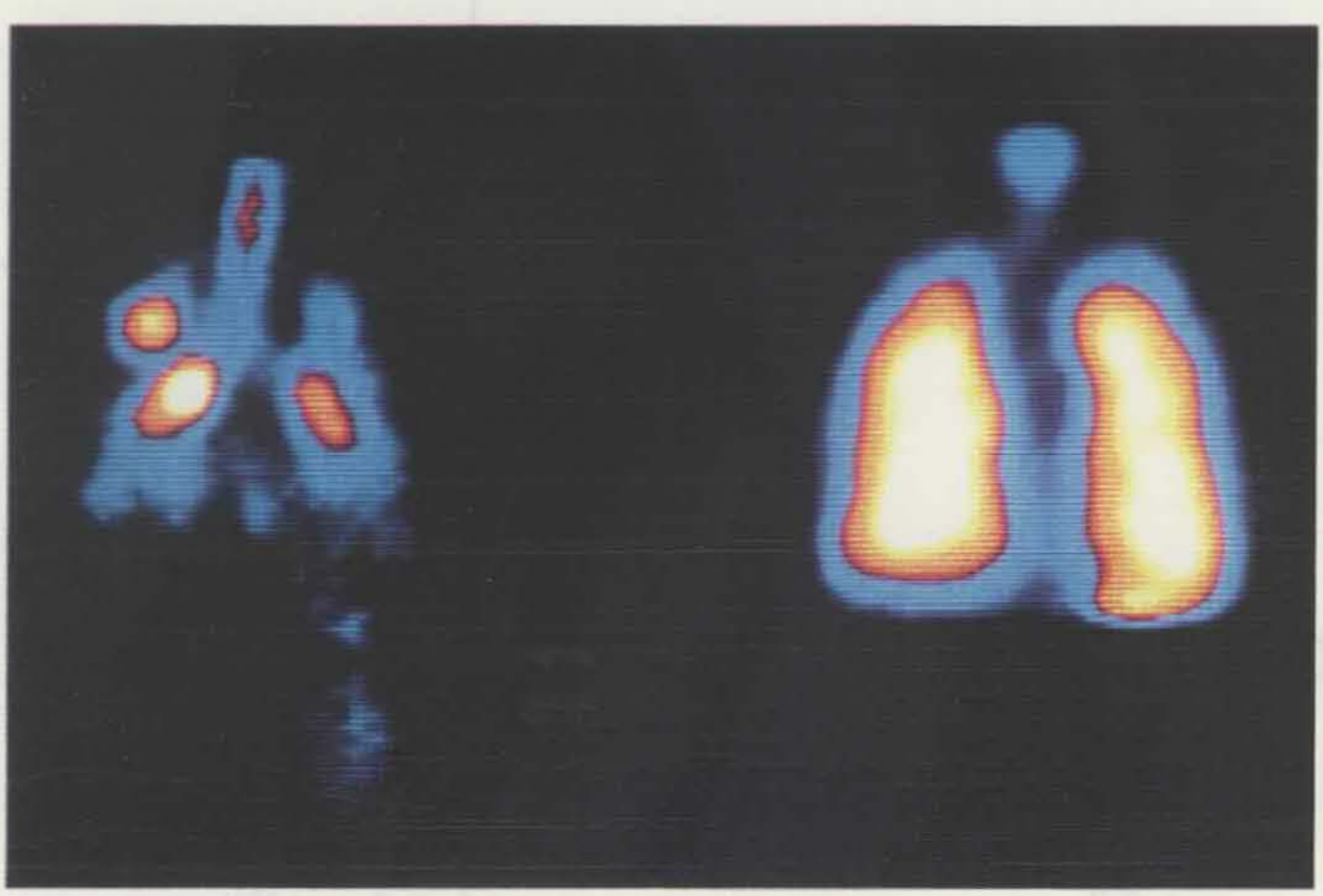

Figure 5. Plot of penetration index d values against the difference in baseline FEV_1 (circles) and the difference in post-challenge FEV_1 (squares) between the iso- and hyper- tonic aerosols. (d values expressed in %).

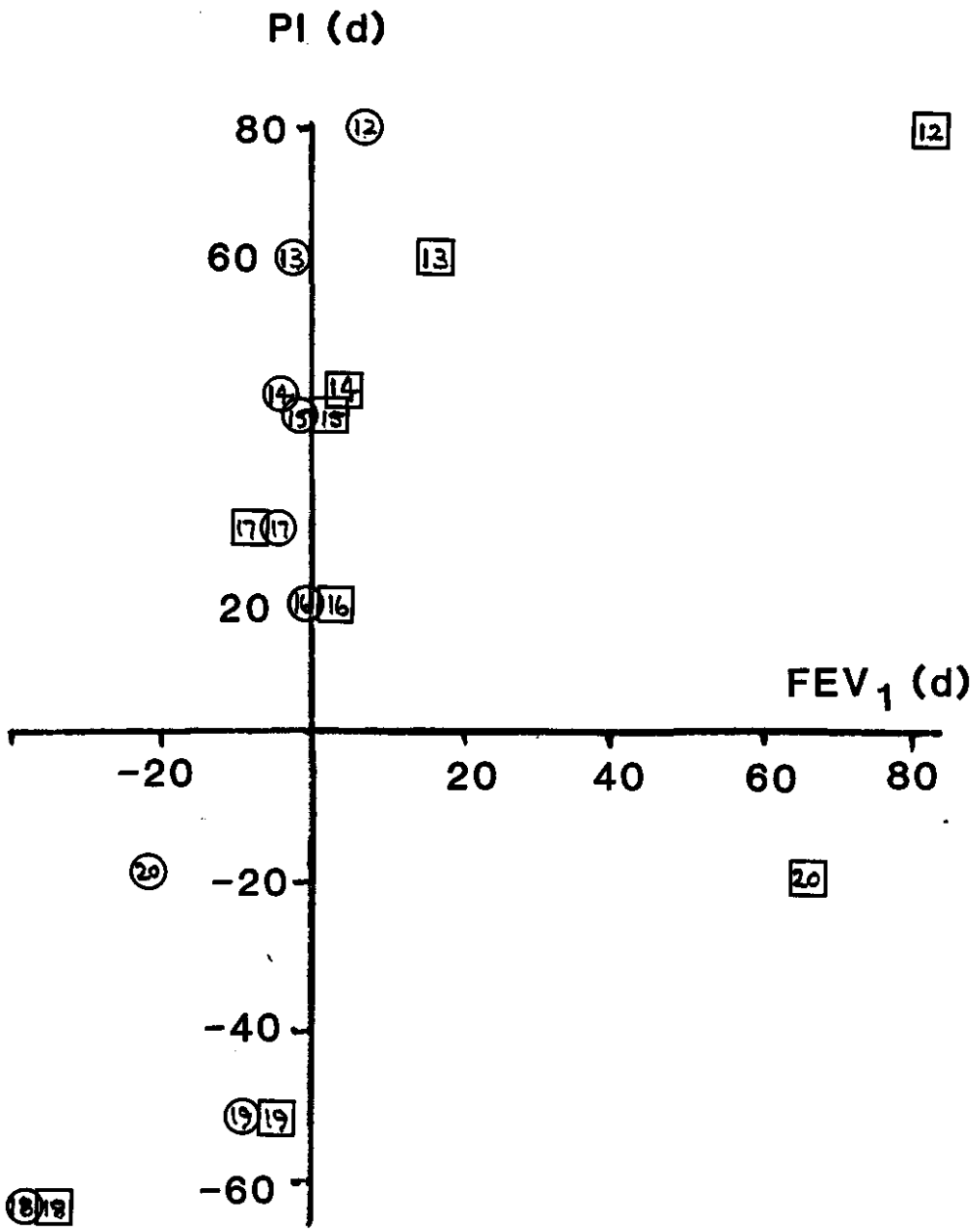

8.4. Discussion

The characteristics of the Mist-O_2-Gen ultrasonic nebuliser output have been previously determined (Phipps and Gonda 1990 [Chapter 3]). With a Hans Rudolf valve included in the delivery system, it has a higher output than the Up-Draft of 0.49 ml/min (Smith 1988) and droplets of a suitable size for penetration into the airways (mass median aerodynamic diameter of 3.6 μm and geometric standard deviation 1.1, Phipps and Gonda 1990 [Chapter 3]). Droplets of this initial size containing 4.5% saline, on reaching equilibrium with the isotonic fluid in the lungs, will grow in diameter to 6.3 μm. Conversely, droplets of the same initial size consisting of 0.3% saline will evaporate to an equilibrium size of 2.6 μm (Figure 6).

1. Penetration index of hyper- and hypo- tonic aerosols in normal subjects.

Using the same sensitive techniques, isotonic aerosol droplets of 2.6 and 5.5μm have been shown to deposit with markedly different deposition patterns in normal individuals (Phipps et al, 1989 [Chapter 7]). The mean % reduction in PI from the small to the large droplet study, using coronal mid-lung slices and including the trachea in the central region, was found to be 72.1 % (Table 6). Had the hypo-and hyper- tonic aerosol droplets used in this study reached their equilibrium size immediately upon entering the respiratory tract (2.4 and 6.3 μm respectively), the difference in PI measured after the 0.3 and 4.5 % saline aerosols would have been expected to be at least as great.

Figure 6. Diagram of hygroscopic growth and shrinkage to equilibrium size during inspiration of hyper- and hypo- tonic droplets of the same initial size (3.7μm) in the respiratory tract.

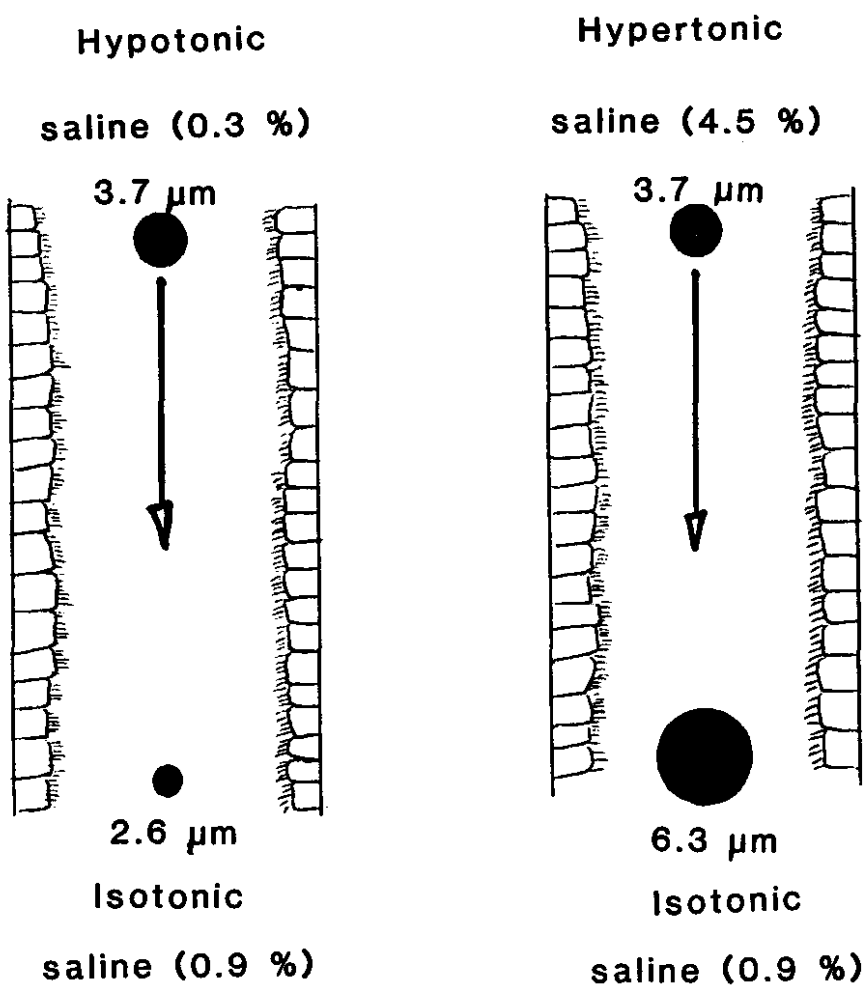

However, although the difference in PI was smaller, the regional deposition patterns of the two aerosols were still markedly different. A number of factors may have been operating to reduce the maximum differences in deposition pattern between the two aerosols:

a) *As the hypertonic aerosol passes through the airways, water is absorbed onto the droplets as they grow. This water is provided by evaporation from the airway surface which becomes hypertonic. The equilibrium diameter will then be greater as the airway fluid osmolarity approaches that of the droplets and the drive for hygroscopic growth will be reduced. Similarly, the opposite will occur for the hypotonic aerosol, water evaporating from the droplets will condense on the airway walls, reducing tonicity and further droplet shrinkage.*

b) *As the hypo- or hyper- tonic aerosols deposit on the airway surface, the tonicity will decrease or increase respectively, with effects as described above.*

c) *The tonicity of tracheal airway fluid is thought to be 10% greater than isotonicity (Boucher et al, 1980), so this will also reduce the driving force for hygroscopic droplet growth. However, the evaporation of the hypotonic droplets would be increased.*

d) *The velocity of the aerosol stream is high in the large airways and the largest droplets deposit by impaction in this region. The larger droplets also take longer to reach equilibrium. These factors work against complete attainment of equilibrium size and deposition of the large droplets before leaving the large airways. Smaller droplets that would normally escape deposition in the large airways, however, will grow more rapidly and deposit by impaction or shrink more rapidly and escape deposition in the large airways. The speed of growth is therefore of critical importance.*

e) *Water from the airway walls must diffuse to or from the centre of the aerosol stream. In the small airways, the amount of airway fluid is large compared to that of the aerosol, which, together with the low velocity of the aerosol stream provides optimum conditions for growth. Any droplet that remains hypo- or hyper- tonic will therefore grow or shrink rapidly and deposit by sedimentation in the small airways and alveoli, the droplets at this point may be closer to isotonicity when they deposit so the airway fluid concentration will tend to remain unchanged after deposition. In contrast, water has further to diffuse in the large airways (assuming no turbulence), less water is available and the droplet size is greater, therefore, growth or shrinkage is slower and incomplete.*

Therefore, although the ratio of peripheral to central deposition is greater for

the hypotonic aerosol compared to the hypertonic, there are a number of mechanisms that limit the preferential deposition in the large airways and augment deposition in small airways and alveoli of the hypertonic aerosol, while the hypotonic droplets tend to have a lower deposition in both large and small airways.

A striking finding was the increased count found in the trachea after the hypertonic aerosol, compared to either the hypotonic used in the normal subjects or the isotonic in the asthmatic subjects (in all but two of the 20 subjects total). Although mucociliary clearance (MCC) has been shown to be faster after hypertonic aerosols (Pavia et al, 1983), hypotonic aerosols have been reported to have a similar effect in some normal subjects (Pavia 1984; Foster et al, 1976). However, the delay between aerosol inhalation and imaging was short (up to 10 minutes) and differences of a similar magnitude were seen in the static images collected immediately after aerosol inhalation (Table 5). Some of the activity in the trachea may, however, have originated from the first or second bifurcation. This effect may be due to hygroscopic growth occurring in the upper airways and trachea causing greater deposition at or close to the carina and subsequent mucociliary clearance up the trachea.

The ratio of peripheral to central airway deposition was greater for the hypotonic aerosol, suggesting that the large airways received a greater proportion of the hypertonic aerosol compared to the distribution of the hypotonic aerosol. From these experiments it is difficult to deduce to what

extent the differences in PI are due to hygroscopic growth or shrinkage. The two likely explanations are that i) the hypertonic aerosol grows to increase central deposition at the cost of reduced peripheral deposition and ii) the hypotonic aerosol has a lower central and increased peripheral deposition due to shrinkage. Regional aerosol delivery is therefore not equivalent with hypo- and hyper- tonic aerosols due to changes in droplet diameter as a result of hygroscopic growth and/or shrinkage.

Persons et al (1987) considered the use of hypertonic aerosols as a means of maximising alveolar deposition of medicinal aerosols. Predictions of total and regional deposition were made using a mathematical model of hygroscopic growth and deposition probability specifically developed by them. They found that pulmonary deposition could be maximised by using hypertonic aerosols of at least 3.5% saline and a droplet size of 2-3 μm. From the results of Persons et al the fractional deposition of 4 μm droplets (σg = 1.8, breathing frequency = 15 min^{-1} and tidal volume = 1000 ml, assuming a relative humidity of 85% for mouth and pharynx and 99.5% for lung) are as follows:

	Total	Tracheo-bronchial (TB)	Pulmonary (P)	P/TB
Hypertonic (3.5 %)	71	20	31	1.55
Hypotonic (0.45 %)	58	12	28	2.33

The predicted deposition fractions show similar alveolar deposition for both aerosols but a greater proportion of tracheobronchial deposition for the hypertonic aerosol than the hypotonic. These predictions are confirmed by our results, although the difference is not as great as measured by us, probably due because: a) the assignments of the regions in the model and experimental data are different, b) the model does not take into account the possible effect of the aerosol tonicity on that of the airway fluid, c) Persons et al only treat the limiting case of a single droplet passing through the respiratory tract.

The calculations of Persons et al predict that the total deposition of the 3.5% aerosol will be increased by 22% compared to the 0.45% aerosol. This is important in challenge testing because the total dose, especially to the large airways will be increased.

Many therapeutic, diagnostic and environmental aerosols are hygroscopic in nature for example, some mucolytics (Pavia et al, 1983), dry particulate drugs such as disodium chromoglycate in its dry powder form and in nebuliser solutions (Fois et al, 1986) and even droplets generated from isotonic

nebuliser solutions may become hypertonic before reaching the airways (Phipps and Gonda 1990 [Chapter 3]). The effects of hygroscopic growth or shrinkage must therefore be taken into account for the prediction of the regional and total deposition of these drugs.

2. *Penetration index of hyper- and iso- tonic aerosols in asthmatic subjects.*

Airway narrowing has been shown to alter regional deposition in favour of the large airways (Richards et al, 1988; Laube et al, 1986; Pavia et al, 1977; Dolovich et al, 1976) in studies where bronchoconstriction prior to administering the imaging aerosol was deliberately induced. Our aim was to assess the effects of baseline lung function and bronchoconstriction during the challenge test on regional deposition.

Six of the nine asthmatic subjects (subjects 12 to 17) had positive d values for PI, in three of these, there was a direct relationship between the differences in % fall in FEV_1 and PI on the two study days (subjects 12 to 14). The small variations in baseline and post- challenge FEV_1 values for both study days in the second three of the six subjects with positive d values for PI (subjects 15 to 17) would suggest that hygroscopic growth may be the major cause of the lower penetration of the hypertonic aerosol. Figure 5 shows the effect of baseline and post challenge FEV_1 changes on PI in graphical form. Small changes in baseline lung function appear to cause the greatest differences in PI, and where the baseline FEV_1 was greater on the hypertonic day ('d' value is negative), the PI was also greater on the hypertonic day ('d' value also

negative) even though there was marked bronchoconstriction on the hypertonic day (subject 20, Figure 5).

In a similar way to the effects of hygroscopic growth, bronchoconstriction increases the fraction of the dose to the central airways while peripheral airway dose is reduced (Dolovich et al, 1976). Thus, if the response depends on regional deposition then it will be altered by the effects of the challenge itself. Therefore, as constriction continues, the stimulus to the large airways will be greater. These challenge tests are not generally carried out on subjects who have a very poor lung function, but changes in baseline from one day to the next may alter the apparent responsiveness to challenge agents that depend on site of deposition for their effect. Apart from variations in baseline lung function, these results show that there is a large variability in regional deposition pattern in asthmatics due to airway narrowing during the challenge and hygroscopic growth of the aerosol droplets in the lungs.

The fact that the response to hypertonic aerosol in asthmatics has been shown to plateau (Smith and Anderson 1989b), suggests that as aerosol dose is increased, more generations are recruited in the hypertonic response up to a limit that may occur at generation 12 where the volume of periciliary fluid rises sharply (Anderson et al, 1989). This observation supports the theory that the delivery of aerosol to the large airways may be the major force in provoking airway narrowing. The fact that aerosol delivery to the large airways is likely to be sensitive to small changes in regional deposition pattern

is therefore of significance. A minor change in deposition pattern resulting in the central deposition of a small proportion of aerosol that would otherwise deposit in the lower airways and alveoli will result in disproportionately large increases in droplet delivery to the large airways. Because the large airways have a relatively small surface area, there could be a very considerable change in the concentration of the substance delivered by the aerosol in the large airways.

8.5. Summary

1. Hygroscopic growth and/or shrinkage is likely to occur to some degree with the aerosols used in this study. Although the effects of tonicity on regional deposition are complex and depend on the droplet size and concentration of the aerosol, the hypertonic aerosol deposited more centrally than the hypotonic in this study, but not by the magnitude expected assuming that all potential growth to equilibrium with isotonic fluid at 37°C had occurred immediately upon entering the respiratory tract.

2. The challenge test itself alters the regional deposition of the aerosol in sensitive subjects and it is related to the fall in FEV_1.

3. The baseline FEV_1 alters the regional deposition as expected.

4. The greater tracheal deposition of the hypertonic aerosol is a feature that may be at least partly due to rapid hygroscopic growth in the oropharynx and

trachea.

These results suggest that the hygroscopic nature of aerosols should be taken into account with regard to total deposition and regional variations in aerosol delivery, especially if the response to the aerosol is known to be dependent on regional deposition.

The intrasubject variability of regional deposition was not directly measured in these studies due to ethical considerations of repeated radioaerosol inhalations in the same subject. However, by considering the group of normal subjects as a whole, intrasubject variability will be accounted for in the statistical treatment of the results. In fact, intrasubject variability may account for the fact that statistical significance was not reached in some of these studies and a greater number of subjects may be more rewarding in this regard.

Intersubject variability is relatively low as described by the standard deviation of the 'd' values of penetration index for the large and small droplet deposition studies (Figure 5, Chapter 7). Intrasubject variability is likely to be less than this. Variability in PI values is likely to be greater for the asthmatic subjects due to the nature of their lung disease. Future studies may benefit from an assessment of intrasubject variability of regional deposition and its relationship to lung function parameters.

Chapter 9

Summary

9.1. Conclusions

It is hoped that the work described in this thesis is contributing to the understanding of factors involved in delivering aqueous aerosols to the lungs by nebulisation. By estimating the rate of aerosol delivery to the target site within the lung and the factors that control this, aerosol generators can be evaluated with greater effectiveness to provide appropriate aerosol delivery for many therapeutic and diagnostic uses. The design of nebuliser systems in the future will also benefit from a full understanding of the inadequacies of the present equipment.

We have shown that the characteristics of nebulised aerosol droplets alter with time of generation. The droplet solute concentration may rise sharply and the size fall as aerosol generation progresses due to evaporation between the generator and mouthpiece. The fact that the humidity of the air inhaled along with the aerosol stream also alters the droplet characteristics means that droplet size distribution measurements should be carried out under standard conditions for comparisons between investigators. These findings are also important with respect to the prediction of regional and total deposition.

The delivery of hypertonic aerosols has been shown to cause bronchoconstriction in hypersensitive subjects. If nebuliser systems deliver hypertonic droplets from initially isotonic nebuliser solutions, airway narrowing and cough may occur in some patients.

The accurate measurement of regional deposition is important for many studies of aerosol deposition and clearance and especially in studies where deposition patterns of two aerosols are to be compared. With the aid of three-dimensional gamma scintigraphy, we have been able to assess regional deposition with greater sensitivity than previously possible with two-dimensional imaging. We then applied these new techniques to compare the deposition patterns of the hyper- and hypo- tonic aerosols currently used in asthma diagnosis.

Hypertonic droplets have the potential to grow, and hypotonic to shrink, in the respiratory tract. For the first time, we have some evidence of the effects of this phenomenon on regional deposition. In normal subjects, there is a difference in the deposition patterns of hyper- and hypo- tonic aerosols of the same initial droplet size and inhaled under the same breathing conditions. These results may be important if, as suspected, the deposition site of the non-isotonic challenge aerosols is critical in the response to them.

Asthmatic subjects may bronchoconstrict during challenge tests and their baseline lung function is often variable. Both of these factors, together with

hygroscopic growth were found to alter regional deposition. Therefore, small changes in baseline lung function, the amount and speed of airway narrowing and the extent of hygroscopic growth will all alter the relative amounts of aerosol depositing in large versus small airways.

9.2. Future work

Although differences in deposition pattern were found between hyper- and hypo- tonic aerosols, the magnitude was much lower than predicted. Hygroscopic growth or shrinkage may be maximised by a number of experimental changes:

i) Use of a less dense aerosols to reduce the change in airway tonicity due to direct deposition of the non-isotonic droplets.
ii) Increase in the saline concentration to maximise hygroscopic growth.
iii) By using hyper-, hypo- and iso- tonic aerosols the contribution of growth and shrinkage to any differences in deposition pattern may be assessed.
iv) By using different initial sizes.

The transmission scanning can enable the accurate determination of attenuation coefficients for attenuation correction of the emission studies (Macey and Marshall 1982). The regional amounts of absolute activity could then be determined which would enable comparison between patients and measurement of total deposition which is thought to be effected by hygroscopic growth (Persons et al, 1987b).

It has been postulated that hypertonic aerosols exert much of their effect in the large airways, the major site of inspired air conditioning during exercise (Anderson et al, 1989). A study to determine the bronchoconstrictive effect of similar doses of aerosol delivered to different parts of the respiratory tract would help to determine the site of action of these challenge aerosols.

Appendix I

Mass balance predictions of droplet solute concentration.

The derivation ignores the mass of dry air associated with the aerosol. We consider sampling at two points: the nebuliser and the mouthpiece. The total mass output from the nebuliser M_I is the sum of the mass flow of droplets M_{dI} and vapour M_{vI}

$$M_I = M_{dI} + M_{vI} \qquad \text{Eqn. 1}$$

At the point of generation, the concentration of solute in the droplets, C_I, is given by the solute output M_{sI} and the droplet output M_{dI}

$$C_I = M_{sI} / M_{dI} \qquad \text{Eqn. 2}$$

M_{sI} may be measured directly from the change in mass and solute concentration in the nebuliser:

$$M_{sI} = (C_{ni} \times M_{ni}) - (C_{nf} \times M_{nf})$$

Where C_{ni} = Initial nebuliser concentration.

M_{ni} = Initial nebuliser solution mass.

C_{nf} = Final nebuliser concentration.

M_{nf} = Final nebuliser solution mass.

The total mass of aerosol arriving at the mouthpiece, M_{II}, is

$$M_{II} = M_{dII} + M_{vII} \qquad \text{Eqn. 3}$$

where M_{dII} and M_{vII} are the mass flow of droplets and vapour at the mouthpiece. From mass balance, M_{II} must be equal to M_I plus any vapour added between the two sampling points by the dilution air, mass flow M_{III}, less any losses of droplets, vapour and solute, ML:

$$M_{II} = M_I + M_{III} - ML = M_{dII} + M_{vII} \qquad \text{Eqn. 4}$$

The concentration of solute in the droplets at the mouthpiece is C_{II}

$$C_{II} = M_{sII} / M_{dII} \qquad \text{Eqn. 5}$$

Substituting from the previous equation

$$C_{II} = M_{sII} / (M_{II} - M_{vII}) \qquad \text{Eqn. 6}$$

The vapour content at the mouthpiece per unit volume V_{II} multiplied by the volumetric flow rate at that point, Q_{II}, is equal to M_{vII}

$$M_{vII} = V_{II} Q_{II} \qquad \text{Eqn. 7}$$

Assuming ideal behaviour in the gas phase, V_{II} is obtained from the ideal gas equation

$$V_{II} = P_{II} M_w / (R T_{II}) \qquad \text{Eqn. 8}$$

where P_{II} and T_{II} are the vapour pressure and temperature at the mouthpiece, and R and M_w are the universal gas constant and molecular weight of water, respectively.

The vapour pressure P_{II} can be calculated on the assumption that the droplets of aerosol are in equilibrium with the surrounding atmosphere. In principle, P_{II} is a function of the droplet size, temperature (T_{II}) and the concentration C_{II}. Ignoring the Kelvin effect (ie the size of the droplet), P_{II} can be calculated from the saturation vapour pressure (P_o) of water at temperature T_{II} [$P_o (T_{II}) = P_{oII}$] and water activity a_{wII}:

$$P_{II} = a_{wII} P_{oII} \qquad \text{Eqn. 9}$$

a_w, of course, depends on the solute concentration C_{II}. P_{oII} can be obtained from tables, or from empirical equations for P_o as a function of temperature (Melwyn Huges?.). M_{vII} thus becomes (eqns 7-9)

$$M_{vII} = Q_{II} P_{oII} a_w(C_{II}) M_w / (R T_{II}) \qquad \text{Eqn. 10}$$

This leads to an implicit equation for C_{II}: from equations 6 and 8:

$$C_{II} = \frac{M_{sII}}{M_{II} - \frac{Q_{II} P_{oII} M_w a_w(C_{II})}{R T_{II}}} \qquad \text{Eqn. 11}$$

In ideal solutions, the water activity a_w is equal to the mole fraction of water Xw which, in turn can be expressed in terms of C_{II} (Appendix II) and the ratio of the molecular weight of the water to that of the solute r:

$$X_{wII} = (1 - C_{II}) / (r\, C_{II} + 1 - C_{II}) \qquad \text{Eqn. 12}$$

Thus, the substitution of 12 into 11 and rearrangement gives a quadratic equation for C_{II}:

$$C_{II}^2 [M_{II} (r-1) + Q_{II} V_{oII}] + C_{II} [M_{II} - Q_{II} V_{oII} - M_{sII} (r-1)] - M_{sII} = 0 \qquad \text{Eqn. 13}$$

where V_{oII} is the saturation vapour content at temperature T_{II}.

Alternatively, a_w for non-ideal solutions can be obtained from suitable theoretical, or empirical expressions. Cinkotai (1971) gave an expression for a_w for sodium chloride solutions at 36°C in the concentration range up to 26.7% which can be written as:

$$a_w = 1 + \alpha\, C_{II} + \beta\, C_{II}^2 \qquad \text{Eqn. 14}$$

where α = -0.486 and β = -1.55.

Since water activity of sodium chloride solution depends only weakly on temperature, this equation is a useful approximation for temperatures other than 36°C.

Substitution of this equation into 11 and rearrangement gives a cubic equation for C_{II}:

$$C_{II}^3 + \alpha/\beta\ C_{II}^2 + [1/\beta - M_{II} / (Q_{II}\ V_{oII}\ \beta)]\ C_{II} + M_{sII} / (Q_{II}\ V_{oII}\ \beta) = 0 \qquad \text{Eqn. 15}$$

The expression used to calculate V_{oII} in our work is from Melwyn Hughes textbook of Physical Chemistry 2nd edition:

$$\log_{10}\ P_o = a - (b \log_{10}\ T_{II}) - (c / T_{II}) \qquad \text{Eqn. 16}$$

where P_o = Saturated vapour pressure (mmHg)

a = 24.068883

b = 5.138

c = 2975

Then

$$V_{oII} = P_o(T_{II})\ M_w / (R\ T_{II}) \quad \text{(from ideal gas equation)}$$

Any change in the concentration of the solution in the droplets must be related to the change of the mass (and therefore the size) of the droplets.

The conversion from concentration to mass can be done by substitution of

$$M_{dII} = M_{sII} / C_{II} \qquad \text{(eqn 5)}$$

in equation 13, or 15, and rearrangement.

Therefore, if we assume ideal behaviour:

$$M_{dII}^2 - M_{dII}\,[M_{II} - Q_{II}\,V_{oII} - M_{sII}(r-1)] - M_{sII}\,[M_{II}(r-1) + Q_{II}\,V_{oII}] = 0 \qquad \text{Eqn. 17}$$

Using the empirical expression for a_w of sodium chloride solutions (Cinkotai 1971)

$$M_{dII}^3 + M_{dII}^2\,([Q_{II}\,P_{oII}\,M_w / (R\,T_{II})] - M_{II}) + \alpha\,M_{dII}\,Q_{II}\,P_{oII}\,M_w\,M_{sII} / (R\,T_{II}) + \beta\,M_{sII}^2\,Q_{II}\,P_{oII}\,M_w / (R\,T_{II}) = 0 \qquad \text{Eqn. 18}$$

The number output of droplets at the mouthpiece n_{II} and their average mass m_{dII} is related to the mass flow of droplets at this stage:

$$M_{dII} = n_{II}\,m_{dII} \qquad \text{Eqn. 19}$$

so that the average droplet mass can then be calculated either by modification of eqn 17 (ideal solutions):

$$m_{dII}^2 - 9m_{dII} / n_{II})\,[M_{II} - Q_{II}\,V_{oII} - M_{sII}(r-1)] - M_{sII}\,[M_{II}(r-1) + Q_{II}\,V_{oII}] / n_{II}^2 = 0 \qquad \text{Eqn. 20}$$

or for non-ideal sodium chloride solutions (eqn 18):

$$m_{dII}^3 + m_{dII}^2\,[Q_{II}\,P_{oII}\,M_w / (R\,T_{II}) - M_{II}] / n_{II} + Q_{II}\,P_{oII}\,M_w\,M_{sII}\,\alpha\,m_{dII} / (R\,T_{II}\,n_{II}^2) + [Q_{II}\,P_{oII}\,M_w / (R\,T_{II}\,n_{II}^3)]\,\beta\,M_{sII}^2 = 0 \qquad \text{Eqn. 21}$$

The average droplet mass m_d defined by equations 20 and 21 is not usually measured directly. It could be obtained by a combination of total mass flow

measurement and particle counting. However, it is more desirable to relate it to droplet size distribution. Assuming that the distribution is log-normal, the diameter of the droplet of average mass d_w is related to the mass median diameter MMD and the geometric standard deviation σg and the droplet density, ρ.

$$d_w = MMD \exp(-1.5 \ln^2\sigma_g) = \sqrt[3]{(6m_d / \pi \rho)} \qquad \text{Eqn. 22}$$

In cases where an aerodynamic sizing method is used, MMD can be obtained from the mass median aerodynamic diameter MMAD; ignoring the slip correction and shape factors:

$$MMD = MMAD \sqrt{\rho} \qquad \text{Eqn. 23}$$

where ρ is the density of the droplet (according to Ferron for the ideal solution assumption (REF):

$$\rho = (100 \times 2.165) / (100 \times 2.165 + C \times 1.165)$$

where C is expressed as % w/w or according to Cinkotai for the empirical equations (Cinkotai 1971).

$$\rho = 0.995 + (0.00752\ C_{II}) + (0.00000174\ C_{II}^2)$$

where ρ is in g/cm^3 and C in % w/w.

If losses between the generator and the mouthpiece are insignificant, further simplifications are possible:

from equation 4: $M_{II} = M_I + M_{III}$ Eqn. 24

$$M_{sI} = M_{sII} \qquad \text{Eqn. 25}$$

$$n_I = n_{II} \qquad \text{Eqn. 26}$$

where n_I is the droplet number output at the generator. Therefore, (i) the concentration of the solution in the droplet at mouthpiece (equations 11 or 15) can be calculated directly from the generator mass output M_I, the vapour mass flow from the dilution air M_{III}, volumetric flow rate at the mouthpiece Q_{II}, saturation vapour content at T_{II} (from equation 16) and the solute output M_{sI}. (ii) for log-normally distributed aerosol, the mass size distribution at the mouthpiece can be obtained from the input parameters required to calculate C_{II} (equations 20 and 21) together with the parameters MMD and σg of the original size distribution in the nebuliser. The number output n_I (which is assumed to be equal to n_{II} for the case of negligible droplet loss) is:

$$n_I = M_{dI} / m_{dI} \qquad \text{Eqn. 27}$$

where m_{dI} is calculated from MMD (cf equation 22).

Summary of symbols and [dimensions] in Appendix I

M = mass output (mass flow), [mass / time].
C = dimensionless, concentration of solution, [mass of solute / mass of solution].
Q = volumetric flow rate [volume / time].
P = vapour pressure [pressure].
T = temperature [absolute temperature].
V = vapour concentration [mass / volume].
R = universal gas constant [Pressure × volume / (moles × temperature)]
a_w = water activity [dimensionless].
r = ratio of molecular weight of water to that of the solute [dimensionless].
ρ = density of solution [mass / volume].

MMD = mass median diameter [length].

MMAD = mass median aerodynamic diameter [length].

σ_g = geometric standard deviation [dimensionless].

M_w = molecular weight of water [weight per mole]

α = constant - 0.486 [dimensionless]

β = constant - 1.55 [dimensionless]

n = droplet output [1 / time]

m = average mass of droplet [mass]

d_m = diameter of droplet of average mass [length]

Subscripts and superscripts

I = at the generator

II = at the mouthpiece

III = from dilution air

d = droplets

v = vapour

s = solute

w = water

Appendix II

Mass balance predictions of droplet size.

The mole fraction of water is

$$X_w = n_w / (n_w + n_s) \qquad \text{Eqn. 1}$$

where nw and ns are the number of moles of water and solute respectively. These can be calculated from the total (m) and molar (M) masses:

$$X_w = (m_w / M_w) / (m_w / M_w + m_s / M_s)$$

$$= 1 / (1 + (r\, m_s) / m_w) \qquad \text{Eqn. 2}$$

where

$$r = M_w / M_s \qquad \text{Eqn. 3}$$

Now, the dimensionless mass concentration C_{II} is :

$$C_{II} = m_s / (m_s + m_w) = (m_s / m_w) / (1 + m_s / m_w) \qquad \text{Eqn. 4}$$

Rearrangement of the last equation gives:

$$m_s / m_w = C_{II} / (1 - C_{II}) \qquad \text{Eqn. 5}$$

which, substituted into equation AII.2 gives equation AI.12.

Appendix III

Radiation dosimetry Calculations.

There is a great deal of variability in the estimation of the radiation dose received by the 'critical organ' and the body as a whole. This is due firstly to the fact that methods of calculation and the rigour to which they are carried out are apt to vary, and secondly, the intersubject variability is usually high.

The calculations made below are taken from a publication by Barber (1985) who realises the importance of urinary clearance for the cumulated absorbed radiation dose to the whole body but especially to the bladder wall. An important part of our protocol is the preliminary hydration and subsequent high fluid intake and voiding rate of our subjects. This is taken into account by Barber.

The dose delivered to a target organ (D_t) is given by:

$$D_t = A_s S_{(t-s)} \qquad (i)$$

Where $S_{(s-t)}$ is the 'S' value given in the MIRD II pamphlet (Snyder et al, 1985) and represents the fraction of the dose absorbed by a target organ (t) as a result of a cumulated activity A (assumed to be uniformly distributed) in the source organ (s).

Barber calculates the cumulated activity in four source organs; lungs (l), kidneys (k), bladder contents (bc) and rest of body (rb). Absorbed doses for each of six target organs are calculated by multiplying cumulative activities by the appropriate S value and summing for all source organs.

'S' values are given for the contribution of each source organ to each target organ except for the rest of the body. In this case, S values for the total body (tb) were modified using organ mass (M) values quoted in MIRD II:

$$S_{(t\text{-}rb)} = S_{(t\text{-}tb)} \cdot (M_{tb}/M_{rb}) - S_{(t\text{-}l)} \cdot (M_l/M_{rb}) - S_{(t\text{-}k)} \cdot (M_k/M_{rb}) - S_{(t\text{-}bc)} \cdot (M_{bc}/M_{rb}) \quad \text{(ii)}$$

The cumulated activity for each source organ was cslculated assuming exponential elimination from the lungs and bi- exponential elimination from the remainder of the body and kidneys. Integration the appropriate expressions with time gives the cumulated activity for each source organ thus:

$$A_l = \frac{A_o}{\delta_l + \delta_p} \quad \text{(iii)}$$

$$A_{rb} = A_o \, \Sigma^2 \, r_i \; 1/(\delta_p + \delta_{ri}) \, (\delta_l + \delta_p) \quad \text{(iv)}$$

$$A_k = A_o \, \Sigma^2 \, k_i \; 1/(\delta_p + \delta_{ki}) \, (\delta_l + \delta_p) \quad \text{(v)}$$

Barber takes into account the voiding time (T) when producing an expression

for the cumulated activity in the bladder contents (bc):

$$\sum_{n=1}^{\infty} B_n = A_0 k_1 [1/1-\exp(-\delta_{k1} + \delta_p)T) (\delta_{k1} - \delta_l)]...\text{etc} \quad \text{(vi)}$$

Where: *

δ_p = physical half life

δ_l = biological half life

$r_1 = 0.541$	$\delta_{r1} = 0.618\ hr^{-1}$
$r_2 = 0.339$	$\delta_{r2} = 0.0746\ hr^{-1}$
$k_1 = 0.0479$	$\delta_{k1} = 2.908\ hr^{-1}$
$k_2 = 0.0122$	$\delta_{k2} = 0.0434\ hr^{-1}$

*These values are taken from Thomas et al, 1984, Diffey and Hilson 1976 and ICRP 1983.

The maximum output of aerosol in each ventilation study is 0.25 ml/min of a 200 MBq/ml solution. Of this output, a maximum of 0.075 ml/min is inhaled assuming the solution output to be 0.15 ml/min (see Chapter 5) and time of inspiration to be half of the total ventilation time. Calculation of cumulated activity values therefore assumes a 30 MBq maximal dose to the lungs and a urine voiding time of 30 mins.

The S values from the rest of the body to the target organ, $S_{(t\text{-}rb)}$ are

calculated from equation (ii), the rest are taken from the MIRD 11 pamphlet together with the organ mass values.

$S_{(l\text{-}l)} = 5.2 \times 10^{-5}$ $S_{(o\text{-}l)} = 9.4 \times 10^{-8}$

$S_{(l\text{-}k)} = 8.5 \times 10^{-7}$ $S_{(o\text{-}k)} = 1.1 \times 10^{-6}$

$S_{(l\text{-}bc)} = 2.4 \times 10^{-8}$ $S_{(o\text{-}bc)} = 7.3 \times 10^{-6}$

$S_{(l\text{-}rb)} = 1.3 \times 10^{-6}$ $S_{(o\text{-}rb)} = 2.5 \times 10^{-6}$

$S_{(k\text{-}l)} = 8.4 \times 10^{-7}$ $S_{(ts\text{-}l)} = 7.9 \times 10^{-9}$

$S_{(k\text{-}k)} = 1.9 \times 10^{-4}$ $S_{(ts\text{-}k)} = 8.8 \times 10^{-8}$

$S_{(k\text{-}bc)} = 2.6 \times 10^{-7}$ $S_{(ts\text{-}bc)} = 4.7 \times 10^{-6}$

$S_{(k\text{-}rb)} = 3.0 \times 10^{-6}$ $S_{(ts\text{-}rb)} = 1.7 \times 10^{-6}$

$S_{(bw\text{-}l)} = 3.6 \times 10^{-8}$ $S_{(tb\text{-}l)} = 2.0 \times 10^{-6}$

$S_{(bw\text{-}k)} = 2.8 \times 10^{-7}$ $S_{(tb\text{-}k)} = 2.2 \times 10^{-6}$

$S_{(bw\text{-}bc)} = 1.6 \times 10^{-4}$ $S_{(tb\text{-}bc)} = 1.9 \times 10^{-6}$

$S_{(bw\text{-}rb)} = 2.8 \times 10^{-6}$ $S_{(tc\text{-}rb)} = 2.3 \times 10^{-6}$

Now,

The dose to any organ is the sum of the doses from each source organ to the target organ in question.

Eg. Dose to lungs (D_l):

$$D_l = A_l S_{(l\text{-}l)} + A_k S_{(l\text{-}k)} + A_{bc} S_{(l\text{-}bc)} + A_{rb} S_{(l\text{-}rb)}$$

For 30 MBq dose to the lungs,

A_l = 10170 μCi hr (μCi = micro Curies)

A_k = 65 μCi hr

A_{bc} = 12 μCi hr

A_{rb} = 1974 μCi hr

Therefore, from equation (vii)

D_l = 0.532 mSv (lungs)

D_{tb} = 0.025 mSv (total body)

D_k = 0.027 mSv (kidneys)

D_{bw} = 0.008 mSv (bladder wall)

D_o = 0.007 mSv (ovaries)

D_{ts} = 0.004 mSv (testes)

The guidelines of the National Health and Medical Research Council state, "The accumulated effective dose equivalent to any individual subject in any year shall not exceed 5 millisievert." (NH&MRC 1984).

Background radiation (Rosen 1985)

'Average Annual Effective Whole Body Dose Equivalent'

= 2.10 mSv yr^{-1}

Some accepted annual dose equivalents : (Rosen 1985)

Less than: 0.50 mSv Within background variations

Less than: 5.00 mSv Within dose limits for the public

Less than: 50.00 mSv Within dose limits for radiation workers

Grtr than 50.00 mSv Special exposure.

References

ABERNATHY, J.D. (1968). Effects of inhalation of an artificial fog. Thorax, 23, 421-426.

AGNEW, J.E. (1984). Aerosol contributions to the investigation of lung structure and ventilatory function. In: Aerosols and the lung, clinical and experimental aspects. Clarke, S.W. and Pavia, D. eds. Butterworths. London p92-126.

AGNEW, J.E., BATEMAN, J.R.M., PAVIA, D. & CLARKE, S.W. (1982a). Radioaerosol and ^{81M}Krypton assessment of regional ventilation in asymptomatic asthma. Thorax, 37, 235.

AGNEW, J.E., LITTLE, F., PAVIA, D. & CLARKE, S.W. (1982). Mucociliary clearance from the airways in chronic bronchitis - smaokers and ex-smokers. Bull Eur Physiopath. Resp., 18, 473-484.

AGNEW, J.E., PAVIA, D. & CLARKE, S.W. (1985). Factors affecting the 'alveolar deposition' of 5 μm inhaled particles in healthy subjects. Clin. Phys. Physiol. Meas., 6, 27-36.

AGNEW, J.E., BATEMAN, J.R.M., WATTS, M., PARAMANANDA, V., PAVIA, D., & CLARKE, S.W. (1981a). The importance of aerosol penetration for lung mucociliary clearance studies. Chest (suppl.), 80, 843-846.

AGNEW, J.E., PAVIA, D. & CLARKE, S.W. (1981b). Airways penetration of inhaled radioaerosol: an index to small airways function? Eur. J. Respir. Dis., 62, 239-255.

AGNEW, J.E., SUTTON, P.P., PAVIA, D. & CLARKE, S.W. (1986). Radioaerosol assessment of mucociliary clearance: towards definition of a normal range. Brit. J. Radiol., 59, 147-151.

ALDERSON, P.O., BIELLO, D.R., GOTTSCHALK, A., HOFFER, P.B., KROOP, S.A., LEE, M.E., RAMANNA, L., SIEGEL, B.A. & WAXMAN, A.D. (1984). Tc-99m-DTPA aerosol and radioactive gases compared as adjuncts to perfusion scinigraphy in patients with suspected pulmonary embolism. Radiology, 153, 515-521.

ALLEGRA, L., BIANCO, S., PETRIGINI, G. & ROBUSCHI, M. (1974). Lo Sforzo muscolare e la nebulizzazione ultrasonica di H_2O come tests di provocazione aspecifica del bronchospasmo. progressi in medicina respiratoria '74. Pasargiklian and Bocca eds. Edizioni Scientifiche Terme e Grandi Alberghi di Sirmione, Sirmione p 81.

AMDUR, M.O., SILVERMAN, L. & DRINKER, P. (1952). Inhalation of sulphuric acid mist by human subjects. Arch. Ind. Hyg. Occup. Med., 6, 305-313.

ANDERSON, S.D., DAVISKAS, E. & SMITH, C.M. (1989). Exercise-induced asthma: a difference of opinion regarding the stimulus. Allergy. Proc., 10, 215-226.

ANDERSON, S.D., SCHOEFFEL, R.E. & FINNEY, M. (1983). Evaluation of ultrasonically nebulized solutions for provocation testing in patients with asthma. Thorax, 38, 284-291.

ANGER, H.O. & MCRAE, J. (1968). Transmission scintiphotography. J. Nucl. Med., 9, 267-269.

ANSELM, A., GEBHART, J., HEYDER, J. & FERRON, G. (1986). Human inhalation studies of hygroscopic particles in the respiratory tract. In: Aerosols, formation and reactivity. Pergammon press, New York., 252-255.

ASMUNDSSON, T., JOHNSON, R.F., KILBURN, K.H. & GOODRICH, K. (1973). Efficiency of nebulizers for depositing saline in human lung. Am. Rev. Respir. Dis., 108, 506-512.

BAILEY, D.L., HUTTON, B.F. & WALKER, P.J. (1987). Improved SPECT

using simultaneous emission and transmission tomography. J. Nucl. Med., 28, 844-851.

BARBER, R.W. (1985). Radiation doses from ^{99m}Technetium-DTPA administered as an aerosol. J. Nucl. Med., 26, 1190-1194.

BARNES, K.L., CLIFFORD, R., HOLGATE, S., MURPHY, D., COMBER, P. & BELL, E. (1987). Bacterial contamination of home nebulizers. Br. Med. J., 295, 812.

BECQUEMIN, M.H., ROY, M., ROBEAU, D., BONNEFOUS, S., PIECHOWSKI, J. & TEILLAC, A. (1987). Inhaled particle deposition and clearance from the normal respiratory tract. Resp. Physiol., 67, 147-158.

BORHAM, P.W., BAILEY, D.L., PHIPPS, P.R., GONDA, I., BAUTOVICH, G.J., MURRAY, C. & MIEKLE, S. (1987). In vitro assessment of aerosol delivery systems. Aust. N.Z., J. Med., 17, 468.

BOUCHER, R.C., BROMBERG, P.C. & GATZY, J.T. (1980). Airway mucosal permeability . In: Airway reactivity. (ed) FE Hargreave. Hamilton Ontario: McMasters University press, 40-48.

BRAIN, J. D. & VALBERG, P.A. (1979). State of the art, deposition of aerosol in the respiratory tract. Am. Rev. Respir. Dis., 120, 1325-1373.

BURCH, G.E. (1945). Study of water and heat loss from the respiratory tract of man. Arch. Intern. Med., 76, 308-314.

BYRON. P.R. (1986). Prediction of drug residence times in regions of the human respiratory tract following aerosol inhalation. J. Pharm. Sci., 75, 433-438.

BYRON, P.R., DAVIS, S.S., BUBB, M.D., & COOPER, P. (1977). Pharmaceutical implications of particle growth at high relative humidities. Pest. Sci., 8, 521.

CHEN, W.Y. & HORTON, D.J. (1977). Heat and water loss from the airways and exercise induced asthma. Respiration, 34, 305.

CINKOTAI, FF. (1971). The behaviour of sodium chloride particles in moist air. J. Aerosol Sci., 2, 325-329.

CLARKE's Isolation and identification of drugs in pharmaceuticals, body fluids and post-mortem material. Moffat AC, Jackson JV, Moss MS, Widdop B (eds) 2nd Edition 1986. Pharmacuetical Press, London, 859-90.

CLARKE, S.W. & NEWMAN, S.P. (1984). Therapeutic aerosols II. Drugs available by the inhaled route. Thorax, 39, 1-7.

CLAY, M.M. & CLARKE, S.W.(1987). Effects of nebulized aerosol size on lung deposition in patients with mild asthma. Thorax, 42, 190-194.

CLAY, M.M., PAVIA, D., NEWMAN, S.P. & CLARKE, S.W. (1983). Factors influencing the size distribution of of aerosols from jet nebulisers. Thorax, 38, 755-759.

COATES, G. & O'BRODOVICH, H. (1986). Measurement of pulmonary epithelial permeability with ^{99m}Tc-DTPA aerosol. Semin. Nucl. Med., 16, 275-284.

COATES, G. & O'BRODOVICH, H. (1987). Extrapulmonary radioactivity in lung permeability measurements. J. Nucl. Med., 28, 903-906.

COLTON. T. (1974). Statistics in medicine. Little, Brown & Co., Boston, Mass.

CORKERY, K.J., LUCE, J.M. & MONTGOMERY, A.B. (1988). Aerosolised Pentamidine for treatment and prophylaxis of *Pneumocystis carinii* pneumonia: an update. Respiratory Care, 33, 676-685.

COVERT, D.S. & FRANK, R. (1980). Atmospheric particles, behaviour and functional effects. In: Physiology and pharmacology of the airways edited by Nadel J. New York, Dekker, 259-290.

CRIDER, W.L., MILBURN, R.H. & MORTON, S.D. (1956). Evaporation and rehydration of aqueous solutions. J. Meteorol., 13, 540-547.

DAHLBÄCK, M., NERBRINK, O., ARBORELIUS, M. & HANSSON, H-C. (1986). Output characteristics from three medical nebulizers. J. Aerosol Sci., 17, 563.

DAUTREBANDE, L. & WALKENHORST, T. (1960). Über die Retention von Kochsalzteilchen in den Atemwegen, in: Inhaled Particles and Vapours, Davies, C.N., Ed., Pergamon, Oxford, 110.

DAVIS, S.S. (1978). Physico-chemical studies on aerosol solutions for drug delivery I. Water-Propylene glycol systems. Int. J. Pharm., 1, 71-83.

DIFFEY, B.L. & HILSON, A.J.W. (1976). Absorbed dose to the bladder from 99m Tc DTPA. Br. J. Radiol., 49, 196-197.

DOLOVICH, M.B., COATES, G., HARGREAVE, F. & NEWHOUSE, M.T. (1985). Aerosols in diagnosis: ventilation, airway penetrance, airway reactivity, epithelial permeability and mucociliary transport. In: Moren F, Newhouse MT, Dolovich MB. eds. Aerosols in Medicine, principles, diagnosis and therapy. Elsevier, 225-259.

DOLOVICH, M.B., JORDANA, M. & NEWHOUSE, M.T. (1987).

Methodologic considerations in mucociliary clearance and lung epithelial absorption measurements. Eur. J. Nucl. Med. (suppl.), 13, S45-S52.

DOLOVICH, M.B., SANCHIS, J., ROSSMAN, C. & NEWHOUSE, M.T. (1976). Aerosol penetrance: a sensitive index of peripheral airways obstruction. J. Appl. Physiol., 40, 468-71.

DOLOVICH, M.B., RYAN, G. & NEWHOUSE, M.T. (1981). Aerosol penetration into the lung: influence on airway responses. Chest (suppl.), 80, 834-836.

DOSMAN, J., BODE, F., URBANETTI, J., MARTIN, R. & MACLEM, P. (1975). The use of helium-oxygen mixture during maximum expiratory flow to demonstrate obstruction in small airways in smokers. J. Clin. Investig., 55, 1090-1099.

DUSSER, D.J., MINTY, B.D., COLLIGNON, M-AG., HINGE, D., BARRITAULT, L.G. & HUCHEN, G.J. (1986). Regional respiratory clearance of aerosolized 99m-Tc- DTPA: posture and smoking effects. J. App. Physiol., 60, 2000-2006.

EDWARDS, A., VELASQUEZ, T. & FARHI, L. (1963). Determination of alveolar capilary temperature. J. Appl. Physiol., 18, 107-113.

EMMETT, P.C., LOVE, R.G., HANNAN, W.J., MILLAR, A.M. & SOUTAR, C.A. (1984). The relationship between the pulmonary distribution of inhaled fine aerosols and tests of small airway function. Bull. Eur. Physiopathol. Respir., 20, 325-332.

ESCHENBACHER, W.L., BOUSHEY, H.A. & SHEPPARD, D. (1984). Alteration in osmolarity of inhaled aerosols c.ause bronchoconstriction and cough, but absence of a permeant anion causes cough alone. Am. Rev. Respir. Dis., 129, 211-215.

FARR, S.J., KELLAWAY, I.W., PARRY-JONES, D.R. & WOOLFREY, S.G. (1985). 99m-Technetium as a marker of liposomal deposition and clearance in the human lung. Int. J. Pharm., 26, 303-316.

FINDEISEN, W. (1935). Uber das absetzen kleiner in der luft suspendieretere tielchen in der menschlichen lunge bei der atmung. Pfleugers Arch., 236, 367-379.

FERRON, G.A. (1977). The size of soluble aerosol particles as a function of the humidity of the air. Application to the human respiratory tract. J. Aerosol. Sci., 8, 251-267.

FERRON, A., HAIDER, B. & KREYLING, W.G. (1983). Aerosol particle growth in the human airways using a calculated humidity profile. J. Aerosol.

Sci., 14, 196-199.

FERRON, G.A., HAIDER, B. & KREYLING, W.G. (1985). A method for the approximation of the relative humidity in the upper human airways. Bull. Math. Biol., 47, 565-589.

FERRON, G.A., HAIDER, B. & KREYLING, W.G. (1988a). Inhalation of salt aerosol particles - I. Estimation of the temperature and relative humidity of the air in the human upper airways, J. Aerosol Sci., 19, 343.

FERRON, G.A. & HORNICK, S. (1984). Influence of different humidity profiles on the deposition probability of soluble particles in the human lung. J. Aerosol. Sci., 15, 209-211.

FERRON, G.A., HORNIK, S., KREYLING, W.G. & HAIDER, B. (1985). Comparison of experimental and calculated data for the total and regional deposition in the human lung. J. Aerosol. Sci., 16, 133-143.

FERRON, G.A., KERREBIJN, K.F. & WEBER, J. (1976). Properties of aerosols produced with three nebulizers. Am. Rev. Respir. Dis., 114, 899-908.

FERRON, G.A., KREYLING, W. & HAIDER, B. (1981). A remark concerning the relative humidity int he upper human airways in relation to aerosol particle growth. Gewellschaft Aerosolforsch, 9, 31-36.

FERRON, G.A., KREYLING, W.G. & HAIDER, B. (1988b). Inhalation of salt aerosol particles - II. Growth and deposition in the human respiratory tract, J. Aerosol Sci., 19, 611.

FOIS, R.A., GONDA, I. & CHAN, H-K. 1986). Tonicity of some commonly used drug preparations for nebulisation. Aust. J. Hosp. Pharm., 16, 19-21.

FOSTER, W.M., LANGENBACK, E.G., SMALDONE, G.C., BERGOFSKY, E.H. & BOHNING, D.E. (1988). Flow limitations on expiration induces central particle deposition and disrupts effective flow of airway mucus. Ann.Occup.Hyg., supplement Inhaled Particles VI, Dodgson, J., R. I. McCallum, M. R. Bailey and D. R. Fisher. Eds., Pergamon Press, Oxford, 101.

FOULDS, R. A. & SMITHUIS, L.O.M.J. (1983). Comparison of lung deposition of a solution after nebulization by three commonly portable nebulizers. Pharm. Weekblad. Sci., 5, 74-76.

FUCHS, N.A. (1959). Evaporation and droplet growth in gaseous media. R S Bradley (ed) Pergamon, Oxford.

FUCHS, N.A. (1964). The meachanics of aerosols. Pergamon, Oxford.

GERRARD, C.S., GERRITY, T.R., SCHREINER, J.F. & YEATES, D.B.

(1981). Analysis of aerosol deposition in the healthy human lung. Arch. Environ. Health, 36, 184-193.

GERRARD, C.S., GERRITY, T.R. & YEATES, D.B. (1986). The relationships of aerosol deposition, lung size and the rate of mucociliary clearance. Arch. Environ. Health, 41, 11-15.

GOLDBERG, I.S. & LOURENCO, R.V. (1973). Deposition of aerosols in pulmonary disease. Arch. Intern. Med., 131, 888-891.

GONDA, I. (1981). Study of the effect of polydispersity of aerosols on regional deposition in the respiratory tract. J. Pharm. Pharmacol. [suppl.], 33, 52.

GONDA, I., KAYES, J.B., GROOM, C.V. & FILDES, F.J.T. (1982). Characterisation of hygroscopic inhalation aerosols. In: Stanley-Wood NG, Allen T, eds. Particle size analysis 1981. Chichester: Wiley Heyden Ltd., 31-43.

GREENING, A.P., MINIATI, M. & FAZIO, F. (1980). Regional deposition of aerosols in health and in airways obstruction: a comparison with Krypton-81m ventillation scanning. Bull. Eur. Physiopathol. Respir., 16, 287-298.

HARGREAVE, F.E., RYAN, G., THOMSON, N.C., O'BYRNE, P.M.,

LATIMER, K., JUNIPER, E.F. & DOLOVICH, J. (1981). Bronchial responsiveness to histamine or methacholine in asthma: measurement and clinical significance. J. Allergy. Clin. Immunol., 68, 347-355.

HARRIS, R.L., & FRASER, D.A. (1976). A model for deposition of fibers in the human respiratory system. Am. Ind. Hyg. Assoc. J., 37, 73.

HAYES, M. (1980). Lung imaging with radioaerosols for the assessment of airway disease. Semin. Nucl. Med., 10, 243-251.

HAYES, M., TAPLIN, G.V., CHOPRA, S.K., KNOX, D.E. & ELAM, D. (1979). Improved radioaerosol administration system for routine inhalation lung imaging. Radiology, 131, 256-258.

HELEY, A. (1987). Aerosolised pentamidine treatment at home. Lancet, ii, 1092.

HENSLEY, M.J., O'CAIN, C.F., MCFADDEN, E.R. & INGRAM, R.H. (1978). Distribution of bronchodilatation in normal subjects: beta agonist versus atropine. J. Appl. Physiol: Respirat. Environ. Exercise Physiol., 45, 778-782.

HEYDER, J., GEBHART, J., HEIGWER, G., ROTH, C. & STAHLHOFEN, W. (1973). Experimental studies of total deposition of aerosol particles in the

human respiratory tract. J. Aerosol Sci., 4, 191-208.

HICKS, J.F., PRITCHARD, J.N., BLACK, A. & MEGAW, W.J. (1986). Experimental evaluation of aerosol growth in the human respiratory tract, in Aerosols: Formation and Reactivity, Proceedings of the Second International Aerosol Conference, Pergamon, Oxford, 244.

HIGGS, C.M.B., JONES, P. & TANSER, A.R. (1987). Bacterial contamination of home nebulizers. Br. Med. J., 295, 1281-1282.

HINDS, W.C. (1982). Aerosol Technology, J. Wiley & Sons, New York.

HODSON, M.E., PENKETH, A.R.L. & BATTEN, J.C. (1981). Aerosol carbenicillin and gentamicin treatment of Pseudomonas aeruginosa infection in patients with cystic fibrosis. Lancet, ii, 1137-1139.

HUGHES, W.T. (1987). Pathology. In Hughes WT ed. *Pneumocystis carinii* pneumonia. Boca Rotan, Florida: CRC Press Inc., 105-125.

ICRP Publication 38. (1983). Radionuclide transformations. Energy and intensity of emissions. Pergamon press, Oxford.

ILOWITE, J.S., GORVOY, J.D. & SMALDONE, G.C. (1987). Quantitative deposition of aerosolized gentamicin in cystic fibrosis. Am. Rev. Respir. Dis.,

136, 1445-1449.

INGLESTEDT, S.J. (1956). Studies on the conditioning of air in the respiratory tract. Acta. Oto-Laryngol [suppl.], 158, 81-92.

ISAWA, T., TESHIMA, T., HIRANO, T., EBINA, A., ANAZAWA, Y. & KONNO, K. (1987). Effect of bronchodilatation on the deposition and clearance of radioaerosol in bronchial asthma in remission. J. Nucl. Med., 28, 1901-1906.

ITOH, H., ISHII, Y., SUZUKI, T., HAMAMOTO, K., TORIZUKA, K., OYAMADA, H. & YONEYAMA, T. (1976). Inhalation scintigraphy with radioaerosols in bronchogenic carcinoma. Radiology, 119, 623-636.

JENKINS, S., HEATON, R.W., FULTON, T.J. & MOXHAM, J. (1987). Comparison of domiciliary nebulized salbutamol and salbutamol from a metered-dose inhaler in stable chronic airflow limitation. Chest, 91, 804-807.

KELVIN, Lord. (1870). On the equilibrium of vapour at a curved surface of a liquid. Proc. R. Soc. Edinb., 7, 63-68.

KIRKPATRICK, M.B., SANDERS, R.V. & BASS, J.B. (1987). Physiological effects and serum lidocaine concentrations after inhalation of lidocaine from a compressed gas-powered jet nebulizer. Am. Rev. Respir. Dis., 136, 447-449.

LANDAHL, H.D. (1963). Particle removal by the respiratory system. Note on the removal of airborne particles by the human respiratory tract with particular reference to the role of diffusion. Bull. Math. Biophys., 25, 29-39.

LAUBE, B.L., SWIFT, D.L. & ADAMS, K.G. (1984). Single-breath deposition of jet-nebulized saline aerosol. Aerosol. Sci. Technol., 3, 97-102.

LAUBE, B.L., SWIFT, D.L., WAGNER, H.N., NORMAN, P.S. & ADAMS, G.K. (1986). The effect of bronchial obstruction on central airway deposition of a saline aerosol in patients with asthma. Am. Rev. Respir. Dis., 133, 740-743.

LEWIS, R.A. & TATTERSFIELD, A.E. (1980). Cold induced bronchoconstriction: interaction with prostaglandin induced bronchoconstriction. Clin. Sci., 59, 12p.

LEWIS, R., & TATTERSFIELD, A.E. (1982). Bronchial hyperreactivity after inhaled distilled water and saline. Br. Med. J., 284, 47.

LIN, M.S. & GOODWIN, D.A. (1976). Pulmonary distribution of inhaled radioaerosol in obstructive pulmonary disease. Radiology, 118, 645-651.

LIPPMANN, M., YEATES, D.B. & ALBERT, R.E. (1980). Deposition, retention and clearance of inhaled particles. Br. Med. J., 37, 337-362.

LOGUS, J.W., TRAJAN, M., HOOPER, H.R., LENTLE, B.C. & MANN, S.F.P. (1984). Single photon emission tomography of lungs imaged with Tc-labelled aerosol. J. Can. Assoc. Radiol., 35, 133-138.

MACEY, D.J. & MARSHALL, R. (1982). Absolute quantitation of radiotracer uptake in the lungs using a gamma camera. J. Nucl. Med., 23, 731-735.

MANN, J.S., HOWARTH, P.H. & HOLGATE, S.T. (1984). Bronchoconstriction induced by ipratropium bromide in asthma: relation to hypotonicity. Br. Med. J., 289, 469.

MARTINDALE. (1982). The Extra Pharmacopoea, 28th Edition, Reynolds J. E. F. (ed), Pharmaceutical Press, London, England, p982.

MARTONEN, T.B., BARNETT, A.E. & MILLER, F.J. (1985). Ambient sulfate aerosol deposition in man: modeling the influence of hygroscopicity. Environmental Health Perspectives, 63, 11-24.

MARTONEN, T.B., BELL, K.A., PHALEN, R.F., WILSON, A.F. & HO, A. 1982). Growth rate measurements and deposition modelling of hygroscopic aerosols in human tracheobronchial models. Ann. Occup. Hyg. Assoc. J., 26, 93-107.

MARTONEN, T.B. & CLARKE, M.L. (1983). The deposition of hygroscopic phosphoric acid aerosols in ciliated airways of man. Fund. Appl. Toxicol., 3, 10-15.

MATTHYS, H., & KOHLER, D. (1985). Pulmonary deposition of aerosols by different mechanical devices. Respiration, 48, 269-276.

MAXWELL, J,C. (1890). Diffusion. In: The scientific papers of James Clarke Maxwell II, edited by Nivan WD. Cambridge, UK. Cambridge University Press, 625-646.

MCAFEE, J,G., GAGNE, H., ATKINS, H.L., KIRCHNER, P.T., REBA, R.C., BLAUFOX, M.D. & SMITH, E.M. (1979). Biological distribution and excretion of DTPA labeled with Tc-99m and In-111. J. Nucl. Med., 20, 1273-1278.

MELANDRI, C., PRODI, V., TARRONI, G., FORMIGNANI, M., DEZIACOMO, T., BOMPANE, G,F. & MAESTRI, D. (1977). On the deposition of unipolarly charged particles in the human respiratory tract. In:Inhaled particles IV Walton WH (ed). New York, Pergammon Press, 193-201.

MERCER, T.T., (1973). Properties of aerosols, in Aerosol Technology in Hazard Evaluation, Mercer, T.T., Ed., Academic Press, New York.

MERCER, T.T. (1981). Production of therapeutic aerosols, principles and techniques. Chest [suppl.], 80, 813-818.

MERCER, T.T., GODDARD, R.F. & FLORES, R.L. (1968). Output characteristics of three ultrasonic nebulizers. Ann. Allergy, 26, 18-27.

MERCER, T.T., TILLERY, M.I. & CHOW, H.Y. (1968). Operating characteristics of some compressed air nebulizers. Am. Ind. Hyg. Assoc. J., 29, 66-78.

MILBURN, R.H., CRIDER, W.L. & MORTON, S.D. (1957). The retention of hygroscopic dusts in the human lungs. Arch. Ind. Health, 15, 59-62.

MITCHELL, D.M,, SOLOMON, M.A., TOLFREE, S.E.J., SHORT, M. & SPIRO, S.G. (1987). Effect of particle size of bronchodilator aerosols on lung distribution and pulmonary function in patients with chronic asthma. Thorax, 42, 457-461.

MONTGOMERY, A. (1988). Therapy and prophylaxis of Pneumocystis carinii pneumonia by pentamidine aerosol. J. Aerosol. Med., 1, 164-166.

MONTGOMERY, A.B., DEBS, R.J., LUCE, J.M., CORKERY, K.J., TURNER, J., BRUNETTE, E.N., LIN, E,T, & HOPEWELL, P.C. (1987). Aerosolised Pentamidine as sole therapy for *P carinii* in patients with AIDS.

Lancet, ii, 480.

MONTGOMERY, A.B., LUCE, J.M., TURNER, J. et al. (1987). Aerosolised pentamidine as sole therapy for pneumocystis carinii pneumonia in patients with acquired immunodeficiency syndrome. Lancet, ii, 480-483.

MORROW, P.E. (1986). Factors determining hygroscopic aerosol deposition in airways. Physiological Reviews, 66, 330-376.

NAIR, P., VOHRA, K.G. (1975). Growth of aqueous sulfuric acid droplets on a function of relative humidity. J. Aerosol. Sci., 6, 265-271.

NEWHOUSE, M. & DOLOVICH, M. (1987). Aerosol therapy: nebulizer vs metered-dose inhaler. Chest, 91, 799-800.

NEWMAN, S.P. (1984). Therapeutic inhalation agents and devices: effectiveness in asthma and bronchitis. Postgrad. Medicine, 76, 194-207.

NEWMAN, S.P. & CLARKE, S.W. (1983). Therapeutic aerosols 1 - Physical and practical considerations. Thorax, 38, 881-886.

NEWMAN, S.P., MILLAR, A.B., LENNARD-JONES, T.R., MOREN, F. & CLARKE, S.W. (1984). Improvement of pressurised aerosol deposition with spacer Nebuhaler device. Thorax, 39, 935-941.

NEWMAN, S.P. & PAVIA, D. (1985). Aerosol deposition in man. In: Moren F, Newhouse MT, Dolovich MB. eds. Aerosols in Medicine. Principles, diagnosis and therapy. Amsterdam: Elsevier, 193-217.

NEWMAN, S,P,, PAVIA, D., MOREN, F., SHEAHAN, N.F. & CLARKE, S.W. (1981). Deposition of pressurised aerosols in the human respiratory tract. Thorax, 36, 52-55.

NEWMAN, S.P., PELLOW, P.G.D. & CLARKE, S.W. (1986a). Droplet size distributions of nebulized aerosols for inhalation therapy. Clin. Phys. Physiol. Meas., 7, 139-146.

NEWMAN, S.P., PELLOW, P.G.D. & CLARKE, S.W. (1986b). Choice of nebulizers and compressors for delivery of carbenicillin aerosol. Eur. J. Resp. Dis., 69, 139.

NEWMAN, S.P., PELLOW, P.G.D. & CLARKE, S.W. (1987a). Efficient nebulization of powdered antibiotics. Int. J. Pharm., 36, 55-60.

NEWMAN, S.P., PELLOW, P.G.D. & CLARKE, S.W. (1987b). Flow pressure characteristics of compressors used for inhalation therapy. Eur. J. Resp. Dis., 71, 122-126.

NEWMAN, S.P., PELLOW, P.G.D., CLAY, M.M. & CLARKE, S.W. (1985).

Evaluation of jet nebulizers for use with gentamicin solution. Thorax, 40, 671-676.

NEWMAN, S.P., WOODMAN, G. & CLARKE, S.W. (198). Deposition of carbenicillin aerosols in cystic fibrosis: effects of nebulizer system and breathing pattern. Thorax, 43, 318-322.

O'CALLAGHAN, C., CLARKE, A.R. & MILNER, A.D. (1989). Inaccurate calculation of drug output from nebulisers. Eur. J. Paediatr., 148, 473-474.

O'DOHERTY, M.J., PAGE, C.J., CROFT, N. & BATEMAN, N.T. (1985). Regional lung epithelial leakiness in smokers and nonsmokers. Nucl. Med. Commun., 6, 353-357.

O'DOHERTY, M.J., PAGE, C., BRADBEER, C., THOMAS, S., BARLOW, D. & NUNAN, T.O. (1988). Differences in relative efficiency of nebulizers for pentamidine administration. Lancet, ii, 1283-1286.

OLDENBURG, F.A., DOLOVICH, M.B., MONTGOMERY, J.M. & NEWHOUSE, M.T. (1979). Effects of postural drainage, exercise and cough on mucus clearance in chronic bronchitis. Am. Rev. Respir. Dis., 120, 739-745.

OSBORNE, W.A. (1913). Water in expired air. J. Physiol. Lond., 47, 12-16.

PALMES, E.D. (1973). Measurement of pulmonary air spaces using aerosols. Arch. Intern. Med., 131, 76-79.

PAVIA, D. (1984). Lung mucociliary clearance. in: Aerosols and the Lung: Clinical and Experimental Aspects. Clarke, S.W., and D. Pavia, D. Eds., Butterworths, London, 127.

PAVIA, D., THOMPSON, M.L., CLARKE, S.W. & SHANNON, H.S. (1977). Effect of lung function and mode of inhalation on penetration of aerosol into the human lungs. Thorax, 32, 194-197.

PAVIA, D., BATEMAN, J.R.M., SHEAHAN, N.F. & CLARKE, S.W. (1980). Clearance of lung secretions in patients with chronic bronchitis: effect of terbutaline and ipratropium bromide aerosols. Eur. J. Respir. Dis., 61, 245-253.

PAVIA, D., SUTTON, P.P., LOPEZ-VIDRIERO, MT., AGNEW, J.E. & CLARKE, S.W. (1983). Drug effects on mucociliary function. Eur J. Respir. Dis. (suppl. 128), 64, 304-317.

PERSONS, D.D., HESS, G.D., MULLER, W.J. & SCHERER, P.W. (1987a). Airway deposition of hygroscopic heterodispersed aerosols: results of a computer calculation. J. Appl. Physiol., 63, 1195-1204.

PERSONS, D.D., HESS, G.D. & SCHERER, P.W. (1987b). Maximization of pulmonary hygroscopic aerosol deposition. J. Appl. Physiol., 63, 1205-1209.

PHIPPS, P.R., BAILEY, D.L., BORHAM, P.W. & GONDA, I. (1986). Rapid droplet size analysis of diagnostic aerosols. J. Hosp. Pharm., 16, 60.

PHIPPS, P., BORHAM, P., GONDA, I., BAILEY, D., BAUTOVICH, G. & ANDERSON, S. (1987). A rapid method for the evaluation of radioaerosol delivery systems. Eur. J. Nuc. Med., 13, 183-186.

PHIPPS, P.R., GONDA, I., BAILEY, D.L., BORHAM, P., BAUTOVICH, G. & ANDERSON, S.D. (1989). Comparisons of planar and tomographic gamma scintigraphy to measure the penetration index of inhaled aerosols. Am. Rev. Respir. Dis., 139, 1516-1523.

PHIPPS, P.R. & GONDA, I. (1990). Droplets produced by medical nebulizers: some factors affecting their size and solute concentration. Chest, 97, 1327-1332.

POPA, V., MAYS, C. & MUNKRE, B. (1988). Domiciliary metaproterenol nebulization: a bacteriologic survey. J. Allergy Clin. Immunol., 82, 231-236.

PORSTENDORFER, J., GEBHART, J. & ROBIG, G. (1977). Effect of evaporation on the size distribution of nebulized aerosols. J. Aerosol Sci., 8,

371-380.

PRUPPACHER, H.R. & KLETT, J.D. (1978). Microphysics of clouds and precipitation. Reidel, Boston.

REMINGTON, S. & MEAKIN, G. (1986). Nebulized adrenalin 1:1000 in the treatment of croup. Anaethesia, 41, 923-926.

RICHARDS, R., HAAS, A., SIMPSON, S., BRITTEN, A., RENWICK, A. & HOLGATE, S. (1988). The effect of methacholine induced bronchoconstriction on the pulmonary distribution and plasma pharmacokinetics of inhaled sodium cromoglycate in subjects with normal and hyperreactive airways. Thorax, 43, 611-616.

ROSEN, R. (1985). Human subjects and experimental irradiation. Radiation protection in Australia, 3, 156-158.

ROYSTON, D., MINTY, B., JONES, J.G. & MCLEOD, M. (1984). A simple separator to generate half microm aqueous particles for lung imaging. Br. J. Radiol., 57, 223-228.

RUFFIN, R.E., KENWORTHY, M.C. & NEWHOUSE, M.T. (1978a). Response of asthmatic patients to fenoterol inhalation: a method of quantifying the airway bronchodilator dose. Clin. Pharmacol. Ther., 23,

338-345.

RUFFIN, R.E., DOLOVICH, M.B., WOLFF, R.K. & NEWHOUSE, M.T. (1978b). The effects of preferential deposition of histamine in the human airway. Am. Rev. Respir. Dis., 117, 485-492.

RUFFIN, R.E., DOLOVICH, M.B., OLDENBURG, F.A. & NEWHOUSE, M.T. (1981). The preferential deposition of inhaled isoproterenol and propranol ol in asthmatic patients. Chest [suppl.], 80, 904-906.

RYAN, G., DOLOVICH, M.B., OBMINSKI, G., COCKCROFT, D.W., JUNIPER, E., HARGREAVE, F.E. & NEWHOUSE, M.T. (1981a). Standardization of inhalation provocation tests: influence of nebulizer output, particle size, and method of inhalation. J. Allergy Clin. Immunol., 67, 156-161.

RYAN, G., DOLOVICH, M.B., ROBERTS, R.S., FRITH, P.A., JUNIPER, E.F., HARGREAVE, E. & NEWHOUSE, M.T. (1981b). Standardization of inhalation provocation tests: two techniques of aerosol generation and inhalation compared. Am. Rev. Respir. Dis., 123, 195-199.

SABINE, A.B., ARECHIGA, A.F., CASTRO, J.F., ALBRECHT, P., SEVER, J.L. & SHEKARCHI, I. (1984). Successful immunization of children with and without maternal antibody by aerosolized measles vaccine II. Vaccine comparisons and evidence for multiple antibody response. J. Am. Med. Assoc.,

251, 2363-2371.

SCHOEFFEL, R.E., ANDERSON, S.D. & ALTOUNYAN, R.E.C. (1981). Bronchial hyperreactivity in response to inhalation of ultrasonically nebulised solutions of distilled water and saline, Br. Med. J., 283, 1285-1287.

SIMONDS, A.K., NEWMAN, S.P., JOHNSON, M.A., TALAEE, N., LEE, C.A. & CLARKE, S.W. (1989). Simple nebulizer modification to enhance alveolar deposition of pentamidine. Lancet, ii, 953.

SIRR, S.A., ELLIOTT, G.R., REGELMANN, W.E., JUENEMANN, P.J., MORIN, R.L., BOUDREAU, R.J., WARWICK, W.J. & LOKEN, M.K. (1986). Aerosol pentration ratio: A new index of ventilation. J. Nucl. Med., 27, 1343-1346.

SMALDONE, G.C., PERRY, R.J. & DEUSCH, D.G. (1988). Characteristics of nebulizers used in the treatment of AIDS related *Pneumocystis carinii* pneumonia. J. Aerosol Med., 1, 113-126.

SMITH, C.M. (1988). The role of osmotic stimuli in the provocation of asthma. PhD Thesis, chapter 7, p97.

SMITH, C.M. & ANDERSON, S.D. (1986). Hyperosmolarity as the stimulus to asthma induced by hyperventilation? J. Allergy Clin. Immunol., 77, 729-736.

SMITH, C.M. & ANDERSON, S.D. (1989a). Provocation tests for asthma using non-isotonic aerosols. J. Allergy Clin. Immunol., 84, 781-790.

SMITH, C.M. & ANDERSON, S.D. (1989b). A comparison between the airway response to isocapnic hyperventilation and hypertonic saline in subjects with asthma. Eur. Resp. J., 2, 36-43.

SNEDECOR, G.W. & COCHRAN, W.G. (1967). Statistical methods. 6th editions, Ames, Iowa State University Press.

SNYDER, W.S., FORD, M.R. & WARNER, G.G. (1985). 'S' Absorbed dose per unit cumulated activity for selected radionuclides and organs. MIRD Pamphlet No 11, New York Soc. Nucl. Med.

STAHLHOFEN, W. (1984). Human data on deposition in lung modelling for inhalation of radioactive materials. In: Smith H, Gerber G, eds. Lung modelling for inhalation of radioactive materials. Proceedings of the meeting of the Commission of European Communities and Nat Radiol Protection Board. Brussels, Luxembourg, 39-59.

STAHLHOFEN, W., GEBHART, J., HEYDER, J. & SCHEUCH, G. (1983). Deposition pattern of droplets from medical nebulizers in the human respiratory tract. Bull. Europ. Physiopath. Resp., 19, 459-463.

STERK, P.J., PLOMP, A., CROBACH, M., VAN DE VATE, J.F. & QUANJER, P.H. (1983). The physical properties of a jet nebulizer and their relevance for the histamine provocation test. Bull. europ. Physiopathol. resp., 19, 27-36.

STERK, P.J., PLOMP, A., VAN DE VATE, J.F. & QUANJER, P.H. (1984). Physical properties of aerosols produced by several jet- and ultrasonic nebulizers. Bull. Europ. Physiopath. Resp., 20, 65.

SUSSKIND, H., BRILL, B. & HAROLD W.H. (1986). Quantitative comparison of regional distributions of inhaled Tc-99m DTPA aerosol and Kr-81m gas in coal miners' lungs. Am. J. Physiol. Imag., 1, 67-76.

SVARTENGREN, M., LINNMAN, L., PHILIPSON, K. & CAMNER, P. (1987). Regional deposition in human lung of 2.5μm particles. Experim. Lung. Res., 12, 265-279.

TAPLIN, G.V., TASHKIN, D.P., CHOPRA, S.K., ANSELMI, O.E., ELAM, D., CALVARES, B., COULSON, A., DETELS, R. & ROKAW, S.N. (1977). Early detection of chronic obstructive pulmonary disease using radionuclide lung imaging procedures. Chest, 71, 567-575.

THOMAS, S.R., ATKINS, H.L., MCAFEE, J.G. et al. (1984). Radiation absorbed dose from 99m-Tc diethyltriaminepentaacetic acid (DTPA). J. Nucl.

Med., 25, 503-505.

THOMSON, M.L. & PAVIA, D. (1974). Particle penetration and clearance in the human lung. Arch. Environ. Health, 29, 214-219.

TRAJAN, M., LOGUS, J.W., ENNS, E.G. & MAN, S.P.F. 1984). Relationship between regional ventilation and aerosol deposition in tidal breathing. Am. Rev. Respir. Dis., 130, 64-70.

TSANAKAS, J.N., WILSON, A.J. & BOON, A.W. (1987). Evaluation of nebulizers for bronchial challenge tests. Arch. Dis. Childhood, 62, 506-508.

TURNER, J.R., CORKERY, K.J., ECKMAN, D., GELB, A.M., LIPAVSKY, A. & SHEPPARD, D. (1987). Equivalence of continuous flow nebulizer and metered dose inhaler with reservoir bag for treatment of acute airflow obstruction. Chest, 93, 476-481.

VIDGREN, M.T., KARKKAINEN, A., PARONEN, T.P. & KARJALAINEN, P. (1987). Respiratory tract deposition of ^{99m}Tc-labelled drug particles administered via a dry powder inhaler. Int. J. Pharm., 39, 101-105.

WAGNER, P.E., (1982). Aerosol growth by condensation, In: Topics in current Physics. Aerosol Microphysics II; Chemical Physics of Microparticles, Marlow, W.H., Ed., Springer-Verlag, Berlin, 129.

WANNER, A. & RAO, A. (1980). Clinical indications for and effects of bland, mucolytic, and antimicrobial aerosols. Am. Rev. Respir. Dis., 122(Pt 2), 79-87.

WEIBEL, E.R. (1963). Morphometry of the human lung. Springer-Verlag, Berlin.

WHARTON, J.M., COLEMAN, D.L., WOFSEY, C.B. et al. (1986). Trimethoprim-sulphamethoxazole or pentamidine for *Pneumocystis carinii* pneumonia in the acquired immunodeficiency syndrome: A prospective randomised trial. Ann. Intern. Med., 105, 37-44.

WOLLMER, P., ERIKSSON, L. & ANDERSON, A-C. (1985). Clinical assessment of a commercial delivery system for aerosol ventilation scanning by comparison with Krypton-81m. J. Nucl. Med. Technol., 13, 63-67.

YAN, K., SCHOEFFEL, R., SALOME, C., HUTTON, B. & WOOLCOCK, A.J. (1983). Changes in lung function produced by methacholine using two different inhalation techniques in normal and asthmatic subjects. Nandi PL, Lam WK. eds. Proceedings of 7th Asia-Pacific congress, Hong Kong. 118-123.

YU, C.P., NICOLAIDES, P. & SOONG, T.T. (1979). The effect of random airway sizes on aerosol deposition. Am. Ind. Hyg. Assoc. J., 40, 999-1005.

YU, C.P. & TAULBEE, D.B. (1977). A theory predicting respiratory tract

deposition of inhaled particles in man. In: Walton WH, McGovern B, eds. Inhaled Particles IV Part1. Pergamon Press, Oxford, 35-476.

Aust. J. Hosp. Pharm. (1986), 16, 60.

Rapid Droplet Size Analysis of Diagnostic Aerosols

Phipps PR[a], Bailey DL[b], Botham PW[a], Gonda I[a], Department of Pharmacy, The University of Sydney[a] and the Department of Nuclear Medicine, Royal Prince Alfred Hospital[b], Sydney, N.S.W. 2050

Aerosols made from aqueous solutions of diagnostic agents are used widely in hospitals for testing of bronchial sensitivity and gamma scintillation imaging of the human respiratory tract. The nature of the formulation, the aerosol generator and the nebulisation conditions may affect the droplet size distribution and hence the regional distribution of the aerosol. A rapid technique is therefore useful to control the quality of diagnostic aerosols.

Cascade impactor slides[1] spiked with known amounts of radioactivity (^{99m}Tc-DTPA in isotonic saline) were placed on a collimated gamma camera and the counts were recorded for 5 minutes and collected on computer. The counts were repeated at several later times to test linearity. The images were displayed on the computer screen and regions of interest were drawn around each slide. After correcting for background, % of total activity on each slide was calculated. In all experiments, the response of the gamma camera was linear over the range $\sim 10^2$-10^5 cpm ($r^2 > 0.99$). The technique was found to be precise and robust provided the total cpm $> 10^4$.

A 7-stage cascade impactor was used at a flow rate of 12.5 L/min to measure the droplet size distribution[1]. Aerosols were generated from a nebuliser using compressed air. The 'dilution' air required to make up the flow through the cascade impactor was conditioned either 'dry' or 'wet' (equilibrated with saturated solutions of LiCl or water, respectively). Upon generation, impactor slides were counted as above. The results were analysed for the mass median aerodynamic diameter (MMAD) and geometric standard deviation (σg) using an interactive least squares program.[1]

There was no significant intra- or inter-nebuliser variation with 'wet' dilution air. As the proportion of the 'dry' dilution air increased, a reduction of MMAD became apparent. This observation suggests that dilution air from diagnostic aerosols should be humidified.

Reference

1. Gonda I, Kayes, JB, Groom CV, Fildes FJT. In: Stanley-Wood NG, Allen T, eds. Particle size analysis. Chichester, Wiley-Heyden Ltd, 1982: 31-43.

Aust. N.Z. J. Med., (1987), 17 [suppl. 2], 468.

IN VITRO ASSESSMENT OF RADIOAEROSOL DELIVERY SYSTEMS.

+P.W.Borham*,++P.R.Phipps, +D.L.Bailey,++I.Gonda, +G.J. Bautovoch, +C.Murray, +S.Miekle. +Department of Nuclear Medicine, Royal Prince Alfred Hospital, Sydney.++Department of Pharmacy, University of Sydney.

Optimal characteristics of radioaerosol delivery systems (RDS) include high output of droplets of a suitable size for pulmonary deposition. Reduced extra-pulmonary deposition and a shorter inhalation time mean reduced exposure to patients and administering personnel. Effective delivery (ED) and wasted delivery (WD) were defined as the delivery from the mouthpiece in MBq/min of droplets below, (ED) or above (WD) a respiratory size range of below 3.3 μm mass median aerodynamic diameter (MMAD). Four commercially available RDS were assessed. 5 ml of 100 MBq/ml Tc-pertechnetate in normal saline was nebulised for 1 min and the droplets collected by a 7-stage cascade impactor. The impactor stage slides were counted on a previously calibrated collimated gamma camera. MMAD, geometric standard deviation (σg) and output of droplets below and above stage 3 of the impactor (3.3 μm, 50% cut-off diameter) were calculated.

RESULTS: Mean of 3 determinations (SD).

RDS	MMAD (μm)	σg	ED (MBq/min)	WD (MBq/min)
ULTRAVENT	1.1(0.1)	1.7(0.1)	6.1(0.5)	0.05(0.02)
VENTICIS	1.0(0.1)	1.8(0.1)	8.1(0.9)	0.02(0.01)
MISTYNEB	3.7(0.1)	1.5(0.1)	11.3(0.2)	15.40(0.50)
CADEMA	2.3(0.1)	1.4(0.1)	14.0(0.8)	1.24(0.61)

The Ultravent and Venticis had low ED and WD values requiring longer inhalation or higher activity concentration. The Mistyneb had a high delivery rate but a high proportion of the droplets were outside the respiratory range. The Cadema had optimal characteristics of high ED and low WD.

Aust. N.Z. J. Med., (1987), 17 [suppl. 2], 483.

QUANTITATIVE SPECT AEROSOL PENETRATION INDEX

Phipps PR, Bailey DL, Gonda I, Borham PW, Bautovich GJ and Anderson SD.
Departments of Nuclear Medicine and Thoracic Medicine, Royal Prince Alfred Hospital, and Department of Pharmacy, Sydney University, Sydney, AUSTRALIA. 2050.

A study was undertaken to examine aerosol penetration index (PI) measurements from SPECT lung studies. The aim was to compare PI values from mid sections of the lung with the whole lung, as encountered in planar imaging. ^{99m}Tc-DTPA

5 healthy subjects inhaled aerosol on 2 separate occasions with different droplet sizes, to target the small and large airways. The data acquired consisted of transmission (153Gd) and rapid emission tomographic acquisitions (< 12 min for 360°). The emission and transmission (attenuation) tomograms were reconstructed in both transverse (T) and coronal (C) planes. The transverse sections were corrected for attenuation after reconstruction using the attenuation section μ values. The attenuation sections were also used to define the lung outlines.

The PI's for the small droplets on the isolated mid portions were significantly higher than for the whole lung (T:+21.3%;$p < 0.05$, (C:+24.0%;$p < 0.01$). In contrast, the large droplets showed no significant difference in PI (T:+4.9%;$p > 0.7$, C:-0.9%;$p > 0.8$). This may be due to the inclusion of peripheral small airways, seen only in the small droplet studies, in the central ROI on the whole lung studies. This suggests that SPECT PI measurements reflect true aerosol deposition more accurately.

J. Pharm. Pharmacol., (1987), 39 (suppl.), 72p.

COMPARISON OF METHODS FOR THE MEASUREMENT OF REGIONAL AEROSOL DEPOSITION

P.R.Phipps*, I.Gonda*, D.L.Bailey+, P.Borham+, G.Bautovich+ and S.D.Anderson[X], *Department of Pharmacy, University of Sydney, +Departments of Nuclear Medicine and [X]Thoracic Medicine, Royal Prince Alfred Hospital, Sydney, Australia.

Two-dimensional (2D) gamma scintigraphy has been used to visualise the deposition of therapeutic and diagnostic aerosols in the human respiratory tract by taking posterior (P) or anterioposterior geometric mean (AP) views. Quantitative analysis of the 2D data in terms of regional deposition in the large central versus small peripheral airways has been difficult because in reality there are small airways superimposed over the large airways located in the centre of the lung.

Development of aerosol formulations with a desired pattern of regional deposition and possibly extended duration of residence in the respiratory tract requires methods capable of better distinction between central and peripheral deposition. The new generation of gamma cameras are able to provide data for three dimensional (3D) reconstructions of deposited radioaerosol on a time scale which should be short enough to avoid significant corruption of the initial deposition image by mucociliary transport. In order to discriminate better between central and peripheral deposition, 3D imaging was carried out. 7 healthy volunteers inhaled isotonic saline aerosols containing ^{99m}Tc-DTPA on two separate occasions under the same controlled conditions. The aerosols contained droplets with mass median aerodynamic diameters of 5.5 and 2.6 m and geometric standard deviations of 1.7 and 1.4 respectively. A gamma camera was used to obtain P, AP and coronal (C) slices taken from the mid portion of the lung; outlines of the lung fields were obtained by transmission. The penetration index (PI) was calculated as the ratio of the radioactivity in quantitatively defined peripheral and central regions.

PI for 2.6 (S) and 5.5 (L) m droplets from P, AP and C mid-slice images:

— = Mean values

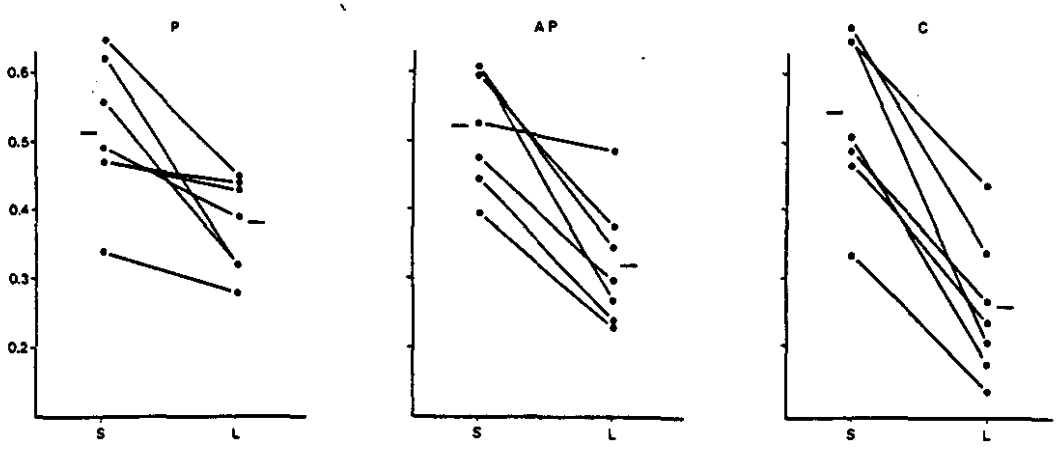

The results (see graphs above) show: 1) The PI was smaller for the large droplets in all subjects and all studies, thus quantitatively validating the usual 2D methods. 2) Removal of the peripheral airways in the C mid-lung slices showed a consistently better discrimination between the deposition of large and small droplets than the AP and especially the P images. We suggest that tomography offers a more sensitive method to evaluate the effect of formulation on the initial regional deposition of aerosols and their subsequent clearance than the conventional 2D methods.

J. Pharm. Pharmacol., (1987), 39 (suppl.), 74p.

CONCENTRATION OF SOLUTION IN AQUEOUS AEROSOL DROPLETS

P.R.Phipps and I.Gonda, Department of Pharmacy, University of Sydney, Sydney, NSW 2006, Australia.

Aerosol droplets made from aqueous solutions are unstable unless their vapour pressure is the same as that of the environment. Two main causes of evaporation of aerosol droplets exist: 1) During inspiration, unsaturated dilution air is added to supplement the airflow used for aerosol generation (Phipps et al.,1987). 2) The nebuliser temperature falls during generation and thus the vapour phase is unsaturated when the aerosol reaches ambient temperature (AT). To find the magnitude of these effects, aerosols were generated from a Cadema air-jet nebuliser by 8 or 10 l/min of oxygen. The nebuliser was connected via 2 cm diameter tubing to a cascade impactor stage. Air of 48.7 (± 3.0)% or 99.7 (± 0.4)% relative humidity (RH) supplied as in patient use, made up the total flow to 12.5 l/min. The initially isotonic nebuliser solution was kept at constant temperatures with a water bath and small heater. The aerosol was collected on the impactor slide which was immediately sealed in plastic and weighed. Droplet concentrations were measured for various nebuliser conditions (Fig. 1) by vapour pressure osmometry.

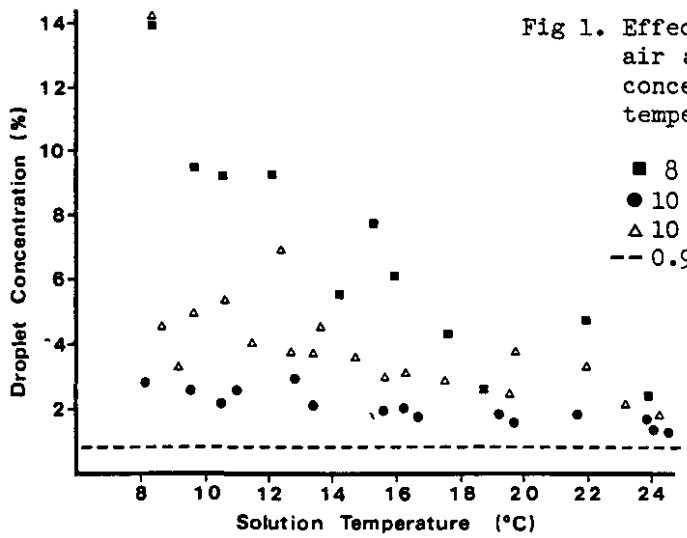

Fig 1. Effect of proportion of dilution air and its humidity on droplet concentration at various solution temperatures.

The results (fig.1) show that: a) The smallest change from the original concentration was obtained when the nebuliser was kept, by heating, at AT thus removing a major cause of initial unsaturation of the aerosol vapour. b) Even with dilution air of 99.7 % RH at AT, there was a substantial increase in droplet solution concentration when aerosols were generated below AT, as would be the case in unheated nebulisers. c) The combination of unsaturated dilution air and generator temperature below AT produced highly concentrated droplets and poorly reproducible behaviour. These results confirm our previous findings of poor reproducibility of droplet size under such generation conditions (Phipps et al., 1987), and can be explained by mass balance analysis.

These observations are of concern in view of the brochoconstrictive properties of certain non-isotonic aerosols (Mann et al., 1984). Changes in droplet solution concentration also parallel changes in droplet size (Phipps et al., 1987), thus they could be a source of variability of regional deposition of diagnostic and therapeutic aerosols.

Mann, J.S. et al (1984) Br. Med. J. 289: 469
Phipps, P.R. et al (1987) Eur. J. Nucl. Med. (in print)

Eur J Nucl Med (1987) 13:183–186

European Journal of Nuclear Medicine

A rapid method for the evaluation of diagnostic radioaerosol delivery systems

Paul Phipps[1], Peter Borham[2], Igor Gonda[1,*], Dale Bailey[2], George Bautovich[2], and Sandra Anderson[3]

[1] Pharmacy Department, University of Sydney, Sydney, NSW 2006, Australia,
Departments of [2] Nuclear Medicine and [3] Thoracic Medicine, Royal Prince Alfred Hospital, Camperdown, NSW 2050, Australia

Abstract. The effective delivery (ED) in MBq/min of a 100 MBq/ml nebuliser solution was defined as the rate of delivery of droplets in the respirable size range (aerodynamic diameter below 3.3 μm) to the mouthpiece of the aerosol delivery system (ADS). Wasted delivery (WD) was defined as the rate of delivery of droplets above 3.3 μm. ED and WD were measured on four types of commercially available ADS. The aerosols were sampled at the mouthpiece of each system and droplet size distribution measured with a seven stage cascade impactor. The effect of ambient air humidity on the droplet size produced by the Cadema delivery system was also evaluated. The ED values ranged from 6 to 15 MBq/min and WD values from 0.01 to 15 MBq/min. Two ADS produced low ED and WD values (6.1–9.0 and 0.01–0.07 MBq/min, respectively) due to a low output, while another produced higher ED and WD values [11.3 ± 0.2 (SD) and 15.4 ± 0.5 (SD) MBq/min, respectively] due to a larger droplet size. The Cadema delivery system gave the optimum characteristics of high ED [13.9 ± 0.8 (SD) MBq/min] and low WD [1.24 ± 0.61 (SD) MBq/min] values. The mass median aerodynamic diameter (MMAD) of the Cadema ADS fell by 22 % ($P < 0.01$) as the ambient dilution air was dried from a high relative humidity (RH) (88 %–100 %) to a low RH (12 %–17 %). The variability of both MMAD and geometric standard deviation (σg) was increased with dry dilution air ($P < 0.01$).

Key words: Aerosols – Radioaerosols – Aerosols-delivery systems – Aerosols-evaluation – Aerosols-diagnostic

Radioaerosol ventilation agents such as those containing ^{99m}Tc-DTPA are used for the assessment of regional ventilation and alveolar clearance. They are produced and delivered to patients via radioaerosol delivery systems (ADS) consisting of jet nebulisers and associated tubing. To be effective, these systems must produce a uniform peripheral aerosol deposition while minimizing a) the radiation dose to the patient, b) the radiation exposure to personnel administering the dose and c) the cost of the procedure. It is therefore important to reduce as much as possible both the duration of administration and the unuseable portion of the radioactive aerosol, the latter including that depositing in the delivery tubing, mouth, oropharynx and central airways and that exhaled by the patient. Regional deposition of aerosols is determined by their physical characteristics, such as size distribution and droplet composition together with patient parameters, such as inhalation flow rate and severity of lung disease; the variability of all of these has complicated previous clinical assessments of ADS (Hayes et al. 1979; Foulds and Smithuis 1983; Trajan et al. 1984; Alderson et al. 1984; Matthys and Kohler 1985; Wollmer et al. 1985).

Nuclear medicine departments are responsible for the choice of ADS and the quality control of radioaerosols. We therefore wished to define meaningful parameters for the assessment of the quality of radioaerosols used for ventilation studies, and to develop rapid experimental methods to measure those parameters, using as far as possible equipment already available in a typical nuclear medicine department (Borham et al. 1986).

The droplet size distribution of ADS is known to depend on operating parameters (Mercer et al. 1965; Ferron et al. 1976; Ryan et al. 1981; Clay et al. 1983; Sterk et al. 1984) and also on environmental conditions (Porstendorfer et al. 1977). In many ADS, ambient dilution air is inhaled along with the aerosol. A potential therefore exists for the humidity of the dilution air to affect the aerosol droplet size and this was also investigated.

Materials and methods

Droplet size determination. Particle size distribution, expressed as the mass median aerodynamic diameter (MMAD) and the geometric standard deviation (σg) was measured using a seven stage cascade impactor (DCI6, Delron, Columbus, Ohio, USA). ^{99m}Tc-pertechnetate in normal saline was added to the nebuliser solution to an approximate concentration of 100 MBq/ml. The aerosol was generated from the nebuliser using compressed oxygen. The dilution air required to make up a fixed flow of 12.5 l/min through the impactor was humidified or dried by bubbling through water or a saturated solution of lithium chloride, respectively.

After generation of the aerosol for approximately 60 s, the impactor slides, precoated with silicone fluid (Dow Corning 200/60000 cs, Midland, Michigan, USA) were removed and simultaneously counted on a large field of view gamma camera (GE 400AT, Milwaukee, Wisconsin, USA) fitted with a low energy, all purpose, colimator. A 5 min

Offprint requests to: I. Gonda (address see above)

image was recorded by an on line computer (DEC PDP11, Maynard, MA, USA). Regions of interest were drawn around the image of each slide and total counts within each were recorded. These values, corrected for background and expressed as a percentage of the total count, together with the previous impactor calibration results for particles and droplets (Gonda et al. 1982) were analysed by a least squares program to determine the MMAD and σg of the aerosol sample. Dead time correction was not necessary at the count rates observed.

The method was validated by placing small volumes of 100 MBq/ml ^{99m}Tc-pertechnetate on to seven coated impactor slides from a pipette (Phipps et al. 1986). The activity in the pipette was measured by a dose calibrator (Capintec Inc. New Jersey, USA) before and after application. The slides were counted for 5 min on the gamma camera five times over a period of 48 h and the results pooled to test for linearity. The activity values ranged from 14.91 to 0.00524 MBq per slide. The correlation equation produced was then used to convert impactor slide counts into activity values. In the experimental runs, the highest activity on any one slide was approximately 6 MBq and 0.1 % of the lowest total activity was still greater than the lowest point on the calibration.

Aerosol delivery system characterisation. Droplet size distribution measurements as described above were carried out in triplicate on four commercially available ADS; Ultravent (Mallinckrodt Inc., St. Louis, USA), Venticis (Cis UK Ltd., North Finchley, London.), Mistyneb (Airlife Inc., Montclair, California, USA) and Cadema (Cadema Medical Products Inc., Middletown, N.Y., USA). Each system was set up as for patient use with the mouthpiece of the delivery tubing connected to the impactor. The aerosol was generated by compressed oxygen at the manufacturer's recommended flow rate (10 l/min in each case) and supplemented with humid dilution air.

The results from the droplet size analysis were used to calculate both the mass fraction of droplets in the respirable size range and the total activity caught in the impactor per min. The respirable size range was taken to be the cumulative activity below stage three of the cascade impactor [50 % cutoff diameter = 3.3 μm (Gonda et al. 1982)]. All results were corrected for decay and to an original nebuliser concentration of 100 MBq/ml.

The effective delivery (ED) of each ADS was calculated as the amount of activity leaving the mouthpiece in MBq/min contained in droplets in the respirable size range. The wasted delivery (WD) was defined as the amount of activity leaving the mouthpiece outside the respirable range, i.e., the amount of activity in droplets depositing on or above stage three of the impactor. The results were expressed as the mean ± standard deviation of three determinations.

Effect of dilution air humidity on the droplet size distribution of the Cadema ADS. The droplet size distribution was measured on the Cadema ADS as described above, with dilution air comprising 4.5 l/min and aerosol 8.0 l/min of the 12.5 l/min total flow through the impactor. Several determinations were carried out on three nebulisers using humid and dry dilution air. The MMAD and σg values for dry and humid dilution air were then compared with the use of a Mann-Whitney U test and the standard deviations with an F-test.

Table 1. ED, WD and aerosol characteristics of four ADS

	MMAD (μm)	σg	($F \times 100$) % below Stage 3	Mean ED[a] MBq/min	Mean WD[a] MBq/min
Ultravent	1.1 (0.1)	1.7 (0.1)	99.2 (0.3)	6.44 (0.46)	0.05 (0.02)
Venticis[b, c] (2) (3)	1.0 (0.1)	1.8 (0.1)	99.8 (0.1)	8.06 (0.86)	0.02 (0.01)
Mistyneb	3.7 (0.1)	1.5 (0.1)	42.3 (0.8)	11.3 (0.2)	15.4 (0.5)
Cadema	2.3 (0.1)	1.4 (0.1)	92.0 (3.1)	14.0 (0.8)	1.24 (0.61)

Values expressed as mean of three results (standard deviation)
[a] Corrected for decay and activity concentration in the nebuliser to 100 MBq/ml
[b] The Venticis aerosol delivery system includes a settling bag which fills during patient use but not during the particle size determination due to the continuous negative pressure supplied to the system
[c] The first run on the Venticis used some of the output to soak the ball bearing filled filter system

Results

The pooled data from the gamma camera calibration was used to plot counts (Y in units of cpm) against activity (X in MBq). The equation of the regression line produced was

$$Y = 9492\ (\pm 1.8\ \%)X + 91.4\ (\pm 787\ \%) \quad (1)$$

where standard deviation in % is given in parentheses, $n = 35$ (pooled results of 7 slides at 5 times) and $r^2 = 0.9997$.

The regression equation (1) shows that a 25 % error is found at a count rate over 4×10^3 cpm. From experience, it was noted that up to 10 % of the total cpm could vary by as much as 25 % without changing the calculated values of MMAD and σg to one decimal place. Therefore a total cpm of over 4×10^4 is required for suitable precision of the method.

Values of activity were calculated from impactor slide counts (A in units of cpm) using Eq. (1), to give the ED and WD values shown in Table 1 from:

$$\mathrm{ED} = (A/T_g) \times F \quad (2)$$

and

$$\mathrm{WD} = (A/T_g) \times (1 - F) \quad (3)$$

where

T_g = generation time (min)
F = fraction depositing below stage three.

The effect of dilution air humidity on the MMAD of droplets produced by the three Cadema ADS is shown in Table 2. The mean MMAD of the pooled results for humid dilution air is 2.55 ± 0.10 μm (SD) where $n = 22$, indicating a low inter and intra nebuliser variability. Dry dilution air reduces the pooled mean MMAD by 22 % ($P < 0.01$) and increases the variability [mean = 1.99 ± 0.32 μm (SD), $n = 17$]. The standard deviations of the dry dilution air MMAD and σg results were both significantly greater ($P < 0.01$) than those of humid dilution air.

Table 2. Effect of ambient dilution air humidity on MMAD and σg of droplets produced by the Cadema ADS

Nebuliser No.	Humid dilution air 88 %–100 % RH			Dry dilution air 12 %–17 % RH		
	No. of repeats	MMAD (μm)	σg	No. of repeats	MMAD (μm)	σg
1	5	2.64 (0.04)	1.40 (0.04)	5	2.41 (0.08)	1.37 (0.03)
2	8	2.51 (0.07)	1.36 (0.04)	8	1.77 (0.15)	1.62 (0.11)
3	9	2.53 (0.13)	1.34 (0.02)	4	1.90 (0.25)	1.55 (0.12)

Values expressed as mean (standard deviation)

Discussion

The effect of droplet size on the regional deposition of aerosols in the human respiratory tract has now been well documented by both in vivo determination and mathematical models (see reviews, e.g., Ferron et al. 1985; Stahlhofen 1984). Particles of mass median aerodynamic diameter between 3 and 1 μm, at resting inhalation flow rates, are of the optimum size for pulmonary deposition. Larger particles tend to deposit in the central airways or mouth while particles in the region of 0.5 μm are exhaled. A better estimation of the effective aerosol delivery may therefore be obtained by excluding those droplets likely to be exhaled. We chose to disregard the exhaled portion of the aerosol in defining our respirable range but droplets of around 0.5 μm may easily be excluded from the results. As the droplet size decreases below 0.5 μm, the alveolar deposition increases, starting from a minimum of around 10 % (Ferron et al. 1985). However, the fraction of radioactivity carried by such small droplets is low in ADS used clinically at present, as shown by our results.

Marked differences in the performance of different ADS are shown in Table 1. The Venticis and Ultravent produce droplets all within the respirable size range but their output is low, requiring either a high nebuliser activity concentration or a long inhalation time. The Venticis incorporates a settling bag as part of the delivery tubing which failed to fill during the droplet size analysis, due to the constant negative pressure applied. If some of the larger droplets settle in this bag the MMAD will decrease (possibly increasing the proportion exhaled). The output will also decrease as a result, but this may be offset by the storage capacity of the bag during exhalation. The Mistyneb nebuliser has a high output of droplets in the respirable range but it produces an even larger portion that deposits outside the pulmonary region. The Cadema nebuliser, however, has optimum operating characteristics with a high delivery rate and little waste of aerosol.

The aerosol samples for the droplet size measurements were taken at the mouthpiece of the delivery system which did not take into account the amount of aerosol depositing in any unshielded tubing, an important hazard consideration. The amount of aerosol caught in the tubing would depend on droplet size, flow rate and tubing geometry so ADS with high WD values and tortuous tubing are more likely to deposit aerosol before the mouthpiece.

The droplet size distribution and output from a nebuliser may change markedly with generation flow rate (Mercer 1973; Ryan et al. 1981; Clay et al. 1983) and this will in turn lead to different ED and WD values. It may thus be possible to modify the effectiveness of an ADS by changing its operating flow rate.

Table 2 shows the results of changing the dilution air humidity passing through the Cadema ADS. Dilution air mixes with the aerosol at the exit from the nebuliser in all of the systems tested. Dry dilution air caused the droplets to evaporate and probably concentrate, and in so doing the droplet size was reduced by 22 % and became more variable. During inhalation of diagnostic radioaerosols, patients require dilution air to supplement the 8 or 10 l/min flowing through the nebuliser with a flow rate often far in excess of the aerosol flow. The humidity of this dilution air, and the proportion of it, will effect the droplet size and variability of the aerosol leaving the mouthpiece to a greater extent than in the reported experiments, and this may have some effect on the droplet deposition. A theoretical explanation and the practical implications of the greater sensitivity of the droplet size and σg to fluctuation of water content at a low relative humidity, is the subject of another paper. However, it is possible that the variability of the results of penetration of aerosols in the diagnosis of chronic obstructive pulmonary disease (Ruffin et al. 1981) could have been due, not to clinical variability, but to variable radioaerosol delivery. The pooled σg values and their variability are also increased with dry dilution air ($P<0.01$) and this, too, may have an effect on the deposition of the aerosols (Gonda 1981).

The breathing pattern is also important in relation to the general deposition of the droplets. A high inspiratory flow rate will cause greater deposition of the larger droplets outside the pulmonary region by impaction, while a low flow rate will increase the pulmonary deposition of those same droplets (Agnew et al. 1985). Therefore, the respirable size ranges and hence the values of ED and WD will change with inhalation flow rate, which could be readily accommodated in new definitions of ED and WD.

Lung disease may effect the ED values by a number of mechanisms. Increased inhalation flow rate, bronchoconstriction and excessive mucous secretions may all lead to reduced pulmonary deposition of aerosol (Taplin et al. 1977) making fine droplets preferable for imaging the alveoli.

The continuous output of the nebulisers makes it possible to estimate the total dose inhaled by the patient as half the sum of ED and WD values if expiration and inhalation times are assumed to be equal and exhaled dose ignored (with the exception of the Venticis which stores aerosol in a settling bag during expiration).

Conclusions

These results show that it is possible to characterise and compare ADS by a simple, quick in vitro method using readily available equipment as an aid to the evaluation of aerosol delivery systems.

The droplet sizing technique was found to be suitably precise provided the total impactor slide counts were greater than 4×10^4 cpm. The system was linear over the range 10^2–10^5 cpm per slide.

Environmental conditions such as ambient air humidity

may have an effect on the droplet size distribution produced by some ADS.

Acknowledgements. The authors would like to thank the Asthma Foundation of NSW for a generous equipment grant. P.R.P. has been the recipient of a Commonwealth Postgraduate Award (Australia). We are also grateful for the assistance of Christine Murray in the initial stages of this study.

References

Agnew JE, Pavia D, Clarke SW (1985) Factors affecting the 'alveolar deposition' of 5 μm inhaled particles in healthy subjects. Clin Phys Physiol Meas 6:27–36

Alderson PO, Biello DR, Gottschalk A, Hoffer PB, Kroop SA, Lee ME, Ramanna L, Siegel BA, Waxman AD (1984) Tc-99m-DTPA aerosol and radioactive gases compared as adjuncts to perfusion scintigraphy in patients with suspected pulmonary embolism. Radiology 153:515–521

Borham PW, Bailey DL, Phipps PR, Gonda I, Bautovich GJ, Murray C, Miekle S (1986) In vitro assessment of aerosol delivery systems. Abstracts of the 17th Annual Science Meeting, Aust NZ Soc Nucl Med, Hobart (Australia), March 1986. Aust NZ J Med (to appear)

Clay MM, Pavia D, Newman SP, Clarke SW (1983) Factors influencing the size distribution of aerosols from jet nebulisers. Thorax 38:755–759

Ferron GA, Hornik S, Kreyling WG, Haider B (1985) Comparison of experimental and calculated data for the total and regional deposition in the human lung. J Aerosol Sci 16:133–143

Ferron GA, Kerrebijn KF, Weber J (1976) Properties of aerosols produced with three nebulisers. Am Rev Respir Dis 114:199–908

Foulds RA, Smithius LOMJ (1983) Comparison of lung deposition of a solution after nebulisation by three commonly used portable nebulisers. Pharm Weekblad [Sci] 5:74–76

Gonda I (1981) Study of the effects of polydispersity of aerosols on regional deposition in the respiratory tract. J Pharm Pharmacol [Suppl] 33:52

Gonda I, Kayes JB, Groom CV, Fildes FJT (1982) Characterisation of hygroscopic inhalation aerosols. In: Stanley-Wood N, Allen T (eds) Particle Size Analysis 1981. John Wiley, Chichester, England, p 31

Hayes M, Taplin GV, Chopra SK, Knox DE, Elam D (1979) Improved radioaerosol administration system for routine inhalation lung imaging. Radiology 131:256–258

Matthys H, Kohler D (1985) Pulmonary deposition of aerosols by different mechanical devices. Respiration 48:269–276

Mercer TT (1973) ch. 9 In: Mercer TT (ed) Aerosol technology in hazard evaluation. Academic Press, New York

Mercer TT, Goddard RF, Flores RL (1965) Output characteristics of several commercial nebulisers. Ann Allergy 23:314–326

Phipps PR, Bailey DL, Borham PW, Gonda I (1986) Rapid droplet size analysis of diagnostic aerosols. Aust J Hosp Pharm 16:60

Porstendorfer J, Gebhart J, Robig G (1977) Effect of evaporation on the size distribution of nebulised aerosols. J Aerosol Sci 8:371–380

Ruffin RE, Dolovich MB, Oldenburg FA, Newhouse MT (1981) The preferential deposition of inhaled isoproterenol and propranolol in asthmatic patients. Chest [Suppl] 80:904–906

Ryan G, Dolovich MB, Obminski G, Cockroft DW, Juniper E, Hargreave FE, Newhouse MT (1981) Standardisation of inhalation provocation tests: influence of nebuliser output, particle size and method of inhalation. J Allergy Clin Immunol 67:156–161

Stahlhofen W (1984) Human data on deposition. In: Smith H, Gerber G (eds) Lung modelling for inhalation of radioactive materials. Proceedings of the Meeting of the Commission of Eur Communities and Nat Radiol Protection Board. Brussels, Luxembourg, p 39

Sterk PJ, Plomp A, van de Vate JF, Quanjer EH (1984) Physical properties of aerosols produced by several jet- and ultrasonic nebulisers. Bull Eur Physiopathol Respir 20:65–72

Taplin GV, Tashkin DP, Chopra SK, Anselmi OE, Elam D, Calvarese B, Coulson A, Detels R, Rokaw SN (1977) Early detection of chronic obstructive pulmonary disease using radionuclide lung imaging procedures. Chest 71:567–575

Trajan M, Logus JW, Enns EG, Man SFP (1984) Relationship between regional ventilation and aerosol deposition in tidal breathing. Am Rev Respir Dis 130:64–70

Wollmer P, Eriksson L, Andersson A-C (1985) Clinical assessment of a commercial delivery system for aerosol ventilation scanning by comparison with krypton-81m. J Nucl Med Technol 13:63–67

Received October 20, 1986 / March 18, 1987

J. Aerosols in Med., (1988), 1, 208-209.

STUDIES OF REGIONAL DEPOSITION OF AQUEOUS AEROSOLS IN THE HUMAN RESPIRATORY TRACT.

P.R.Phipps[1], I.Gonda[1]*, D.L.Bailey[2], P.Borham[2], S.D.Anderson[3] and G. Bautovich[2], [1]Department of Pharmacy, University of Sydney, Sydney NSW 2006, and Departments of [2]Nuclear and [3]Thoracic Medicine, Royal Prince Alfred Hospital, Camperdown, NSW 2050, Australia.

Aqueous aerosols are intrinsically unstable as they can exchange water with the environment depending on the surrounding vapour pressure. The results of this dynamic process are changes in droplet size (Phipps et al., 1987a) and concentration of the solution in the droplets (Phipps and Gonda, 1987). While the latter may affect the intensity of the pharmacological effects elicited by the solutes, the former is likely to lead to a modified regional deposition of the aerosol. Since aqueous aerosols are widely used for therapy and diagnosis in bronchial provocation tests and lung scanning, it is important to prepare well-defined aqueous aerosols and to quantify their deposition in the human respiratory tract. Aerosols were generated from solutions of ^{99}Tc-DTPA in normal saline using oxygen at 8 l/min in a small droplet (S) aerosol generator (Cadema Medical Products Inc., Middletown, USA), or in a nebulizer of unknown origin at 6 l/min giving large droplets (L). In order to prevent droplet evaporation, the dilution air supplementing the oxygen flow through the generator was humidified and the temperature of the nebulizer solution was kept constant by a miniature heater. The droplet size distributions of the two aerosols had mass median aerodynamic diameters (MMAD) 2.6 and 5.5 μm and geometric standard deviations 1.4 and 1.7, respectively. These sizes were selected deliberately to simulate the growth (or shrinkage) of a hypertonic (or hypotonic) aerosol with an intermediate MMAD, the type used in tests of bronchial hyperreactivity (Anderson et al.,1983). The concentration of the solutions in the droplets (Phipps & Gonda, 1987) was found to be near-isotonic (1.1 $\pm$ 0.1%). These aerosols were inhaled on two separate occasions by healthy volunteers under controlled respiratory conditions. In order to distinguish between aerosol deposition in the large airways and the lung parenchyma (which might overlie the former), a 3-dimensional (3D) gamma scintigraphic technique was employed (Phipps et al., 1987b). Penetration index (PI) was calculated as the ratio of the counts per second per pixel in peripheral to central regions. PI calculated from well defined mid-lung transverse sections was found to be the most sensitive measure to discriminate between the deposition of S and L aerosols: PI was significantly lower ($p < 10^{-5}$) for the L aerosols in all subjects, the overall relative difference between L & S being (56.5 $\pm$ 11.4) %. Thus, a) small aerosols with a low degree of polydispersity were shown to deposit to a much greater extent in the lung parenchyma than large droplet aerosols; b) the 3D tomographic technique for calculation of PI appears to be sufficiently sensitive to study the possible consequences of changes of aerosol droplet size 'in vivo'.

REFERENCES

Anderson, S.D.; Schoefel, R.E. and Finney, M. (1983) Thorax 38:284.

Phipps, P.; Borham, P.; Gonda, I.; Bailey, D.; Bautovich, G. and Anderson, S. (1987a) Eur.J.Nucl.Med. 13:183.

Phipps, P.; Gonda, I.; Bailey, D.C.; Borham, P.; Bautovich, G. and Anderson, S.D. (1987b) J.Pharm.Pharmacol. 39 (Suppl): 78P.

Phipps, P.R. and Gonda, I. (1987) ibid. 74P.

Comparisons of Planar and Tomographic Gamma Scintigraphy to Measure the Penetration Index of Inhaled Aerosols[1-3]

PAUL R. PHIPPS,[4] IGOR GONDA, DALE L. BAILEY, PETER BORHAM, GEORGE BAUTOVICH, and SANDRA D. ANDERSON

SUMMARY The quantitative measurement of regional aerosol deposition in human lungs using two-dimensional (2D) gamma scintigraphy has proven to be useful in therapeutic and diagnostic aerosol studies. The penetration index (PI) has been defined as the ratio of activity in a peripheral lung zone to a central lung zone, but the ability to discriminate between aerosol deposition in the large airways and lung parenchyma is reduced by the fact that the latter overlies the former in the central zone. To overcome this, we used a three-dimensional (3D) technique. Seven healthy subjects inhaled isotonic saline aerosols containing ^{99m}Tc-DTPA on two occasions. The droplets had a mass median aerodynamic diameter (MMAD) of either 2.6 or 5.5 μm (with geometric standard deviations [σg] of 1.4 and 1.7, respectively). Transmission tomography was performed on each subject to delineate lung boundaries in 2D and 3D. After inhalation, anterior (A) and posterior (P) images were collected and a tomographic study performed. Mid-lung slices were taken from coronal (CC) and transverse (TC) sections. PI was calculated on the 2D images (AP and P) and the 3D slices (CC and TC) using exactly defined regions. The PI values were smaller for the large droplet aerosol (5.5 μm) in all subjects and methods. The relative differences in PI between large and small (2.6 μm) droplet studies (d values) were greater and less variable for the 3D methods (TC, 56.5 ± 11.4% and CC, 52.4 ± 12.3%) compared to the 2D methods (P, 25.4 ± 17.1% and AP, 38.3 ± 15%; $p < 0.005$). We found the 3D methods to be more sensitive for discriminating between aerosol deposition in large and small airways than were the conventional 2D methods. AM REV RESPIR DIS 1989; 139:1516-1523

Introduction

The ability to differentiate quantitatively between the deposition of inhaled aerosols in large conducting airways and in lung parenchyma is useful in several areas of respiratory and nuclear medicine. For example, the assessment of the initial deposition pattern is necessary in the measurement of mucociliary clearance (1-11), the "*in vivo*" evaluation of devices for production of aerosols, and the parameters affecting their performance (12-23). The comparison of aerosols with radioactive gases (17, 19, 24-29), aerosol tests for small airways function (25, 27), and standardization of inhalation provocation tests (30-32) all require a measure of the distribution of radioactivity between the conducting airways and parenchyma. Perhaps the greatest need for quantitative information on the regional distribution of inhaled materials is necessary in the study of the deposition and elimination of substances with local pharmacologic activity (18, 20, 21, 33-36) and the pathophysiologic (7, 15, 24-27, 29, 37, 38) and pharmaceutical factors affecting these processes (13, 16, 20-23, 39).

The most common measure to estimate the relative amounts of aerosol deposited in the large airways and the lung parenchyma is the penetration index (PI) (3, 23, 25, 27, 28, 37, 40). This parameter is obtained by defining peripheral and central regions of the respiratory tract and calculating the ratio of radioactive counts in the two regions; a correction based on comparison with ^{81m}Kr scans is sometimes applied (3, 25, 27, 37), particularly when the gas is used to define the lung boundary or a volume correction is required for intersubject comparisons.

Conventionally, two-dimensional (2D) gamma scintigraphy has been used to visualize the deposition of radioaerosols in the human respiratory tract by taking posterior or anteroposterior geometric mean views. The central and peripheral regions of interest for the calculation of PI have been selected with the assumption that the former would contain predominantly large conducting airways, whereas the latter would represent mostly deposition in the small peripheral airways and, primarily, in the alveoli. It is well known that in reality, there are small airways and parenchyma as well as large airways located in the center of the lung because of its three-dimensional (3D) structure.

Logus and colleagues (41) showed the great value of the 3D technique of single photon emission computed tomography (SPECT) for lung imaging. In animals, SPECT detected ventilation defects caused by artificial obstructions that were not detected by other more conventional methods, whereas in patients with abnormal lung function, SPECT provided much better information about the regional aerosol deposition than either the posterior or anterior planar views. These investigators also studied the qualitative effect of two different breathing patterns on regional aerosol deposition, but they could detect no difference either by the 2D or 3D method, presumably because the aerosol was fine enough (mass median aerodynamic diameter [MMAD] = 1.2 μm, geometric standard deviation [σg] = 1.8) to deposit primarily in the alveoli (42).

We wished to develop a consistent and sensitive method of PI measurement that would enable us to discriminate between deposition in lung parenchyma and conducting airways. To this end, we employed aerosols of different sizes with expected depositions predominantly in these two distinct regions. In order to avoid the possibility of bias due to the effect of different rate and depth of breathing on the individual subject's aerosol deposition (43), we measured PI in each subject for

(*Received in original form March 14, 1988 and in revised form November 17, 1988*)

[1] From the Department of Pharmacy, University of Sydney, Sydney and the Departments of Nuclear Medicine and Thoracic Medicine, Royal Prince Alfred Hospital, Camperdown, Australia.

[2] Supported by the Asthma Foundation of New South Wales, Australia.

[3] Correspondence and requests for reprints should be addressed to Dr. I. Gonda, Department of Pharmacy, University of Sydney, Sydney, NSW 2006, Australia.

[4] Recipient of a Commonwealth Postgraduate Award.

the two aerosol sizes, inhaled using the same pattern of breathing on both occasions. We employed a gamma camera with tomographic acquisition capability to measure radioaerosol deposition on a time scale short enough to avoid significant change of the initial deposition pattern by mucociliary transport and absorption.

Methods

Subjects

Seven healthy, nonsmoking subjects were studied, five men and two women of mean age 34 yr (range, 26 to 39 yr). Lung volumes were obtained from each subject, and dynamic lung function tests were performed immediately before each inhalation study. The study protocol was approved by the Hospital Ethics Review Committee, and written informed consent was obtained from each subject prior to the studies after full explanation of the protocol.

Transmission Study

A transmission study (44, 45) was carried out on each subject to delineate lung fields. Each subject was placed in a supine position over a gamma camera (GE 400AT; General Electric, Milwaukee, WI) fitted with a low energy, all purpose, collimator and linked to an on-line computer (DEC PDP 11; Digital Electronic Corp., Maynard, MA). A flood source containing approximately 1.5 GBq of ^{153}Gd in water was fixed to a frame in front of the subject's chest. Two ^{57}Co markers were placed on premarked positions on the subject's chest, and anteroposterior images were collected. The markers were then removed with the subject remaining in the same position before a 64-angle tomographic study of 10 to 12 s/angle (approximately 15 min total duration) was acquired in a 64 × 64w matrix. The attenuation images collected were then reconstructed to provide low definition anatomical data in coronal and transverse planes.

Aerosol Deposition

Two radioaerosols with different particle size distributions were inhaled on two occasions by each subject. The aerosols were generated with oxygen from a medical gas cylinder from either a Cadema nebulizer (Cadema Medical Products Inc., Middletown, NY) at 8.0 L/min or a nebulizer of unknown origin at 6 L/min. The humidity of the dilution air supplementing the flow to the mouthpiece and the change in temperature of the nebulizer solution during generation were found to affect the droplet characteristics (46, 47). As a result of these observations, a miniature resistive heater was positioned inside each nebulizer. Power was then applied through a variac to keep the nebulizer as close as possible to room temperature. Dilution air was humidified with the aid of a medical humidifier placed in-line. Droplet sizing was performed on the radioaerosols produced by the nebulizers under these conditions with the aid of a calibrated seven-stage cascade impactor (DCI-6; Delron, Columbus, OH) (48). The coated glass impactor slides containing the deposited radioaerosol were counted on a previously calibrated gamma camera (47) and the droplet size distribution calculated by a least squares fit to the data (48). The droplet sizes of the two aerosols were 2.6 and 5.5 μm MMAD and 1.4 and 1.7 σg, respectively.

Inhalation Circuit

A closed aerosol inhalation circuit was used to monitor and record the subject's breathing. A target was thus provided to reproduce the breathing pattern on the subsequent inhalation with the aerosol of different size (figure 1).

The circuit consisted of a bag in a box system with the humidifier and nebulizer in the inspiratory line and filter and CO_2 absorber in the expiratory line. The volume respired was displaced from the "box" by the "bag," which then entered a bell spirometer (Gould Godart BV., Bilthoven, the Netherlands) via a respiratory flow transducer (Hewlett-Packard 47304A; Hewlett-Packard, Waltham, MA) and a pneumotachograph (Hewlett-

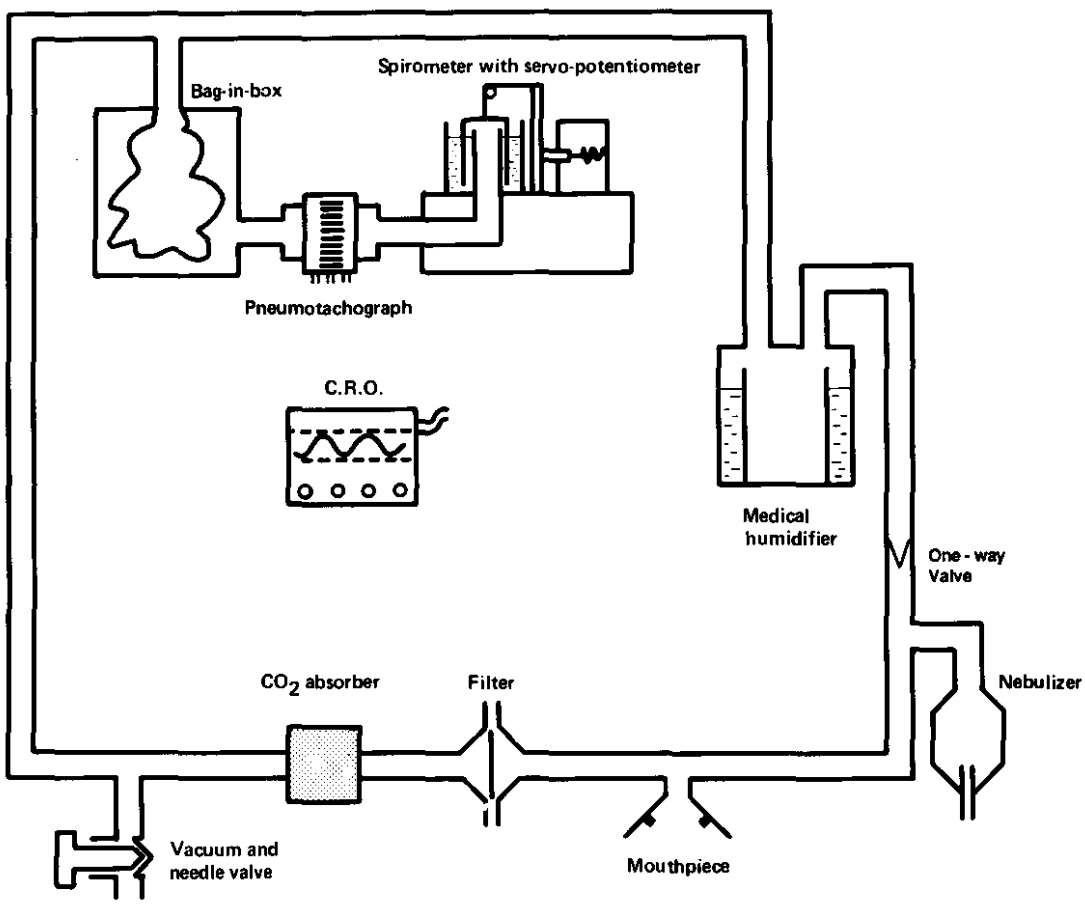

Fig. 1. Diagram of aerosol inhalation breathing circuit.

Packard 21073B). The flow signal from the pneumotachograph was integrated (respiratory integrator 8815A; Hewlett-Packard) and displayed on a cathode ray oscilloscope (184A and 1805A amplifier; Hewlett-Packard). A vacuum was applied to the circuit via a needle valve to evacuate from the system an appropriate amount of air to keep the system isovolumetric.

Inhalation

Each subject was seated at the mouthpiece of the aerosol delivery circuit and breathed tidally via the mouth for a few minutes to determine their natural tidal volume, peak flow, and frequency of breathing. The target volume or inspiratory flow was then displayed on the oscilloscope as a baseline and target line. The subject followed the tidal volume, or inspiratory flow line, as it moved between the target lines. A facility on the integrator allowed for any small changes in baseline by resetting after the end of every breath. The inspiratory flow was measured from a trace of the original flow signal and tidal volume from the spirometer graph. A metronome was used to provide a target for frequency of breathing. Approximately 5 ml of 100 MBq/ml ^{99m}Tc-DTPA in normal saline was then injected into the nebulizer through a rubber septum while the subject remained on the system. The inhalation period was three to four minutes with a further inhalation if lung counts were found to be below 2000 counts per second over the posterior thorax.

Imaging

Immediately after aerosol inhalation, water was gargled and expectorated and the subjects placed in a supine position over the gamma camera. Two-minute anterior and posterior images were then collected before a 10 to 12 s/angle SPECT study, in a 64 × 64w matrix.

Data Treatment

The images obtained by the gamma camera were displayed on the computer screen in a 64 × 64w matrix (Gamma 11; Digital Electronic Corp.). The transmission data were converted to attenuation values and transverse sections reconstructed using conventional convolution back-projection methods (Nuclear Medicine Package; Analogic Corp., Worcester, MA). The emission data were reconstructed by convolution back-projection and a first-order Chang attenuation correction performed employing a constant attenuation coefficient (49) derived from the attenuation values described above.

Coronal and transverse sections were formed from the reconstructed images. A number of coronal and transverse central slices were then taken from the midportion of the right lung and summed together as shown in figure 2. The right lung only was assessed to avoid corruption by activity in the stomach adjacent to the left lung. The reconstructed transmission tomographic images were used to define right lung boundaries in transverse, coronal, and anteroposterior views for each subject. These were used to derive central and peripheral zones by computer-based predefined criteria related to the dimensions of the lung. The central region was drawn along the medial boundary edge of dimensions as shown in figure 2. The peripheral region was defined by scanning from a point midway down the medial side of the lung image, around the lung, drawing a peripheral strip a set distance (one-third of the lung height) inside the outer boundary (figure 2). Once a region was defined for a subject, it was stored for all future uses.

The PI was then defined as:

$$PI = \frac{\text{Counts per second (cps)/pixel in peripheral region}}{\text{cps/pixel in central region}}.$$

PI measurements were performed on the following images: planar methods: (*1*) the 2D posterior image (P), not corrected for attenuation; (*2*) anteroposterior geometric mean image (AP), not corrected for attenuation; tomographic methods: (*3*) transverse central slices (TC) taken through the midportion of the lung in transverse view of thickness approximating 50% of the lung height; (*4*) coronal central slices (CC) taken through the midportion

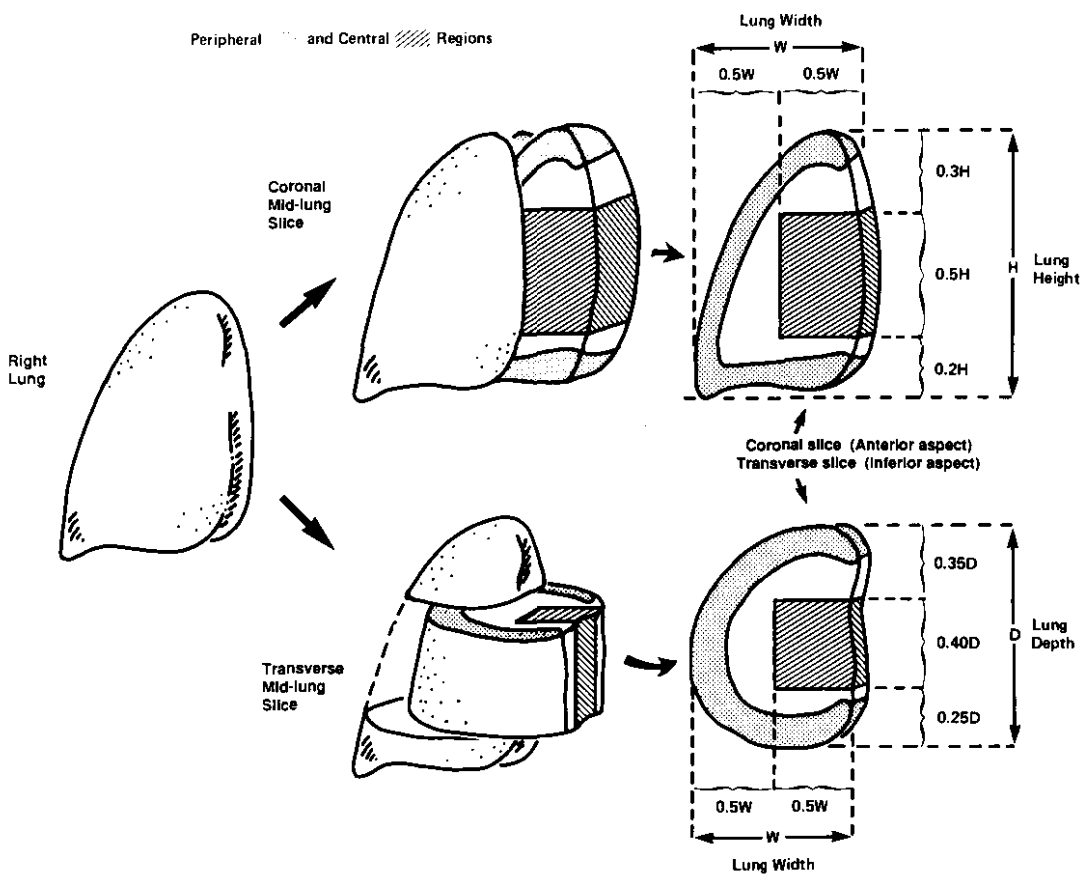

Fig. 2. Diagram of peripheral and central regions and mid-lung slicing.

of the lung in coronal view of thickness approximating 40% of the lung depth.

Results

All subjects' spirometric and lung function results were within the normal range, and there was negligible intrasubject variability in performance between "small" (MMAD = 2.6 μm, σg = 1.4) and "large" (MMAD = 5.5 μm, σg = 1.7) aerosol studies (table 1). This was confirmed by the two-tailed paired *t* test (50) and the two-tailed Wilcoxon rank sum test (51), which demonstrated no statistically significant intrasubject differences ($p < 0.1$) between the two studies for mean peak inspiratory and expiratory flow, tidal volume, and duration of respiratory cycle (table 2). These are the primary breathing parameters believed to affect the regional deposition of aerosols in the aerodynamic size range used in this work (43).

Typical AP and CC images for the small and large droplet studies in Subject 2 are shown in figure 3. A small qualitative difference in the deposition pattern of the right lung can be observed with the AP images, whereas a much greater difference in the deposition pattern between large and small droplets with the CC images can be observed.

Figure 4 shows that the PI was smaller for the large droplets in all subjects and in all methods employed. The highest statistical significance was obtained for the transverse ($p < 10^{-5}$) and coronal ($p < 10^{-3}$) midlung slices, whereas the planar (P) images exhibited the least significant difference ($p = 0.014$). To examine the group response more closely, these differences were further evaluated by calculating the relative increase in PI of the small droplet study compared to the large droplet study as a percentage (d):

$$d\,\% = \frac{\text{PI (small droplets)} - \text{PI (large droplets)} \times 100}{\text{PI (small droplets)}}.$$

These results are shown in figure 5. The d values obtained from the 3D (TC and CC) images are significantly greater than those from the 2D (P and AP) ($p < 0.005$), whereas there was no difference between the two 3D methods or between the two 2D methods ($p > 0.1$) The d value from the P images was inferior to all other methods tested.

The standard deviation of the mean d values are also shown in figure 5. PI from TC and CC can be seen to display the most consistent pattern in the subject population and aerosols studied.

TABLE 1

SUBJECT DETAILS

Subject	Sex	Age (yr)	Height (cm)	Weight (kg)	VC (%) S	VC (%) L	FEV_1 (%) S	FEV_1 (%) L	FEV_1/VC (%) S	FEV_1/VC (%) L	FEF_{50} (%)
1	F	39	154	54	105	97	98	79	84	59	62
2	M	39	182	71	107	105	113	85	83	101	106
3	M	26	191	78	103	103	104	82	84	101	98
4	M	38	154	59	111	116	113	83	88	77	78
5	M	38	165	63	108	111	102	86	89	102	96
6	M	26	171	65	119	130	128	86	87	103	96
7	F	29	166	67	114	104	109	83	86	74	78

Definition of abbreviations: VC = vital capacity (% predicted); FEV_1 = forced expiratory volume in 1 s (% predicted); FEV_1/VC = FEV_1 as percent of VC; FEF_{50} = forced expiratory flow at 50% VC (% predicted) (51); S = "small" aerosol droplet study (MMAD = 2.6 μm); L = "large" aerosol droplet study (MMAD = 5.5 μm).

Discussion

Among the various quantitative measures of the distribution of deposited radioaerosols between the airways and the lung parenchyma, the PI is almost certainly the most convenient and readily measurable. However, planar measurements of aerosol deposition suffer from the problem of the inclusion of overlying "peripheral" airways in the central "large" airway region (41).

It has been suggested before (52) that tomography should be better suited to distinguish between deposition in the small and large airways than should the conventional 2D images. We therefore attempted to further separate central and peripheral airways by the use of these tomographic techniques. Our results show that in comparison with the conventional techniques based on planar imaging, tomographic methods of measuring regional deposition are superior, with the coronal and transverse midlung slices giving a more discriminating measure of PI. This is also likely to be the case with aerosols of different droplet size characteristics to those used, as long as there is a

TABLE 2

MEAN BREATHING PARAMETERS*

Subject	Study†	MPIF (L/min)	MPIF (CV %)	MPEF (L/min)	MPEF (CV %)	MTV (ml)	MTV (CV %)	DRC (s)	DRC (CV %)
1	S	25.1	8.9	20.6	7.2	491.7	6.9	4.45	3.3
	L	25.9	9.4	19.2	9.5	493.9	8.9	4.40	3.8
	d	3.2		−6.8		0.5		1.10	
2	S	23.2	26.7	16.7	13.4	713.8	9.1	8.11	3.8
	L	28.4	23.7	17.5	17.8	730.2	15.0	7.96	4.0
	d	22.4		4.8		2.3		1.80	
3	S	41.9	6.9	31.1	6.6	614.7	5.3	5.21	4.4
	L	40.4	4.7	27.3	6.3	574.8	5.3	5.18	4.1
	d	−3.6		−9.6		−6.5		0.6	
4	S	30.4	15.9	21.7	7.5	682.6	11.3	4.91	3.2
	L	8.1	11.5	20.5	7.2	74.6	7.7	4.90	3.1
	d	−7.6		−5.5		−1.2		0.2	
5	S	43.3	16.1	34.4	11.6	987.6	3.8	6.26	4.4
	L	31.1	8.1	31.1	9.6	1,000.1	3.4	6.28	4.8
	d	−28.2		−9.6		1.3		0.3	
6	S	31.0	12.7	34.3	8.8	1,254.8	8.1	6.43	3.4
	L	34.1	8.7	29.6	12.7	1,244.2	14.2	6.44	4.7
	d	10.1		−13.7		−0.8		0.2	
7	S	29.1	13.7	19.5	13.7	495.0	12.1	3.65	4.2
	L	35.3	10.7	24.6	9.3	633.9	13.0	3.60	4.6
	d	21.3		26.5		28.1		1.4	

Definition of abbreviations: S = "small" aerosol droplet study (MMAD = 2.6 μm); L = "large" aerosol droplet study (MMAD = 5.5 μm); d = % difference between large and small study, 100 (L − S)/S; MPIF = mean peak inspiratory flow (L/min); MPEF = mean peak expiratory flow (L/min); MTV = mean tidal volume (ml); DRC = duration of respiratory cycle (s); CV = coefficient of variation (%).

* Values are mean ± standard deviation.

† Study.

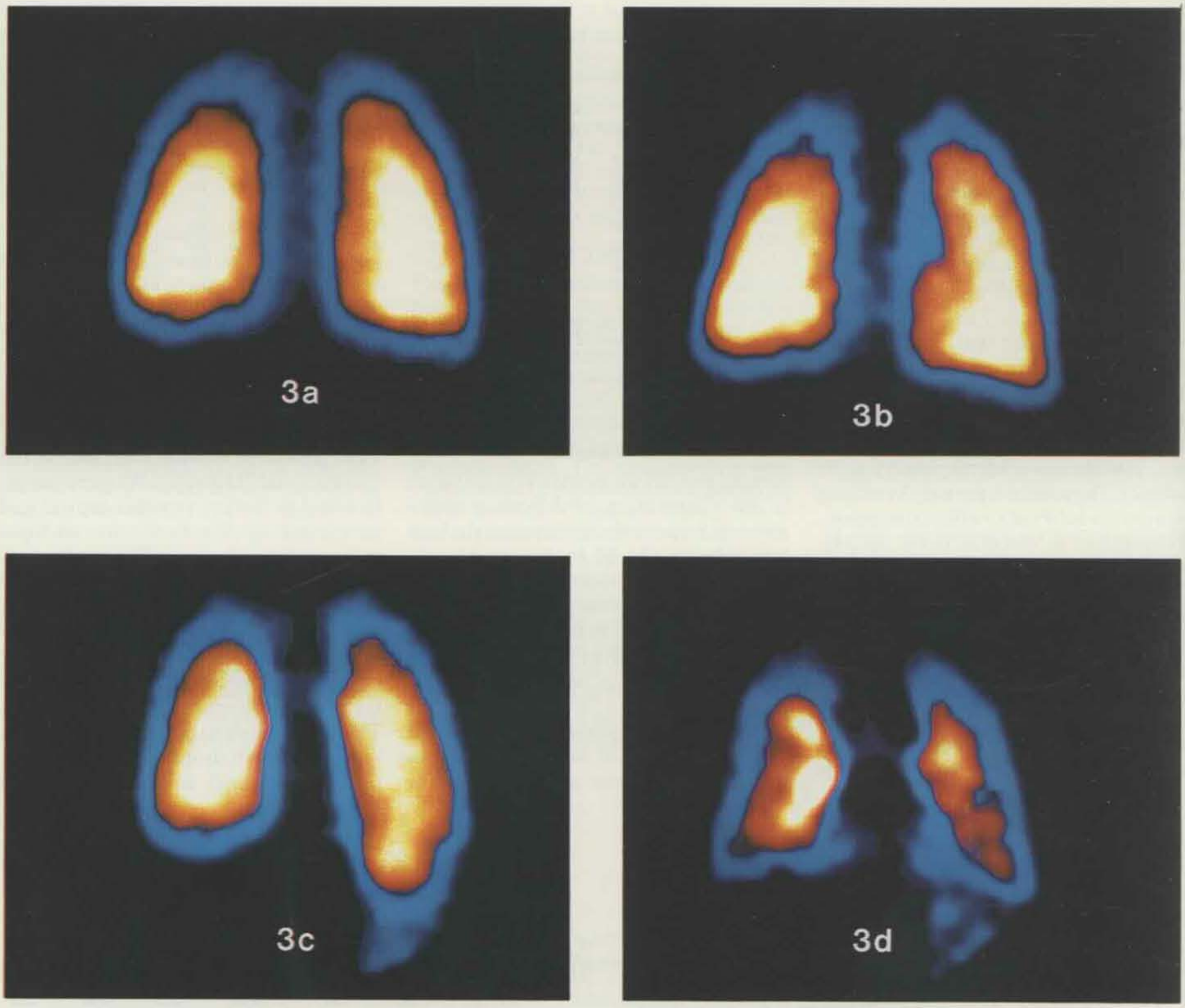

Fig. 3. Deposition images of the small aerosol (3a and 3b) and large aerosol (3c and 3d) in Subject 2. Images 3a and 3c are anteroposterior (AP) images, whereas 3b and 3d are coronal mid-lung slices (CC). The CC images show a larger qualitative difference in deposition pattern between the large and small studies.

proportion of both peripheral and central deposition.

Mildly polydisperse aerosols with MMAD of 5.5 and 2.6 μm were used because the former aerosol would be expected to have a substantially smaller PI than the latter (48, 53, 54). Impaction in the conducting airways is probably the predominant mechanism of deposition of the "large" droplets, whereas sedimentation in the small airways and alveoli becomes important for smaller droplets. The results indicate that the choice of the regions of interest is consistent with the idea that the "central" region contains mainly large conducting airways and the "peripheral" region consists probably of bronchioli and alveoli; otherwise, we would not expect to obtain such clear differences in PI between the two aerosols in all subjects and methods used. Although there was a difference in the breathing patterns between the large and small aerosol studies in some subjects, there was no significant trend and the changes in PI could not be explained by this. Nevertheless, we would recommend that attempts be made to reproduce as much as possible the breathing pattern in an individual for studies of changes in PI, particularly in subjects with abnormal and variable airway function (55).

After the initial deposition, the inhaled aerosol undergoes dynamic changes due to absorption and mucociliary clearance (8). Although a longer time is required for SPECT image acquisitions (up to 15 min), these changes are likely to have little effect on the calculated PI values for the following reasons: in normal subjects, the absorption rate half-life of Tc-DTPA is 86 ± 26 min (56) and this varies little throughout the respiratory tract over the SPECT acquisition time, especially mediolaterally (57–59). Therefore, this route of elimination of the radioactivity will affect approximately equally both the peripheral and the central regions. Similarly, the "background" radioactivity appearing in the bloodstream will be small and distributed quite uniformly and it will be cleared rapidly with 58% clearing with a biologic half-time of 3.8 min, 24% with 15.6 min, and 18% greater than 118 min in subjects with normal renal function (60). With regard to the mucociliary clearance, it can be envisaged that

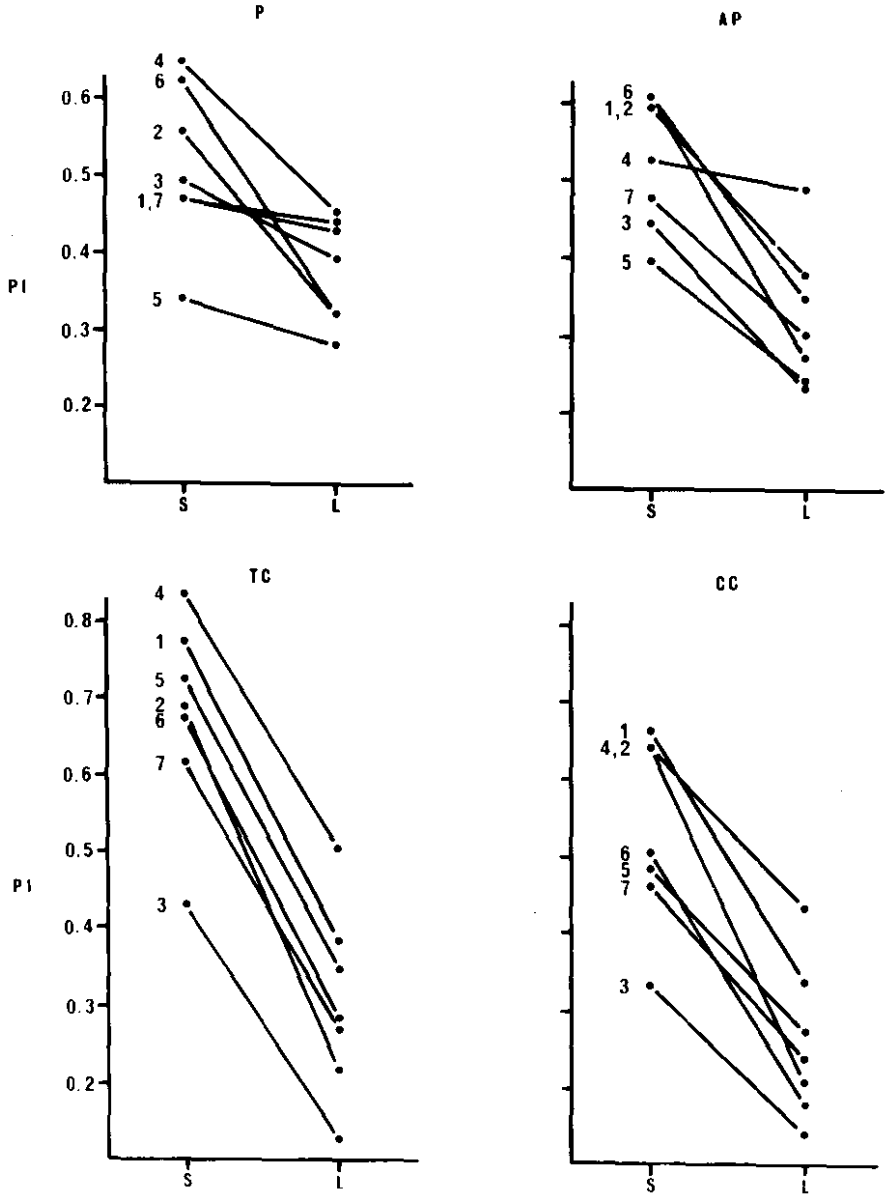

Fig. 4. Penetration index (PI) values for small (S) and large (L) droplets. Posterior image (P), anteroposterior image (AP), transverse mid-lung slices (TC), and coronal mid-lung slices (CC). Where a single point for the S aerosol represents two subjects, the first number refers to the subject with a higher PI for the L aerosol.

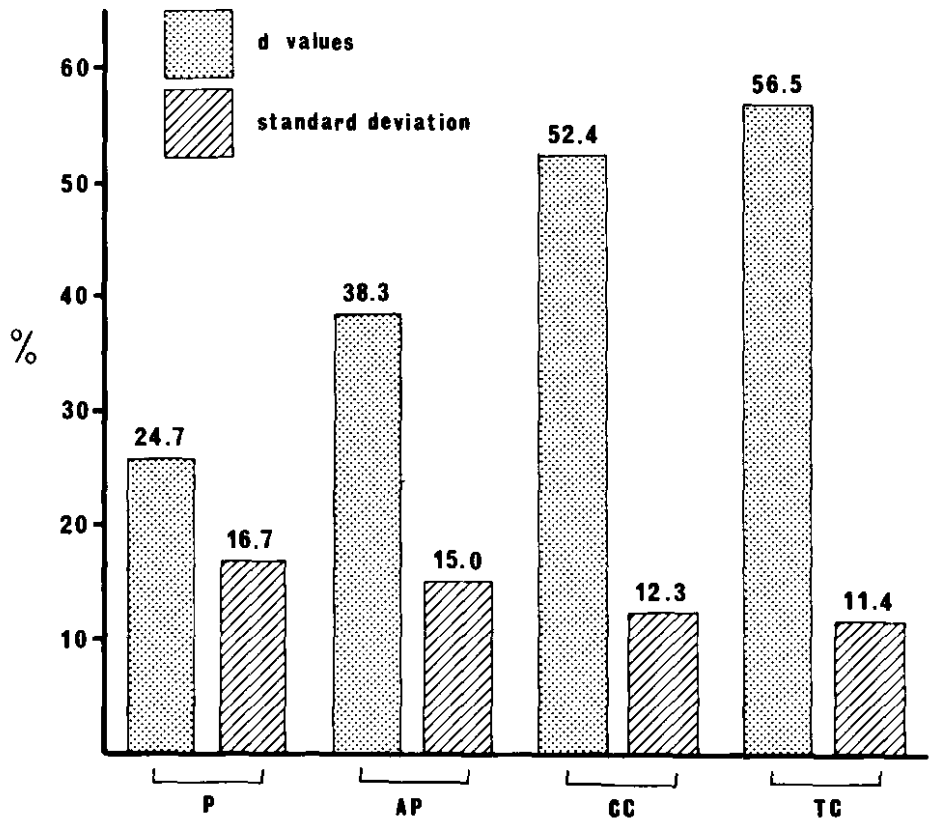

Fig. 5. Chart of d values as the relative difference in penetration index between large and small droplet studies (d values) and standard deviations for posterior (P), anteroposterior (AP), transverse mid-lung slices (TC), and coronal mid-lung slices (CC).

at least in normal subjects, this process is at steady state, whereby there exists a balance between the rates of supply and removal of material in the more proximal ciliated regions of the respiratory tract. Therefore, we would not expect this process to significantly affect the radioactive counting in the central region over the time period of the SPECT studies. The peripheral region probably contains many nonciliated surfaces that are therefore not subject to mucociliary clearance. Moreover, all the above processes have half-lives longer than the duration of our SPECT studies (61, 62).

In conclusion, we have shown that there were significant reductions in the PI values in normal adults when they inhaled two aerosols with MMAD of 2.6 μm (σg = 1.4) and 5.5 μm (σg = 1.7), respectively, under controlled conditions. These reductions were most pronounced when the PI was calculated from mid-lung coronal or transverse slices obtained by SPECT reconstruction; this former method also gave the most consistent pattern of changes in PI in the subject population studied. The conventional planar images showed the same qualitative behavior, but their ability to distinguish between deposition of the large and small aerosols was substantially lower, particularly for the posterior images.

This is the first time that quantitative deposition measurements have been undertaken using SPECT, and the advantages of PI obtained in this way are likely to be important in studies requiring a high degree of discrimination between the deposition of aerosols on conducting and respiratory surfaces of the respiratory tract.

References

1. Sanchis J, Dolovich M, Chalmers R, Newhouse M. Quantitation of regional aerosol clearance in the normal human lung. J Appl Physiol 1972; 33: 757–62.
2. Foster WM, Langenback E, Bergofsky EH. Measurement of tracheal and bronchial mucus velocities in man: relation to lung clearance. J Appl Physiol 1980; 48:965–71.
3. Agnew JE, Bateman JRM, Watts M, Paramananda V, Pavia D, Clarke SW. The importance of aerosol penetration for lung mucociliary clearance studies. Chest 1981; 80(Suppl:843–6).
4. Weiss T, Dorrow P, Roland F. Continuous aerosol inhalation scintigraphy in the evaluation of early and advanced airways obstruction. Eur J Nucl Med 1984; 9:62–7.
5. Agnew JE, Pavia D, Clarke SW. Factors affecting the "alveolar deposition" of 5 μm particles in healthy subjects. Clin Phys Physiol Meas 1985; 6: 27–36.
6. Agnew JE, Sutton PP, Pavia D, Clarke SW. Radioaerosol assessment of mucociliary clearance: towards definition of a normal range. Br J Radiol 1986; 59:147–51.
7. Gerrard CS, Gerrity TR, Yeates DB. The relationships of aerosol deposition, lung size and the rate of mucociliary clearance. Arch Environ Health 1986; 41:11–5.
8. Lippmann M, Yeates DB, Albert RE. Deposition, retention, and clearance of inhaled particles. Br J Med 1980; 37:337–62.
9. Pavia D. Lung mucociliary clearance. In: Clarke SW, Pavia D, eds. Aerosols and the lung. London: Butterworths, 1984; 127–55.
10. Dolovich MB, Jordana M, Newhouse MT. Methodologic considerations in mucociliary clearance and lung epithelial absorption measurements. Eur J Nucl Med 1987; 13(Suppl:S45–S52).
11. Clarke SW, Agnew JE. Current status of nuclear medicine in chronic airflow limitation. Eur J Nucl Med 1987; 13(Suppl:S20–3).
12. Asmundsson T, Johnson RF, Kilburn KH, Goodrich JK. Efficiency of nebulizers for depositing saline in human lung. Am Rev Respir Dis 1973; 108:506–12.
13. Newman SP, Pavia D, Moren F, Sheahan NF, Clarke SW. Deposition of pressurized aerosols in the human respiratory tract. Thorax 1981; 36:52–5.
14. Foulds RA, Smithuis LOMJ. Comparison of lung deposition of a solution after nebulization by three commonly used portable nebulizers. Pharmaceut Weekbl (Sci Ed) 1983; 5:74–6.
15. Laube BL, Swift DL, Adams KG III. Single-breath deposition of jet-nebulized saline aerosol. Aerosol Sci Technol 1984; 3:97–102.
16. Newman SP, Millar AB, Lennard-Jones TR, Moren F, Clarke SW. Improvement of pressurized aerosol deposition with spacer Nebuhaler device. Thorax 1984; 39:935–41.
17. Royston D, Minty DB, Jones JG, McLeod M. A simple separator to generate half micron aqueous particles for lung imaging. Br J Radiol 1984; 57:223–8.
18. Matthys H, Kohler D. Pulmonary deposition of aerosols by different mechanical devices. Respiration 1985; 48:269–76.
19. Wollmer P, Eriksson L, Andersson A-C. Clinical assessment of a commercial delivery system for aerosol ventilation scanning by comparison with krypton-81m. J Nucl Med Technol 1985; 13:63–7.
20. Vidgren MT, Karkkainen A, Paronen TP, Karjalainen P. Respiratory tract deposition of ^{99m}Tc-labelled drug particles administered via a dry powder inhaler. Int J Pharm 1987; 39:101–5.
21. Vidgren MT, Paronen TP, Karkkainen A, Karjalainen P. Effect of extension devices on the drug deposition from inhalation aerosols. Int J Pharm 1987; 39:107–12.
22. Newman SP. Therapeutic aerosols. In: Clarke SW, Pavia D, eds. Aerosols and the lung. London: Butterworths, 1984; 197–224.
23. Newman SP, Pavia D. Aerosol deposition in man. In: Moren F, Newhouse MT, Dolovich MB, eds. Aerosols in medicine. Principles, diagnosis and therapy. Amsterdam: Elsevier 1985; 193–217.
24. Taplin GV, Tashkin DP, Chopra SK, *et al.* Early detection of chronic obstructive pulmonary disease using radionuclide lung-imaging procedures. Chest 1977; 71:567–75.
25. Agnew JE, Pavia D, Clarke SW. Airways penetration of inhaled radioaerosol: an index to small airways function? Eur J Respir Dis 1981; 62:239–55.
26. Trajan M, Logus JW, Enns EG, Man SFP. Relationship between regional ventilation and aerosol deposition in tidal breathing. Am Rev Respir Dis 1984; 130:64–70.
27. Emmett PC, Love RG, Hannan WJ, Millar AM, Soutar CA. The relationship between the pulmonary distribution of inhaled fine aerosols and tests of small airway function. Bull Eur Physiopathol Respir 1984; 20:325–32.
28. Kohn H, Klech H, Anglberger P, *et al.* Dry aerosol of monodisperse millimicrospheres for ventilation imaging: production, delivery system, and clinical results in comparison with ^{81m}krypton and ^{127}xenon. Eur J Nucl Med 1985; 10:411–6.
29. Susskind H, Brill B, Harold WH. Quantitative comparison of regional distributions of inhaled Tc-99m DTPA aerosol and Kr-81m gas in coal miners' lungs. Am J Physiol Imag 1986; 1:67–76.
30. Ryan G, Dolovich MB, Obminski G, *et al.* Standardization of inhalation provocation tests: influence of nebulizer output, particle size, and method of inhalation. J Allergy Clin Immunol 1981; 67:156–61.
31. Ryan G, Dolovich MB, Roberts RS, *et al.* Standardization of inhalation provocation tests: two techniques of aerosol generation and inhalation compared. Am Rev Respir Dis 1981; 123:195–9.
32. Yan K, Schoeffel R, Salome C, Hutton B, Woolcock AJ. Changes in lung function produced by methacholine using two different inhalation techniques in normal and asthmatic subjects. In: Nandi PL, Lam WK, eds. Proceedings of seventh Asia-Pacific congress, Hong Kong, 1983; 118–23.
33. Ruffin RE, Kenworthy MC, Newhouse MT. Response of asthmatic patients to fenoterol inhalation: a method of quantifying the airway bronchodilator dose. Clin Pharmacol Ther 1978; 23: 338–45.
34. Ruffin RE, Dolovich MB, Wolff RK, Newhouse MT. The effects of preferential deposition of histamine in the human airway. Am Rev Respir Dis 1978; 117:485–92.
35. Ruffin RE, Dolovich MB, Oldenburg FA, Newhouse MT. The preferential deposition of inhaled isoproterenol and propranolol in asthmatic patients. Chest 1981; 80(Suppl:904–6).
36. Dolovich MB, Ryan G, Newhouse MT. Aerosol penetration into the lung: influence on airway responses. Chest 1981; 80(Suppl:834–6).
37. Dolovich MB, Sanchis J, Rossman C, Newhouse MT. Aerosol penetrance: a sensitive index of peripheral airways obstruction. J Appl Physiol 1976; 40:468–71.
38. Pearson MG, Chamberlain MJ, Morgan WKC, Vinitski S. Regional deposition of particles in the lung during cigarette smoking in humans. J Appl Physiol 1985; 59:1828–33.
39. Farr SJ, Kellaway IW, Parry-Jones DR, Woolfrey SG. 99m technetium as a marker of liposomal deposition and clearance in the human lung. Int J Pharm 1985; 26:303–16.
40. Agnew JE. Aerosol contribution to the investigation of lung structure and ventilatory function. In: Clarke SW, Pavia D, eds. Aerosols and the lung. London: Butterworths, 1984; 92–126.
41. Logus JW, Trajan M, Hooper HR, Lentle BC, Mann SFP. Single photon emission tomography of lungs imaged with Tc-labeled aerosol. J Can Assoc Radiol 1984; 35:133–8.
42. Yu CP, Taulbee DB. A theory predicting respiratory tract deposition of inhaled particles in man. In: Walton WH, McGovern B, eds. Inhaled particles IV, part 1. Oxford: Pergamon Press, 1977; 35–47.
43. Stahlhofen W. Human data on deposition in lung modelling for inhalation of radioactive materials. In: Smith H, Gerber G, eds. Lung modelling for inhalation of radioactive materials. Proceedings of the meeting of the Commission of European Communities and National Radiology Protection Board. Brussels: Commission of the European Communities, 1984; 39–59.
44. Anger HO, McRae J. Transmission scintiphotography. J Nucl Med 1968; 9:267–9.
45. Bailey DL, Hutton BF, Walker PJ. Improved SPECT using simultaneous emission and transmis-

sion tomography. J Nucl Med 1987; 28:844–51.
46. Phipps PR, Gonda I. Concentration of solution in aqueous aerosol droplets. J Pharm Pharmacol 1987; 39(Suppl:74P).
47. Phipps PR, Borham P, Gonda I, Bailey DL, Bautovich G, Anderson S. A rapid method for the evaluation of diagnostic radioaerosol delivery systems. Eur J Nucl Med 1987; 134:183–6.
48. Gonda I, Kayes JB, Groom CV, Fildes FJT. Characterization of hygroscopic inhalation aerosols. In: Stanley-Wood NG, Allen T, eds. Particle size analysis 1981. Chichester: Wiley Heyden Ltd., 1982; 31–43.
49. Chang LT. A method for attenuation correction in radionuclide computed tomography. IEEE Trans Nucl Sci 1978; NS-25:638–43.
50. Snedecor GW, Cochran WG. Statistical methods. 6th ed. Ames: Iowa State University Press, 1967.
51. Colton T. Statistics in medicine. Boston: Little, Brown and Co., 1974.
52. Dolovich MB, Coates G, Hargreave F, Newhouse MT. Aerosols in diagnosis: ventilation, airway penetrance, airway reactivity, epithelial permeability and mucociliary transport. In: Moren F, Newhouse MT, Dolovich MB, eds. Aerosols in medicine. Principles, diagnosis and therapy. Amsterdam: Elsevier, 1985; 225–59.
53. Gonda I. Study of the effect of polydispersity of aerosols on regional deposition in the respiratory tract. J Pharm Pharmacol 1981; 33:(Suppl:52).
54. Ferron GA, Hornik S, Kreyling WG, Haider B. Comparison of experimental and calculated data for the total and regional deposition in the human lung. J Aerosol Sci 1985; 16:133–43.
55. Laube JW, Swift DL, Wagner HN, Norman PS, Adams GK III. The effect of bronchial obstruction on central airway deposition of a saline aerosol in patients with asthma. Am Rev Respir Dis 1986; 133:740–3.
56. Coates G, O'Brodovich H. Measurement of pulmonary epithelial permeability with ^{99m}Tc-DTPA aerosol. Semin Nucl Med 1986; 16:275–84.
57. O'Doherty MJ, Page CJ, Croft N, Bateman NT. Regional lung epithelial leakiness in smokers and nonsmokers. Nucl Med Commun 1985; 6: 353–7.
58. Dusser DJ, Minty BD, Collignon M-AG, Hinge D, Barritault LG, Huchen GJ. Regional respiratory clearance of aerosolized 99m-Tc-DTPA: posture and smoking effects. J Appl Physiol 1986; 60: 2000–6.
59. Coates G, O'Brodovich H. Extrapulmonary radioactivity in lung permeability measurements. J Nucl Med 1987; 28:903–6.
60. McAfee JG, Gagne H, Atkins HL, *et al.* Biological distribution and excretion of DTPA labeled with Tc-99m and In-111. J Nucl Med 1979; 20: 1273–8.
61. Byron PR. Prediction of drug residence times in regions of the human respiratory tract following aerosol inhalation. J Pharm Sci 1986; 75:433–8.
62. Becquemin MH, Roy M, Robeau D, Bonnefous S, Piechowski J, Teillac A. Inhaled particle deposition and clearance from the normal respiratory tract. Respir Physiol 1987; 67:147–58.

Droplets Produced by Medical Nebulizers*

Some Factors Affecting Their Size and Solute Concentration

Paul R. Phipps, B. Pharm.†; and Igor Gonda, B.Sc., Ph.D.

The effect of nebulizer solution temperature and dilution air humidity on the size and solute concentration of aqueous aerosol droplets were studied. Four combinations of jet-nebulizers with air compressors or oxygen sources and one ultrasonic nebulizer were tested. The temperature to which the nebulizer solution of each system fell during generation was measured. The nebulizers were then kept at set temperatures, generated aerosols collected and either droplet size or solute concentration measured. The droplet solute concentration was found to increase. The droplet size decreased along with the droplet solute concentration increase. The ultrasonic nebulizer also was tested: its high output made the concentration of the solution in the droplets much more stable. However, the proportion of droplets depositing in the tubing and valves changed markedly with aerosol flow rate. The potential for large changes in droplet solute concentration, droplet size and output during nebulization should be considered in therapeutic and diagnostic applications of nebulized aerosols.

(Chest 1990; 97: 1327-32)

Nebulized aerosols are used extensively in therapy and diagnosis of respiratory diseases. This mode of administration also has proven useful in ventilation imaging as an aid in the diagnosis of pulmonary embolism. In fact, it is the ease with which solutions or suspensions of therapeutic and diagnostic agents can be nebulized which makes the use of this type of aerosol so widespread.

The importance of the characterization of nebulizer systems for clinical applications has been recognized by a number of authors.[1-7] The clinical efficacy of nebulized aerosol treatment depends primarily on the amount of active substance depositing at various sites in the respiratory tract, which in turn is dependent on the droplet size[8,9] and output from the nebulizer as well as patient parameters such as inspiratory flow rate, respiratory tract morphology and disease state of the lungs.[10] The wide variation in performance of nebulizer delivery systems[5,6,11-13] makes it likely that a failure in therapy often may be explained by poor aerosol delivery rather than by a poor response to the drug therapy.

It is well known that the nebulizer solution cools and concentrates during nebulization,[14,15] and it has been reported that the humidity of the air inhaled along with the aerosol affects droplet characteristics.[7,16] We wished to look directly at the effects of nebulizer cooling and dilution air humidity on *(a)* the size and *(b)* the concentration of solutes in the aerosol droplets generated by a number of different medical nebulizer systems.

Methods

The following products were assessed: Cadema nebulizer (Cadema Medical Products Inc., Middletown, NY) with compressed oxygen at 8 L/min; Up-Draft nebulizer (Hudson Up-Draft Oxygen Therapy Sales Co., Temecula, CA) with compressed oxygen at 8 L/min; Up-Draft with Flatus Mk.V air compressor (Maymed, Anaesthetic Supplies Pty. Ltd, Sydney, Australia)—this system is equivalent to Tote-A-Neb, Hospitak Inc., Lindenhurst, NY (private communication, Laura Martinazzi); Up-Draft with Aerosol-One air compressor (Medical Industries America, Des Moines, IA); Mist-O_2-Gen ultrasonic nebulizer (Model EN143A, Timeter, PA).

These systems are representative of equipment used in the diagnosis of pulmonary embolism (Cadema nebulizer), non-isotonic challenge testing in asthma diagnosis[17] (Mist-O_2-Gen) or for drug delivery in the treatment of various respiratory diseases (Up-Draft nebulizer, Up-Draft with Flatus Mk.V air compressor and Up-Draft with Aerosol-One air compressor). The flow rate produced by the Flatus Mk.V and the Aerosol-One air compressors through the UpDraft nebulizer containing 5 ml normal saline solution was found to be 6.3 and 5.0 L/min, respectively as measured by rotameter (Platon Ltd, Basingstoke, Harts, UK)

The change in temperature of each system was measured with an esophageal thermistor probe (YSI series 400, temperature recorder model 46TUC, Yellow Springs Instruments Co. Inc, Yellow Springs, OH) placed in the nebulizer solution, and the temperature was recorded at set times during aerosol generation until the temperature had reached a steady value (T_s). The initial volume of solution in the nebulizer was 5 ml (jet nebulizers) or 200 ml (ultrasonic nebulizer). The ambient temperatures varied between 23 and 24°C.

The concentration of sodium chloride in the aerosol droplets generated by the jet nebulizers was measured for different, constant, nebulizer solution temperatures. The lowest temperature used for each nebulizer was approximately the value reached after running the nebulizer without heating to a steady temperature T_s, determined as described previously. The nebulizer bowl, containing 5 ml normal saline solution, was cooled to a nominated temperature by immersion in a cold water bath. The aerosol was then generated and the nebulizer solution temperature kept at the nominated value by immersion in a warm water bath. The temperature of the nebulizer solution was monitored with the miniature esophageal thermistor probe. The temperature was controlled to ±0.3 degrees during a generation time of 10 to 25 min and generated volume of 1 to 3 ml. The aerosol was passed via a short length of tubing (30 cm) through the last two stages of a cascade impactor (DCI6, Delron, Columbus, OH) and collected in a small container of similar dimensions to a cascade impactor slide. The flow through the impactor stages was 12.5 L/min, and the dilution air necessary to supplement the flow through the nebulizer was supplied either at ambient temperature (23 to 24°C) and humidity (65 to 75 percent) or fully humidified at ambient temperature via a Douglas bag. After collection of the aerosol droplets, the containers were re-weighed and droplets diluted with normal saline solution if their volume was

*From the Department of Pharmacy, Sydney University, Sydney, Australia.
†Recipient of a Commonwealth Postgraduate Scholarship.
Manuscript received July 18; revision accepted December 1.

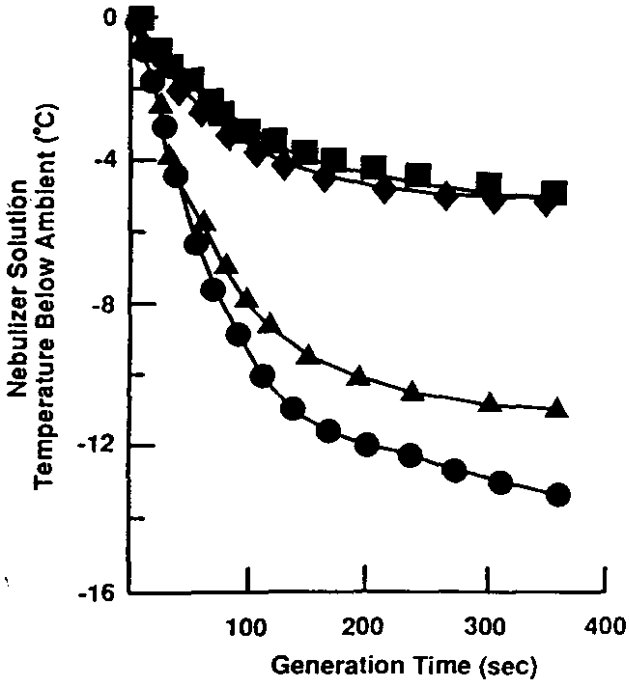

FIGURE 1. Graph of nebulizer solution temperature below ambient (23 to 24°C) vs time of generation for the four jet nebulizer systems: Up-Draft/Aerosol-One *(squares)*, Up-Draft/Flatus *(diamonds)*, Cadema/compressed oxygen *(circles)* and Up-Draft/compressed oxygen *(triangles)*.

insufficient for the determination of their solute concentration by vapor pressure osmometry (model 1100, Knauer, Bad Homberg, West Germany).

The solute concentration of the aerosol droplets generated by the Mist-O_2-Gen nebulizer was measured by the previously noted methods, except that aerosol droplets were collected in 30-s samples at set times during continuous nebulization.

The output of nebulizer solution from the jet nebulizer systems was measured by weighing after generation for different periods of time, whereas for the ultrasonic nebulizer it was measured continuously. The output from the mouthpiece with a two-way valve (model 2700, Hans Rudolf Inc, Kansas City, MO) in line, also was tested at various flow rates.

The droplet size of the jet nebulizers at a number of operating solution temperatures was measured in separate experiments. The nebulizer was cooled to a set temperature and aerosol generated as in the concentration measurements for 2 min. The nebulizer solution contained approximately 100 MBq/ml of $^{99m}Tc\ O_4^-$ in normal solution. The aerosol was sized by cascade impaction as described previously.[7]

The size of the droplets produced by the ultrasonic nebulizer was measured with and without the two-way valve in line, using the same methods as previously described.

RESULTS

The fall in temperature with time of nebulization for each of the nebulizer-generator systems is shown in Figure 1. For the jet nebulizers, the temperature falls to a steady value T_S which is 5 to 6°C below the ambient temperature at the lower flow rates of the air compressors, and 11 to 15°C at 8 L/min flow rate from a gas cylinder. Most of this temperature change occurs in the first 4 min of aerosol generation. By contrast,

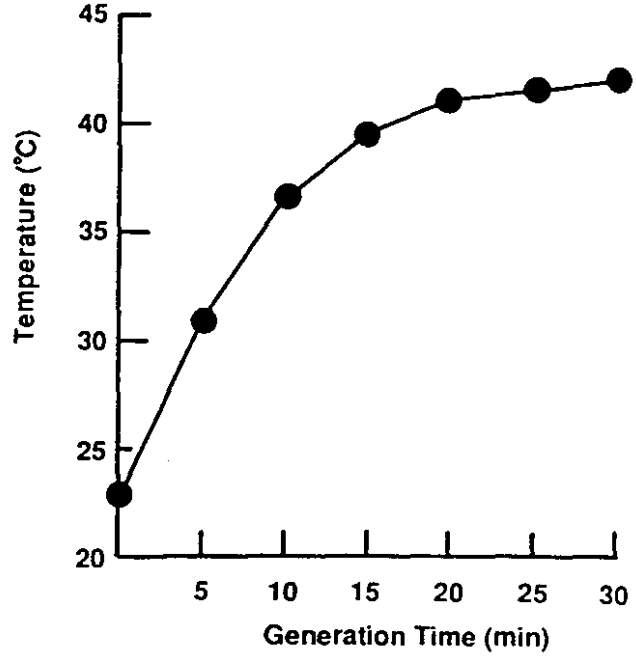

FIGURE 2. Graph of nebulizer solution temperature vs generation time for the Mist-O_2-Gen ultrasonic nebulizer.

the ultrasonic nebulizer increases in temperature by approximately 18°C and over a longer period of time (approximately 20 min [Fig 2]).

The total outputs of the jet nebulizer systems are plotted against generation time in Figure 3. The total output fell during nebulization for all of the jet nebulizer systems tested. The magnitude of the fall was similar for both the Cadema and Up-Draft with reductions in total output of approximately 45 to 65 mg/min for temperature falls of 11 to 15°C (over 6 min of generation).

The reduction in output with generation time for the two air compressor-driven systems was lower; approximately 15 and 27 mg/min for the Aerosol-One and the Flatus, respectively, after a temperature fall of 5 to 7°C during 6 min of generation.

The ultrasonic nebulizer solution output is much larger than that of the jet nebulizers. The output vs time graph is shown in Figure 4. The output without tubing or valve was found to be approximately constant at 4.8 ml/min over the time period tested. The output through the two-way valve was found to be greatly reduced and was dependent on the flow rate of the aerosol through it (Fig 4).

The change in concentration of solution in the nebulized aerosol droplets can be seen for each nebulizer system in Figure 5. The solute concentration contained in the aerosol produced by the jet nebulizers increases significantly with the fall in nebulizer temperature and with the reduction in the dilution air humidity. At the steady temperature T_S the droplet solution reaches 5.8 and 9.2 percent sodium chloride for the Cadema and Up-Draft nebulizers, respectively,

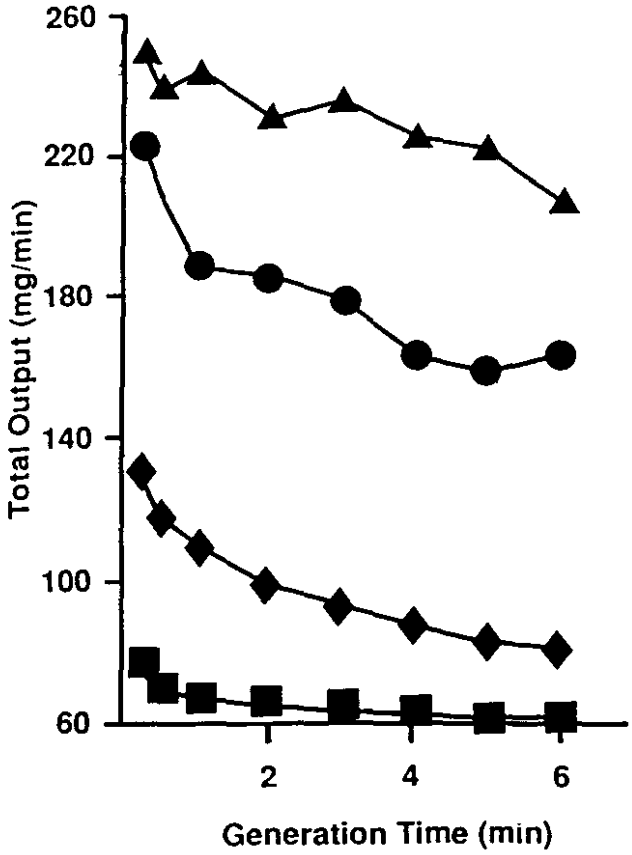

FIGURE 3. Graph of nebulizer output vs generation time for the four jet-nebulizer systems: Up-Draft/Aerosol-One *(squares)*, Up-Draft/Flatus *(diamonds)*, Cadema/compressed oxygen *(circles)* and Up-Draft/compressed oxygen *(triangles)*.

using 8 L/min of compressed oxygen as the generation gas. The Flatus/Up-Draft system reaches a little less than 5 percent and the Aerosol-One/Up-Draft reaches approximately 36 percent saline solution after the same generation time.

The effect of dilution air humidity alone on the droplet solute concentration with the nebulizer at room temperature for each jet nebulizer system can be seen in Table 1.

The droplet solute concentration reaches 1.1 to 1.5 percent with saturated dilution air at ambient temperature. Ambient dilution air with relative humidity of 65 to 75 percent at ambient temperature increased the droplet solute concentration to 1.86 and 2.46 percent for the Up-Draft and Cadema, respectively, generated with compressed oxygen. The effect with the air compressors was greater with the Up-Draft, the Flatus compressor producing a concentration of 3.45 percent and the Aerosol-One, 13.5 percent.

The droplet solution concentration generated from the ultrasonic nebulizer changes very little with time. The maximum effect is seen at the start of generation (0.93 percent saline from 0.9 percent initial value), and as nebulization progresses, the concentration returns toward isotonic, reaching it after approximately 13 min.

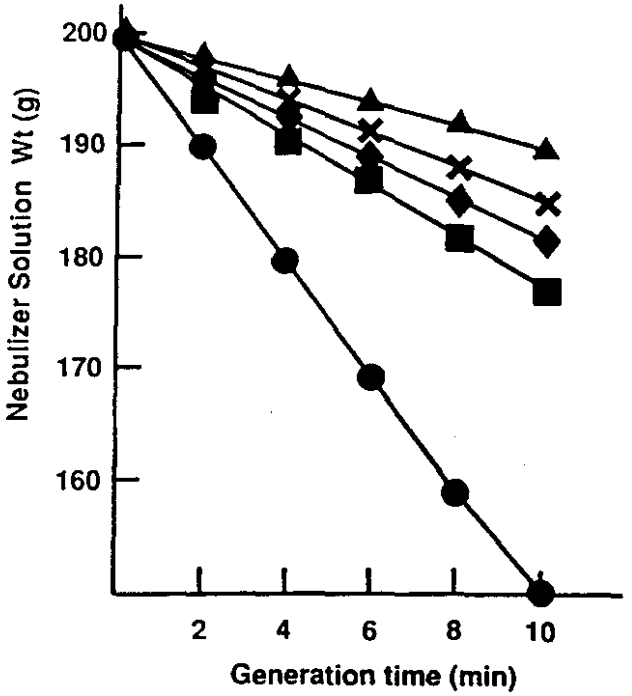

FIGURE 4. Graph of output vs generation time for the Mist-O_2-Gen ultrasonic nebulizer: no tubing or valve *(circles)*, Bennett tubing and valve (model 2700, Hans Rudolf Inc., Kansas City, MO) attached; 10 L/min flow rate *(triangles)*, 20 L/min *(squares)*, 30 L/min *(diamonds)* and 50 L/min *(crosses)*.

The droplet size distributions of the jet-nebulizer

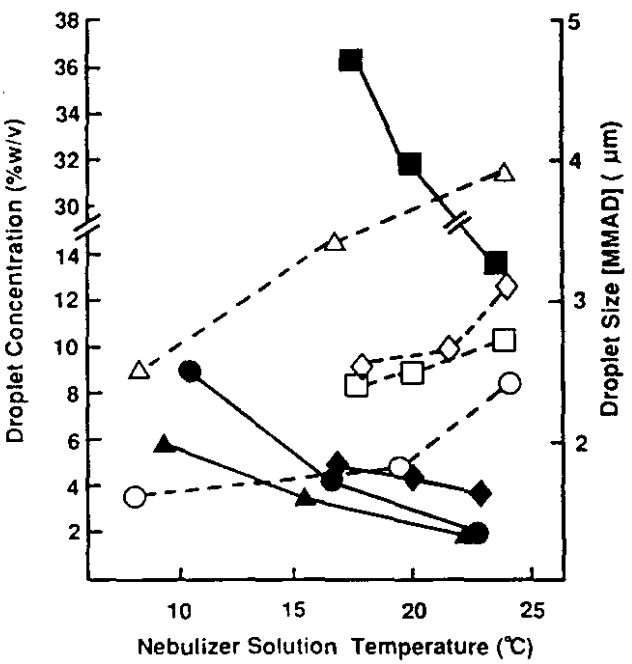

FIGURE 5. Graph of droplet solute concentration *(solid symbols, % W/V)* and mass median aerodynamic diameter *(open symbols, μm)* *vs* nebulizer solution temperature for the four jet-nebulizer systems: Up-Draft/Aerosol-One *(squares)*, Up-Draft/Flatus *(diamonds)*, Cadema/compressed oxygen *(circles)* and Up-Draft/compressed oxygen *(triangles)*. Note that the ambient temperature is the highest value on each graph.

Table 1—*Effect of Dilution Air Humidity on Droplet Solute Concentration at Ambient Temperature*

Nebulizer/Generator System	Droplet Solute Concentration (% W/V Saline)*	
	100% Relative Humidity	65-75% Relative Humidity
Up-Draft/Aerosol-One	1.5±0.3	13.5±1.8
Up-Draft/Flatus	1.1±0.1	3.5±0.6
Up-Draft/Compressed O_2	1.3±0.2	1.9±0.3
Cadema/Compressed O_2	1.5±0.2	2.5±0.2

*Results expressed as mean ± range (number of determinations = 2 or 3).

systems fall with reduced dilution air humidity and with the falling temperature in the nebulizer, in parallel with the increase in solute concentration in the aerosol droplets. Figure 5 shows the effect of nebulizer temperature on aerosol droplet size. The effect of temperature change is greater when compressed oxygen is used at 8 L/min, the droplet size falling by 33 and 36 percent of the size at ambient temperature for the Cadema and Up-Draft, respectively. With Flatus and Aerosol-One generation, the size change is smaller (19 and 11 percent fall from ambient temperature value, respectively). Conversely, the effect of dilution air humidity at ambient temperature is greater with the air compressor generation than with the compressed oxygen (Table 2). The changes that would be seen in practice with unheated nebulizers are shown in Table 3.

The ultrasonic nebulizer droplet size changes when a two-way valve is included in line but is not affected by changes in relative humidity of the dilution air (Table 4).

Discussion

The fact that the nebulizer solution temperature of jet nebulizers falls during generation has been well documented. The heat loss is due to the evaporation of the nebulizer solution to saturate the gas used to

Table 2—*Effect of Dilution Air Humidity on Droplet Size at Ambient Temperature*

Nebulizer/Generator System	Mass Median Aerodynamic Diameter in μm* (Geometric Standard Deviation†)	
	100% Relative Humidity	65-75% Relative Humidity
Up-Draft/Aerosol-One	4.2±0.3 (1.5)	2.7±0.3 (1.5)
Up-Draft/Flatus	4.1±0.2 (1.6)	3.1±0.3 (1.6)
Up-Draft/Compressed O_2	4.2±0.1 (1.4)	3.9±0.2 (1.5)
Cadema/Compressed O_2	2.7±0.1 (1.4)	2.4±0.2 (1.4)

*Results expressed as mean ± range (number of determinations = 2 or 3).

†Geometric standard deviation values all ±0.1.

Table 3—*Change of Concentration and Droplet Size Between Ambient and Steady State Temperature, T_s (65-75% Relative Humidity Dilution Air)*

Nebulizer/Generator System	Droplet Size, % Fall*	Droplet Concentration, % Rise*
Up-Draft/Aerosol-One	11.1	170
Up-Draft/Flatus	5.2	39.1
Up-Draft/Compressed O_2	35.9	392
Cadema/Compressed O_2	2.4	244

*Calculated as:

$$\frac{|X(T_s) - X(T_a)|}{X(T_a)} \times 100$$

where X = droplet size or droplet solution concentration at ambient temperature T_a or steady state temperature T_s (lowest steady temperature reached by each system).

generate the aerosol and some cooling due to adiabatic expansion of the generating gas.[14,18] This evaporation also leads to an increase in solute concentration of the nebulizer solution.[18] The gas from a compressed gas cylinder contains no water vapor, while an air compressor supplies air of ambient humidity. Less vapor is therefore required from the nebulizer solution to saturate the air from an air compressor and heat loss is therefore reduced. Of the energy imparted to the solution of an ultrasonic nebulizer, however, part is used to overcome the surface tension to disperse solution droplets and part to heat the solution itself. The nebulizer solution therefore warms during generation (Fig 2).

The initial output from the nebulizer depends on the type, the flow rate and the saturation of the generating gas. The change in jet nebulizer output measured during generation depends almost solely on the temperature of the nebulizer solution. The nebulizer solution provides both the solution output and the output of vapor necessary to saturate the generation gas with water vapor at the nebulizer temperature. Therefore, the amount of vapor carried by the generation gas decreases as the temperature falls and the reduction in total output mirrors these changes.

As the temperature of the ultrasonic nebulizer solution increases, the extra water needed to saturate the air is likely to come from the dense aerosol cloud within the nebulizer chamber. The output therefore is

Table 4—*Size of Droplets Generated by the Mist-O_2-Gen Ultrasonic Nebulizer**

Ambient Temperature, °C	Dilution Air Relative Humidity, %	Mouthpiece and Valve	Mass Median Aerodynamic Diameter (μm)	Geometric Standard Deviation
19.5±0.3	99.0±1	Yes	3.6±0.1	1.1±0.1
19.0±0.3	53.1±1	Yes	3.5±0.2	1.1±0.1
19.0±0.3	53.5±1	No	5.7±0.1	1.4±0.1

*Results expressed as mean ± range (number of determinations = 2 or 3).

not likely to change as the nebulizer temperature rises as suggested by the results (Fig 4). The two-way valve situated before the mouthpiece of the ultrasonic nebulizer filters a high proportion of the larger droplets from the aerosol stream. The effect therefore is to reduce the output and mass median aerodynamic diameter of the droplets. This effect depends on the flow rate of the aerosol stream and hence the velocity of the droplets. There is an optimum flow rate, however, due to opposing effects: At the lower flow rate, the droplets tend to settle into the nebulizer solution or within the tubing and the output is reduced. At the higher flow rates, the droplets are more likely to impact within the tubing and on the valve. The optimum flow rate for this system was found to be approximately 20 L/min (Fig 4).

Although it is known that the concentration of the solution in the jet nebulizer bowl increases with generation due to the release of vapor in addition to the liquid droplets,[14,15] the changes in solution concentration in the droplets measured in the experiments reported here are generally much greater. This is because the cold aerosol droplets generated from the jet nebulizer solution will evaporate a substantial amount of water as they rapidly warm up to room temperature. Therefore, the concentration of solute in the droplets increases to a value determined by the difference between the ambient temperature and the temperature of the nebulizer solution and to a lesser extent due to the gradual increase of the concentration in the nebulizer.

The nebulizer solution equilibrates to a lower steady temperature T_s when the dry gas from a compressed gas cylinder is used to generate the aerosol, compared with the air compressors. The droplet solute concentration thus increases to a greater extent (relative to the value at ambient temperature) as a result (Table 3).

The ambient air inhaled along with the aerosol that makes up the inspiratory flow is likely to have a lower relative humidity than that corresponding to the nebulizer solution; therefore, it has the effect of drying the aerosol droplets as it mixes before inhalation.[7] This concentrating effect is quite marked, especially when the generation flow and the output of solution from the nebulizer is low. The consequence of the low output is that there is only a small volume of water present in the droplets to resaturate the aerosol stream (see results for Up-Draft/Flatus and especially the Up-Draft/Aerosol-One systems, Fig 5 and Table 1). The ambient relative humidity was comparatively high during these experiments (65 to 75 percent), and a lower ambient relative humidity, such as that found in air-conditioned rooms, would be expected to greatly enhance these effects.

The ultrasonic nebulizer has a higher output and larger droplet size, so more water is available for saturation of the dilution air and the concentration change of the droplet solution hence is much smaller than that of the jet nebulizers. The droplet concentration therefore starts off greater than isotonic, but as the tubing becomes saturated, this is able to supply the vapor necessary to saturate the dilution air. Although the nebulizer solution temperature is increasing, the droplets do not become hypotonic due to water vapor condensing on them as the aerosol stream cools; rather, the excess vapor will condense on the walls of the conducting tubing.[19]

Schoeffel et al[20] found that small amounts of hypertonic (3.6 percent sodium chloride) aerosol caused bronchoconstriction in asthmatic subjects. Lewis and Tattersfield[21,22] found that a number of asthmatic subjects had bronchoconstriction after inhaling a jet nebulized aerosol of isotonic saline solution, but not to an aerosol generated by a nebulizer heated to 37°C. This was explained in terms of a reduction in airway cooling by the warm aerosol, but it may have been due to a reduction in the concentrating effects that the nebulizer temperature fall imparted on the droplets. The possibility that initially isotonic, or even hypotonic, solutions may produce hypertonic aerosol droplets should therefore be accounted for when delivering therapeutic aerosols to patients with hyperreactive airways.

The necessity for nebulization to be reproducible for bronchial challenge testing, has led to some careful characterization of nebulizers;[23-25] the nebulizer temperature change may, however, add to the variability in dose and site of delivery of challenge agents.

The size of the aerosol droplets falls with generation time in conjunction with the increase in concentration. The magnitude of this is variable but it is likely to affect the deposition pattern of aerosol within the lungs.[8] Large differences in regional deposition as measured by "penetration index" on tomographic slices have been found in normal subjects inhaling aerosols with mass median aerodynamic diameters of 2.6 and 5.5 μm.[26] The smaller droplet size showed a much higher relative deposition in the small airways and lung parenchyma. The change in droplet size, depending on the time since the start of generation and the humidity of dilution air (for example, from an initial droplet size of 4.2 μm with 100 percent relative humidity dilution air to 2.4 μm after the equivalent of 4 min generation for the Up-Draft/Aerosol-One system) may be important in therapeutic, diagnostic or experimental applications when reproducibility of aerosol deposition or clinical response is important.[27,28] It is, of course, very likely that some subsequent adjustment of droplet size will take place in the respiratory tract.[29]

The Flatus compressor produces a droplet size

similar to the Aerosol-One, with the Up-Draft nebulizer, but with the higher flow rate of the Flatus, a smaller droplet size may be expected. The discrepancy may be due to the fact that the Aerosol-One droplets are evaporating to a greater extent than with the Flatus at ambient temperature and saturated dilution air (1.5 and 1.14 percent, respectively [Table 1]). The lower output of the Aerosol-One/Up-Draft system is likely to be responsible for this.

The effect of the increase in temperature of the ultrasonic nebulizer solution on the droplet solute concentration is small. Also, the effect of dilution air humidity on the droplet size (and presumably the droplet solute concentration) is small due to the much higher output from the Mist-O_2-Gen nebulizer. The larger droplet size generated by the ultrasonic nebulizer means that they are more easily deposited on the tubing and valves within the system.

To reduce the evaporation effects in jet nebulizers, the generating gas and dilution air should be saturated with water vapor at ambient temperature and the nebulizer solution should be maintained at ambient temperature. As these changes may affect the outcome of therapy, clinical studies to measure any alterations in response should be carried out.

The higher output and droplet size occurring with the Mist-O_2-Gen ultrasonic nebulizer makes the droplet size and solute concentration less susceptible to large changes during nebulization. However, the presence of tortuous tubing, valves and high inhalation flow rate will cause a large reduction in the output available to the patient because the large droplets will deposit in the apparatus.

ACKNOWLEDGMENTS: The authors would like to thank Mr. Ian Spiers for the preliminary data on the Mist-O_2-Gen ultrasonic nebulizer, colleagues in the Departments of Thoracic and Nuclear Medicine at the Royal Prince Alfred Hospital Camperdown for assistance and encouragement, and the Asthma Foundation of New South Wales for financial support.

REFERENCES

1 Newman SP, Pellow PGD, Clarke SW. Droplet size distributions of nebulized aerosols for inhalation therapy. Clin Phys Physiol Meas 1986; 7:139-46
2 Newman SP, Pellow PGD, Clarke SW. Flow pressure characteristics of compressors used for inhalation therapy. Eur J Respir Dis 1987; 71:122-26
3 Foulds RA, Smithuis LOMJ. Comparison of lung deposition of a solution after nebulization by three commonly portable nebulizers. Pharm Weekblad Sci 1983; 5:74-76
4 Matthys H, Kohler D. Pulmonary deposition of aerosols by different mechanical devices. Respiration 1985; 48:269-76
5 Newman SP, Woodman G, Clarke SW. Deposition of carbenicillin aerosols in cystic fibrosis: effects of nebulizer system and breathing pattern. Thorax 1988; 43:318-22
6 Newman SP, Pellow PGD, Clay MM, Clarke SW. Evaluation of jet nebulizers for use with gentamicin solution. Thorax 1985; 40:671-76
7 Phipps P, Borham P, Gonda I, Bailey D, Bautovich G, Anderson S. A rapid method for the evaluation of radioaerosol delivery systems. Eur J Nuc Med 1987; 13:183-86
8 Stahlhofen W, Gebhart J, Heyder J, Scheuch G. Deposition pattern of droplets from medical nebulizers in the human respiratory tract. Bull Europ Physiopath Resp 1983; 19:459-63
9 Ferron GA, Hornik S, Kreyling WG, Haider B. Comparison of experimental and calculated data for the total and regional deposition in the human lung. J Aerosol Sci 1981; 16:133-43
10 Ilowite JS, Gorvoy JD, Smaldone GC. Quantitative deposition of aerosolized gentamicin in cystic fibrosis. Am Rev Respir Dis 1987; 136:1445-49
11 Newman SP, Pellow PGD, Clarke SW. Dropsizes from medical atomisers (nebulizers) for drug solutions with different viscosities and surface tensions. Atomisation Spray Technol 1987; 3:1-11
12 Sterk PJ, Plomp A, van de Vate JF, Quanjer PH. Physical properties of aerosols produced by several jet- and ultrasonic nebulizers. Bull Eur Physiopathol Respir 1984; 20:65
13 Dahlbäck M, Nerbrink O, Arborelius M, Hansson HC. Output characteristics from three medical nebulizers. J Aerosol Sci 1986; 17:563
14 Davis SS. Physico-chemical studies on aerosol solutions for drug delivery: I. Water-propylene glycol systems. Int J Pharm 1978; 1:71-83
15 Mercer TT, Tillery MI, Chow HY. Operating characteristics of some compressed air nebulizers. Am Ind Hyg Assoc J 1968; 29:66-78
16 Porstendorfer J, Gebhart J, Robig G. Effect of evaporation on the size distribution of nebulized aerosols. J Aerosol Sci 1977; 8:371-80
17 Anderson SD, Schoeffel RE, Finney M. Evaluation of ultrasonically nebulized solutions for provocation testing in patients with asthma. Thorax 1983; 38:284-91
18 Mercer TT. Production of therapeutic aerosols, principles and techniques. Chest 1981; 80(suppl):813-18
19 Mercer TT, Goddard RF, Flores RL. Output characteristics of three ultrasonic nebulizers. Ann Allergy 1968; 26:18-27
20 Schoeffel RE, Anderson SD, Altounyan REC. Bronchial hyperreactivity in response to inhalation of ultrasonically nebulized solutions of distilled water and saline. Br Med J 1981; 283:1285-87
21 Lewis RA, Tattersfield AE. Cold induced bronchoconstriction: interaction with prostaglandin induced bronchoconstriction. Clin Sci 1980; 59:12
22 Lewis R, Tattersfield AE. Bronchial hyperreactivity after inhaled distilled water and saline. Br Med J 1982; 284:47
23 Tsanakas JN, Wilson AJ, Boon AW. Evaluation of nebulizers for bronchial challenge tests. Arch Dis Childhood 1987; 62:506-08
24 Sterk PJ, Plomp A, Crobach MJJS, van de Vate JF, Quanjer PH. The physical properties of a jet nebulizer and their relevance for the histamine provocation test. Bull Europ Physiopathol Resp 1983; 19:27-36
25 Ryan G, Dolovich MB, Obminski G. Cockroft DW, Juniper E, Hargreave FE, et al. Standardisation of inhalation provocation tests: influence of nebulizer output, particle size and method of inhalation. J Allergy Clin Immunol 1981; 67:156
26 Phipps PR, Gonda I, Bailey DL, Borham P, Bautovich G, Anderson SD. Comparisons of planar and tomographic gamma scintigraphy to measure the penetration index of inhaled aerosols. Am Rev Respir Dis 1989; 139:1516-23
27 Clay MM, Clarke SW. Effects of nebulized aerosol size on lung deposition in patients with mild asthma. Thorax 1987; 42:190-94
28 Mitchell DM, Solomon MA, Tolfree SEJ, Short M, Spiro SG. Effect of particle size of bronchodilator aerosols on lung distribution and pulmonary function in patients with chronic asthma. Thorax 1987; 42:457-61
29 Morrow PE. Factors determining hygroscopic aerosol deposition in airways. Physiol Rev 1986; 66:330

Aerosols: science, industry, health and environment. (1990). Eds. Masuda, S and Takahashi, K. Pergamon Press, Oxford, vol. 1. p 227-230.

SOME CONSEQUENCES OF INSTABILITY OF AQUEOUS AEROSOLS PRODUCED BY JET AND ULTRASONIC NEBULIZERS

I. GONDA and P.R. PHIPPS

Department of Pharmacy, University of Sydney, Sydney, NSW 2006, Australia.

ABSTRACT

Medical aerosols prepared by nebulization of aqueous solutions are unstable: they may undergo evaporation or uptake of water prior to, or after, entry to the human respiratory tract (RT). These dynamic changes modify the results of characterization of aerodynamic droplet size. We analyse the changes of the aerodynamic diameter (D) by mathematical models and show experimentally that the evaporation and condensation phenomena also affect the deposition of aerosols 'in vivo'.

KEYWORDS

Aerosols - therapeutic, diagnostic; Nebulizers; Aerosols - deposition; Aerosols - hygroscopic; Droplet size analysis.

INTRODUCTION

Nebulization of aqueous solutions is a common method of aerosol production in medicine (Gonda, 1990). It has been pointed out that these aerosols are unstable (Mercer, 1973; Porstendorfer et al., 1977): they will exchange heat and water with the environment until their vapour pressure becomes equal to the ambient, or the droplets are transformed into solid particles. These processes occur on time scales similar to the time it takes to deliver droplets from the nebulizer to a size measurement device, or to the area of deposition in RT. Therefore, both the measurement (Porstendorfer et al., 1977) and the deposition of medical aerosols are affected by water exchange. Theoretical comparison of regional deposition of hygroscopic and stable aerosols was made by numerous authors but there is little experimental evidence to support the models (Gonda, 1990). In order to evaluate the deposition of 'hygroscopic' aqueous aerosols in RT, it is necessary to have methods to obtain their aerodynamic size distribution reliably. Small droplets of non-isotonic solutions can equilibrate rapidly with the air in the airways. It is therefore a reasonable objective to determine the size distribution of the aerosol

when it is equilibrated at 37 ^{o}C with isotonic solution (Hickey et al., 1990); alternatively, the particle size of the dried aerosol can be determined and the droplet size of the equilibrated aerosol calculated (Gonda et al., 1982; Mercer, 1973).

We have shown (Phipps et al., 1987; Phipps and Gonda, 1990a) that aerosol droplets from jet nebulizers can undergo marked changes in size and solute concentration before reaching the outlet of the aerosol delivery system. In the first part, a mass balance model is summarized which helps to correct the measured D for the effect of evaporation or condensation. In the second part, experimental evidence for change of droplet size in RT and its effect on regional deposition is presented.

ESTIMATE OF DROPLET SIZE AND CONCENTRATION CHANGES 'IN VITRO'

The output of a nebulizer m_1 consists of droplets and vapour. It is thought that, initially, the concentration of the solution in the droplets is the same as in the nebulizer, c_1, and that the vapour pressure is at equilibrium with this solution at temperature T_1. When the aerosol droplets reach the ambient temperature T_2, evaporation or condensation takes place. To supplement the aerosol with an adequate volume of gas for inhalation or size measurement, it is often mixed with dilution air supplying a mass of vapour per unit time, m_3. Consequently, a further exchange of water and heat is possible. The following mass balance models can be derived (Phipps and Gonda, 1990b) [only the models ignoring the losses of aerosol in the equipment and the Kelvin effect (Gonda et al., 1982) are presented here]:

I. Assuming ideal solution behaviour (Ferron, 1977), the concentration c_2 in the droplets can be calculated from the quadratic equation

$$(c_2)^2[m_2(r-1)-v_2q_2]+c_2[m_2-v_2q_2-m_s(r-1)]-m_s = 0 \qquad (1)$$

where c_2 = final concentration of solution in droplets (g solute/g solution); r = ratio of the molecular mass of water to that of solute; v_2 = saturation vapour content of pure water at temperature T_2 (g/l); q_2 = total flow rate (aerosol + dilution air) (l/min); $m_2 = m_1+m_3$ = total mass flow rate (aerosol + dilution air) (g/min); m_s = output of solute (g/min). m_s can be measured directly or calculated as the total nebulizer output less the water carried in the droplets and in the vapour. The latter is obtained from the vapour pressure at equilibrium with solution at c_1 and T_1.

II. Similarly, using an empirical expression for the dependence of vapour pressure on saline concentration (Cinkotai, 1971), c_2 can be obtained from a cubic equation

$$(c_2)^3+(a/b)(c_2)^2+c_2[1/b-m_2/(q_2v_2b)]+m_s/(q_2v_2b) = 0 \qquad (2)$$

where a=-0.486 and b=-1.55 are empirical constants.

Neglecting the slip correction, the ratio of aerodynamic diameter D_1 of the initially generated droplet containing solution of concentration c_1, to the size D_2 of droplet with concentration c_2 is

$$D_1/D_2 = (d_1/d_2)^{1/6}(c_2/c_1)^{1/3} \quad (3)$$

where d_1 and d_2 are the densities of the solutions obtained from the theoretical (Ferron, 1977) or empirical (Cinkotai, 1971) relationship between d and c. Some representative results are shown in the Table I:

Table I. Dependence of the final concentration in the droplets c and D on the total output O, the ratio R of aerosol/dilution air and RH of dilution air for initial c=0.9% and D=3 μm at 20 ^{o}C. The subscripts refer to the ideal and empirical vapour pressure and density approximations of Ferron (1977) (i) and Cinkotai (1971) (e).

O (g/min)	R (l/l)	RH (%)	c_i (g/g)	c_e (g/g)	D_i (μm)	D_e (μm)
	10:10	50	100.0	21.4	0.7	1.1
0.2		90	2.1	1.9	2.3	2.3
	10:1	50	1.3	1.3	2.7	2.7
		90	0.96	0.95	2.9	2.9
		0	18.9	12.2	1.1	1.3
0.5	10:20	50	1.9	1.9	2.4	2.4
		90	1.0	1.0	2.9	2.9

It is noticed that the changes in D become very significant when the output of the aerosol is low and a large quantity of dry dilution air is mixed with the aerosol. However, even for a nebulizer with a moderate output (0.2 g/min in 10 l/min of air) mixed 10:10 with dilution air [relative humidity (RH) 50%, ambient temperature] there is about a 3-fold reduction in D as a result of drying. High RH of the dilution air is required to prevent evaporation of this aerosol because even with dilution air of RH=90%, about 25% reduction of D is predicted. Even greater shrinking of D would take place if the nebulizer temperature were allowed to drop as often happens in practice (Phipps and Gonda, 1990a). Another interesting observation for this aerosol is that the calculation based on ideal solution behaviour can be grossly in error for prediction of the concentration but, because of the cube root dependence of D on c, there is not much error incurred in D compared to the calculation based on the real behaviour of salt solutions.

DEPOSITION OF HYGROSCOPIC AEROSOLS 'IN VIVO'

We used a recently developed sensitive tomographic method to measure the penetration index (PI) of inhaled radiolabelled aerosols (Phipps et al., 1989). Because we observed significant deposition in the trachea, the method was modified to include this deposition in the central region. Both in our inhalation studies and during size measurement, the nebulizers were kept at ambient T and the dilution air was appropriately humidified to minimize size changes of droplets after their generation. Five normal subjects inhaled aerosols with mass median aerodynamic diameter MMAD= 3.7 μm and geometric standard deviation GSD=1.4 on two occasions. The difference in the tests was the tonicity of the aerosols; the saline

concentration was either 0.3 or 4.5%. These concentrations and sizes were selected so that if these aerosols equilibrated to become isotonic (as they would in the lung) before deposition, their MMAD would be 2.6 and 6.3μm, respectively. The figure (below) indicates that some changes of size of the droplets in the anticipated direction, sufficient to be detected as differences in PI, occurred in the RT of 4/5 subjects.

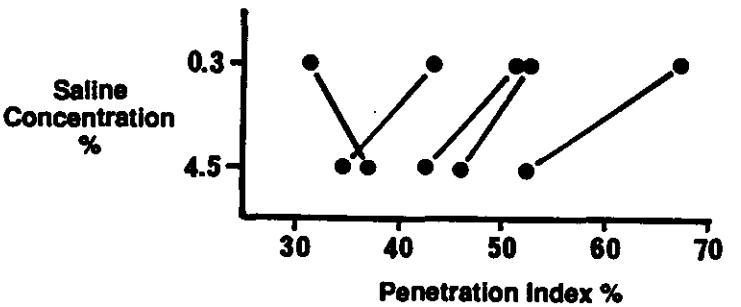

In conclusion, the ability of droplets of aqueous solutions to change in size during measurement and before, or after, the entry into RT has important consequences for interpretation of 'in vivo' and 'in vitro' studies.

REFERENCES

Cinkotai, F.F. (1971). The behaviour of sodium chloride particles in moist air. Aerosol Sci., 2, 325-329.

Ferron, G.A. (1977). The size of soluble aerosol particles as a function of the humidity of the air. Application to the human respiratory tract. J.Aerosol Sci., 8, 251-267.

Gonda, I. (1990). Aerosols for delivery of therapeutic and diagnostic agents to the respiratory tract. Crit.Rev.Therap.Drug Deli.Systems, 6, 273-313.

Gonda, I., Kayes, J.B., Groom, C.V. and Fildes, F.J.T. (1982). Characterization of hygroscopic inhalation aerosols. In: Particle Size Analysis 1981. (N.G. Stanley-Wood and T. Allen, Eds.). Wiley Heyden, Chichester, pp.31-43.

Hickey, A.J., Gonda, I., Irwin, W.J. and Fildes, F.J.T. (1990). The effect of hydrophobic coating upon the behavior of a hygroscopic aerosol powder in an environment of controlled temperature and relative humidity. J.Pharm.Sci. (in press).

Mercer, T.T. (1973). Aerosol Technology in Hazard Evaluation. Academic Press, New York.

Phipps, P.R. and Gonda, I. (1990a). Droplets produced by medical nebulizers: Some factors affecting their size and solute concentration. Chest (July issue, in press).

Phipps, P.R. and Gonda, I. (1990b) (manuscript in preparation).

Phipps, P.R., Borham, P., Gonda, I., Bailey, D., Bautovich, G. and Anderson, S. (1987). A rapid method for the evaluation of radioaerosol delivery systems. Eur.J.Nuc.Med., 13, 183-186.

Porstendorfer, J., Gebhart, J. and Robig, G. (1977). Effect of evaporation on the size distribution of nebulized aerosols. J.Aerosol Sci., 8, 371-380.